PB-221 280

LEAD/ACID BATTERY DEVELOPMENT FOR HEAT ENGINE/ELECTRIC HYBRID VEHICLES

J. Giner, et al

Tyco Laboratories

Prepared for:

Environmental Protection Agency

November 1971

DISTRIBUTED BY:

NTIS

National Technical Information Service
U. S. DEPARTMENT OF COMMERCE
5285 Port Royal Road, Springfield Va. 22151

PB 221 280

APTD-1346

Final Report

LEAD/ACID BATTERY DEVELOPMENT FOR HEAT ENGINE/ELECTRIC HYBRID VEHICLES

November 1971

Prepared for DIVISION OF ADVANCED AUTOMOTIVE
POWER SYSTEMS DEVELOPMENT
U.S. ENVIRONMENTAL PROTECTION AGENCY
Ann Arbor, Michigan

Contract No. EHSH 71-009

By

J. Giner
A.H. Taylor
F. Goebel

Tyco Laboratories, Inc.
16 Hickory Drive
Waltham, Massachusetts 02154

Reproduced by
NATIONAL TECHNICAL
INFORMATION SERVICE
U S Department of Commerce
Springfield VA 22151

194

ABSTRACT

A program has been undertaken to develop a lead acid battery system for use in a hybrid heat engine/electric vehicle. The basic requirements are that the battery be capable of supplying high rate power pulses and of accepting high rate charge pulses, both of short duration. The maximum power ratings specified are for 92.5 KW for a 10 sec period with an average maximum power output of 70.5 KW over a 25 sec period. The maximum recharge rate is 39 KW and in the most severe cycle 980 Whr of energy are transferred to or from the battery. A five year lifetime is envisaged and the battery must withstand a total of 200,000 cycles but not all at the above high rates. The minimum working voltage is 200 V with a minimum of 1.5 V/cell. The preferred battery weight is 450 lb maximum with a projected cost of no greater than $550.

The feasibility of developing a bipolar lead acid battery system which conforms to these specifications has been investigated using a modular approach to system design. The candidate test plates, herein defined as "quasi-bipolar" plates, are approximately one-sixth full scale and have a thermoplastic substrate as active material support. In the preferred design, a vertical array of lead strips placed on either side of each substrate are connected with adjacent strips on the opposite side only over the top of the substrate to provide electrical conduction through the substrate. Inter-cell leakage is minimized by removing these conduction points from direct contact with the acid. The full-size plate is made relatively long (8in.) and shallow (4 in.) to minimize resistance losses. The strips are held at fixed points to the plastic substrate by an overlying plastic grid so as to permit unidirectional expansion of the Pb down the plate without buckling it. Each complete quasi-bipolar plate is 60 mil total thickness with a maximum paste thickness of 20 mil on both the positive and negative sides. No Sb is present in the design.

The plates were tested at 30°C by repetitive cycling at currents and for times equivalent to those required to achieve the most severe ratings specified by EPA in the preliminary power profile (page 1 of this report) using a full scale battery system based on these plates. Thus, the plates were discharged at 150 mA/cm^2 corresponding to the 55 KW rate and were charged at up to the 40 KW rate (83 mA/cm^2). Prior to cycling experiments small additions of H_3PO_4 were made to the 1.28 sp gr. electrolyte. Following each group of 100 high rate cycles, the capacity retained by each test plate was evaluated at the C/5 rate. Results were compared with those on fresh thin plates (Pb/Sb grids) from a commercial SLI battery tested under slightly less severe conditions, that is, at currents corresponding to the 47.5 KW and 25.9 KW ratings on discharge and charge respectively using a full size battery system based on the conventional plates. The actual

currents used were 175 mA/cm^2 and 72 mA/cm^2. No H_3PO_4 additions were made to the electrolyte in the latter case. Note also that the bipolar system operates at lower current densities than does the conventional system to achieve the same power rating.

The conventional monopolar positive plates lasted for a maximum of 350 complete high rate cycles prior to failure. After 300 cycles the C/5 capacity retained by three positive test plates was 57%, 23% and 3.5%. The conventional negative plates still performed well after 500 complete cycles, losing only ~30% of their original C/5 capacity. In contrast five "quasi-bipolar" test plates retained 87%, 102%, 90%, 91% and 89% of their C/5 capacity after 300 cycles. Furthermore, four of these five plates lasted for 1000 complete high rate cycles before showing signs of failure and the capacity retention at this point was still 47%, 61%, 51% and 48%. The fifth plate failed only after 730 complete cycles. Failure is denoted here as the point at which the voltage fell below 1.5 V/cell before completion of a (25 sec) discharge cycle.

Calculations show that a full size modular battery system based on the quasi-bipolar plates can operate at 143 mA/cm^2 to achieve the maximum average power output of 70.5 KW (for 25 sec). Each module weighs 54.5 lb and 10 parallel modules are employed each with 133 plates in series. The power density is 128 W/lb. Alternatively, to achieve the maximum specified power output of 92.5 KW (for 10 sec) within the desired weight requirement of 450 lb maximum, only 8 parallel modules may be employed and the operating current density is increased to 234 mA/cm^2 (212 W/lb). However, a preferred approach to achieve such a power output with minimum modifications to the present system is to decrease the paste thickness by 25% (i.e., from 20 mil to 15 mil/electrode) when the operating current density per plate may be reduced to < 190 mA/cm^2. No design difficulties or manufacturing problems are anticipated and the active material per electrode is still about five times that required for the most severe cycle specified in the final power profile (980 Whr on one cycle).

Final Report

LEAD/ACID BATTERY DEVELOPMENT FOR HEAT ENGINE/ELECTRIC HYBRID VEHICLES

November 1971

Prepared for DIVISION OF ADVANCED AUTOMOTIVE
POWER SYSTEMS DEVELOPMENT
U.S. ENVIRONMENTAL PROTECTION AGENCY
Ann Arbor, Michigan

Contract No. EHSH 71-009

By

J. Giner
A.H. Taylor
F. Goebel

Tyco Laboratories, Inc.
16 Hickory Drive
Waltham, Massachusetts 02154

FOREWORD

This report contains a summary of work performed by Tyco Laboratories for the Division of Advanced Automotive Power Systems Development, Environmental Protection Agency under Contract No. EHSH 71-009.

ACKNOWLEDGEMENTS

Problems associated with the development and operation of a high power density lead acid battery were discussed with Mr. John Nees of N.L. Industries (Heightstown, N.J.), Dr. Everett Ritchie of I.L.Z.R.O. (Joplin, Missouri), Mr. Cooke also of I.L.Z.R.O. (New York) and Mr. Rooney of W.R. Grace Co. (Cambridge, Mass.). Information and materials resulting from these discussions were used in the course of the contract, and we would like to thank these gentlemen and also Mr. Bob Bowen of Tyco's Mule Battery Division for their help. The helpful discussions with our contract monitor, Mr. Charles Pax (Ann Arbor, Michigan), and, with Dr. Mark Salamon (D.O.T. Cambridge) and Mr. Bill Robertson (NASA Lewis) are also appreciated. We would also like to acknowledge the work of Mr. L. Gaines (Tyco Laboratories, Inc.) in the development of preliminary concepts and calculations for the bipolar plate and modular battery system.

Table of Contents

Section No. Page No.

ABSTRACT vii

SUMMARY OF WORK xiv

I. INTRODUCTION 1

II. TASK I: INVESTIGATION OF THE STATE OF THE ART. 7
- A. Cycle Life Testing, Equipment and Procedure 7
- B. Performance Evaluations of Commercial SLI Plates 9

III. TASK II: PRELIMINARY DESIGN STUDIES 21
- A. Design Concepts. 21
- B. Design Equations and Concepts for a Preliminary Bipolar Concept A 22
- C. Design Analysis for Preliminary Concept A. 28

IV. TASK III: STUDY OF ELECTROCHEMICAL PROBLEM AREAS RELEVANT TO DESIGN OF A HIGH POWER DENSITY BATTERY . . . 35
- A. Utilization of Active Material. 35
- B. Effect of Sb and H_3PO_4 on Paste Performance 42
- C. Factors Not Varied in the Study of Electrochemical Performance . . 54
- D. Conclusions. 55

V. TASK IV: CORROSION OF SUBSTRATE MATERIALS. 57
- A. Metal Substrates 57
- B. Plastic Substrates. 68

Table of Contents (Continued)

Section No. Page No.

VI. TASK V: DEVELOPMENT AND MECHANICAL TESTING OF STRUCTURES 79
- A. Factors Influencing Choice of Design Materials and Techniques 79
- B. Conclusions 94
- C. Preliminary Plate Development 94
- D. Second Design Plate 96
- E. Final Plate Design 98
- F. Construction of the Battery Using Quasi-Bipolar Plates 100
- G. Method of Construction of the Quasi-Bipolar Plate 101
- H. Modifications to the Final Design Structure 110
- I. Design in Which the Plastic Substrate is Conductive 112

VII. LIFE TESTING OF NEW DESIGN PLATES 117
- A. Test Cell and Test Procedure 117
- B. Test Results 119

VIII. BATTERY DESIGN AND PRELIMINARY COST ANALYSIS 135
- A. Design, Operation, and Characteristics of a Quasi-Bipolar Battery System Based on the Preliminary Power Profile Specified by EPA 135
- B. Design, Operation and Characteristics of a Quasi-Bipolar System Based on the Final Power Profile Specified by EPA 140
- C. Energy Density of a Full-Size Battery System Based on the Quasi-Bipolar Plates (Concept I) 144
- D. Preliminary Cost Estimate for the Quasi-Bipolar Battery (Concept I) 145

IX. SUMMARY OF ACHIEVEMENTS, EVALUATION OF THE MAIN AREAS REQUIRING FURTHER DEVELOPMENT, AND PRELIMINARY WORK PLAN 147
- A. Summary of Achievements 147
- B. Areas Requiring Further Development 148
- C. Work Plan 149

X. REFERENCES 151

Table of Contents (Continued)

Page No.

APPENDIX I: Calculation Details for a Full Size Battery Based on the Preliminary Bipolar Concept A, with Plastic Substrate and Pb Conductors, Using the Preliminary Power Profile. 155

APPENDIX II: New Design Equations for the Preliminary Bipolar Concept B with a Plate Dimension of 8 in. × 4 in. Using the Preliminary Power Profile 159

APPENDIX III: Comparison of Battery Systems Based on the Preliminary Power Profile and on the Two Different Bipolar Plates Outlined in Preliminary Concepts A and B. 161

APPENDIX IV: Energy Density Comparison of Thin Plate Conventional SLI and Quasi-Bipolar Batteries (Final Design Plates) at High and Low Discharge Rates. 163

APPENDIX V: Curing and Formation Techniques 165

APPENDIX VI: Engineering Data for Battery Materials of Possible Interest 167

List of Illustrations

Figure No. Page No.

1. Battery maximum power design curve for 6 passenger hybrid car 3

2. Performance characteristics of a fresh thin conventional SLI positive plate under severe cycling conditions - Plate 1 11

3. Performance characteristics of a fresh thin conventional SLI positive plate under severe cycling conditions - Plate 2 12

4. Performance characteristics of a fresh thin conventional SLI positive plate under severe cycling conditions - Plate 3 13

5. Photograph of a typical thin commercial SLI positive plate prior to cycling 14

6. Photograph of a typical thin commercial SLI positive plate after 500 cycles 14

7. Photograph illustrating plate buckling in a conventional thin positive SLI plate after 500 cycles 15

8. Performance characteristics of a fresh thin conventional SLI negative plate under severe cycling conditions - Plate 1 17

9. Performance characteristics of a fresh thin conventional SLI negative plate under severe cycling conditions - Plate 2 18

10. Photograph of a typical thin conventional SLI negative plate prior to cycling 19

11. Photograph of a typical thin conventional SLI negative plate after 500 cycles 19

12. Illustration of the production of a basic bipolar plastic plate as in Preliminary Concept A 24

13. Initial visualization of bipolar plates with plastic support and "lead fingers" folded over the top of the support 25

14. Graph of the coulombic efficiency of the active materials as a function of current density 29

15. Plots of the system weight versus the substrate thickness for various lead plates using the Preliminary Concept A 30

16. Plots of the system weight versus the ratio (F) of the required capacity/initial capacity using the Preliminary Concept A 31

17. Photograph of anodized aluminum mold used in the preparation of iR-free plate laboratory test structures 37

List of Illustrations (cont)

Figure No. Page No.

18. Schematic of anodized aluminum mold used in the preparation of iR-free plate laboratory test structures 38

19. Photograph of an as-cast, pure Pb, iR-free laboratory test structure having a grid structure 44 mil in depth 39

20. Performance of Barton VLY positive paste in iR-free laboratory test grids as a function of paste thickness 40

21. Performance of universal Grenox positive paste in iR-free laboratory test grids as a function of paste thickness 41

22. Cycling performance characteristics of Universal Grenox positive material pasted in an idealized iR-free, one-sided laboratory test Pb/Sb grid to a depth of 20 mil – Pb/Sb-1 45

23. Cycling performance characteristics of Universal Grenox positive material pasted in an idealized iR-free, one-sided laboratory test Pb/Sb grid to a depth of 20 mil – Pb/Sb-2 46

24. Cycling performance characteristics of Universal Grenox positive material pasted in an idealized iR-free, one-sided laboratory test Pb/Sb grid to a depth of 20 mil – Pb/Sb-3 47

25. Cycling performance characteristics of Universal Grenox positive material pasted in an idealized iR-free, one-sided laboratory test Pb grid to a depth of 20 mil and with H_3PO_4 added to the electrolyte – Pb H_3PO_4-7 48

26. Cycling performance characteristics of Universal Grenox positive material pasted in an idealized iR-free, one-sided laboratory test Pb grid to a depth of 20 mil and with H_3PO_4 added to the electrolyte – Pb H_3PO_4-8 49

27. Cycling performance characteristics of Universal Grenox positive material pasted in an idealized iR-free, one-sided laboratory test Pb grid to a depth of 20 mil and with H_3PO_4 added to the electrolyte – Pb H_3PO_4-9 50

28. Cycling performance characteristics of Universal Grenox positive material pasted in an idealized iR-free, one-sided laboratory test Pb grid to a depth of 20 mil and with no additions – Pb-5................. 51

29. Cycling performance characteristics of Universal Grenox positive material pasted in an idealized iR-free, one-sided laboratory test Pb grid to a depth of 20 mil and with no additions – Pb-6................ 52

30. Corrosion current of Pb, Pb/Ca and Pb/Sb grid samples held at 1.25 V (Hg/Hg_2SO_4) in 1.28 sp gr H_2SO_4 at 30°C 60

31. Corrosion currents of Pb, Pb/Ca and Pb/Sb grid samples held at 1.25 V (Hg/Hg_2SO_4) in 1.28 sp gr H_2SO_4 at 60°C 61

List of Illustrations (cont)

Figure No. Page No.

32. Corrosion currents of Pb, Pb/Ca and Pb/Sb grid samples held at 1.25 V (Hg/Hg_2SO_4) in 1.28 sp gr at 90 °C 62

33. Photograph of "bare" grids after corrosion in 1.28 sp gr H_2SO_4 at 1.25 V (Hg/Hg_2SO_4) at 90 °C after 60 days 63

34. Photograph of grids corroded in 1.28 sp gr H_2SO_4 (with an overcoating of PbO_2) at 90 °C for 60 days 66

35. First mold design for plastic plate manufacture 97

36. Typical photograph of an unpasted "quasi-bipolar" plate newly thermoformed 99

37. Schematic of an individual module 102

38a. Dimensions of aluminum mold for quasi-bipolar plate manufacture 103

38b. Photograph showing one face of the mold used to thermoform the final quasi-bipolar plate 104

39. Preparation sequence for quasi-bipolar plate manufacture 105

40. Section through the various components of the bipolar plate prior to thermoforming 109

41. Photograph of a quasi-bipolar plate prior to pasting with a surface treatment of Dynel fibers to enhance paste adhesion 111

42. Construction of a bipolar plastic plate with conduction at the top and bottom of the plate and at those points where the Pb strips and plastic grid intersect on the surface of the plate 113

43. Photographs of a pasted and cured quasi-bipolar plate and of a formed quasi-bipolar plate 118

44. Performance of quasi-bipolar plate no. 6 "repasted" under severe cycling conditions 120

45. Performance of quasi-bipolar plate no. 8 "repasted" under severe cycling conditions 121

46. Performance of quasi-bipolar plate no. 10 under severe cycling conditions 122

47. Performance of quasi-bipolar plate no. 11 under severe cycling conditions 123

48. Performance of quasi-bipolar plate no. 12 under severe cycling conditions 124

List of Illustrations (cont)

Figure No. Page No.

49. Performance of quasi-bipolar plate no. 22 under severe cycling conditions 125

50. Performance of quasi-bipolar plate no. 13 under severe cycling conditions 126

51. Performance of quasi-bipolar plate no. 23 under severe cycling conditions 127

52. Capacity retention (C/5) for the limiting electrode of quasi-bipolar test plates as a function of the number of prior high rate cycles undergone. The dotted curves show the equivalent data for three conventional positive plates tested under slightly less severe conditions 128

53. Photographs of the positive (a) and negative (b) electrodes of plate no. 8 after extended (1000) high rate/shallow discharge cycles 131

54. Photographs of the positive (a) and negative (b) electrodes of plate no. 12 after extended (1000) high rate/shallow discharge cycles 132

List of Tables

Table No. Page No.

I. Design Equations for the Preliminary Bipolar Concept A. 26

II. Design Values for the 150 mA/cm^2 Operating Point. 27

III. Design Analysis for Preliminary Concept A 28

IV. Comparison of the Weight Losses (g) of Pb and Pb Alloys in 1.28 sp g. H_2SO_4 at Various Temperatures After 60 Days Immersion. . 64

V. Comparison of Weight Changes (%) in Pb and Pb Alloy Grids With and Without an Overpasting of Positive Active Mass When Immersed in 1.28 sp gr H_2SO_4 at Constant Potential for 60 Days. 65

VI. A Comparison of the Relative Advantages (+) and Disadvantages (-) of Three Grid Materials in Lead Acid Batteries 67

VII. Weight Changes of Various Plastics in 1.28 sp gr H_2SO_4 at (30°C, 60°C and 90°C) 69

VIII. Chemical Resistance of Unfilled Epon 828 as a Function of Curing Agent in 25% Sulfuric Acid Over a 189-Day Immersion Period 73

IX. Chemical Resistance of EMI-24 Versus CL Cured Epon 823 Castings 74

X. Properties of Glass Fabrics 75

XI. Properties of Glass Fabrics 81

List of Tables (Continued)

Table No. Page No.

XII. Technical Data for Carbon and Graphite Cloth. 83

XIII. Pricing Schedules for Carbon and Graphite Fabrics 84

XIV. Properties of Prepreg 85

XV. Price Schedules for Thermoplastic Materials 86

XVI. Lexan Resin Bonding Data. 89

XVII. Heat Deflection Temperatures of EPON Systems. 92

XVIII. Construction Details on Bipolar Plates with Plastic Substrate and Pb Conductors 114

XIX. Basic Assumptions and Design Parameters of a Full-Size Battery Based on the Quasi-Bipolar Plate with Conduction Over the Top (Concept I) 139

XX. Summary of Weight Requirements for Each Module Based on the Quasi-Bipolar Plates (Concept I) and Operating Under the Preliminary Power Profile 139

XXI. Percentage Weight Distribution Comparison in Conventional and Quasi-Bipolar Batteries. 140

XXII. Summary of the Weight Requirements for Each Module Based on the Quasi-Bipolar Plates (Concept I) and Operating Under the Final Power Profile 142

XXIII. Preliminary Large Volume Material Costs and Individual Component Cost Estimates for a Module Conforming to the Final Power Profile and Incorporating the Quasi-Bipolar Plates Outlined in Concept I. 145

SUMMARY OF WORK

The following summary incorporates a review of the many aspects of battery development examined in the program, and brief conclusions are drawn on each, irrespective of whether or not the information obtained was used in the final design concept. This summary follows the sectional outline of the report itself.

SUMMARY OF SECTION I. INTRODUCTION

The preliminary power profile specified by EPA for development of design concepts and plate testing is given. The final power profile for ultimate design and performance evaluations is included. It is noted that fresh thin plate SLI batteries already have the necessary discharge power density but that the main problem is the effect of cycling and standby life on subsequent performance. Little data are available on this, especially under the specific cycling regime supplied.

The concept of a bipolar plate was first introduced and the following advantages and disadvantages were noted.

A. Advantages

1. The active material can be distributed over a greater area without incurring too great a weight penalty.

2. The active material is discharged evenly over the entire plate.

3. External intercell connections are not necessary.

4. Intercell resistance losses are minimized.

B. Disadvantages

1. Since all the cells of a battery module operate in series, greater demands are made on reliability and reproducible behavior from each electrode.

2. Intercell electrolyte leakage could cause discharge of the plate by an electrochemical mechanism.

3. Corrosion of the substrate could produce leakage and plate buckling.

SUMMARY OF SECTION II. INVESTIGATION OF THE STATE OF THE ART

Typical plates from a thin plate conventional SLI battery were examined under a specific cycling regime designed to simulate the most severe conditions specified by EPA in the preliminary power profile. The effect of the cycling was investigated by C/5 capacity evaluations after every ~ 100 high rate cycles. The following results were recorded.

1. Performance is limited by the positive plates which last only a maximum of 350 complete high rate cycles. The C/5 capacity retained after 300 complete cycles on each of the three positive test plates was 57%, 23%, and 3.5%.

2. Positive plate expansion and consequent poor paste adhesion, particularly close to the current takeoff terminal, apparently limit the performance of the positive plates.

3. Fresh commercial negative plates stand up very well to such cycling and a decrease of only ~ 30% of total capacity (capacity after full charge) is noted after 500 cycles.

The following more general conclusions were also evident.

4. The positive plates in fresh conventional thin plate SLI batteries are marginal in obtaining the high discharge power densities required for hybrid vehicle purposes. They are less than satisfactory in providing adequate power after extended cycling life.

5. Particularly on cycling, there is a serious problem with conventional positive, thin SLI battery plates which is caused by longitudinal resistance losses along and down the grid. This results in uneven utilization of active mass and, therefore, high local depth of discharge even when the overall depth of discharge is shallow. Paste shedding results particularly close to the current takeoff terminal. Designs which overcome this problem are desirable.

SUMMARY OF SECTION III. PRELIMINARY DESIGN STUDIES

This task was aimed at developing preliminary design concepts suitable for use in a high power density/long life battery. Provision was made in the designs for the reduction of electronic iR gradients along each plate and for decreasing active mass thickness. Further important considerations were those of improving plate reliability and minimizing corrosion, plate buckling, and intercell electrolyte leakage problems, all of which can adversely affect performance. The basic design concepts considered were:

1. Bipolar plate with a nonconductive plastic substrate as support for the active material and with metal strips as electronic contact. The strips, which are laid vertically down the plate and in a parallel array along the plate, on both sides, are in contact with the adjacent strips on the opposite side only over the top of the plate. The contact points are all encased in a plastic border.

2. Same as (1) but with contact at the top and bottom of each plate, the latter points also being encased in a plastic border.

3. Same as (2) but with contact also at localized points down and across the plate surface via holes through the plate. The latter points are also covered with plastic.

Two additional bipolar designs were considered:

4. A bipolar plate with plastic substrate as active material support. The substrate, however, is also electronically conductive. Conductivity is achieved either by using a conducting filler, e.g., graphite powder, or by sandwiching a layer of carbon or graphite cloth between plastic sheets. In both cases, however, it is not necessary for the strips to make physical contact over, under, or through the plate. The conduction path is via the Pb strips, to the graphite and then through to the Pb strips on the opposite side of the plate. The plastic isolates the graphite conductor (which also reinforces the structure) from the H_2SO_4 and so prevents electrolyte leakage through the plate.

5. Bipolar plate with conductive, corrosion resistant, light weight/high strength metal backing.

The approach of developing a high power density, long life lead acid battery system based on a preliminary bipolar concept was illustrated using a modular approach to the problem. The effects of various design variables on system weight were demonstrated and the most crucial design values were found to be the operating current density and the electrochemical yield of the paste (Ahr/gm of active paste).

SUMMARY OF SECTION IV. STUDY OF ELECTROCHEMICAL PROBLEM AREAS RELEVANT TO THE DESIGN OF A HIGH POWER DENSITY BATTERY

There are several problem areas associated with the use of lead-acid batteries for high power density batteries. The most important of these problem areas were examined in the course of this program, and the following major conclusions were drawn.

1. To optimize a lead acid battery for use in hybrid electric vehicles, a large number of thin plates should be used. The operating current density is thus reduced. Paste utilization is substantially increased in thin plates compared to that in conventional plates operating at the same current density.

2. Particularly on cycling, there is a serious problem with conventional plates operating at high power densities which is caused by longitudinal resistance losses along and down the grid. This results in uneven utilization of active mass and, therefore, high local depth of discharge even when the overall depth of discharge is shallow. Paste shedding results. When these resistance losses are minimized there is a marked improvement in paste performance at the same, high operating power densities.

3. To maintain cycle life in a battery which contains no Sb in the grid, paste or electrolyte (for example, when pure Pb is used as grid material), small additions of H_3PO_4 to the electrolyte are very effective.

SUMMARY OF SECTION V. CORROSION OF SUBSTRATE MATERIALS

The literature was reviewed and a wide range of plastics and metals were studied in 1.28 sp gr. H_2SO_4 at up to 90 °C. The following conclusions were drawn.

A. Metals

1. Metals such as Ti, TiN, Al and Mg either with or without conductive coatings, Pb overplating, etc. are not suitable for use in Pb acid batteries without additional development work. The materials all corrode severely or form oxides which act as a dielectric.

2. Pb or Pb alloys cannot be used in sheet form as active mass support and current conductor in a practical bipolar high power density battery for hybrid vehicles. To resist corrosion and to be mechanically capable of supporting the active mass, the sheets have to be of impractical thickness with particular regard to battery weight limitations.

3. The use of Pb or its alloys as current conductors in conjunction with a plastic substrate material support is not precluded from a corrosion or expansion aspect. Pure Pb is the material of choice by virtue of its corrosion resistance in acid compared to Pb/4.5% Sb and Pb/0.08% Ca alloys. It also has less expansion problems than the Pb/0.8% Ca alloy. It is estimated that a covering of active mass will reduce Pb corrosion in H_2SO_4 by at least 20%.

B. Plastics

1. The majority of thermoplastics, for example, Lexan, polystyrene, polysulfone, PVC, polypropylene and Noryl are stable in 1.28 sp gr. H_2SO_4 at ambient temperature for extended periods. From this aspect they are suitable for use as substrate material.

2. Reinforced laminates with thermosetting resins are subject to attack by H_2SO_4 at the resin to glass reinforcement bond. The base resins, and particularly epoxy and phenolic resins, if suitably selected and carefully cured, can be quite resistant to acid attack.

3. The major outlet for thermosets in Pb acid batteries is not as a structural paste support material, but as an adhesive or sealant in selected areas of the plate or battery.

4. No data have yet been generated on the corrosion resistance of reinforced thermoplastics in H_2SO_4. Literature information suggests that this is generally as good as that of the unreinforced plastics.

SUMMARY OF SECTION VI. DEVELOPMENT AND MECHANICAL TESTING OF STRUCTURES

The additional aspects of plate development not already considered in previous sections were examined here. Due to corrosion problems, structures involving metals other than Pb or Pb alloys were not considered further. Emphasis was placed on those alternative designs outlined in Section III of this report. The selection of materials and techniques for further study was closely controlled by the results of corrosion and other parameters influencing design which are described in earlier sections. Literature surveys of material performance capabilities were carried out and, where necessary, these were backed up by laboratory tests. The following specific factors were considered.

1. Strength
2. Ease of fabrication
3. Cost and availability
4. Bonding of the plastic to Pb or Pb alloys
5. Adhesion of active mass to the plastic
6. Oxidation of the plastic by PbO_2
7. Temperature and corrosion resistance
8. Ease of handling (e.g., brittleness) and sealing (plastic to plastic) in a battery case.

Only plastic materials were investigated since it was clear by this stage that the maximum chance of success lay in the use of plastic substrate materials as active mass support in the grid.

The following specific conclusions were drawn as a result of this study.

1. Both thermoplastics and thermosets have adequate mechanical strength to support the active mass in practical design configurations. With thermosets a reinforcement medium is required for this purpose, especially for substrates of ≤ 20 mil thickness. Engineering thermoplastics may be suitable as support material in the unreinforced form, especially when strengthened by the incorporation of a thicker plastic rim surrounding the main substrate area. For substrates of < 20 mil thickness, the thermoplastics also require reinforcement.

2. A wide range of reinforcement techniques is available using glass, carbon and graphite cloths, or chopped fibers as reinforcing media. Suitable surface treatments are applied to these materials to enhance their compatibility with the plastic of choice.

3. Whereas thermosets are most usually reinforced with cloth material, thermoplastics generally use chopped fibers. Hot press techniques are used to form structural laminates with thermosets. Reinforced thermoplastics are formed to shape by injection molding methods. The latter technique is not suited to the thin plate structures desired here because of inadequate mold filling.

4. A thermoforming technique is suggested when fabricating plates from thermoplastics. The latter may be reinforced if desired by hot pressing a suitable cloth between thin sheets of the plastic in question.

5. Mainly because of H_2SO_4 corrosion stability, thermoplastics are preferred to thermosets as substrate material.

6. Thermosets form superior bonds with Pb than do thermoplastics. The former may then be used to provide seals in plates at localized points if desired. Careful choice of the resin and its curing technique and curing agent are, however, necessary.

7. Because carbon and graphite can be used as reinforcement, a means of obtaining conductive plastic substrates is offered if concurrent problem areas can be solved.

8. Lexan thermoplastic is an ideal starting material for substrate fabrication. It is relatively low cost, is thermoformable, stable in H_2SO_4, light weight/medium strength, is easy to handle, and is resistant to oxidation by PbO_2.

9. There are techniques available to enhance sealing of thermoplastics to Pb. Also, paste adhesion to such substrates may be enhanced by suitable surface treatments.

10. No temperature stability problems are anticipated with the plastics.

A plate, defined here as a "quasi-bipolar" plate, was constructed based on the above and additional information obtained in previous sections. The most important aspects of this plate are summarized below.

1. It is approximately 1/6 full size and may be scaled up to full size directly. Final plate dimensions (pasting area) are 8 in. × 4 in. The 4-in. dimension is in the vertical direction. Relatively long and shallow plates result. The reason for this can be seen from the current conduction paths which in this plate are over the top of the plate only. By making the plate relatively shallow, resistance losses down the plate are minimized.

2. The materials of construction are Lexan as substrate and pure Pb as current conductors. Lexan is a light weight/high strength plastic which permits relatively easy handling of the plate with sufficient flexural strength capabilities. Pure Pb has minimal corrosion problems and also is quite good from an expansion viewpoint.

3. The current conductors of Pb have been held at 20-mil thickness.

4. The conductors are separated by 0.15-in. intervals along the plate. This separation permits easy charge and discharge of active mass without introducing excessive resistive losses. The separation is equivalent to that of horizontal grid members in conventional lead acid batteries, but since each lead strip carries only the current generated around it, the additional leads used in conventional plates to collect the current at the terminal are not necessary here.

5. A plastic rim is provided to facilitate sealing of each plate within a case (Lexan). Lexan is an extremely easy material to handle from this aspect.

6. Paste thickness is held at 20 mil per positive and negative electrode with a plastic substrate thickness of 20 mil also. Pasting thickness is governed by the plastic border round the circumference of the plate (as is the case with the outside rim in conventional plates). The rim also adds rigidity to the structure.

7. Paste adhesion to the plastic substrate is enhanced using glass mats or dynel fibers attached to the substrate surface in a prior step. Very good paste adhesion has been observed so far.

8. Current is removed from each electrode over the top of each plate only, using Pb conductors looped over the base plate prior to layup. The points where each conducting strip make contact with its equivalent strip on the opposite face of the substrate are not directly immersed in electrolyte. The problem of intercell leakage is thus minimized significantly.

9. The Pb conductors are held mechanically to the plastic substrate by a plastic overlying grid only at those points where the plastic and the Pb intersect down and across the plate. During cycling, this setup permits expansion of the Pb down the plate without introduction of any stresses resulting in plate buckling and poor paste adhesion.

10. As discussed, production of the entire plate is relatively easy. It appears that it can be carried out on a large scale basis.

11. There is scope in the design for both thinner base plates and also thinner pastes. No substantial changes are required. The plastic base plate can easily be reinforced with glass cloth to provide sufficient flexural rigidity in < 20 mil thicknesses. Paste thicknesses < 20 mil also give superior paste utilization and reduce weight requirements.

The construction of designs (1) - (5), Section III, are outlined in this section together with the production of a basic module. Designs (1) - (3) could be made relatively easily whereas there were problems associated with the manufacture or operation of designs (4) and (5) which were insurmountable in the time period of this contract.

SUMMARY OF SECTION VII. LIFE TESTING OF NEW DESIGN PLATES

The construction of test cells and steps leading up to the high rate cycle testing of the quasi-bipolar plates is described. H_3PO_4 was added to all test cells (Sb-free) prior to cycling. The cycling regime was again at currents corresponding to the 55 KW and up to the 40 KW rates on discharge and charge respectively for a full scale battery system built with the plates. As before, the capacity (C/5) retained by the test plates was periodically measured (~ every 100 cycles). The performance of five plates tested (design (1), Section III) was extremely good and four of these withstood 1000 high rate cycles before signs of failure were observed. With the fifth plate, failure was observed after 730 complete cycles. Comparatively, with the conventional positive plates tested in a similar cycling regime, only 350 complete cycles at best could be obtained. After 300 complete cycles, the capacity retained (C/5) was 57%, 23%, and 3.5% for the three positive conventional plates. Even after the 1000 cycles, the (C/5) capacity retained by the four "quasi-bipolar" test plates was 47%, 61%, 51%, and 48%.

A plate made according to design (3) , Section III, stood up to 1158 complete high rate cycles without showing any signs of failure, and its capacity retention (C/5) at the latter point was 74%.

SUMMARY OF SECTION VIII. BATTERY DESIGN AND PRELIMINARY COST ANALYSIS and

SUMMARY OF SECTION IX. SUMMARY OF ACHIEVEMENTS, EVALUATION OF THE MAIN AREAS REQUIRING FURTHER DEVELOPMENT AND PRELIMINARY PROPOSED WORK PLAN

The design of a module and complete battery system conforming first to the preliminary power profile and then to the final power profile specified by EPA is discussed. The choice of design parameters is rationalized. The preliminary cost estimate for the quasi-bipolar battery is given and an estimate of the energy density of a typical bipolar system at both high (55 KW) and moderate (C/5 rate) rates is given and compared with that of a conventional thin plate SLI battery operating at the same rates. Problem areas requiring further development are outlined and a proposed plan of work is included. The following conclusions were drawn.

1. A new quasi-bipolar plate has been developed in which the active material support is plastic, and conduction through the plate is achieved by parallel Pb strips laid vertically over the top of each plate and along it. The conduction paths through the support are so arranged as to be not immersed in electrolyte during normal cell operation. The possibility of short circuits via intercell electrolyte leakage is thus minimized.

2. The Pb conductors are held at fixed points to the plastic substrate via a plastic grid with horizontal cross-members. Expansion is thus permitted in a vertical direction without introduction of excessive strains resulting in plate buckling.

3. The plate uses dynel fiber or glass mass backing to enhance paste adhesion. Pure Pb strips act as conductors and no Sb is used in the plate components. Cycling life is maintained using H_3PO_4 additions to the electrolyte.

4. On operation at high rates of charge and discharge (150 mA/cm^2), the bipolar plates show very good performance characteristics. They last typically for 1000 high rate/shallow discharge cycles and capacity retention at the C/5 rating is also extremely good. Comparatively, fresh commercial battery positive plates degrade excessively after ≤ 350 cycles and capacity retention is relatively poor.

5. In the preliminary power profile the maximum discharge rate specified is 55 KW and the minimum desired power density is 100 W/lb. In a full size system using the above quasi-bipolar plates, 14 parallel modules may be used each with 100 bipolar plates in series and weighing 40.9 lb/module. The required operating current density per plate is only 110 mA/cm^2. A modular system constructed from the above plates operating to the limits of their tested cycling capabilities, i.e., at 150 mA/cm^2, incorporates 10 parallel modules and exhibits a power density of 136 W/lb.

6. To conform to the specifications given by EPA in their final power profile (Fig. 1), the only change required in the above modular system is to incorporate 133 quasi-bipolar plates in series per module instead of 100 plates/module. Module weight is recalculated at 54.5 lb. At the 70.5 KW average maximum discharge rate and the minimum required power density of 128 W/lb, the operating current density per plate is 143 mA/cm^2 (10 parallel modules). At the preferred operating point of 156.6 W/lb the operating current density is close to 180 mA/cm^2 while to achieve the maximum discharge rate of 92.5 KW for 10 sec (205.5 W/lb) the rate must be increased to 234 mA/cm^2. In the latter two cases only 8 parallel modules are used. Also, though cycling behavior is not demonstrated in the latter cases, the plates with 20 mil thickness of paste per electrode do contain more than sufficient excess of active mass for such deeper discharge cycles.

7. In the preferred mode, it is anticipated that the best module design for operation under the final power profile would again be one incorporating 133 quasi-bipolar plates in series but on each plate the paste thickness would be reduced by at least 25% to 15 mil per electrode. More than sufficient capacity is still available in the plates to meet the most extensive capacity demands (980 Whr on two consecutive cycles for 25 sec at an average 70.5 KW rate). In this manner the operating current density can be reduced to < 190 mA/cm^2 even at a power density of 205.5 W/lb.

8. A battery built from 11 parallel modules, each with 100 quasi-bipolar plates in series and with incorporation of sufficient acid, can operate at ~ 130 mA/cm^2 and its energy density is 9.7 Whr/lb at this rate (100 W/lb). Under the same circumstances, a battery constructed from conventional plates must operate at >200 mA/cm^2 and its energy density here is 5.9 Whr/lb. Such a battery does not perform adequately under extended high rate cycling.

9. At medium discharge rates (C/5-rate), the respective energy densities for the bipolar and conventional systems are 20 Whr/lb and 17.3 Whr/lb respectively.

10. A modification of the quasi-bipolar plate in which multiple Pb conduction paths are made across and down the plate has also been constructed and an initial plate exhibits superior performance on extended cycling (compared to the initial quasi-bipolar plate above).

The most important areas requiring further study to develop the quasi-bipolar plate and battery discussed above are as follows:

1. Extend cycling data on a large number of quasi-bipolar plates under a range of conditions and at higher rates as specified in the more recent EPA requirements. This will establish plate reliability on a more realistic basis.

2. Construct full scale plates to demonstrate structural stability and feasibility of large scale fabrication techniques.

3. Extend evaluations of long term plate corrosion resistance, particularly of the thin cross section Pb conductors but also of the plastic substrate. This will establish a realistic value for the minimum cross-section per conductor which is compatible with cell performance, weight, and reliability.

4. Establish the exact volume of electrolyte and electrode gap separation necessary to permit successful operation of the plates under high rate/shallow discharge cycling. Here the dimensions of separator and retainer are crucial regarding their effect on interelectrode volume and also gas bubble retention between electrodes.

5. Construct prototype modules to develop technology in this area and isolate any plate sealing problems.

6. Complete a more thorough cost analysis particularly with relation to manufacturing and assembly costs.

7. Identify alternate applications for such a system.

8. Investigate the behavior of the bipolar plates under two consecutive high rate power pulses for 25 sec within a 60 sec interval and followed by high rate recharge.*

---

*Such a test has been performed successfully for 6 successive cycles on one of our plates (quasi-bipolar plate no. 6 in the report) which had already been tested for >700 high rate cycles.

I. INTRODUCTION

It has long been recognized that the internal combustion engine is a serious source of air pollution. An attractive alternative to the pure combustion engine vehicle is the hybrid car in which a heat engine produces more nearly a constant power output. A battery, charged by a generator when the requirements of traction at the wheels are low, delivers the pulses for acceleration. This concept, either in the series arrangement,[1] in which all the mechanical energy of the heat engine goes through the alternator, or in the parallel arrangement,[2] in which only a portion of the energy goes through the alternator, offers the advantage of having the heat engine (for instance, an internal combustion engine) working under conditions of minimum pollution. By bypassing the crucial problem of the all-electric car, i.e., the lack of batteries with sufficient energy density, a viable vehicle might be produced with current technology.

The battery required for this vehicle has to be capable of high power pulses of relative short duration. In addition, economic considerations dictate that the battery tolerate a very high number of cycles (although the depth of discharge of these cycles is low). The following operating characteristics of such a battery which were drawn up as a result of preliminary information[3] regarding the operation of a hybrid automobile .

Preliminary Power Profile

1. 55-KW discharge rate sustained for 25 sec and performed for two such 25-sec periods within a 60-sec interval.

2. 30-KW recharge rate sustained for 90 sec directly following the two above discharges of item 1.

Voltage:

200 to 220 V open circuit; 150 minimum working voltage.

Life:

The battery should be capable of operating at the above power rates and durations after operating for 5 years and 200,000 cycles which include the following number and types.

Number of Cycles	Discharge Rate, KW	Charge Rate, KW	Energy Transferred from the Battery per cycle, Whr
500	55	30	380
3000	55	30	130
3000	55	30	80
Balance of 200,000	10	5	30

Weight:

550 lb maximum

Cost:

The battery should be capable of a mass production cost of less than $550.

Operation:

Suitable for safe use in a family automobile without undue care and maintenance.

In the performance of the present contract, the preliminary battery was designed and the plates tested in accordance with the above specifications. Calculations given in Section VIII for final battery performance using the chosen design plate are also based on these initial power levels. The effects on battery weight, performance and operating current density incurred by the more advanced specifications recently received from EPA, and shown below, are discussed also in Section VIII of this report.

The more advanced performance schedule is as follows:

Final Power Profile

1. The power profile of Fig. 1 with peak power of 92.5 KW, and performed for two such 25-sec periods within a 60 sec interval.

2. A minimum recharge rate of 39 KW sustained for 90 sec directly following the two above discharges.

Voltage:

Minimum working voltage of 200 V. Minimum cell voltage of 1.5 V.

Life:

The battery should be capable of operating at the above power rates and durations after operating for 5 years and 200,000 cycles which include the following number and types:

Number of Cycles	Discharge Rate, KW	Charge Rate, KW	Energy Transferred from the Battery per cycle, Whr
500	70.5	39	490
3000	55	30	130
3000	55	30	80
Balance of 200,000	10	5	30

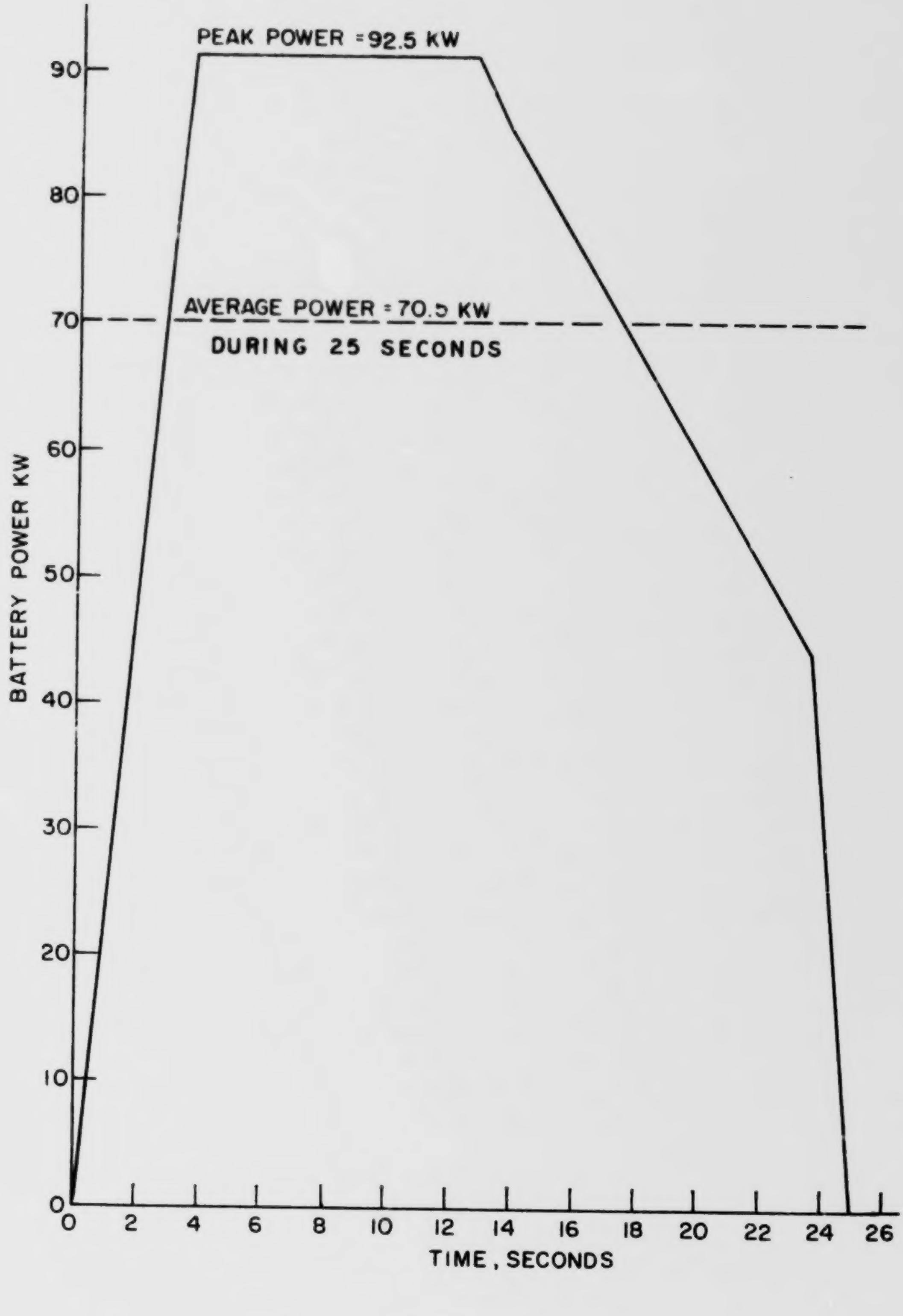

Fig. 1. Battery maximum power design curve for 6 passenger hybrid car

Weight:

550-lb maximum. (Goal 450-lb maximum.)

Cost:

The battery should be capable of mass production cost of less than $550.

Operation:

Suitable for use in a family automobile without undue care and maintenance.

Clearly, the new battery is very different in requirements from batteries being developed for the all-electric cars. In fact, the power demands of this battery are more similar to those encountered by the SLI battery or by the high power, extra thin plate airplane batteries. In particular, the cycling conditions are very specific and very extreme. Designs guided by a careful tradeoff between power density and life are therefore necessary to meet the specific goals.

Preliminary experiments at our laboratories confirmed that new, off-the-shelf SLI batteries already have the necessary discharge power density. Thus, a conventional SLI battery with 0.080-in. positive plates (15 Ahr at the 20-hr rate) gave a discharge of 150 sec at the 10 C rate. Lead-acid batteries used for airplane starting have plates about 0.050 in. thick and show still higher rates of discharge than SLI batteries.

The problem of obtaining the required rate of discharge with fresh batteries did not seem to be a serious one. Aside from the problems related to charge acceptance at the pre-established power densities (which were examined during the performance of the contract), we considered that the main problem was the effect of cycling and standby life on the subsequent performance. Since the cycling regime is a very specific one and there was very little information at the present time on the magnitude of the problem, a thorough study was indicated. Remedial action to achieve a high power density battery with specified long useful life was directed to developing stable battery components and/or obtaining batteries with a reserve of power and energy density which would guarantee the required performance even after part of the power and energy density had degraded as a consequence of the specified cycling and standby waiting periods.

The development of multicycle, long life, high rate lead-acid batteries is a new area of battery technology. The two basic approaches available were to modify existing SLI lead-acid cells to improve and stabilize their power density or to develop a novel lead-acid battery system, for example, a bipolar lead-acid battery. Our major emphasis in this work has been directed at the latter approach since we felt that the advantages of using such a design (over conventional monopolar structures) were such that a more practical and improved power density system would result.

The bipolar battery derives its name from its electrode configuration. The positive electrode of one cell and the negative electrode of the next cell are on two sides of an electrically conductive but electrolyte impermeable substrate. All the current produced by the battery passes across this substrate. Since external intercell connections are not necessary, a bipolar battery can exhibit both high specific power and energy. The use of the bipolar configuration in high rate rechargeable batteries is not a new concept, and the specific advantages of its use are as follows:

1. The active material can be distributed over a greater area without incurring too great a weight penalty.
2. The active material is discharged evenly over the entire plate.
3. External intercell connections are not necessary.
4. Intercell resistance losses are minimized.

The effects of these accrued advantages on battery weight, performance and life were examined in detail in the contract period.

On the other hand, there are the following disadvantages with bipolar designs:

1. Since all the cells of a battery module operate in series, greater demands are made on reliability and reproducible behavior from each electrode.
2. Intercell electrolyte leakage could cause discharge of the plate by an electrochemical mechanism.
3. Corrosion of the substrate could produce leakage and plate buckling.

These problem areas were also the subject of close study in this contract. Experiments were all aimed at generating information on the extent of the problems. Materials and design concepts were investigated with the utlimate aim of overcoming or minimizing the problems.

As a result of this study, a plate was developed which has many of the advantages of the bipolar battery plate without some of its disadvantages. This plate which we call a "quasi-bipolar plate" is described later.

The report is presented in accordance with a schedule of work followed in this program. Comparative data were also recorded on conventional plates from commercial batteries tested under the extreme cycling conditions specified in the preliminary schedule. Several preliminary design concepts were chosen based on a bipolar type plate and a detailed analysis of the effects of variations of the design parameters then carried out. This not only established optimum design figures but also indicated those areas in which subsequent research would provide the most significant improvement in performance. In all of this work, the need for a long life battery was also borne in mind. Provision for the extension of small scale plate and battery fabrication techniques to full scale commercial production was also of prime concern. In later sections of the report fabrication techniques of the final design of choice (and specific reasons for this choice) are given together with extended cycling data on the new plates under the same conditions of test as for the commercial plates. Comparisons between the two are shown and the advantages of the new plates are noted.

II. TASK I: INVESTIGATION OF THE STATE OF THE ART

There were no data available to date on the performance of conventional high power density batteries operated under the conditions specified in this contract, that is, high rate charge discharge cycles with a shallow depth of discharge. Results shown below record the behavior of plates from such batteries under these conditions. Comparative performance evaluations on novel design plates are given later in this report.

A. Cycle Life Testing, Equipment and Procedure

In order to perform cycle life testing within the time frame of this contract, it was necessary to develop an accelerated test. This test, although inadequate to give an absolute value regarding the battery life, has to serve to compare cycling life of novel designs of plates, cells and batteries with those which are in the state-of-the-art under conditions which are relevant to the final use. For this purpose, we chose to use continuous cycling under the most severe charge and discharge conditions specified for the battery; (i.e., currents corresponding to a discharge rate of 55 KW and a charge rate of 30 KW, and times to allow an energy transfer of 380 Whr).[3]

We constructed a cycle tester with ten separated test stations. The system operates by galvanostatically charging and discharging the test batteries which are placed in series. The power current is regulated by a Sorensen power supply with a nominal output of 40 V and 60 A (the actual maximum current is 66 A). Timers are provided to adjust the duration of charge and discharge from 0 to 120 sec. The unit will also permit the application of two consecutive discharges (e.g., two 25-sec discharges within a 60-sec interval, as required for final battery test) followed by a charge. In addition, the timers can be bypassed to allow manual operation.

Voltage cutoffs limits during charge and discharge can be set automatically at each test station within the limits of 0 to 10 V. When an individual cell reaches its preset cutoff limit, it is automatically removed from the circuit, to be reconnected again on completion of the individual cycle in which voltage cutoff occurred.

Initially it was observed that every time a cell was removed from the circuit during charge, a large current pulse of up to ~200 A for ~20 msec passed through the remainder of the cells. This was due to the discharge of the capacitors on the power supply (used to reduce AC ripple). We have overcome this problem by using backup cells. On operation, when the

Preceding page blank

test cell reaches its cutoff point, the backup cell is first connected in parallel and the "failed cell" then removed from circuit. The entire switching operation is completed in ≤ 0.5 sec.

On discharge, the voltage of the output must rise when a test cell fails. Therefore, no transient current surge is observed when a test cell is removed after reaching the cutoff limit on discharge.

A typical test procedure used to test individual battery plates is as follows:

1. Plate is completely discharged at C/5 rate to determine capacity.

2. Plate is completely charged at C/5 rate.

3. Plate is discharged 20% of capacity at C/5 rate.

4. Plate is cycled for 100 cycles, starting with the discharge portion of cycle, under the following conditions.

    a. Charge and discharge currents are those necessary to obtain the 55 KW and 30 KW rates respectively from a battery system built with the test plate.

    b. Durations of discharge and charge are 25 and 61-67 sec, respectively, as long as the cutoff potentials are not exceeded. (These times are calculated using the values of discharge and charge rate, of energy transferred during discharge and of cell potential given in the specifications.)

    c. The cutoff potentials are 2.75-3.0 V for charge and 1.5 V for discharge. On reaching this cutoff voltage, the particular cell is bypassed, but connected again in the next cycle.

5. At the end of the 100th cycle, plate is charged completely at C/5 rate.

6. Plate is completely discharged at C/5 rate to determine capacity. (It is realized that this step adds to the severity of the test.)

7. Repeat from step 2.

The procedure was repeated for 500 cycles or until cell failure. We considered that a cell had failed when it could not be discharged for 25 sec at a voltage higher than 1.5 versus an overdesigned counterelectrode. In addition, the capacity determination after groups of 100 cycles gives a good indication of the effect of cycling on the plate.

For the testing of plates, overdesigned counterelectrodes (Pb or PbO_2, depending on whether we are testing a positive or a negative plate) were used, and both the cell voltage and the potential of the test plate (versus $Hg/HgSO_4$ reference electrode) were recorded.

We chose a test temperature of 30°C for all our cycle testing. This permitted a comparison of individual cell performance under well defined conditions though not necessarily at the final operating temperatures. Our cells contained a relatively large volume of electrolyte (~1400 ml) and during testing we observed no more than a 2°C rise in temperature. Cooling was achieved using glass U-tubes in each individual cell through which thermostatted water was circulated. In practice, temperatures in excess of 40°C can be attained during our test schedule if no cooling is employed. As discussed, however, our cycling procedure is rather severe and we do not anticipate such temperature fluctuations in actual battery operation. In preliminary experiments, we observed that the faster deterioration of the plates expected at high temperatures was more than compensated for by the higher performance of the aged plates at this higher temperature. Therefore, under the selected test cycle, the cycling life was better at 40°C than at 30°C.* Acid specific gravity has been fixed at 1.28, which is typical for high power density batteries.[4]

B. Performance Evaluations of Commercial SLI Plates

Plates were tested from a commercial thin plate, SLI battery having the following specifications:

Number of plates = 90
Plates per cell = 7 positives and 8 negatives
Dimension per plate, in. = 5.2 by 6.1 (including surrounding grid structure)
Thickness of positive plate, in. = 0.060
Thickness of negative plate, in. = 0.050
Weight of paste in positive, g = 126
Weight of grid in positive, g = 70
Weight of paste in negative, g = 100
Weight of grid in negative, g = 70
Capacity of battery at C/20, Ahr = 96
Shipping weight, lb (with 1.28 sp gr acid) = 55
Grid alloy = Pb/Sb

---

*In separate experiments, we examined active and passive component corrosion problems under practical conditions at elevated temperatures (up to 90°C).

In order to conform to the specified weight restrictions (550-lb maximum), we could use ten such batteries (i.e., 420 positives and 480 negative plates). To meet voltage requirements, we would have to rearrange the plates to form 100 cells in series, each cell containing four positives and five negatives in parallel. Effective pasted area of each commercial plate is 377 cm^2 (both sides). Assuming a discharge voltage of 180 V, the maximum current called for at 55 KW is 305 A. The current required per plate is thus 76.25 A or 202 mA/cm^2. On charge at 30 KW and 240 V, the relevant current is 31.25 A (83 mA/cm^2). Note that the calculation is an approximate one, taking no account of precise weight requirements for electrolyte, cases, intercell connections etc., in such a rearranged configuration. It does permit us to evaluate commercial plate performance under realistic conditions.

In practice, the plates were discharged at 66 A (175 mA/cm^2) and charged at 27 A (72 mA/cm^2), respectively, corresponding to the 47.5 KW and 25.9 KW ratings. The use of these slightly lower rates (compared to 55 KW and 30 KW) was necessitated by the limits of the discharge unit which was designed for testing of plates requiring much less current to achieve the battery specification. If anything, longer plate life on cycling would be anticipated than at the 55 KW and 30 KW rates because the cycle is less severe. Discharge time was 25 sec and cutoff voltage 1.5 V/cell. Charge time was 61 sec and cutoff voltage 2.75 V/cell.

Three commercial positive test plates were evaluated and we show the results of cycling in Figs. 2-4. Fig. 2 shows the initial and final cell voltage on the best of these plates during charge and discharge, and the percentage of time for which the plate accepted charge and discharge (i.e., a percentage of 61 sec and 25 sec, respectively). The capacity retained by the plate after each group of cycles is also shown. In this mode of cycling, the plates performed well until a maximum of ≤ 350 complete cycles when each positive plate either had already failed or had begun to fail (Fig. 3). Failure was preceded by an increase in the charging voltage (with early cutoff) and a rapid decrease in voltage on discharge below 1.5 V (with early cutoff also). The capacity retained at the C/5 rate is shown in the figure and was 57% after 300 complete cycles and 34% after 400 cycles, within which period failure on discharge was observed. With the remaining two positive plates, failure occurred after 300 cycles (23% capacity retained) and after 200 cycles (66% capacity retained), respectively. For the latter plate, only 3.5% capacity was retained after 300 complete cycles.

The general trends in the data for all these plates were toward an increase in charging voltage (with consequent greater gas evolution) and, on discharge, a decrease in cell voltage with increase in number of cycles. The cells which failed first of all exhibited the highest voltages on charge and lowest on discharge and showed the greatest reduction in capacity after a given number of cycles. We have examined each of these positive plates visually after the above cycling regime for changes in appearance. Typical photographs are shown in Figs. 5-7 for the plates before and after testing. Fig. 5 shows a typical positive plate prior to testing. After testing, we found excessive buckling of the grids in each plate and in one case the grid itself was actually broken along approximately two-thirds of its length

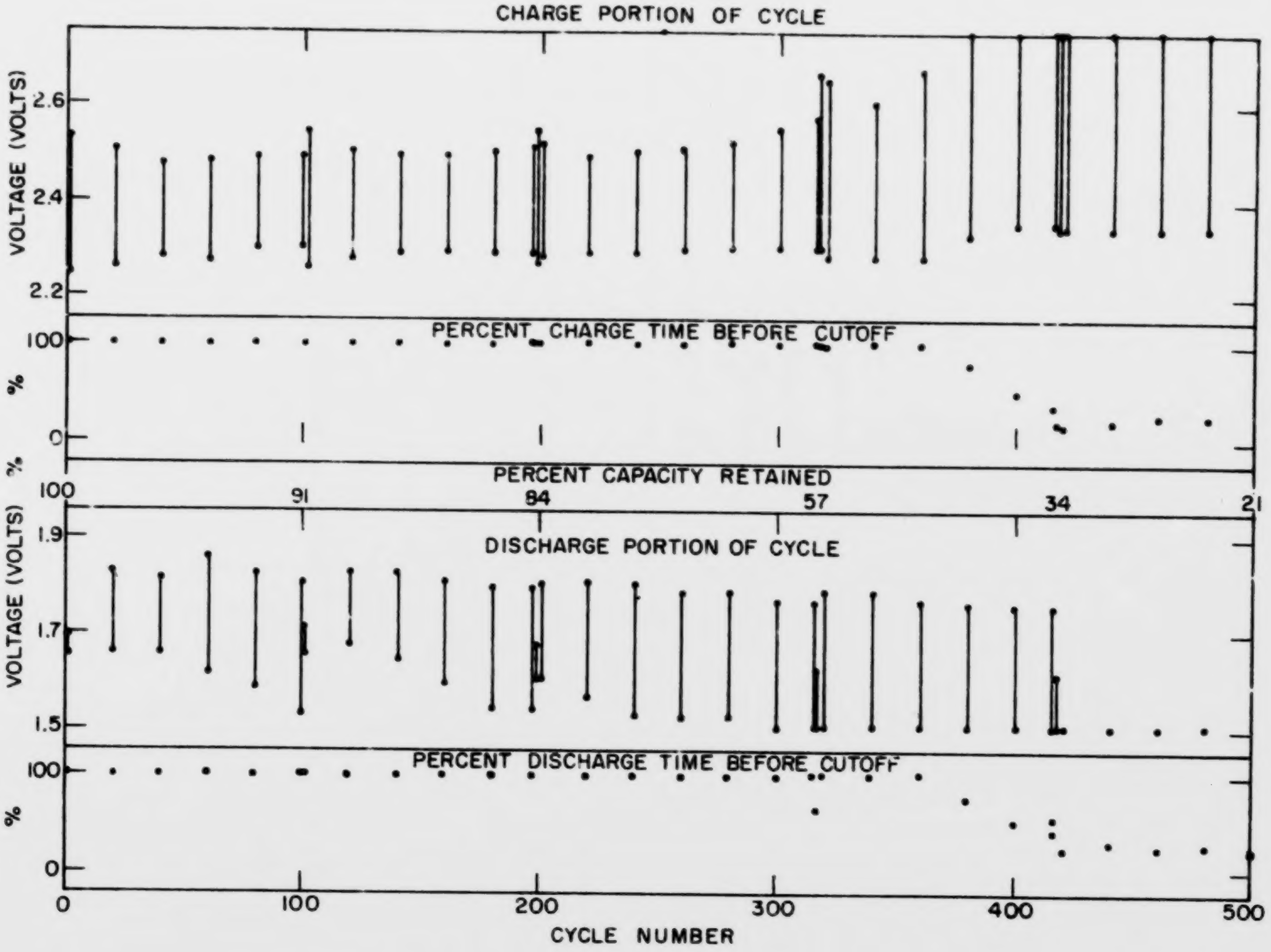

Fig. 2. Performance characteristics of a fresh thin conventional SLI positive plate under severe cycling conditions - Plate 1

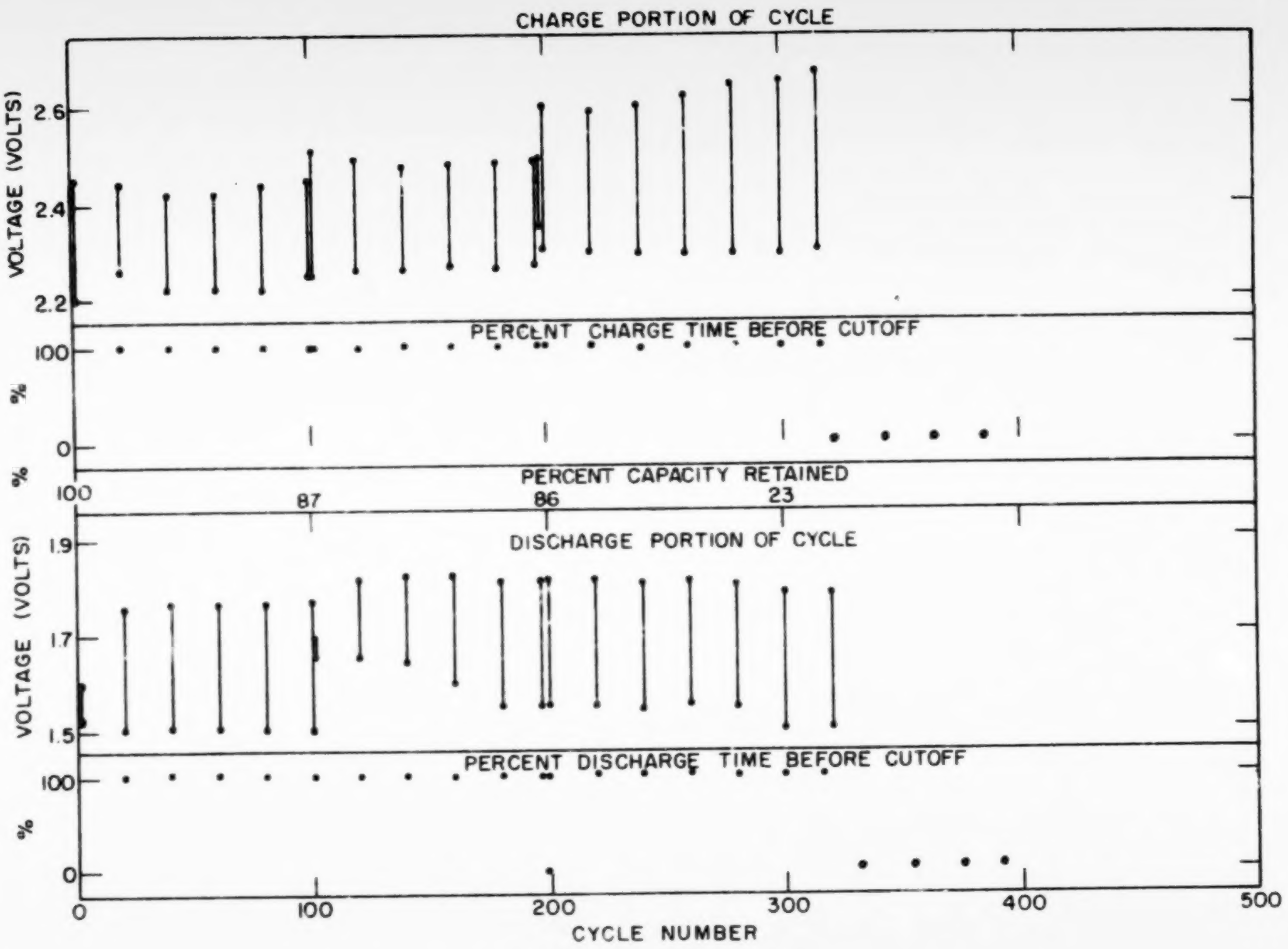

Fig. 3. Performance characteristics of a fresh thin conventional SLI positive plate under severe cycling conditions - Plate 2

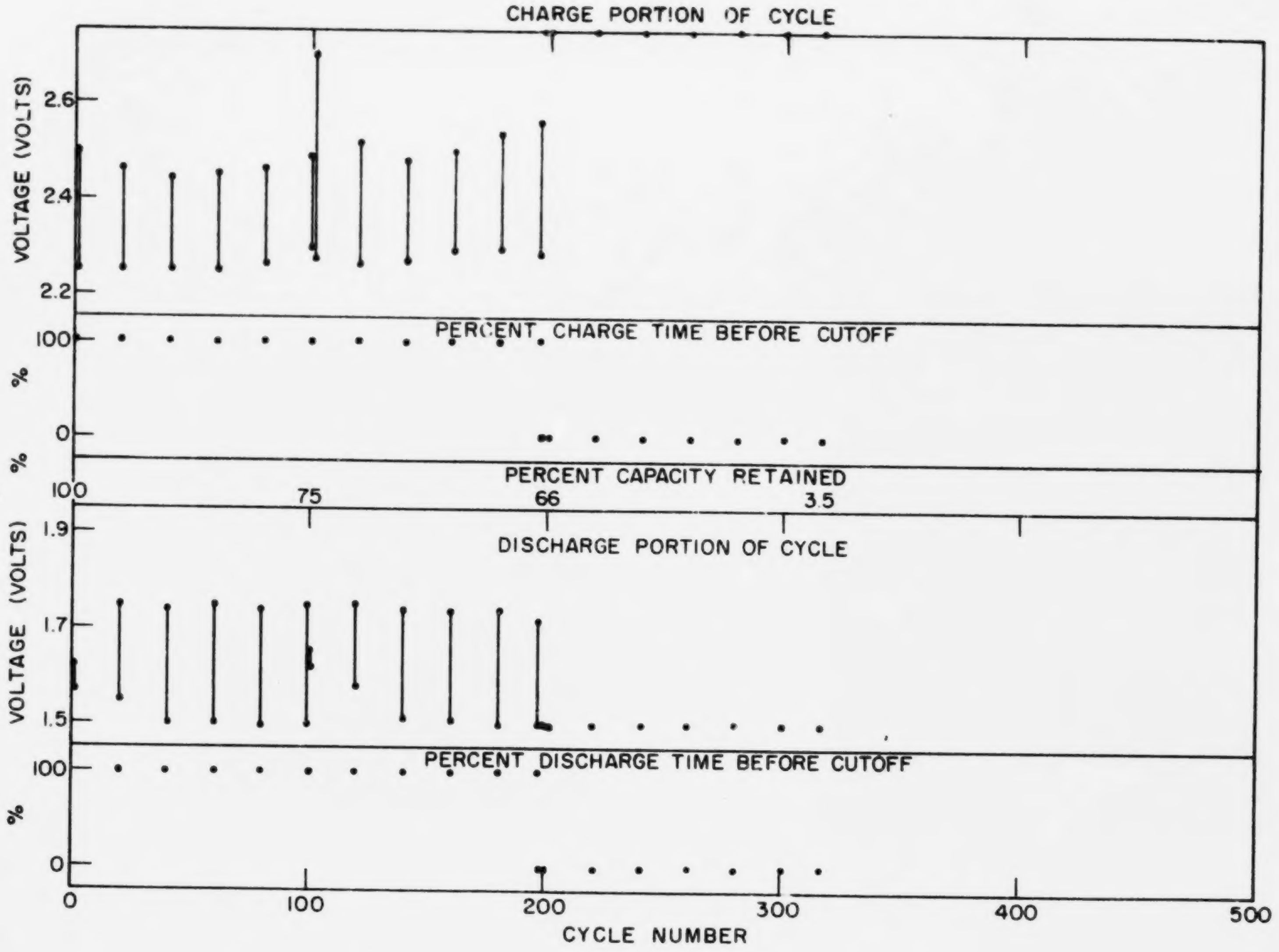

Fig. 4. Performance characteristics of a fresh thin conventional SLI positive plate under severe cycling conditions - Plate 3

Fig. 5. Photograph of a typical thin commercial SLI positive plate prior to cycling

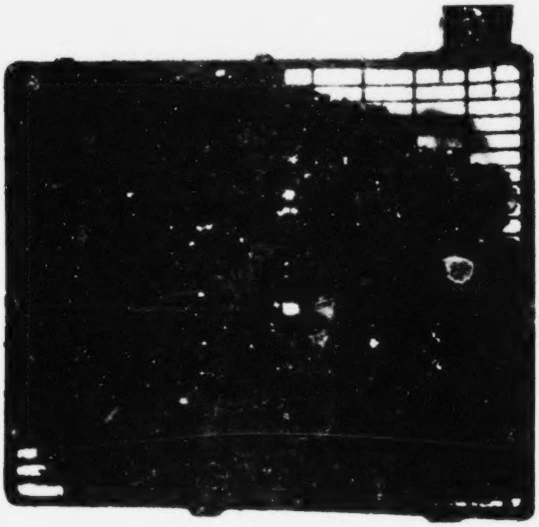

Fig. 6. Photograph of a typical thin commercial SLI positive plate after 500 cycles

✓

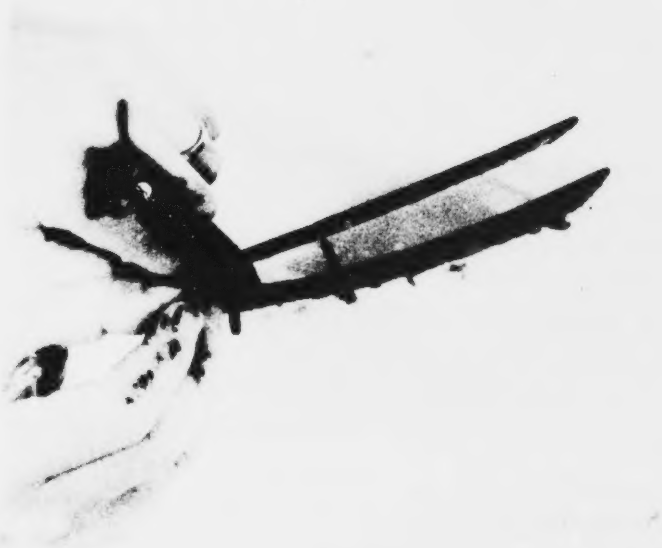

Fig. 7. Photograph illustrating plate buckling in a conventional thin positive SLI plate after 500 cycles

across the plate in the midsection. [It must be noted here that even at the start of the cycling regime, each positive plate was slightly buckled (see Fig. 7), but not so severely as on completion of the cycling]. Paste material was actually widely separated from the grid in many sections (forming "bubbles" over several cm^2 area) of each plate. Retention of material was virtually nonexistent in some plate areas, particularly close to the current takeoff terminal (Fig. 6). The poorer paste retention close to the current takeoff terminal can be interpreted as due to higher local depth of discharge as caused by iR drop along the grid. The predominant failure mechanism appears to be a combination of extensive expansion of each plate during cycling, with consequent buckling of the plate (see Fig. 7) and therefore poor paste adhesion and shedding (see Fig. 6).

We have plotted the data on the two negative test plates in a similar way and these are shown in Figs. 8 and 9. Data on these two plates paralleled each other very closely and even after 500 cycles, 70% and 76% of the original (C/5) capacity still remained in each plate. Cell voltages on charge rarely exceeded 2.5 V maximum (and 2.2 V minimum). On most cycles, there was a distinct trend towards lower maximum voltage on charge in a given group of 100 cycles (suggesting an overall loss in capacity during the sequential discharges). On the last series of cycles, the initial maximum charging voltage was 2.75 V (and 85% charge was accepted); whereas, on the previous groups of cycles, 100% charge was accepted and the maximum voltage was generally ~2.6 V. This is due to having commenced our last series of cycles from the 100% capacity point (and not 80% as before).

On the discharge cycles, there was again a trend towards lower voltages during each group of 100 cycles. As the capacity of each cell fell, the discharge voltages also decreased. In effect, we are apparently shifting from the 80% capacity starting point towards smaller values within each group of 100 cycles. In addition, we observe a steady decrease in total capacity (i.e., capacity after full charge) as cycling proceeds. The decrease is relatively small when compared with positive plate performance. The negative plates, when removed from the test rack, exhibit a much roughened surface structure (Fig. 11) compared to their initial appearance (Fig. 10). No excessive shedding of active mass was observed though the roughening is probably a prelude to such shedding.

Based on these experiments, the following conclusions were drawn on the performance capabilities of these fresh thin commercial SLI battery plates operated at high power density.

1. Performance is limited by the positive plates which last only a maximum of 350 complete high rate cycles. The C/5 capacity retained after 300 complete cycles on each of the three positive test plates was 57%, 23%, and 3.5%.

2. Positive plate expansion and consequent poor paste adhesion, particularly close to the current takeoff terminal, apparently limit the performance of the positive plates.

3. Fresh commercial negative plates stand up very well to such cycling and a decrease of only ~30% of total capacity (capacity after full charge) is noted after 500 cycles.

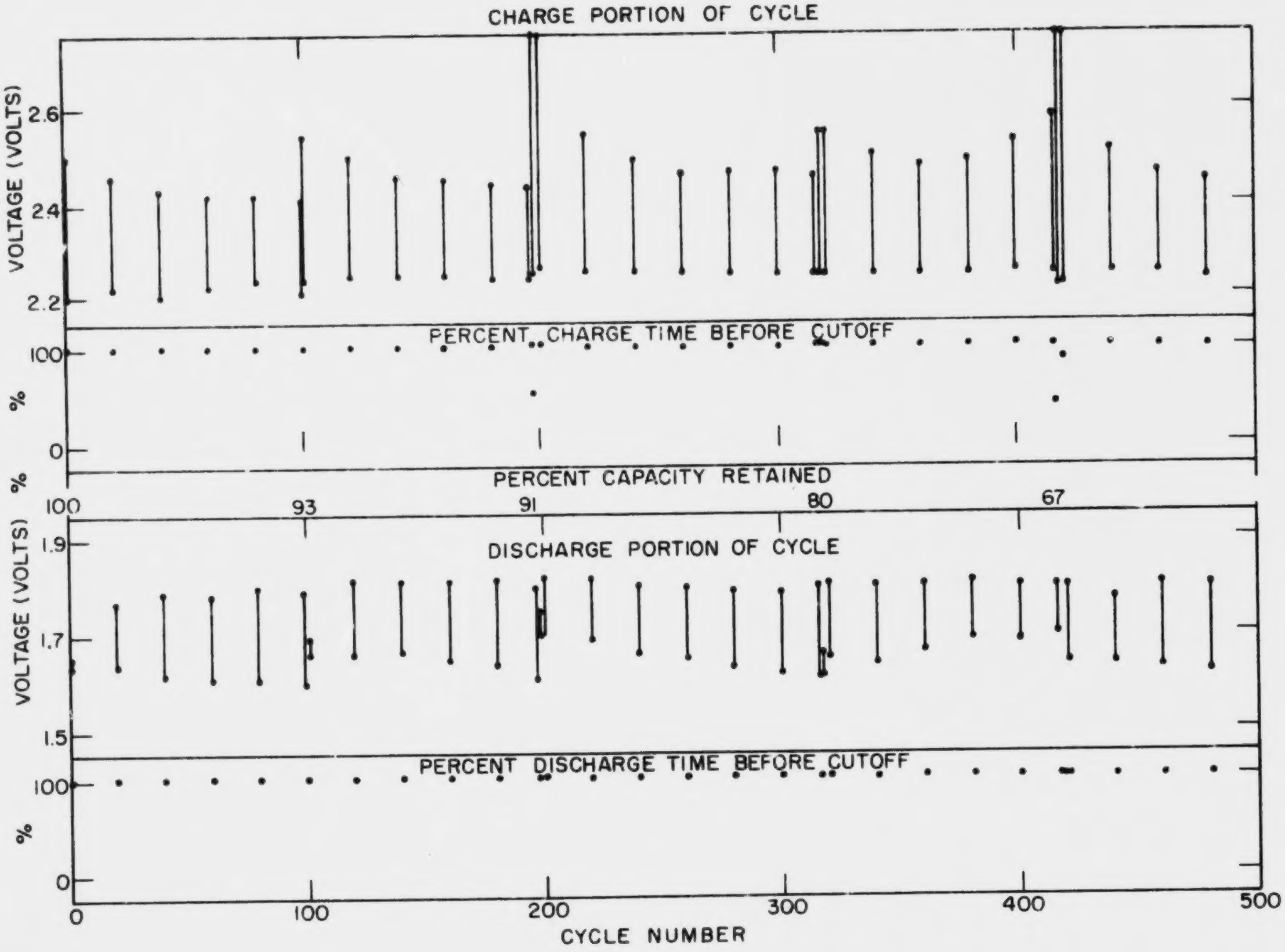

Fig. 8. Performance characteristics of a fresh thin conventional SLI negative plate under severe cycling conditions - Plate 1

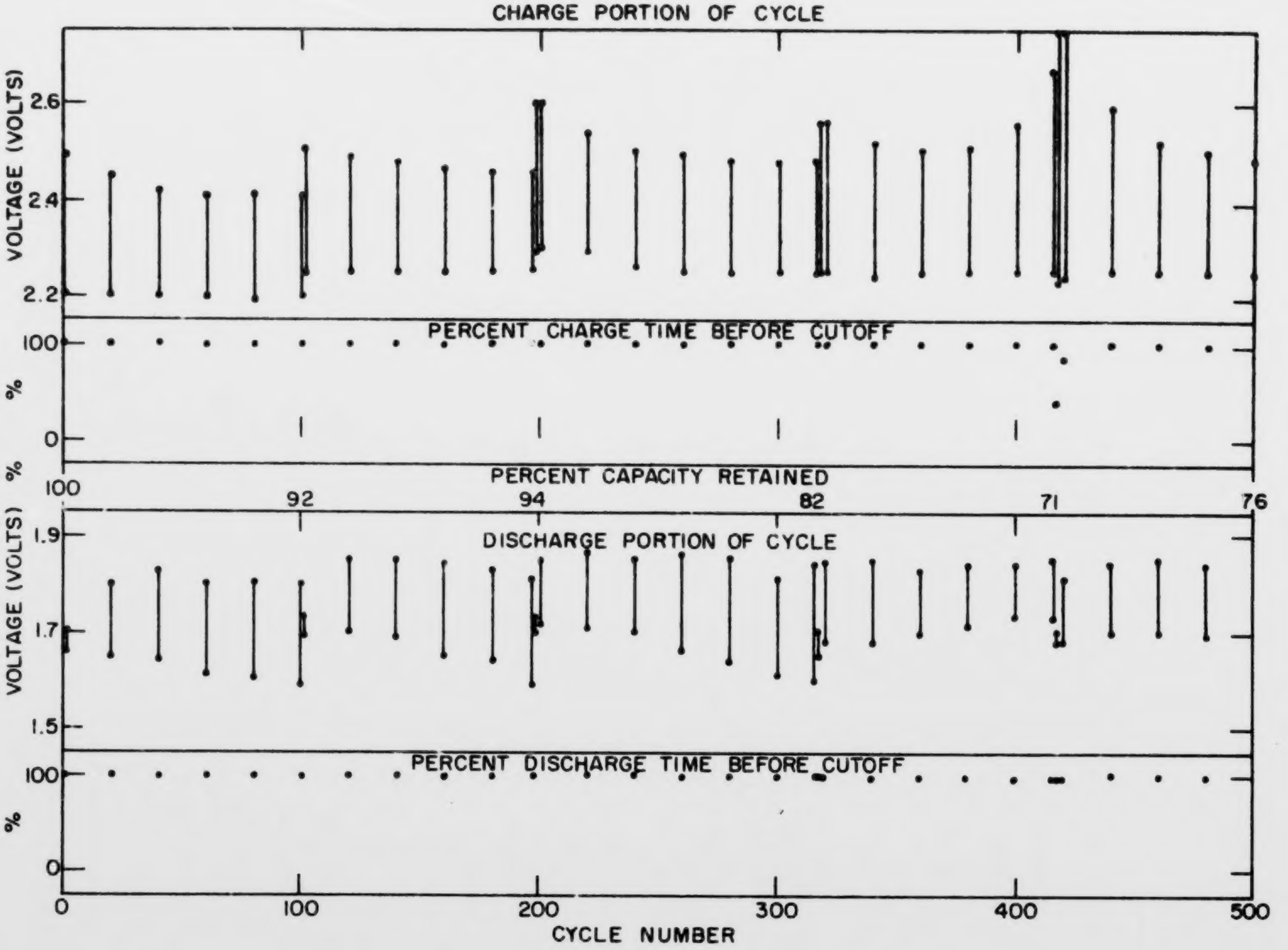

Fig. 9. Performance characteristics of a fresh thin conventional SLI negative plate under severe cycling conditions - Plate 2

Fig. 10. Photograph of a typical thin conventional SLI negative plate prior to cycling

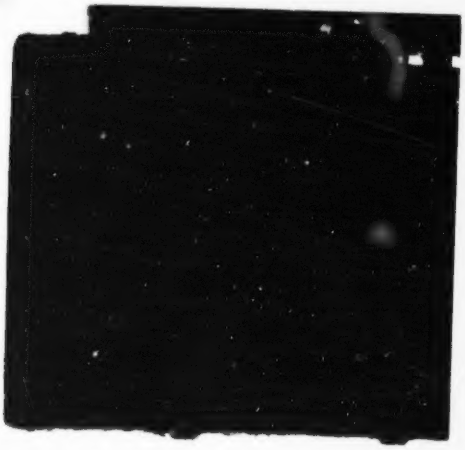

Fig. 11. Photograph of a typical thin conventional SLI negative plate after 500 cycles

Within each group of cycles, the negative plates lose charge steadily, but much of this loss can be recouped by a periodic recharge at regular intervals (every 100 cycles in this case). Charge acceptance on the negative plates appears to be more efficient as the overall state of charge decreases. Such an effect in the positive plates is masked by the overall degradation of the plates.

The following more general conclusions are also evident:

1. The positive plates in fresh conventional thin plate SLI batteries are marginal in obtaining the high discharge power densities required for hybrid vehicle purposes. They are less than satisfactory in providing adequate power after extended cycling life.

2. Particularly on cycling, there is a serious problem with conventional positive, thin SLI battery plate which is caused by longitudinal resistance losses along and down the grid. This results in uneven utilization of active mass and, therefore, high local depth of discharge even when the overall depth of discharge is shallow. Paste shedding results particularly close to the current takeoff terminal. Designs which overcome this problem are desirable.

III. TASK II: PRELIMINARY DESIGN STUDIES

This task was aimed at developing preliminary design concepts suitable for use in a high power density long life battery. Provision was made in the designs for the reduction of electronic iR gradients along each plate and for decreasing active mass thickness. Further important considerations were those of improving plate reliability and minimizing corrosion, plate buckling, and intercell electrolyte leakage problems, all of which can adversely affect performance. All of these aspects are discussed in full later.

A. Design Concepts

The basic bipolar design concepts which we considered in the contract period are outlined below in concepts 1 through 5. Concepts 1 - 3 are the bipolar designs which were considered to be of more practical interest after initial experimentation, literature surveys and design calculations. Concepts 4 and 5 are alternative bipolar designs having both advantages and disadvantages over 1 - 3. It was considered that their disadvantages outweighed their advantages but nevertheless they were examined briefly here. In addition to these designs which were experimentally tested, we also discussed two preliminary conceptual designs: Concept A - on which the feasibility of constructing a full scale high power density battery system was first analyzed and Concept B which is exactly the same as A except that the bipolar plate size is larger. (See Section III.B and Appendices I-III.)

The basic design concepts considered were: -

1. Bipolar plate with a nonconductive plastic substrate as support for the active material and with metal strips as electronic contact. The strips, which are laid vertically down the plate and in a parallel array along the plate, on both sides, are in contact with the adjacent strips on the opposite side only over the top of the plate. The contact points are all encased in a plastic border.

2. Same as (1) but with contact at the top and bottom of each plate, the latter points also being encased in a plastic border.

3. Same as (2) but with contact also at localized points down and across the plate surface via holes through the plate. The latter points are also covered with plastic.

The above designs range from what we have termed a "quasi-bipolar" plate [as in (1)] to modifications which more closely approximate a true bipolar design [particularly as in (3)]. In a true bipolar plate, conduction is achieved over the entire plate area. A major problem in bipolar plates can be encountered as a result of leakage through the plates (e.g., by corrosion attack) causing short circuits. We anticipated that reducing the number of possible leakage paths and locating their geometry so that they were as far removed from corrosive attack as possible would alleviate the problem. In the event that corrosion problems are successfully overcome, the modifications in (2) and (3) permit the more complete realization of the overall advantages of bipolar plates.

Two additional bipolar designs were considered:

4. A bipolar plate with plastic substrate as active material support. The substrate, however, is also electronically conductive. Conductivity is achieved either by using a filler, e.g., graphite powder, or by sandwiching a layer of carbon or graphite cloth between plastic sheets. In both cases, however, it is not necessary for the strips to make physical contact over, under, or through the plate. The conduction path is via the Pb strips, to the graphite and then through to the Pb strips on the opposite side of the plate. The plastic isolates the graphite conductor (which also reinforces the structure) from the H_2SO_4 and so prevents electrolyte leakage through the plate.

5. Bipolar plate with conductive, corrosion resistant, light weight/high strength metal backing.

In both of the above designs, conduction is achieved over the entire substrate area. The advantages of the true bipolar plate are thus fully realized. Unfortunately, so are all the problems - particularly corrosion, and with design (4), the possibility of gas evolution on exposed graphite also exists. All these aspects have been considered in subsequent sections and a balance has been made between the desirability of having reliable and long life plates and that of maximizing plate performance on final design plates.

B. Design Equations and Concepts for a Preliminary Bipolar Concept A

Below, discussion,calculation and design details relevant to the construction of a high power density battery system based on a preliminary concept of a bipolar plate (Concept A) are given. This demonstrated the feasibility of the approach. It also provided useful design values for critical comparison with those on modified and improved designs. Subsequent calculations for a full size battery using the improved designs were basically the same as those given in detail for this Concept A. The effects on battery characteristics of changes in design variables and in particular, changes in the operating current density are also clearly outlined using the Concept A as a particular case. The present section summarizes the results of these calculations which are given in more detail in Appendix I. (Compare Appendices 2 and 3 also).

For a high power density battery system it was initially considered that a large number of thin plates should be employed, imposing quite a severe strain on the mechanical stability of the plate suppport material (the grid). To support the active material, it was felt initially that a plastic substrate might be suitable. Since plastic grids also greatly reduce the constructional problems associated with a bipolar configuration, particularly sealing, it seemed highly advantageous to use both these concepts in the same battery. As described below, the use of thermoplastic structural materials obviates many of the difficulties inherent in the bipolar configuration.

In view of the electrical, weight, and economic constraints given in the work statement, it was felt that a modular approach to the battery system would be most sensible. By building the system from uniform sized components (modules), maintenance, system reliability, as well as the economics of component failure could be made more attractive. In principle, we chose a fixed cross-sectional area for the module and took into account in the influence of the variable parameters by changes in the overall length (in effect, plate thickness and electrode separation). The basic system module as initially conceived consists of a nominal 180-V battery containing 100 bipolar cells with an active area of 15 sq in. per electrode. The external dimensions of the module case are 6 in. wide by 4 in. high. Module length is dependent on the design parameters selected.

Fig. 12 illustrates the preliminary view of the production of the basic plastic plate. The first step involves the casting of individual pure lead ribs. These are subsequently incorporated in the casting of the plastic support, and end up as horizontal protruding ribs from a flat plate. In this configuration, they provide the required interelectrode conductivity. Note that the exposed portions of the ribs are wider away from the electrode face. In this manner, contact of the active material with one grid is optimized.

The entire plastic sheet is then given a thin coating of lead. This lead coat has a dual purpose. Primarily, it provides good electrical conductivity over the entire plate surface. A further objective is to prevent electrolyte from penetrating the plastic-lead interface. The thickness of this layer is dependent on the corrosion rate of lead under the required electrical constraints. Application of the protective lead is currently conceived as a two step process. After an initial layer of lead is vacuum deposited, the bulk of the lead layer is electroplated via standard techniques. As a final step, the plates are pasted and cured in a conventional manner.

Though in principle attractive, several possible problem areas were anticipated with the above design relating primarily to constructional problems, intercell corrosion at the Pb/plastic interfaces extending through the plastic support, and expansion of the positive electrode leading to the plate buckling. Thus the alternative designs summarized in (1)-(3) above were proposed. Numbers (1) and (2) were visualized initially as in Fig. 13. [See Fig. 36 for the final design for (1) and Fig. 42 for the final design for (3)]. The number of corrosion paths is greatly reduced and the path lengthened by folding lead strips over the plastic support. In the first modification, contact between positive and negative plates in each cell is not through the plate but over it, at the top of the plate. In the second modification, electrical contact is

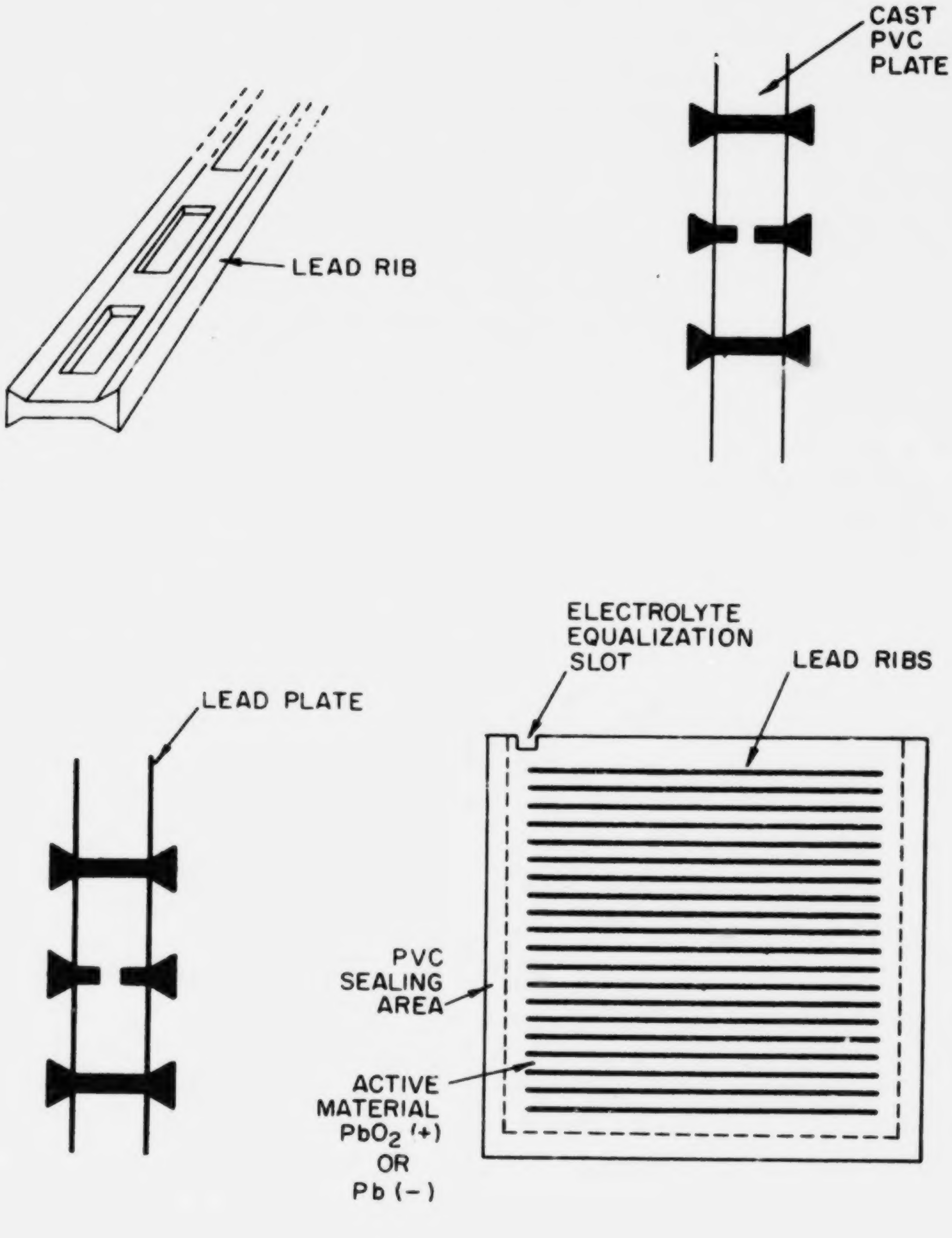
CAST
PVC
PLATE
LEAD RIB
LEAD PLATE
ELECTROLYTE
EQUALIZATION
SLOT
LEAD RIBS
PVC
SEALING
AREA
ACTIVE
MATERIAL
PbO_2 (+)
OR
Pb (−)

Fig. 12. Illustration of the production of a basic bipolar plastic plate as in Preliminary Concept A

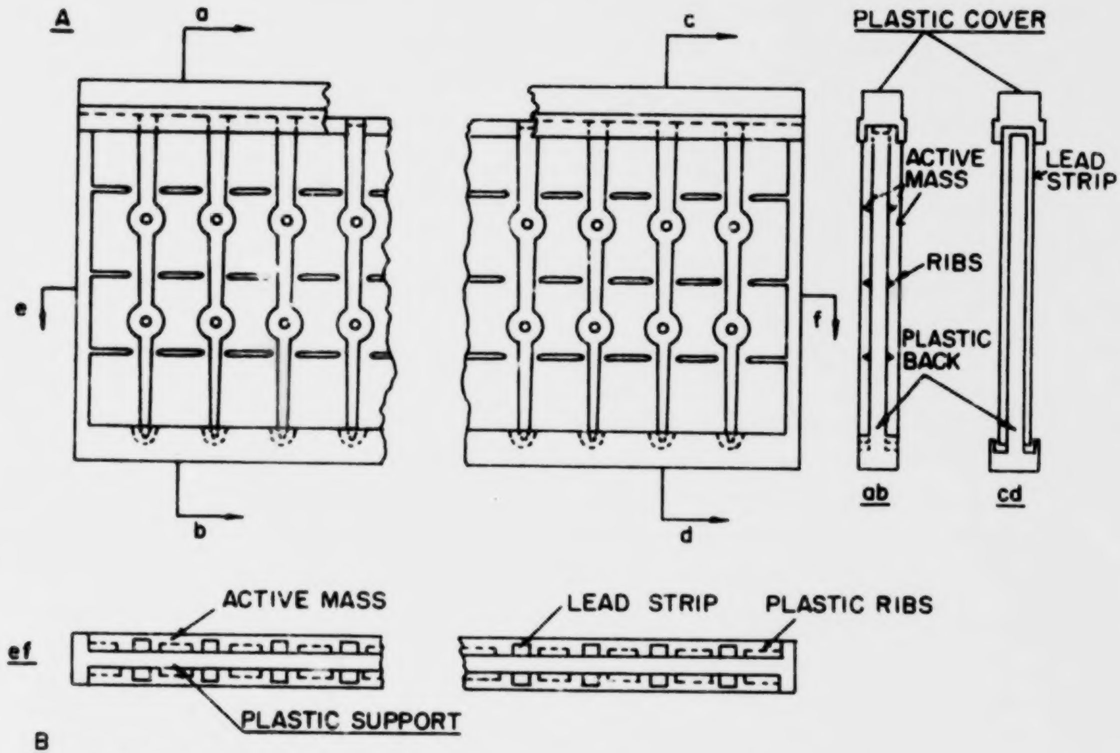
A
a
c
PLASTIC COVER
ACTIVE MASS
LEAD STRIP
RIBS
e
f
PLASTIC BACK
ab
cd
b
d
ACTIVE MASS
LEAD STRIP
PLASTIC RIBS
ef
PLASTIC SUPPORT

B

MODIFICATION OF "A" WITH CONTACTS ON TOP AND BOTTOM

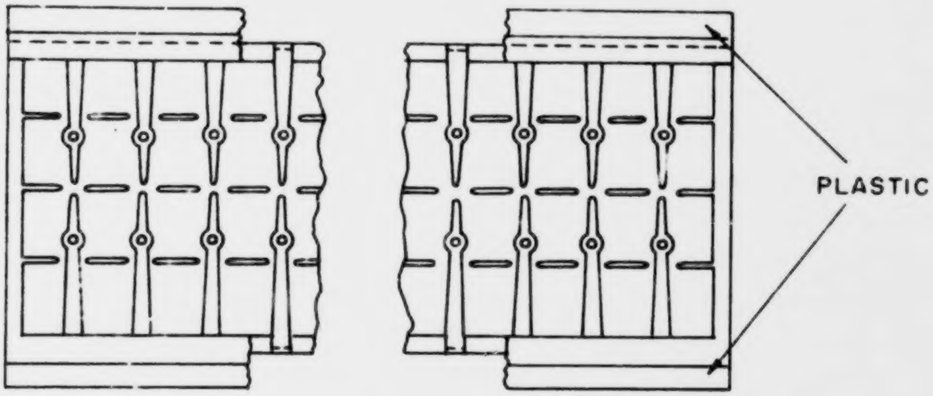

Fig. 13. Initial visualization of bipolar plates with plastic support and "lead fingers" folded over the top of the support [basically, designs (1) and (2) on page 21]. The final construction of this plate is shown in Fig. 36

maintained by the lead strips at both top and bottom of the plate. The latter of course now increases the number of corrosion paths but the path length is still relatively long compared to the original design configuration (Fig. 12). Expansion holes are also provided in the strips on the positive side only. Note also the plastic ribs provided in the plate to give good paste adhesion.

The following design variables were considered to be of major importance and were assigned symbols as indicated below. Though specific to the preliminary Concept A outlined in Fig. 12 above, the calculations are easily modified to include design variations such as those shown in Fig. 13. This has been done in the final design calculations, discussed later. Table I shows the design equations for the preliminary bipolar Concept A.

X = operating current density, mA/cm^2
Y = electrochemical yield Ahr/g of active paste (assumed equal for both positive and negative material)
F = decay allowance, dimensionless (required capacity/initial capacity)
T_p = thickness of the plastic plates, in.
T_L = thickness of the lead ribs, in.
P = thickness of the lead plate, in. each side
S = spacing of the lead ribs, in.
A = acid utilization, dimensionless: this factor incorporates an allowance for the actual ampere hour equivalent (i.e., Ahr/gm H_2SO_4 of a given sp gr.) of the acid compared to the theoretical ampere hour equivalent of the same acid. The factor was estimated from the data of Vinal.[4]

Table I. Design Equations for the Preliminary Bipolar Concept A

Component	Weight/Module, g
Active paste:	$0.269\ X/FY$
Plates:	$5.5 \times 10^5\ P + 5.5 \times 10^4\ T_p + 1.94 \times 10^5\ T_L\ T_p/S + 1.09\ XT_L/SFY$
Acid:	$1.42\ X/A$
PVC case:	$0.53\ X/A + 11500T_p + 2.98 \times 10^{-2}\ X/FY + 276 + 23000P$
Terminal plates:	695
Interelectrode wiring:	60
Number of Modules:	$3150/X$
Battery weight, lb:	$7090/X + 2.07/FY + 4.61 \times 10^5\ T_p/X + 13.4 \times 10^5\ T_L T_p/SX + 7.56\ T_L/SFY + 39.5 \times 10^5\ P/X + 13.5/A$ pounds

The following parameters were not varied:

Module height and width	4 × 6 in.
Plastic case thickness	0.25 in.
Electrode size	3 × 5 in.
Paste density	$4.2\ g/cm^3$*
Acid density	$1.26\ g/cm^3$
Interelectrode wiring	50 g/foot of wire
Module terminals	0.25-in. lead plated aluminum

Consideration of the design requirements showed that the deepest depth of discharge, 764 Whr. occurred at the highest power level, 55 KW. The battery was designed soley with regard to this most severe situation, and hence may be considered to be conservatively rated for the other cycle types. The weight breakdown shown in Table II was summarized from the calculations presented in Appendix I.

Table II. Design Values for the 150 mA/cm^2 Operating Point

Active Paste, lb	3.3	Distance between plates, in.	0.014
Plates (Pb + plastic), lb	10.0	Active paste thickness, in.	0.007***
Acid, lb	0.9	Substrate thickness, in.	0.0038
Plastic Case, lb	2.3	Case thickness, in.	0.250
Terminal Plates, lb	1.5	Module Length (100 cells), ft	0.59
Intermodule Wiring, lb	0.1		
Total Module Weight, lb	18.1		
Separators, lb	(not considered) **		
Retainers, lb	(not considered) **		

---

*Although the paste density is not an important design variable, its basic influence on the performance of the battery electrodes must be considered.

**Separator weight was not included in the preliminary calculations but was later shown to contribute only 1.5% to total battery weight. Similarly glass retainers, also not considered, constribute only 1% to total battery weight.

***The calculated thickness of paste necessary to supply the required capacity is only 7 mil per electrode for two consecutive 25 sec, 55 KW pulses. We chose to use 20 mil initially to facilitate plate fabrication and handling. As is illustrated in Section VIII, a battery prepared from such a plate still conforms to weight requirements and has a sevenfold excess of active mass based on the two consecutive 55 KW pulses for 25 sec each. There is thus wide scope for optimizing the final design even further by reducing the paste thickness. The knowledge gained during the development of the 20 mil pasted plates is directly applicable to thinner structures, e.g., with 15 mil paste thickness, and no problem areas are anticipated.

C. Design Analysis for Preliminary Concept A

The most crucial design values were found to be the operating current density (X) and the electrochemical yield (Y). These two parameters are not independent and hence cannot be selected arbitrarily. Data derived from Berndt[6] was used to prepare Fig. 14 which illustrates how the utilization of active material may be expected to vary as a function of current density. We have examined this aspect also in the contract period. Coulombic capacities range from 0.125 Ahr/g (50% of theoretical) at 2.5 mA/cm^2 to 0.0375 Ahr/g (15% of theoretical) at 250 mA/cm^2. Since these experiments employed relatively thick plates, the results are conservative for present purposes.

As an illustration, three representative cases are shown in Table III; 50 mA/cm^2, 150 mA/cm^2, and 250 mA/cm^2. The other design parameters were held constant at the nominal values shown. In view of the detrimental effect of cell temperature increases, these designs were also evaluated from a heat transfer standpoint. Consideration of convective heat transport from the electrodes to the electrolyte and conductive transport through the case walls showed that these interfaces did not result in significant temperature gradients. At the 55 KW level, the battery temperature rise (assuming adiabatic operation, a worst case) is less than 3° F/min.

Table III. System Designs for Three Different Current Densities

Current Density, mA/cm^2	50	150	250
Coulombic Yield, Ahr/g	0.081	0.054	0.037
Decay Allowance	0.5	0.5	0.5
Plastic Plate, in.	0.03	0.03	0.03
Lead Ribs, in.	0.03	0.03	0.03
Lead Plate, in.	0.004	0.004	0.004
Rib Spacing, in.	0.5	0.5	0.5
Acid Use (parameter "A", dimensionless)	0.5	0.5	0.5
Module Length, ft	0.42	0.47	0.55
Number of Modules	63	21	13
System Weight, lb	868	380	319
System Volume, ft^3	4.2	1.8	1.2

Based on the above results, the 150 mA/cm^2 operating level was selected for detailed analysis since it easily fulfilled the weight requirement and yet permitted operation at approximately three-fifths of the current density of standard SLI batteries discharged at the same power density. The detailed design analysis of the 150 mA/cm^2 operating point is shown in Table II. All data were based on the nominal values given in Table I.

The effect of variations of the other design values were also considered. In particular, the effect on system weight of changes in the lead plate thickness, the plastic plate thickness, the decay factor, and the acid utilization were of interest. These results are summarized in Figs. 15 and 16. All data are at the 150 mA/cm^2 design point.

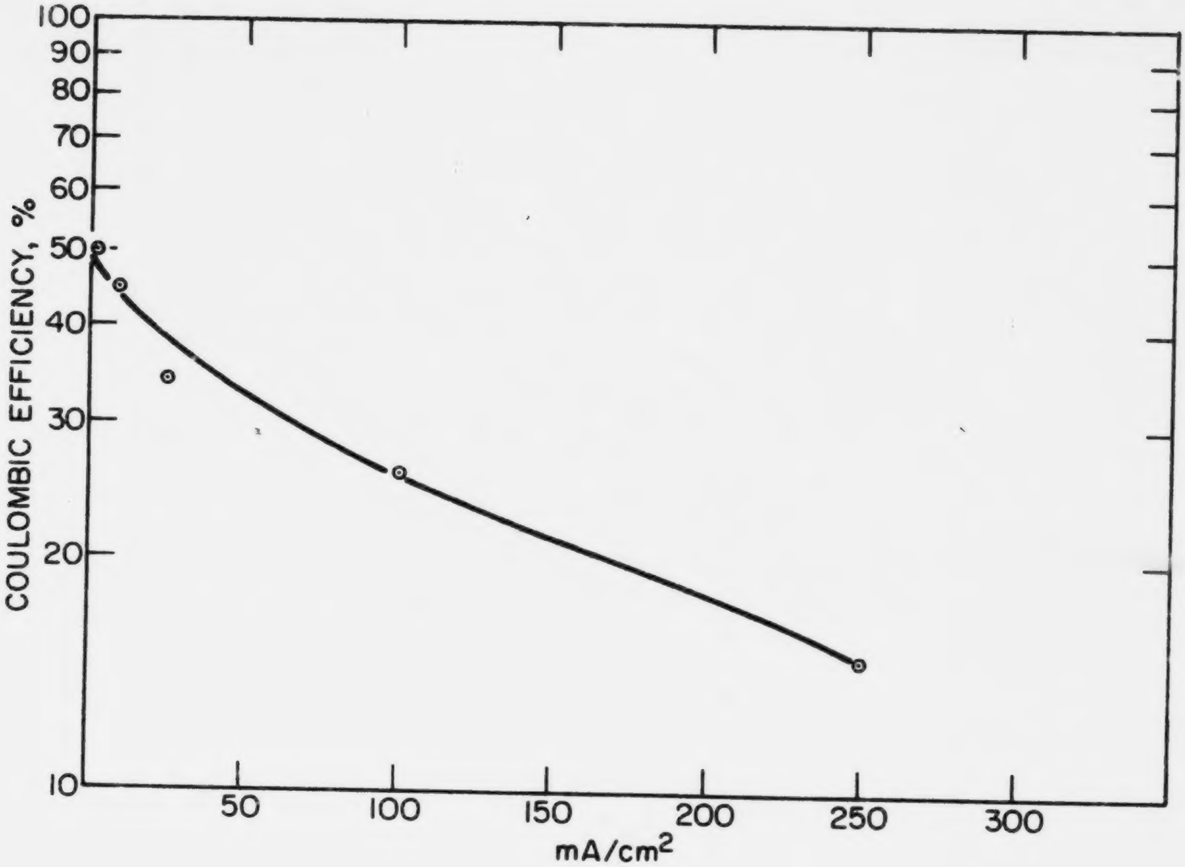

Fig. 14. Graph of the coulombic efficiency of the active materials as a function of current density [data to conventional monopolar thick plate (~ 75 mil) performance as abstracted from the data of Berndt Ref. 6]

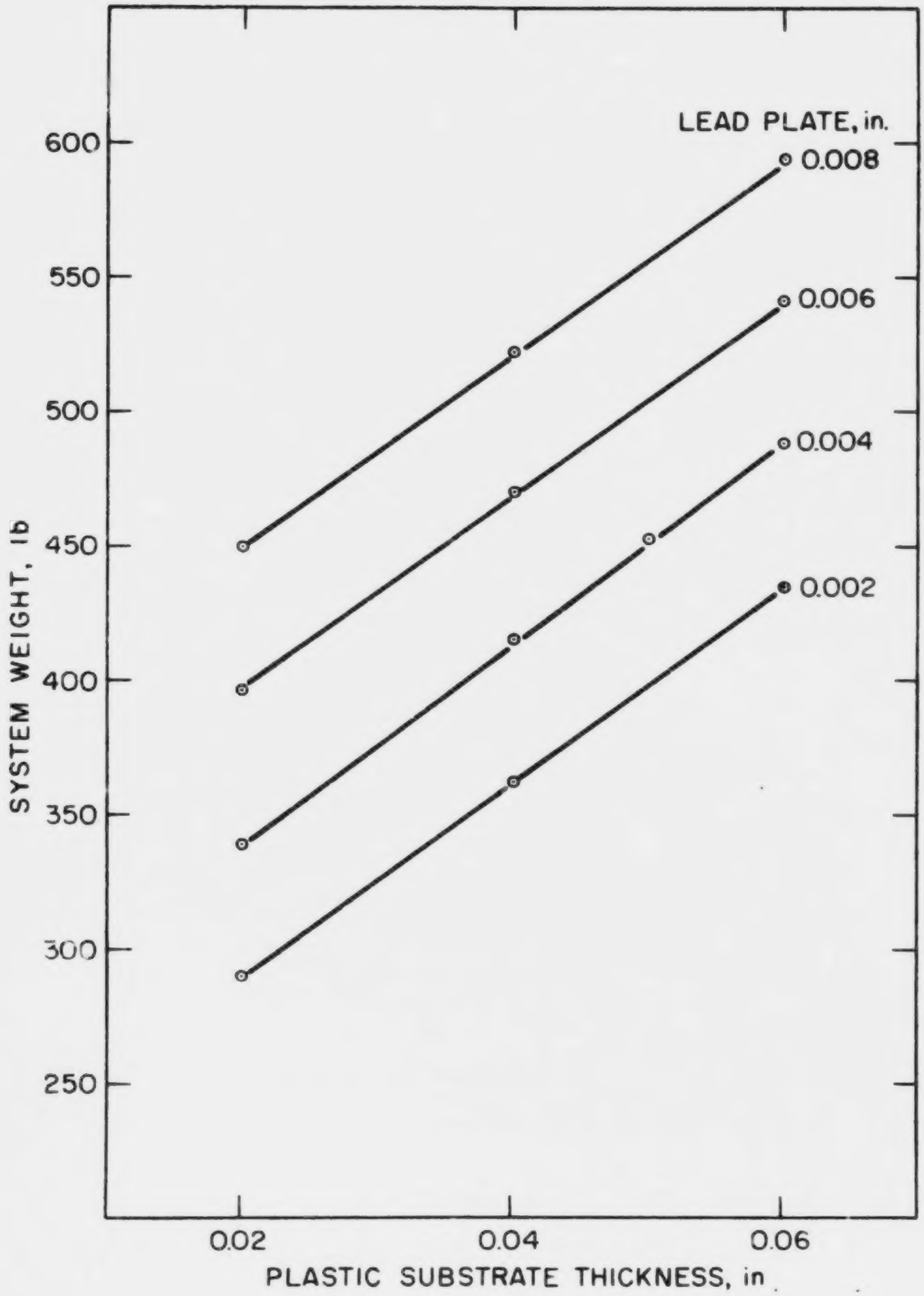

Fig. 15. Plots of the system weight versus the substrate thickness for various lead plates using the Preliminary Concept A (based on the term 39.5×10^5 P/X, where X = operating current density mA/cm^2 and P = lead plate thickness, inches) see Table I on page 28

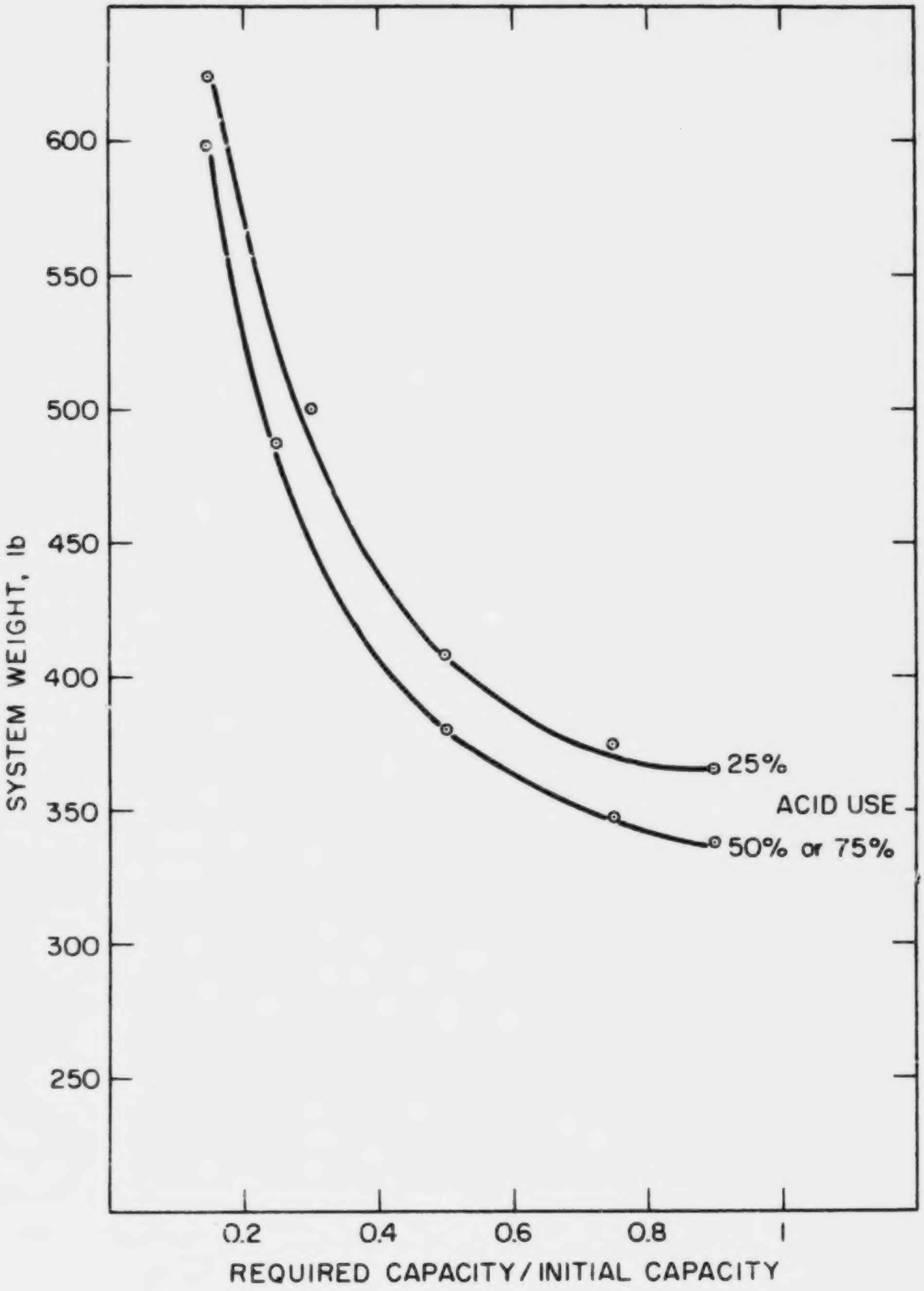

Fig. 16. Plots of the system weight versus the ratio (F) of the required capacity/initial capacity using the Preliminary Concept A (that is, as a function of those terms in Table I on page 28 which contain the factor F. The effect of varying the term "A", the acid use, is also shown)

Fig. 15 depicts the effect of substrate geometry on the system weight. The thickness of the lead plate used to enhance paste adhesion and minimize corrosion through the plastic substrate is determined by the corrosion rate on the positive side of the electrode. As can be seen, a total lead thickness of 0.015 in. is a probable maximum. However, this thickness could be divided unequally with 4 mil on the negative side and 12 mil on the positive side. The necessity of incorporating the Pb plate in the final design was a factor studied in the course of the contract. Note that plastic substrates up to 0.050 in. thick can meet the weight specification of 550 lb. The actual thickness is, of course, a function of the strength and molding behavior of the plastic.

Fig. 16 shows the relatively minor effect of acid usage on overall system weight. Hence, it was concluded that investigation of acid concentration for weight minimization purposes was not a particularly useful approach. Note that the reserve capacity, i.e., the initial ampere-hours available in the electrode divided by the ampere-hours required by the discharge [all determined by Berndt's data,[6] (Fig. 14)] necessitated by the duration and stresses of the cycle regime is of significant impact. The system as designed can tolerate the inclusion of a five-fold excess of active material (a fact which should be borne in mind in view of our later plate designs).

We recalculated these preliminary design equations on a bipolar-battery and based the data on an 8-in. × 4-in. plate dimension. This is defined here as Preliminary Concept B. (See also Appendices 2 and 3). The aim was to have a plate which was relatively long and shallow (for reasons discussed later) and in addition, a weight savings in case materials and intermodule connectors was also anticipated. The calculations in the Appendix (2 and 3) show that at an operating current density of 150 mA/cm^2 the total battery weight is 364 lb. This compares with a value of 380 lb for an equivalent battery with a plate dimension of 5-in. × 3-in. A comparison of design values for each module for the 150 mA/cm^2 operating point indicates where the weight savings is incurred. This was indeed in the case materials and to a minor extent in the intermodule wiring. Because of the greater capacity of the larger area plates (8-in. × 4-in., cf. to 5-in. × 3-in.), fewer modules are required in this latter design - 10 modules compared to 21 modules. It is important to note also that the operating current densities are the same in both designs so no disadvantages in the larger modules were expected here.

The above calculations demonstrate the expected weight of a high power density battery based on a bipolar plate as initially conceived with plastic substrate and Pb conductors. In the course of the contract period, we have not adhered strictly to the design concepts outlined above (see designs 1 - 3 at the start of this Section and also later in the report). For example, the rib spacing has been changed and no lead plate is incorporated in the final design. Paste and substrate thickness have also been varied and the reasons for all these changes are given later. We have, however, used the 150 mA/cm^2 operating point as our reference in all test data and include in Section VIII the final calculations of battery weight based on this current density. This is discussed subsequently. In the following sections, we have considered those factors, e.g., corrosion and strength of the substrate, which we deemed to be important in the choice of a final design structure. The most important aspects of plate design as they affected paste performance e.g., the paste thickness, were also studied. Electrochemical factors governing plate design, e.g., the presence or absence of Sb in the grid, were also of direct concern. These factors are all discussed in the following sections. In all of these, the need for a long life battery was also borne in mind.

IV. TASK III: STUDY OF ELECTROCHEMICAL PROBLEM AREAS RELEVANT TO DESIGN OF A HIGH POWER DENSITY BATTERY

There are several problem areas associated with the use of lead-acid batteries for high power density batteries. The most important of these problem areas were examined in the course of this contract.

A. Utilization of Active Material

High rate charge[10] and discharge capabilities are required for traction purposes. Even at low rates of discharge (low current densities), the coulombic efficiency* of the active material is no greater than 50%.[4,6] As the discharge current density is increased, the paste utilization, as such, also decreases rapidly and can be $< 20\%$ at high discharge rates.[4,6-9]

The above is true for plates of all thicknesses but there is another important consideration. This is that the utilization,* in depth, of active mass at a given discharge rate decreases as plate thickness increases. This is due in a large part to the inability of the electrolyte to diffuse across the electrode thickness. In addition, there are iR losses along the grid of a conventional plate which can affect paste utilization. Whereas the effect of paste thickness on performance has been demonstrated beforehand with relatively thick ($\geq 1/16$ in.) commercial plates,[4] no information is available on performance of thin plates (≤ 40 mil) in the absence of these iR effects (which also can cause poor paste utilization). Studies were carried out with two commercial oxides in iR-free plates described below.

1. Choice of active material

Two materials only have been studied, namely Barton VLY oxide** ($< 2\%$ Pb, 60% orthorhombic PbO, and 40% tetragonal PbO) and Universal Grenox oxide** (25% Pb and a balance of orthorhombic PbO) both from N.L. Industries. Though the curing schedule of the former is ideal in that it permits good control over the amount of tetrabasic lead sulfate formed in the paste (with long needlelike crystals and consequently a good porous interlocking mass), we did not observe good paste adhesion with this material. In contrast, plates pasted with Grenox oxide have, almost without exception, performed well. We consequently confined our studies to plates pasted with the Grenox oxide. This report includes data on those plates pasted with Barton VLY oxide which showed good adhesion and performance capabilities.

---

*we have referred in this report both to coulombic efficiency and more often, to utilization of the active mass. The first term refers to the observed capacity expressed as a percentage of the theoretical capacity calculated from the known amount of electrochemically active material in the plate. The utilization term used here refers to the capacity measured at a given current density and expressed as a percentage of the capacity measured at the C/20 rate. In this sense the 50% and 20% coulombic efficiencies quoted above become 100% and 40% when expressed as paste utilization.

**The curing schedules are given in Appendix V.

2. Design of iR-free plate laboratory test structures

We designed and constructed three anodized aluminum grid molds for casting iR-free grid structures. A photograph of one of the molds is shown in Fig. 17. A schematic is shown in Fig. 18 and a typical as-cast plate is illustrated in Fig. 19. Grid depths in each of these molds are 20, 28, and 44 mil. Pb or Pb/Sb casts were prepared using a loading of ~4 lb. The use of this amount of material permited good grid definition. Before use, a commercial release agent was applied to a heated mold and the casting process then carried out using freshly acid-washed ($HClO_4$ or CH_3COOH) Pb or Pb/Sb to provide clean castings. The actual casting was made at ~450°C in a hydrogen atmosphere. We found that grid thickness in the plate agreed very well with the mold depth. For example, when using the mold with 44-mil grid depth, the height of ribs in the cast alloy was also 44 mil. Each of these grids has an area of 77.8% available for active material. The large bulk of the backing on each plate ensures insignificant problems from iR losses along the plate.

3. Effect of paste thickness

Performance of Barton VLY oxide and Universal Grenox oxide was examined by evaluating capacities as a function of current density up to 310 mA/cm^2. The grids were all cast from Pb 4.5% Sb and pasting area was held at ~90 cm^2.

The results are shown in Figs. 20 and 21 for plates pasted with the above thicknesses of both oxides. We have examined three separate samples of each paste at each thickness. Capacities were all evaluated initially at the C/20 rating. For the Grenox paste, we have plotted the capacity per cubic inch (volume capacity) at each rate of discharge as a function of current density. For the Barton VLY oxide (which did show an identical capacity to thickness ratio at the C/20 rate for each of the three thicknesses of oxide), we have plotted the ratio of the capacity at a given rate to the C/20 capacity versus current density. It is apparent from the figures that, for both pastes, utilization of active mass is greatest for the 20-mil plates over the entire range of current densities. This is especially evident in Fig. 21 obtained with Grenox oxide. There one can see that at, e.g., the 150 mA/cm^2 operating point, the utilization of active mass is almost doubled in the 20-mil plate compared to the 44-mil plate. At the 155 mA/cm^2 operating point for the Barton VLY oxide, the utilization of paste in the 20-mil plates is 53% compared to 39.5% and 31% for the 28 and 44-mil plates, respectively - in good agreement with the trends for the Grenox oxide.

The inference to be drawn from these data is that especially when operating at high rates of discharge, a large number of thin plates should be chosen. For example, to achieve the power density specified in the contract (100 W/lb), a conventional battery (> 60-mil plate thickness) must operate at ~250 mA/cm^2. At this point, the efficiency of paste utilization is only about 27%. As will be discussed, a battery incorporating new design plates can achieve the same 100 W/lb power density when operating at ~105 mA/cm^2. From Fig. 21, the efficiency of active mass utilization is ~48% at this point, that is, almost a twofold improvement with the new design.

Fig. 17. Photograph of anodized aluminum mold used in the preparation of iR-free plate laboratory test structures

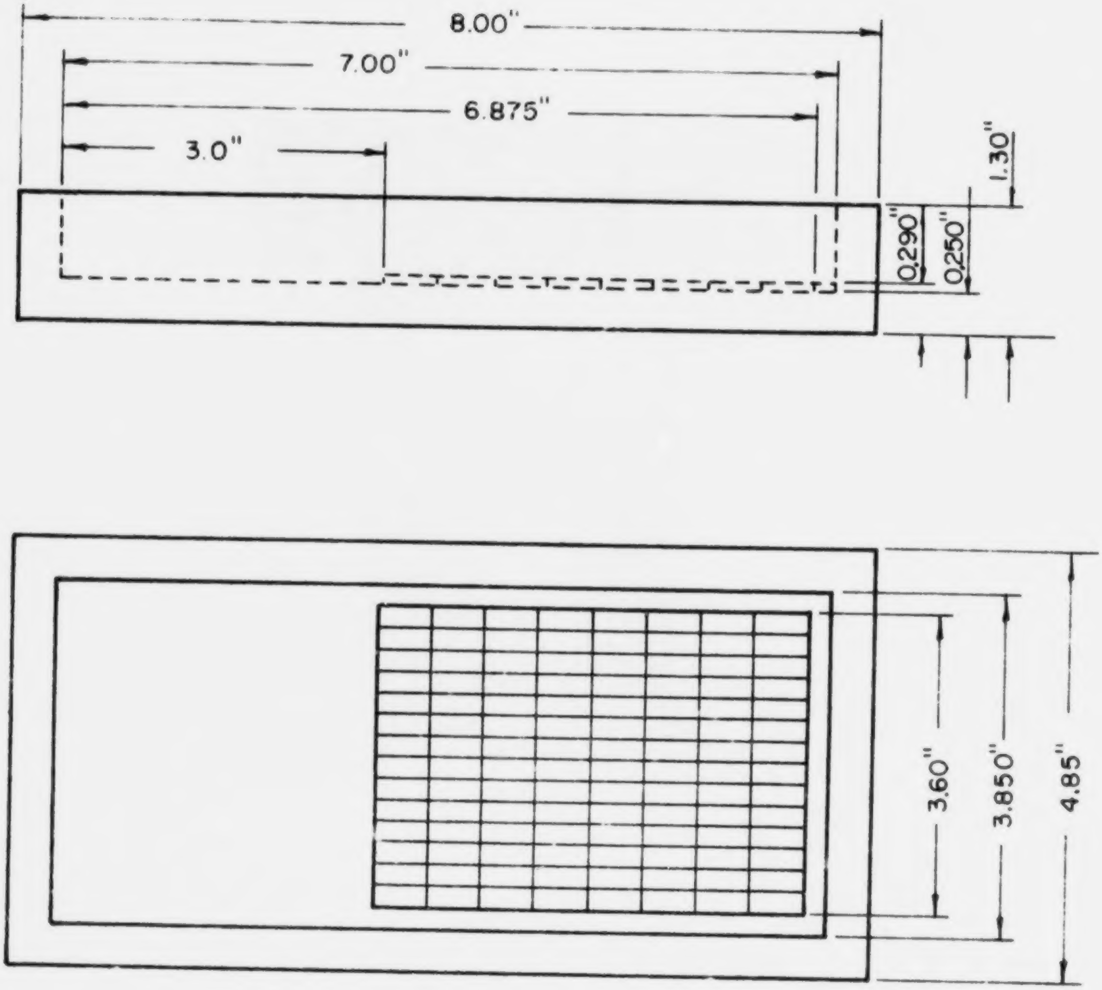
8.00"
7.00"
6.875"
3.0"
1.30"
0.290"
0.250"
3.60"
3.850"
4.85"

Fig. 18. Schematic of anodized aluminum mold used in the preparation of iR-free plate laboratory test structures

Reproduced from best available copy.

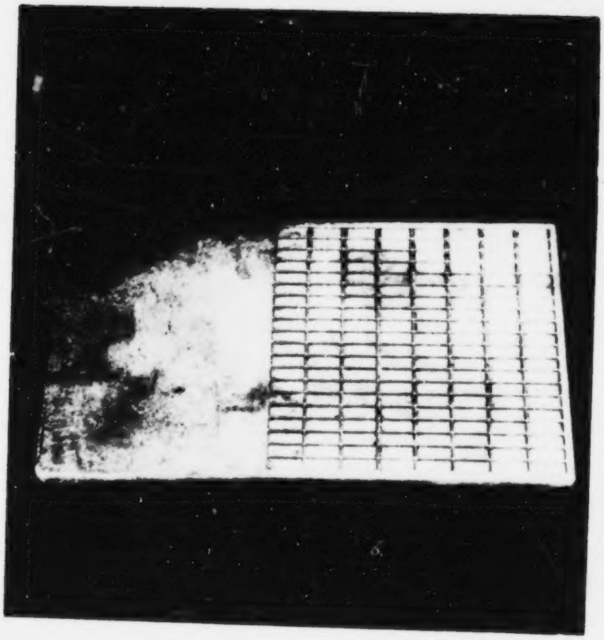

Fig. 19. Photograph of an as-cast, pure Pb, iR-free plate laboratory test structure having a grid structure 44 mil in depth

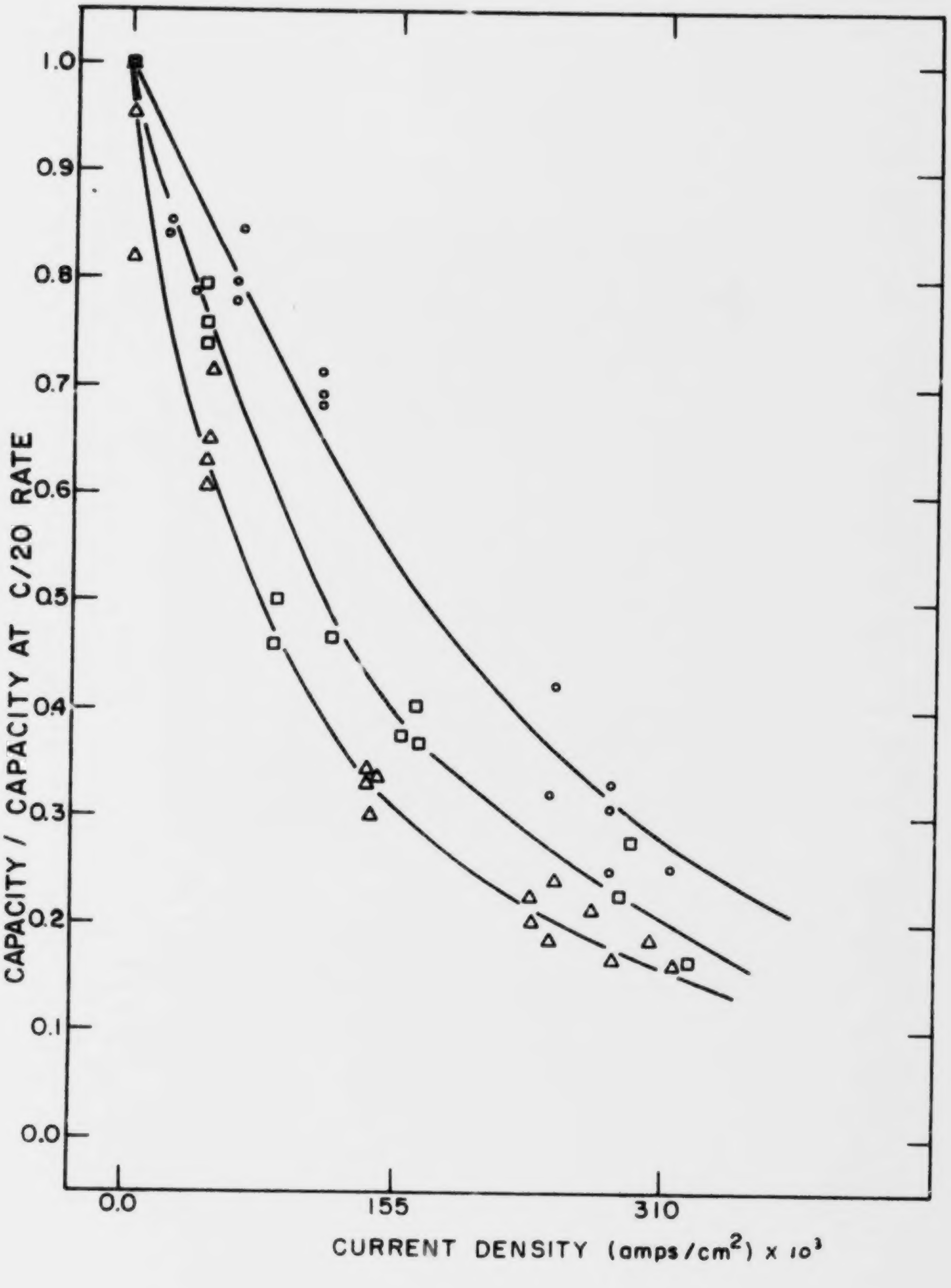

Fig. 20. Performance of Barton VLY positive paste in iR-free laboratory test grids as a function of paste thickness (○, 20 mil; □, 28 mil; Δ, 44 mil) at various current densities

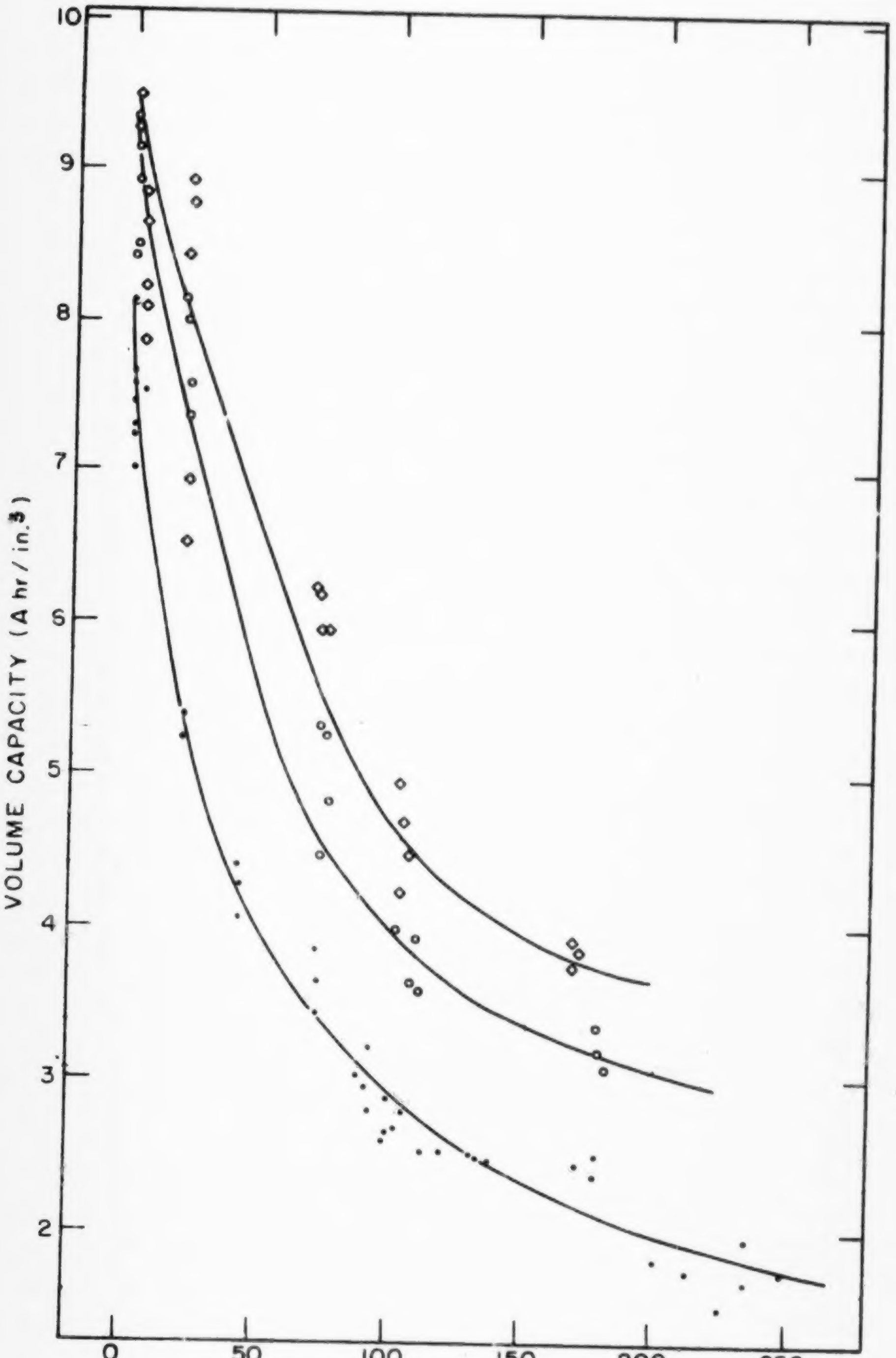

Fig. 21. Performance of universal Grenox positive paste in iR-free laboratory test grids as a function of paste thickness (◊, 20 mil; ○, 28 mil; ●, 44 mil) at various current densities

4. Longitudinal resistive losses affecting paste utilization

In conventional thin battery plates which have a single current takeoff terminal, a possible problem in paste utilization and cycling lifetime is encountered because of iR losses along and down the plate, away from the terminal.[11] Because of the increase in resistance in the latter directions, it is easier to discharge the paste in those areas closest to the takeoff terminal. Poor distribution of active mass utilization and high local depth of discharge can thus occur even if the overall depth of discharge is low. Again, subsequent paste shedding problems would ensue since shedding is worse at high local depth of discharge.[12]

We have also examined this aspect of battery performance. Data on the plates described above (Fig. 21) were compared with similar data on fresh conventional positive plates of 60-mil and 80-mil plate thickness. This is approximately equivalent to our 28-mil and 44-mil one-sided plates, respectively. At the 150 mA/cm^2 operating point, the "volume capacities" for the 28-mil and 44-mil resistance-free structures were 3.3 and 2.2 Ahr/in.^{3} respectively; while they were 3.1 and 2.8 Ahr/in.^{3} for the 60-mil and 80-mil conventional plates respectively. That is, there was no marked difference in paste utilization. At 250 mA/cm^2, however, the volume capacity for the 28-mil one-sided plate was 2.7 Ahr/in.^{3} compared to 1.9 Ahr/in.^{3} for the conventional plate of 60-mil thickness. A similar trend applied to the resistance-free plate of 44-mil thickness compared to the conventional plate of 80-mil thickness.

For a conventional battery to operate at a power density of 100 W/lb, the plates must support current densities > 200 mA/cm^2. Under such conditions, there is an effect of longitudinal iR losses in conventional plates which is manifested by poorer paste utilization compared to that in resistance-free plates. Higher local depth of discharge can thus be anticipated even when the overall depth of discharge is relatively shallow. As noted in previous sections, we have tested conventional positive and negative plates under high rate cycling conditions (equivalent to 47.5 KW on discharge with a 25.9 KW charge) and found that excessive positive paste shedding occurs in the area of the current take off terminal. This is shown in the photographs in Figs. 5 and 6 which are of a positive plate before and after cycling (> 300 complete high rate cycles). Clearly then, designs aimed at eliminating these resistance effects are desirable and should permit a more even utilization of active mass with consequent greater plate life on cycling.

At the 150 mA/cm^2 operating point, we observe no severe discrepancies between conventional plates and resistance-free plates. Thus, at this point, the problem of longitudinal resistance losses is not a serious one with battery plates. We reemphasize that whereas a battery constructed from the new design plate can operate at 150 mA/cm^2 (the power density here is actually 135 W/lb), a battery with conventional plates can not (the power density of a conventional SLI thin plate lead acid battery operating at 150 mA/cm^2 is only 74 W/lb).

B. Effect of Sb and H_3PO_4 on Paste Performance

It has been established[13-17] that, for conventional batteries cycled at relatively deep depths of discharge, Sb presence lead to increased cycle life. Similar results apparently followed H_3PO_4 additions to the electrolyte using pure Pb or Pb/Ca grids.[18-21] Unfortunately, the above data did not consider the very shallow discharge cycles at high rates required in the present case: for this reason, we decided to investigate the effect of Sb and H_3PO_4 on paste performance under these conditions. Our prime concern here was to determine if Sb could be removed from the battery grid without affecting cycling lifetime. Since the present battery has to last for 5 yr, we also anticipated serious restrictions to lifetime from self-discharge, poor charge acceptance and grid corrosion if Sb additions were necessary.

The desirability of having a maintenance free battery also necessitates the removal of Sb from the system. Apart from lowering the Sb content from 4.5% to $\sim$0.5% and using a microporous rubber separator to prevent Sb reaching the negative plate,[26] there is little alternative to overcoming the desirability of Sb presence in regard to enhancing cycling life without the undesirable side-effects quoted above, other than finding an additive which has the same effect on cycling behavior, but not the same adverse effects. The above alternative in fact is also not very feasible since only very small amounts of Sb are required to introduce the undesirable effects of selfdischarge and gassing, etc., on the negative plate.

For this study, we used our iR-free, one-sided plates pasted to a depth of 20 mil. Nine plates were prepared, three from a Pb/4.5% Sb alloy and the remainder from pure Pb. Universal Grenox oxide was cured and formed in the conventional manner and plate capacities determined at the C/5 rating. To the electrolyte in three of the cells with pure Pb grids, H_3PO_4 additions (1.8 vol % of 85% H_3PO_4) were then made. The amount of H_3PO_4 used corresponds to the optimum addition used by Tudor, et al.[21] The additions were made after forming the plates since the latter authors report lower capacity values on prior addition of H_3PO_4. To minimize the temporary early cycle capacity losses in cells containing H_3PO_4, we also cycled each of the above three plates five times (to 1.8 V) prior to our high rate charge/discharge investigations of paste performance. We also cycled all the other plates in the same way so that each plate for testing had exactly the same prior history.

After this conditioning, the C/5 capacities of the three plates containing Pb/4.5% Sb were 2.28, 2.18 and 2.35 Ahr (plates numbered 1-3, respectively). The plates pasted in pure Pb grids and with no H_3PO_4 additions had capacities of 0.83, 1.44 and 1.50 Ahr (plates numbered 4-6, respectively). Interestingly, the capacities of these plates were 1.97, 2.34, and 2.36 Ahr on first measuring the C/5 capacity. (Plate number 4 showed very poor paste adhesion even prior to any cycling.) Degradation in performance is obvious for pure Pb plates even within these relatively few (but deep) discharge cycles. Some degradation was also observed with the Sb containing plates but to a much lesser extent. The initial C/5 capacities of the Pb plates numbered 7, 8, and 9 prior to H_3PO_4 additions to the electrolyte were 2.28, 2.01, and 2.42 Ahr, respectively, and fell to 1.69, 1.39, and 1.61 Ahr immediately after H_3PO_4 additions. After four further cycles to 1.8 V, values of 1.65, 1.60, and 1.70 Ahr, respectively, were recorded.

The cycling tests were perform[illegible]asically as described for the commercial plates. When testing Sb-free positive plates, pure Pb or Pb/0.08% Ca grids were used in the negative plates. The current densities for cycling were 150 mA/cm^2 for discharge and 82 mA/cm^2 for charge (equivalent to 55 KW and 40 KW, respectively, in our design). Discharge time was 25 sec and charge time 61 sec. Only positive plate performance was evaluated in detail and large capacity negatives were used. Test temperature was again 30°C ± 1°C.

The results of these experiments are plotted in Figs. 22-29. These show initial and final voltages during groups of cycles and also the capacity (C/5) retained by each plate after approximately each group of 100 cycles. The cutoff voltage was kept constant at 1.5 V on discharge but was permitted to vary from 2.55 V to ~3.5 V on the charge cycle. The reasons for this were that the negative plate potentials at end of charge in the absence of Sb were shifted to more negative values because of the greater H-overvoltage on pure Pb. Also, the positive plate potential is apparently polarized when no Sb is present. Therefore, when the cutoff voltage was set at 2.75 V on charge for example, we found that the cells containing no Sb cut out excessively early and, as a result, not enough charge was put back into the cell during the charging part of the cycle. When the cutoff point was set at, e.g., 3.0 V, many of the cells responded very well to the cycling conditions without any severe capacity losses. In some cases also, we raised or lowered the cutoff point on charge merely to examine subsequent cell response on discharge. In the figures we have also noted these changes.

Generally, when the cutoff point was raised (and cells stayed in for greater times on charge), the subsequent discharge cycles were at higher voltages throughout and the final discharge voltage gradually increased during cycling. Exactly opposite effects were noted when the cutoff point was lowered. Excessive raising of the cutoff point may induce early cell failure due to excessive gassing of the plates.

1. Overall cell performance of plates with lead-antimony grids

a. The Pb/Sb positive plates all behave well on cycling and show good performance on charge and discharge at least up to 320 complete cycles. The capacity retained after this number of cycles is 45%, 20% and 65% for the three plates. This is better on average than commercial positive plate performance under similar cycling conditions. One of the plates lasted for 430 cycles before beginning to fail. The better cycling behavior of these plates when compared with the commercial plates is probably related to the drastically different grid geometry. It would support the view that the failure mechanism with the latter plates under the test conditions was due to paste shedding caused by grid corrosion and buckling, rather than to paste deterioration.

b. During discharge, the cell voltage falls on average only by 0.13 V when the cells are performing well. This also is much superior to commercial thin SLI positive plate performance (where the average voltage decay on discharge was 0.22 V).

c. At the onset of failure, no significant enhancement in performance is achieved when the voltage cutoff is raised above 2.75 V. On the contrary, excessive gassing and paste shedding result.

d. The final discharge voltage is ~1.75 V when each cell is performing well. Even on fresh conventional plates, the final discharge voltage never exceeded 1.65 V.

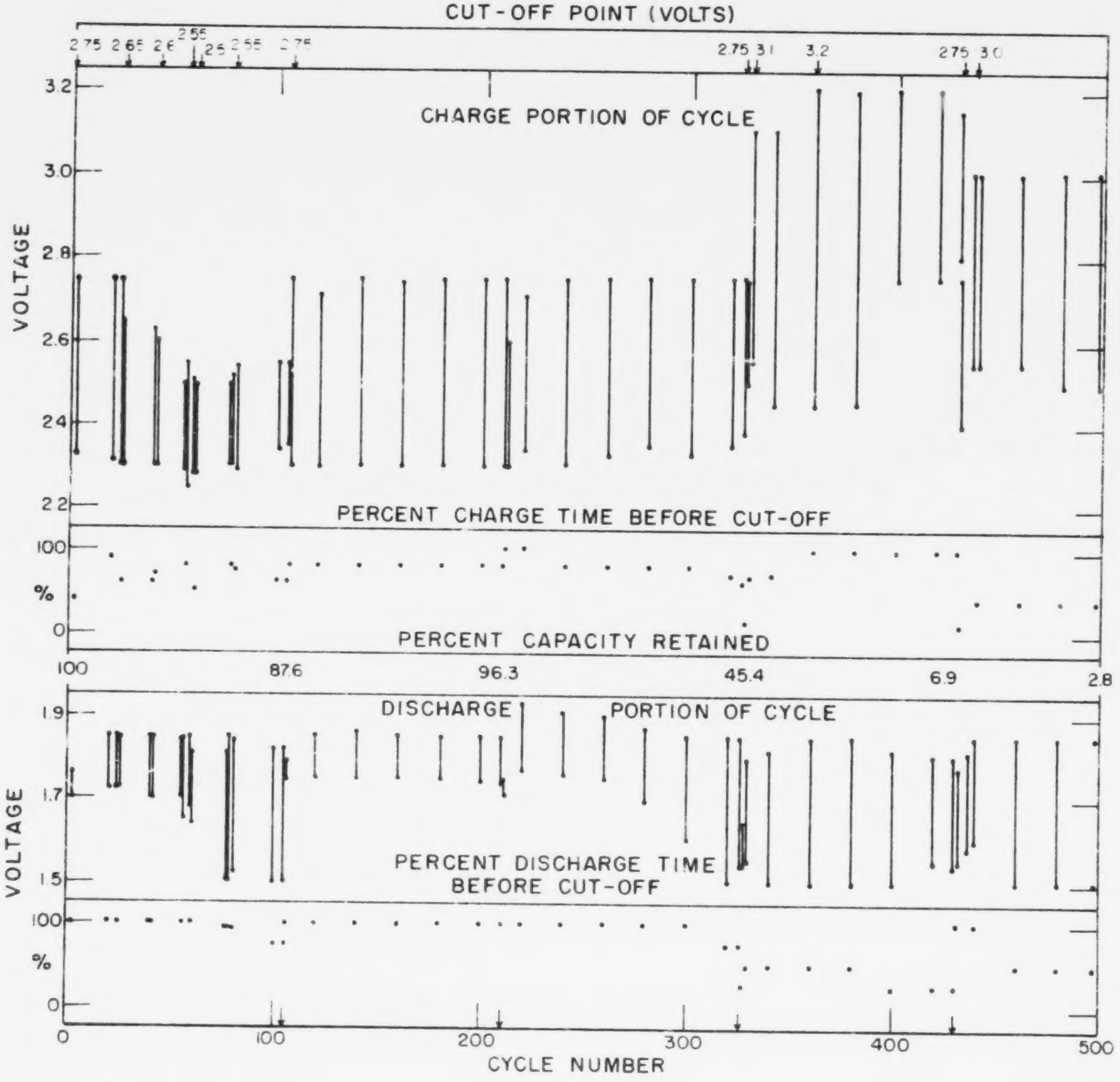

Fig. 22. Cycling performance characteristics of Universal Grenox positive material pasted in an idealized iR-free, one-sided laboratory test Pb/Sb grid to a depth of 20 mil – Pb/Sb-1

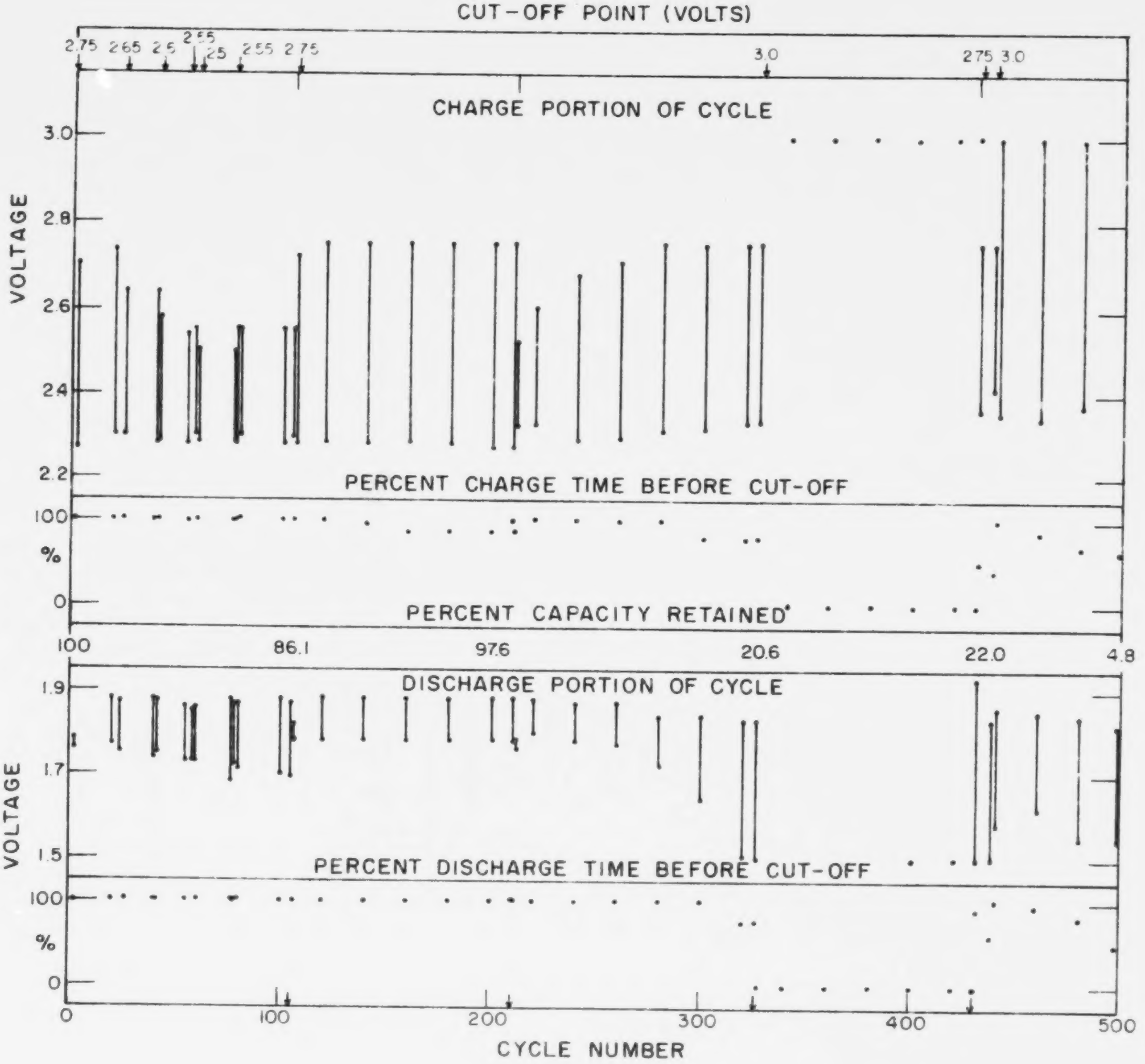

Fig. 23. Cycling performance characteristics of Universal Grenox positive material pasted in an idealized iR-free,one-sided laboratory test Pb/Sb grid to a depth of 20 mil – Pb/Sb-2

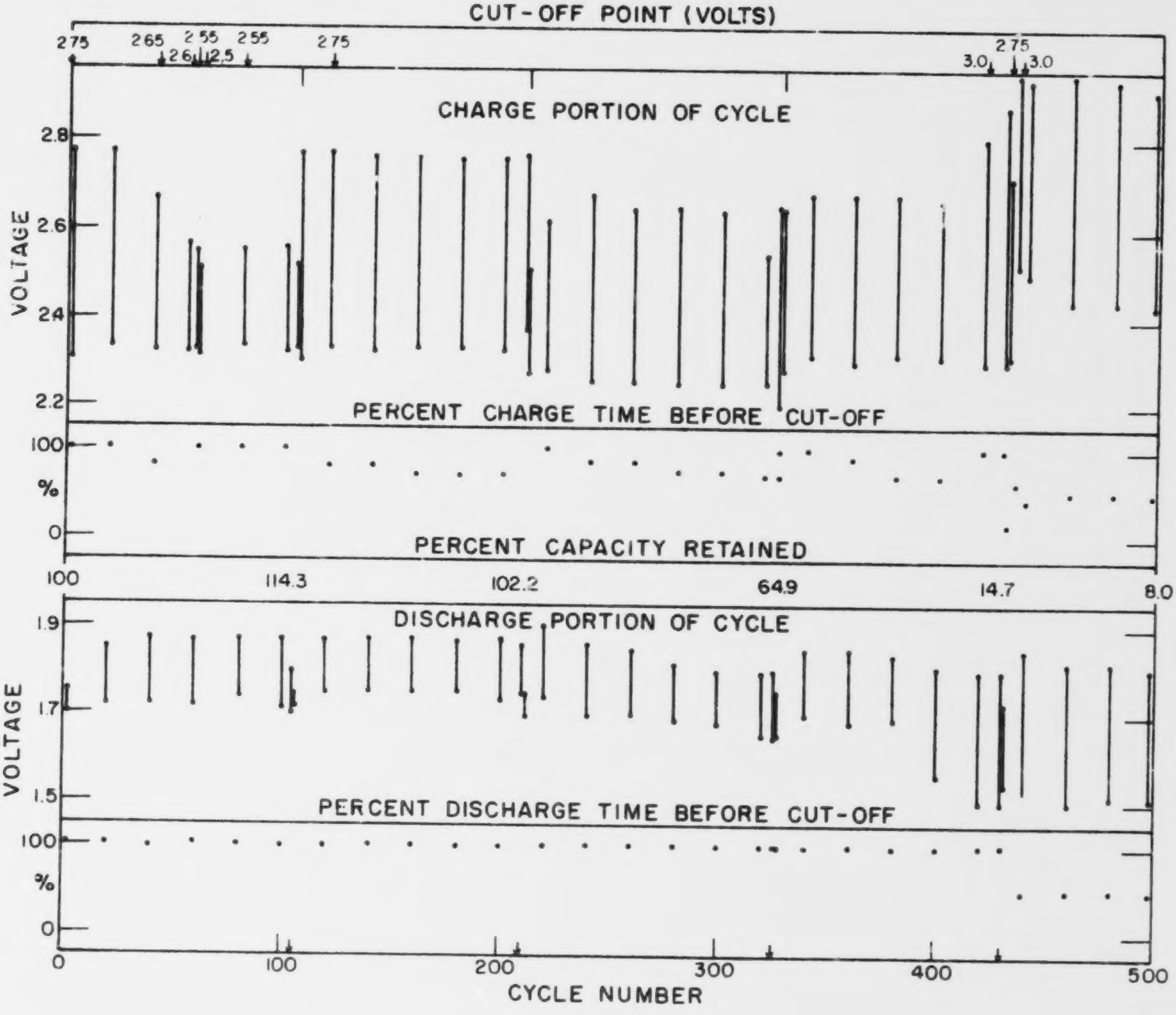

Fig. 24. Cycling performance characteristics of Universal Grenox positive material pasted in an idealized iR-free, one-sided laboratory test Pb/Sb grid to a depth of 20 mil – Pb/Sb-3.

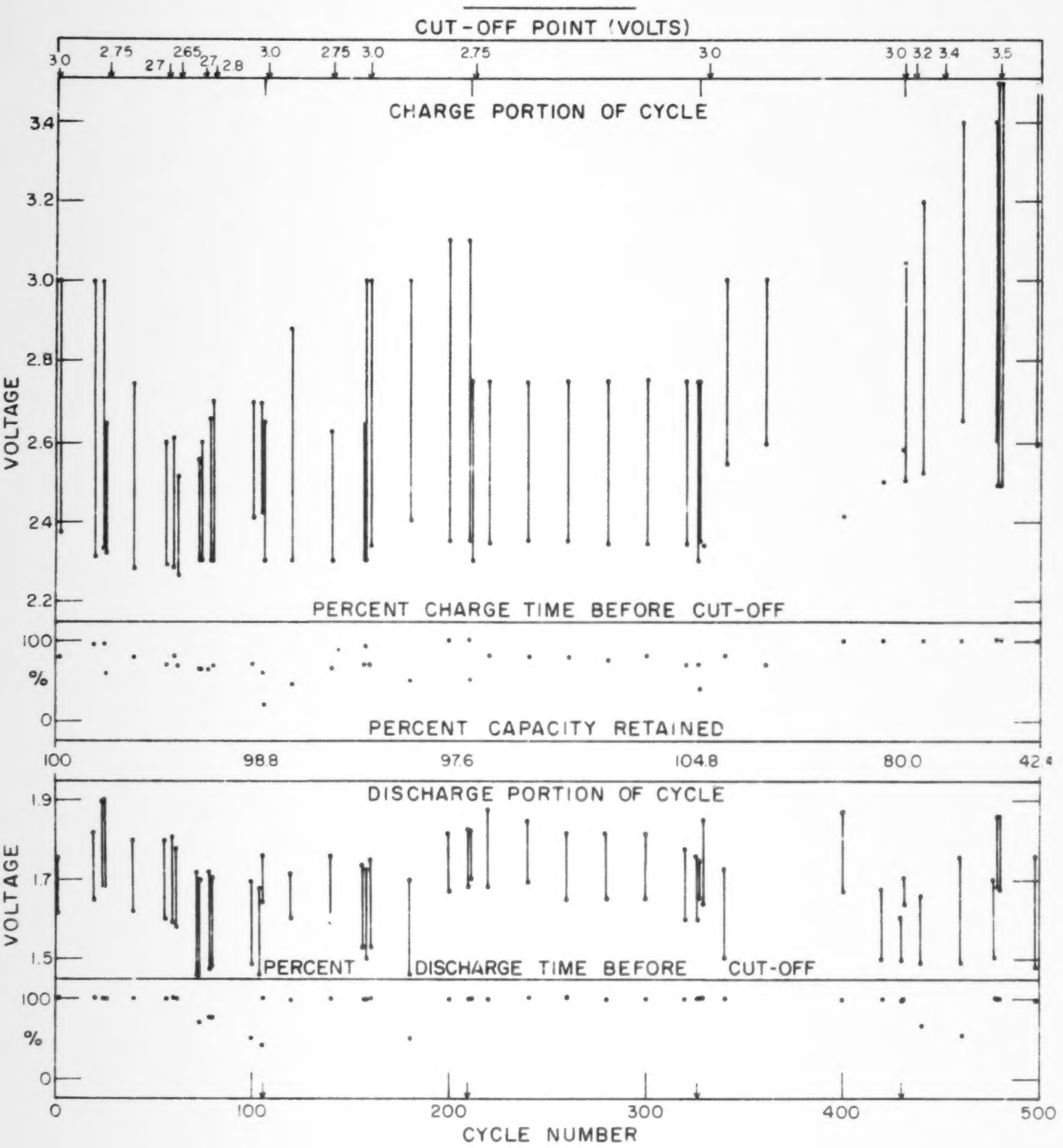

Fig. 25. Cycling performance characteristics of Universal Grenox positive material pasted in an idealized iR-free, one-sided laboratory test Pb grid to a depth of 20 mil and with H_3PO_4 added to the electrolyte – Pb H_3PO_4-7

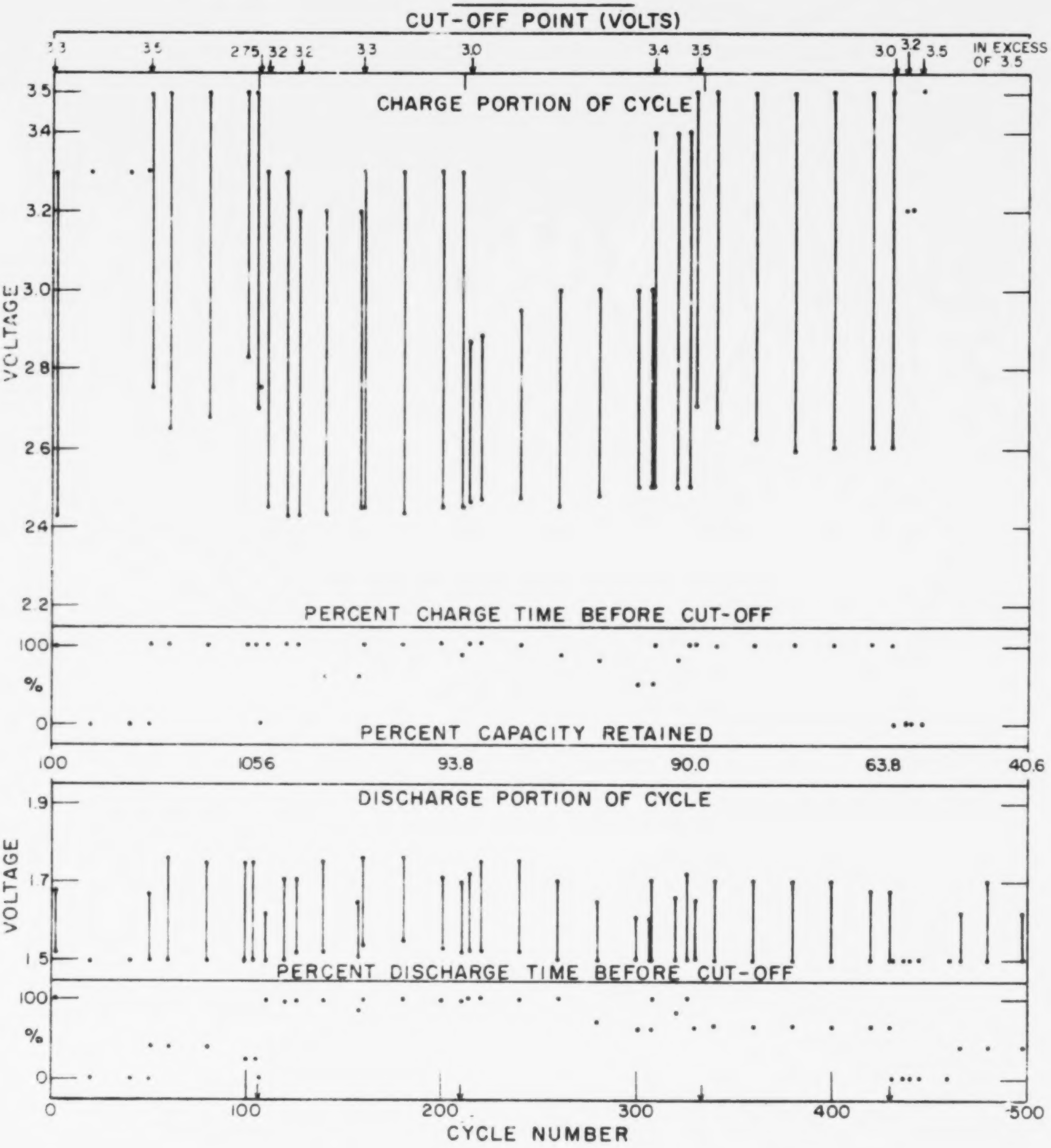

Fig. 26. Cycling performance characteristics of Universal Grenox positive material pasted in an idealized iR-free, one-sided laboratory test Pb grid to a depth of 20 mil and with H_3PO_4 added to the electrolyte – Pb H_3PO_4-8

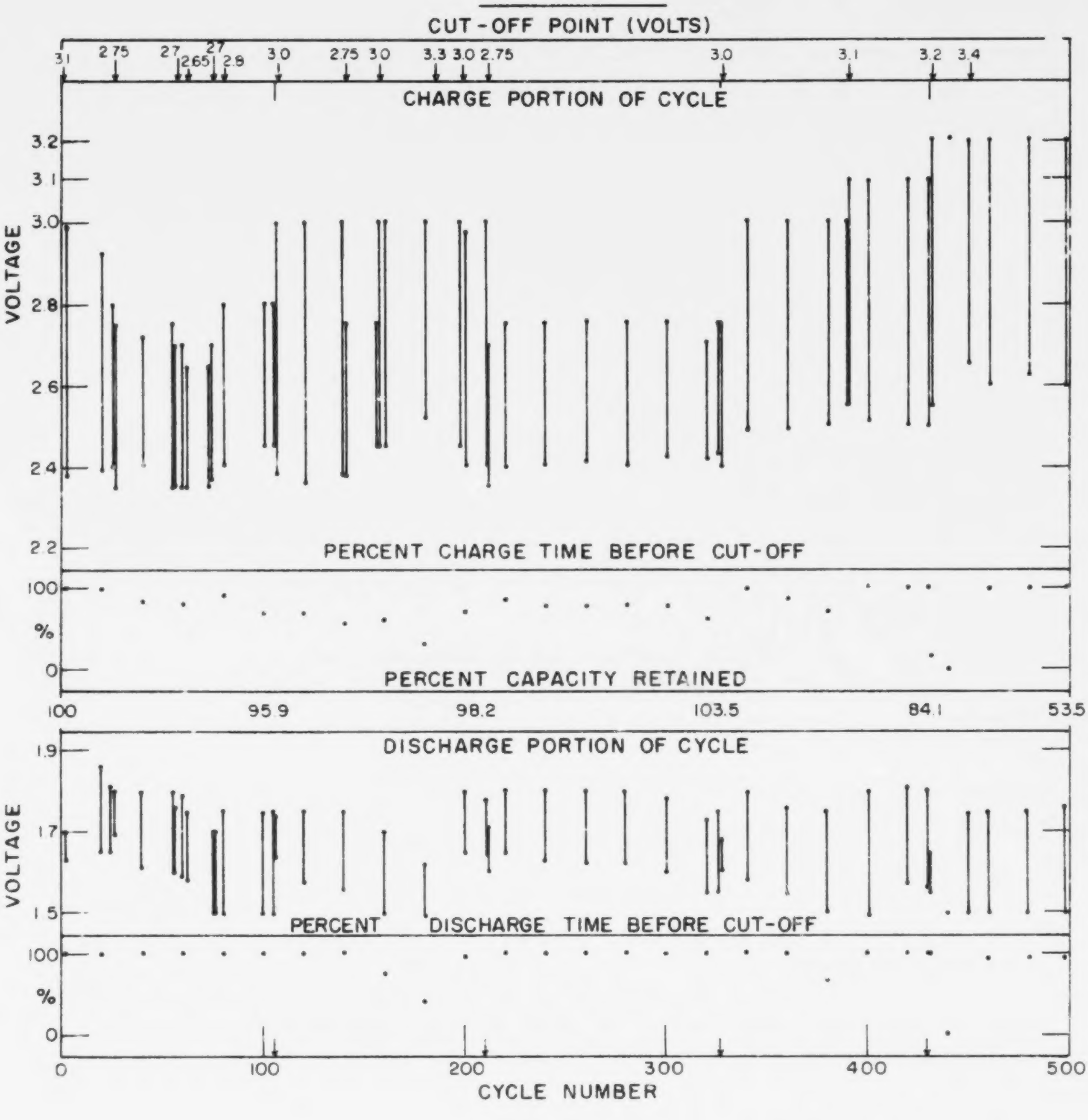

Fig. 27. Cycling performance characteristics of Universal Grenox positive material pasted in an idealized iR-free, one-sided laboratory test Pb grid to a depth of 20 mil and with H_3PO_4 added to the electrolyte – Pb H_3PO_4-9

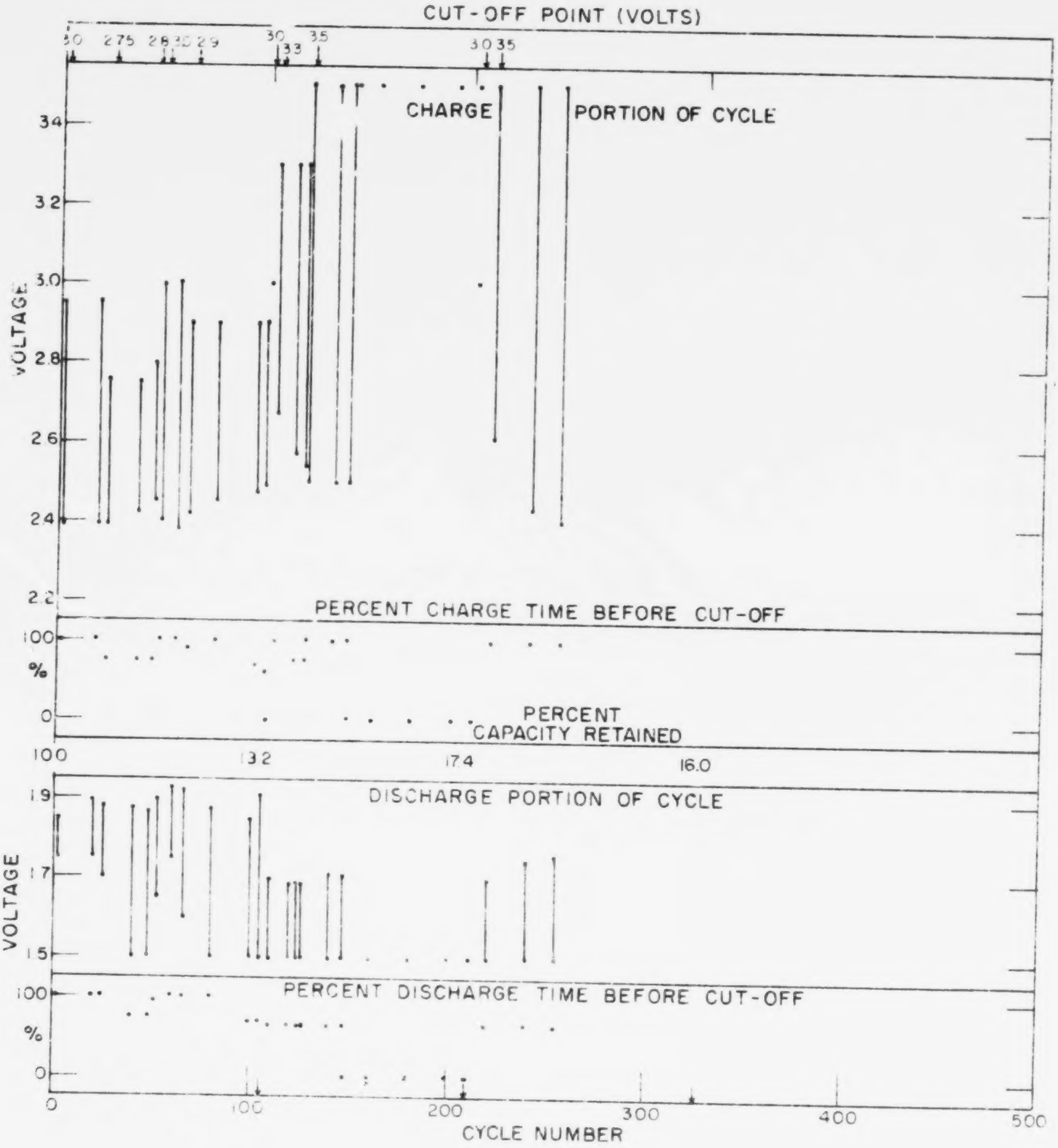

Fig. 28. Cycling performance characteristics of Universal Grenox positive material pasted in an idealized iR-free, one-sided laboratory test Pb grid to a depth of 20 mil and with no additions – Pb-5

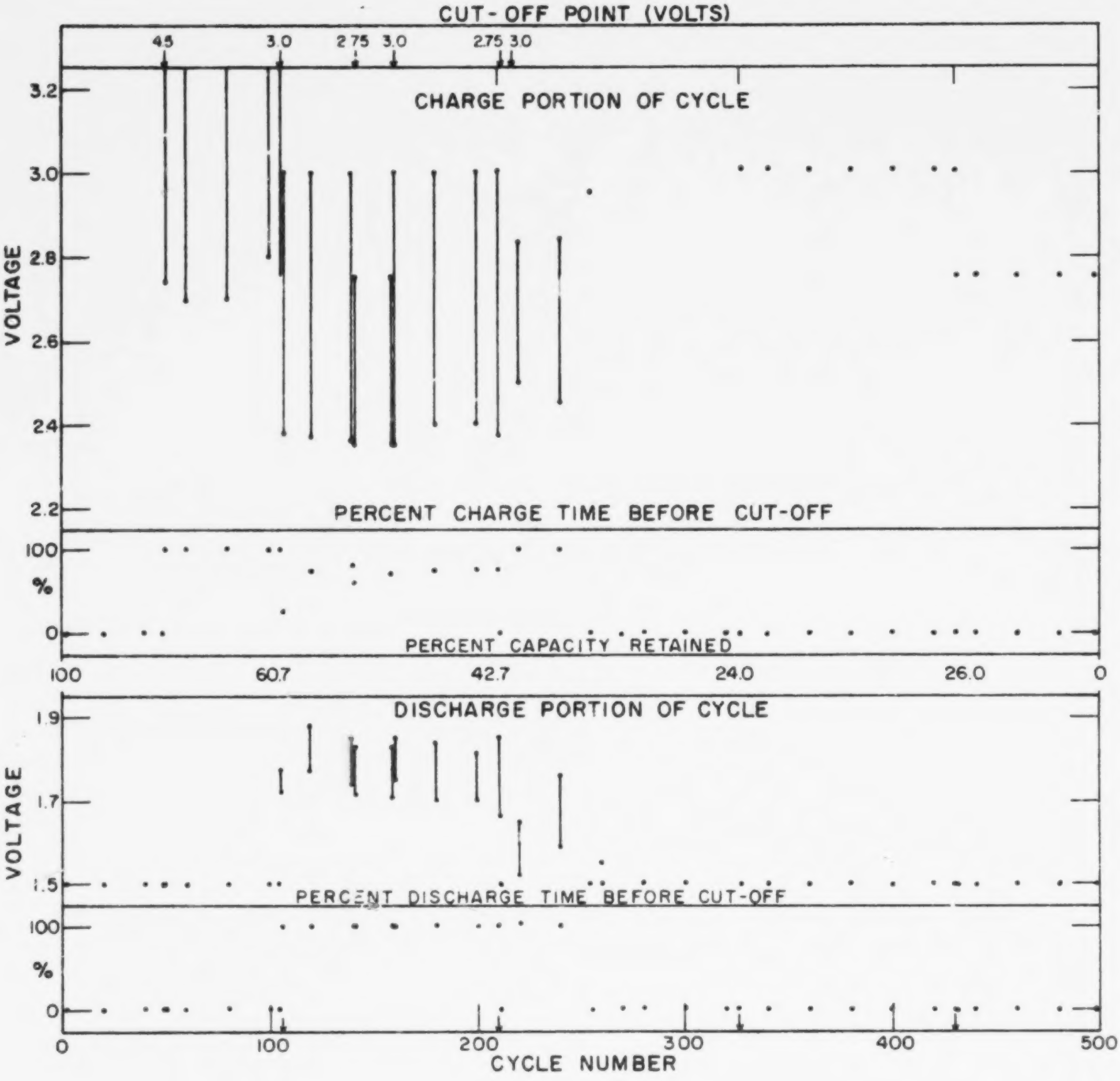

Fig. 29. Cycling performance characteristics of Universal Grenox positive material pasted in an idealized iR-free, one-sided laboratory test Pb grid to a depth of 20 mil and with no additions – Pb-6

e. The oversized negative plates all behaved very well on discharge, generally exhibiting a voltage of ~1.0 V versus Hg/Hg_2SO_4. On charge, negative plate potentials varied somewhat. When the plates were undercharged, the voltage was $\leq$ 1.15 V. When gassing, voltages as high as 1.45 V were recorded.

f. When performing well, positive plate potentials on charge were ~1.45 V at the end of the charge cycle while on completion of the discharge cycle the potential was generally ~0.84 V versus Hg/Hg_2SO_4.

g. Failing cells exhibited positive plate potentials in excess of 1.6 V versus Hg/Hg_2SO_4 on charge and down to 0.6 V on discharge.

h. Failed positive plates exhibited very poor paste adhesion in the onesided iR free grid.

2. Overall cell performance of plates with pure lead grids and H_3PO_4 additions to the electrolyte

a. The Pb/H_3PO_4 positive plates all behave extremely well on cycling over most of 400 complete cycles. After 320 cycles, the capacity retention is 105%, 104% and 90% - far superior to the Pb/Sb plates. After 500 complete cycles, the values are 42%, 54% and 41%.

b. The decay in voltage during discharge is more marked for these plates and occurs also at lower values. When performing well, the voltage decay during a discharge cycle was on average 0.19 V.

c. During charge, cell voltages in excess of 3.0 V were common on completion of the charge cycle.

d. Final discharge voltages are in excess of 1.6 V when each cell is performing well.

e. On charge, the positive plate potentials are of the order of ~1.6 V versus Hg/Hg_2SO_4 when the cell is behaving well. Values in excess of this were recorded towards completion of the cycling experiments. On discharge, the voltage approaches 0.74 V versus Hg/Hg_2SO_4.

f. Negative plate potentials (oversized plates) are constant near 1.0 V versus Hg/Hg_2SO_4 during discharge but depending on the state of charge of the plate, may vary during charge from 1.06 V to > 1.6 V versus Hg/Hg_2SO_4. This is caused by an increase in the hydrogen overvoltage on the plate when no Sb is present and is one reason why such large cell voltages are observed at end of the charging cycle. In addition, there is increased polarization of the positive plate.

g. Even after 500 complete cycles, there was still very good paste retention in the one-sided plates.

3. Overall cell performance of plates with pure Pb grids without H_3PO_4 additions to the electrolyte

Very poor performance was observed with all these plates and most did not last more than 200 complete cycles. After 200 cycles, 19%, 42%, and < 10% capacity was retained by the three test plates. As with the Pb/H_3PO_4 plates, excessively high cell voltages are obtained during charge. The cells have no apparent durability as regards cycling life. Failed cells showed very poor paste adhesion reminiscent of that in the Sb containing cells after more extended cycling tests.

Our basic conclusions with respect to the above are that Sb can be removed from the cells provided H_3PO_4 additions are used instead. Though there is a fall in overall capacity (C/5) following H_3PO_4 additions (~25%), the capacity retention during cycling of the latter plates appears to be better than on the plates containing Sb, when both are cycled in the same manner. The final voltage of laboratory test cells containing Sb is > 0.1 V higher than that of the Pb/H_3PO_4 test cells during discharge. If the negative plates are near full charge, gassing occurs on the Sb-free plates at potentials substantially more negative than on those plates containing Sb. No excessive negative-plate degradation is observed, however. Because the negative plate potential shifts markedly according to its state of charge, it can seriously affect investigations by cutting out cells when the positive plate is still capable of performing well. This is a factor which requires careful consideration in examining the results presented here. The positive plate, when fresh, is polarized by 0.1-0.2 V when Sb is absent from the cells. When the cells have been tested for > 300 cycles, the Pb/Sb plates also have high positive plate potentials on charge. With the H_3PO_4 containing cells, no paste degradation is noted as a result of positive plate polarization.

We have examined the plates visually after cycling and find poor paste retention and softening in those plates with Pb/Sb grids and with pure Pb grids. The plates of pure Pb with H_3PO_4 added to the electrolyte exhibit a much better surface appearance and have not nearly so much shedding. They are still, however, softened somewhat on the sur face of the paste. A "slippery" whitish film is also present on these plates - probably a phosphate containing compound. No X-ray or electron microscopic investigations or paste microstructure were carried out here due to time limitations.

C. Factors Not Varied in the Study of Electrochemical Performance

Mainly because of time limitations the following were not varied in our experiments:

1. Surface area of active material (as defined by additions of Pb_3O_4 to litharge).
2. Separator material: For tests with commercial plates, the separators supplied with the batteries were employed. The same type of separators were used when examining the effect of Sb and H_3PO_4 on paste performance. For tests with novel designs, industrial Daramic separators were employed.[27] This is an extruded polyethylene material.
3. Electrode retainer: For tests with commercial plates and in examining the Sb and H_3PO_4 questions, no retainers were used. For tests with bipolar plates 3-mil glass mat retainers were used.
4. Sulfuric acid concentrations: Constant at 1.28 sp gr.
5. Cycling temperature: Constant at 30°C ± 1°C.

6. Nature and amount of expander in the negative plate: This was kept constant at 2% of an industrial "KX" expander supplied by NL Industries.

7. Specific gravity of H_2SO_4 used in the formation process: This was kept constant at 1.08.

8. Use of tetrabasic lead sulfate based paste instead of lead oxides as starting material: This was not examined.

9. Morphology of the active material (as defined by the curing process and the nature of the original oxide mix): We did attempt to use Barton VLY oxide with and without a high temperature curing schedule. Particularly in the latter case, poor adhesion of paste was observed so we did not extend these evaluations. With Universal Grenox oxide, a conventional room temperature cure was employed at all times.

10. Paste stabilizers: $< 1\%$ of dynel fibers were added to the positive paste to enchance mechanical paste stability during cycling. This is a common industry procedure. With later novel plate designs the same amount of fibers was added to the negative paste for the same purpose.

11. Porosity of active material (as defined by the amount of H_2SO_4 added during the mixing): This was kept constant at 42.5 cc of 1.4 sp gr H_2SO_4 per lb of positive oxide and 38 cc of 1.4 sp gr H_2SO_4 per lb of negative oxide. For early experiments with Barton VLY oxide, this amount was varied but with varying success as indicated by subsequent performance results.

D. Conclusions

The following major conclusions were drawn from the foregoing data:

1. To optimize a lead acid battery for use in hybrid electric vehicles, a large number of thin plates should be used. The operating current density is thus reduced. Paste utilization is substantially increased in thin plates compared to that in conventional plates operating at the same current density.

2. Particularly on cycling, there is a serious problem with conventional plates operating at high power densities which is caused by longitudinal resistance losses along and down the grid. This results in uneven utilization of active mass and, therefore, high local depth of discharge even when the overall depth of discharge is shallow. Paste shedding results. When these resistance losses are minimized there is a marked improvement in paste performance at the same, high operating power densities.

3. To maintain cycle life in a battery which contains no Sb in the grid, paste or electrolyte, (for example when pure Pb is used as grid material) small additions of H_3PO_4 to the electrolyte are very effective.

V. TASK IV. CORROSION OF SUBSTRATE MATERIALS

The problem of corrosion in a lead acid battery is a severe one [22, 28-30] and greatly reduces the number of candidate materials. Particularly in a bipolar design, with thin plate structures, corrosion may be expected to seriously affect plate life if adequate materials are not chosen. This is particularly true in the 1.28 sp gr H_2SO_4 electrolyte chosen[4] to meet the desired high power density applications. Corrosion of the grid, which, in a bipolar design, can be either a conductive, high strength/light weight metal sheet of suitable design, or a system based on a plastic substrate with metal strips as conductors laid on the surfaces of the substrate, was of prime concern. Because there are a number of commercially available separators and retainers of suitable type and dimension,[4, 27] these were not considered further from the corrosion aspect. Choice of appropriate plastic for the battery case was, however, also examined.

The choice of a grid material or materials involves a compromise between the increase in active mass utilization concurrent with a reduction in active mass thickness and the increased likelihood of plate failure by corrosion of thin cross-section grid members. The aim of this study was to provide information on the most suitable material for grid and case construction. In particular, plastic materials, both conductive and nonconductive metal substrates, e.g., Ti, TiN, Al, Mg, C and conventional Pb based grid alloys were investigated.

A. Metal Substrates

1. Metals other than Pb and Pb based alloys

There are several materials of choice, namely Ti, TiN, Al and Mg, all of which are theoretically very desirable. They are light weight/high strength materials and because of their good conductivity can be used both to support the active mass and also to conduct the current over the entire plate area during discharge. Even in thin cross-sections, no reinforcement is necessary (in contrast to Pb or Pb based materials of similar dimensions). Most of these metals have been examined at one time or the other in the past but there are few recorded results of their behavior in Pb acid batteries. Unfortunately, Al and Mg both corrode rapidly when exposed to H_2SO_4 and attempts to protect Al from corrosive attack in H_2SO_4 by an overplating with Pb have also proven unsuccessful due to imperfections in the plate. Ti metal at the potential of the negative lead acid plate also corrodes readily.[31] At the positive plate potential, TiO_2 is formed and inhibits further corrosion but acts as a dielectric.[31] TiN does not corrode in H_2SO_4 at either the positive or negative plate potentials.[31.32] However, on the positive plate at the interface between the nitride and the pasted lead oxides, a dielectric TiO_2 film is again formed.[32] This gives poor paste adhesion and results in insignificant charge and dis-

Preceding page blank

charge capabilities of the paste.[32, 33] The use of a flash of Au on the TiN has been proposed[33] to alleviate the latter problem. In the context of the present contract, this solution was thought to be unacceptable because of the economics involved. Instead, we studied briefly the use of conductive plastic coatings to protect the metals from the corrosive environment while still maintaining electronic contact with the paste.

Tests were initiated on metal plaques using Al, Mg and Ti coated with a conductive epoxy material. The conductive coating was made from epoxy resin no. 828* and curing agent Z,* using 60% TiN powder of 325 mesh as conducting medium. Typically, after the coating process, it was necessary to grind the coating to achieve adequate conductivity. This was because the TiN particles tended to settle during curing of the epoxy. Conductivities varied with coating thickness. For example, at 1-mil thickness, the resistances were 3 Ω/in.^{2} for the coated Al plaque, 4.4 Ω/in.^{2} for the Mg, 3 Ω/in.^{2} for the Ti. For a 2-mil thickness, the Mg plaque exhibited a very high resistance, whereas for Ti the resistance was 4.4 Ω/in.^{2}. Difficulty was encountered in preparing a conductive coating of suitable consistency, in that if the coating was too thin the epoxy tended to flow off the surface and the TiN particles settled rapidly, leaving a rough granular surface of low epoxy content. If the coating was too thick, then it was very difficult to apply. This was an even greater problem with graphite 325 mesh material as conductive medium. Here it was necessary to use a 50 wt % graphite/epoxy mixture to achieve any type of coating. Even after grinding to 1-mil final thickness, such coatings still exhibited 1 KΩ/in.^{2} resistance on each panel. We did not use conductive materials in less than 50 wt % quantities because poor conductivities are observed[34] at values lower than this.

The TiN conductive epoxies coated on Al, Mg and Ti panels were potentiostatted at 1.25 V versus Hg/Hg_2SO_4 in 1.28 sp gr H_2SO_4 at 60°C. After 6 days, the Mg panel showed severe blistering and the current was 60 mA. After 8 days, the Al panel also showed severe blistering and the current was 29 mA. Both Al and Mg panels showed severe dissolution of the underlying metal. After 10 days, the Ti panel showed small blisters in the center of the plate which gradually spread until after 27 days total, the coating showed no adhesion to the panel. The corrosive current was 0.1 mA.

The results emphasized the difficulty in working with metals which corrode in H_2SO_4 media. As has been noted before, e.g., with Pb cladded Al, if any imperfections in the coatings develop, then catastrophic failure occurs. These imperfections were obviously present in our coatings. The Ti did not exhibit such a high corrosion rate because of its protective oxide. Because of these problems, we did not extend our experiments on these metallic substrates any further but concentrated instead on what we felt were the more attractive alternatives of plastic based substrates with Pb based materials as electronic conductors laid on each side of the substrate.

2. Pb and Pb alloys

Pure Pb or Pb alloys can theoretically be used as grid (active mass support and current conductor) in a bipolar design but in practice, the sheets have to be of impractical thickness for this purpose. Thus, there is a problem of corrosion through the sheets which would have to be excessively thin to conform to battery weight requirements. Also, such thin sheets (≤ 40 mil) would in any event be unable, solely, to support the active mass.[4]

---

*Supplied by the Shell Chemical Company.

Due to predominant formation of PbO_2 on the positive side, buckling can also be expected.[28] These factors, however, do not preclude the use of Pb or its alloys as current conductors in a bipolar plate with a plastic substrate to support the active mass. Because of this, we have also examined the corrosion and expansion of these materials in H_2SO_4.

A substantial quantity of data have been published on the corrosion and expansion of Pb and Pb alloys in H_2SO_4.[22,28-30,35] These have been reviewed and, in the following, a brief discussion is given of the factors we considered in the selection between the three conventional current conductors, namely: Pb/Sb alloys and Pb/Ca based alloys and pure lead. Results of corrosion tests in this laboratory are also recorded.

a. Strength: As noted, by itself pure Pb does not have sufficient mechanical strength to support the active mass even in conventional automotive plates. Pb/Sb and Pb/Ca grids are intrinsically much stronger[4] but for the thinner plate structures (< 50 mil) which are desirable for high power density batteries, are themselves marginal. Such thin grids are also more difficult to cast.

b. Corrosion and expansion of positive grid: We have demonstrated earlier that to achieve a high power density lead acid battery, a larger number of thinner plates with minimized resistance losses would be desirable. Setting aside the mechanical strength aspect - which must also be considered in plate thicknesses < 50 mil (even for Pb/Sb or Pb/Ca alloys) - the limiting factor then becomes that of the plate failure by grid corrosion. As the grid thickness is reduced, so the likelihood of this mode of failure is increased. Of the three materials Pb, Pb/Sb and Pb/Ca, the former was believed to be least susceptible to this mode of failure. We carried out corrosion tests on annealed Pb, Pb/4.5% Sb and Pb/0.08% Ca grids at 30, 60 and 90°C over a 60-day period to confirm this. Tests were also carried out on the annealed materials coated with active mass (PbO_2) and on uncoated specimens. The latter were potentiostatted at the potentials attained by the coated specimens in the same solution (close to 1.25 V versus Hg/Hg_2SO_4). The aims were to compare the corrosion rates of the three materials and to investigate differences in corrosion rates as a function of coverage with active mass.

Testing of the uncoated specimens shown in Figs. 30-32 gave the relative corrosion rates of the three materials plotted as corrosion current versus time. As noted by Lander,[36] current measurements should not be taken as an absolute measure of the corrosion rate of Pb alloys since some gas evolution may also occur on the samples. No detailed analysis of the curves was carried out but it is evident that the most severe attack is experienced by the Pb/Sb alloy while the Pb and Pb/Ca samples exhibit similar rates of attack. Fluctuations in measured current are particularly evident with the Pb/Sb alloy possibly due to formation of passivating $PbSO_4$ layers and their periodic shedding from the specimens. Also, with the Pb/Sb alloy, the initial high rate of attack is presumably caused by depletion of Sb in the surface layers of the alloy.

After testing, the samples were removed and cleaned in ammonium acetate solution following the method of Lander.[36] Weight loss measurements are given in Table IV.

Clearly, the data confirm the current measurements and point to an increasing susceptibility to corrosion attack in the order Pb/Sb > Pb> Pb/Ca. This also is somewhat misleading as may be seen from Fig. 33 which is a photograph of the 90°C test samples. The

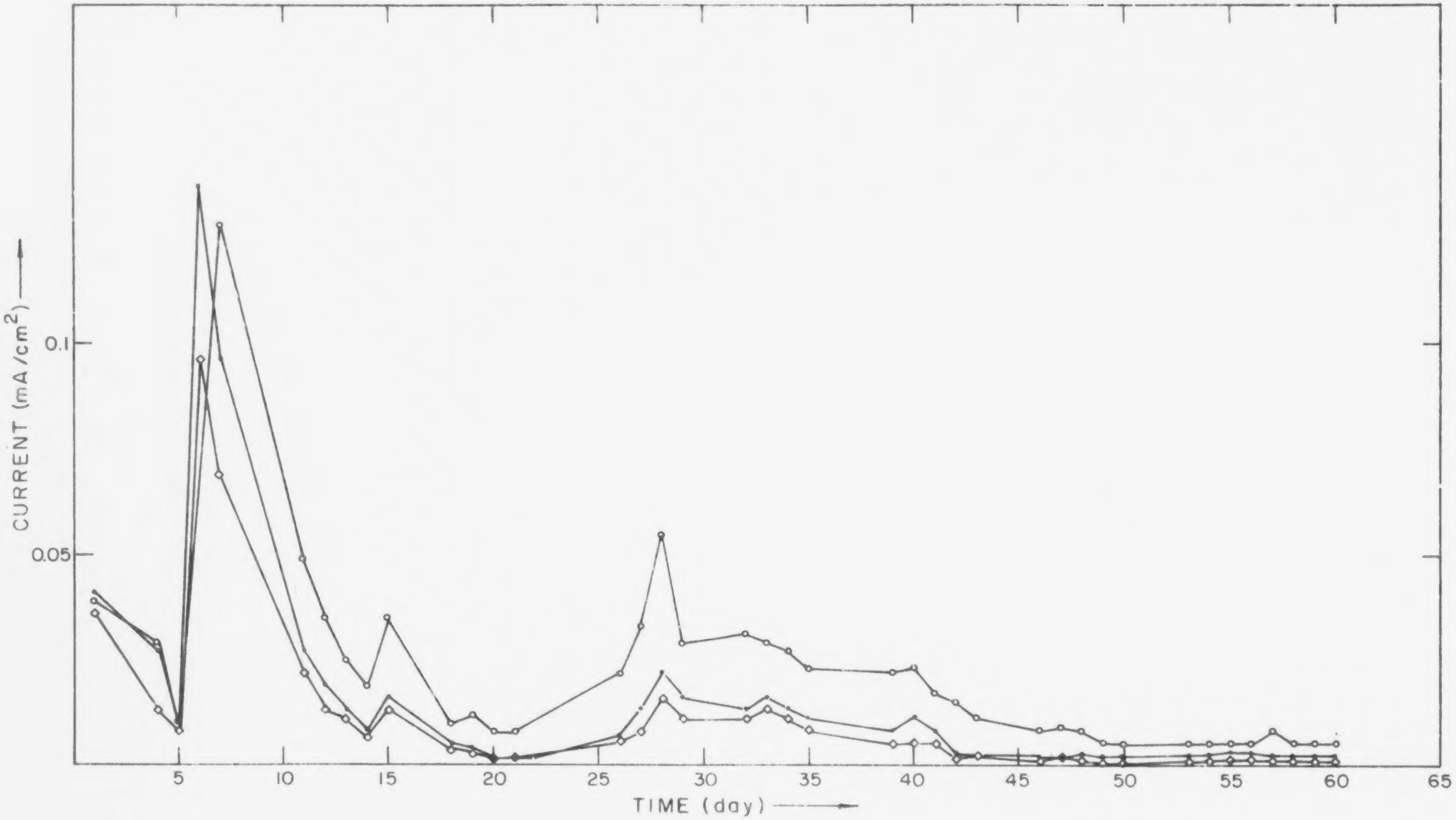

Fig. 30. Corrosion current of Pb, Pb/Ca and Pb/Sb grid samples held at 1.25 V (Hg/Hg_2SO_4) in 1.28 sp gr H_2SO_4 at 30 °C (◇, Pb/Ca; ●, Pb; ○, Pb/Sb)

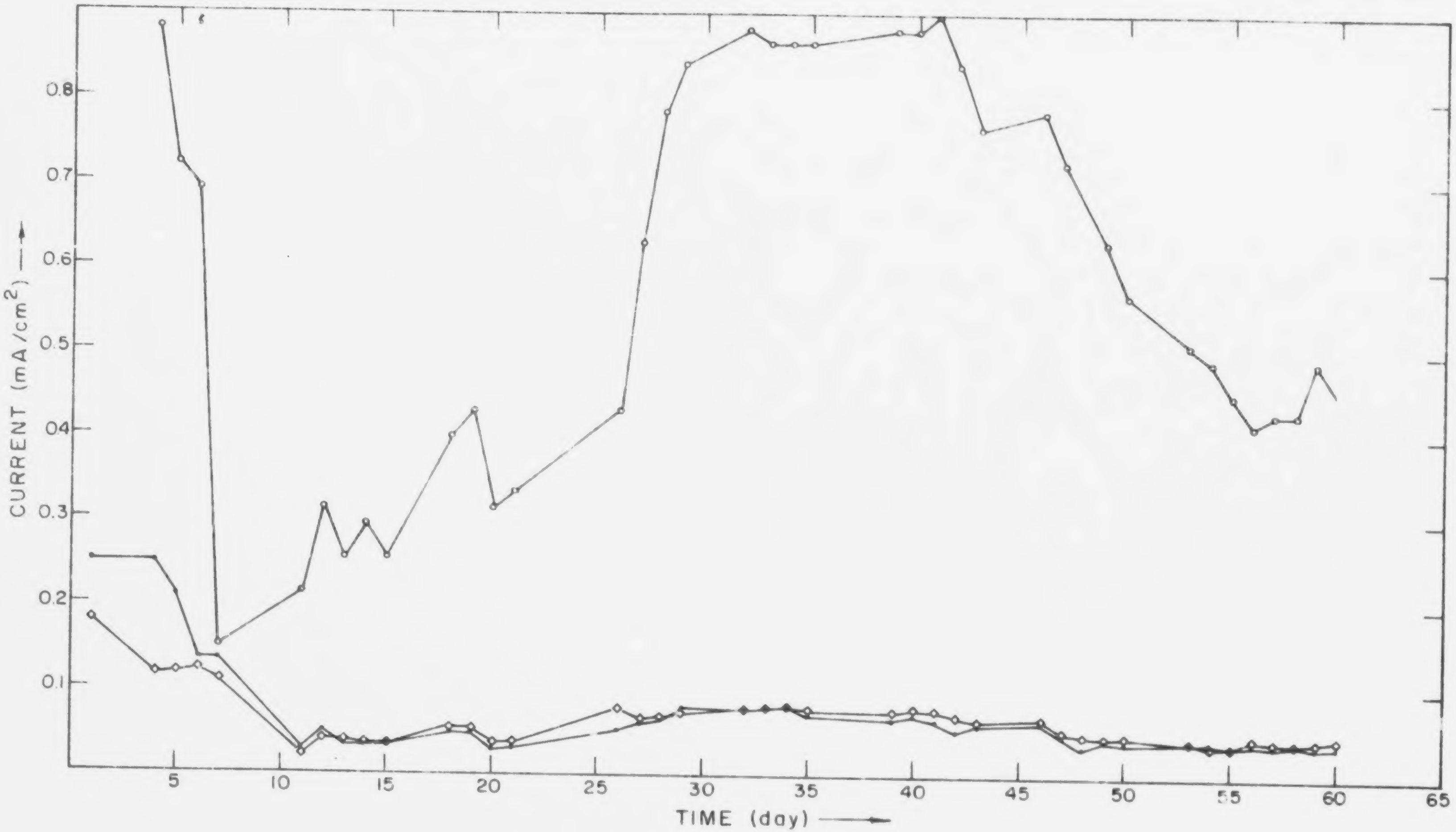

Fig. 31. Corrosion currents of Pb, Pb/Ca and Pb/Sb grid samples held at 1.25 V (Hg/Hg_2SO_4) in 1.28 sp gr H_2SO_4 at 60°C (◇, Pb/Ca; ●, Pb; ○, Pb/Sb)

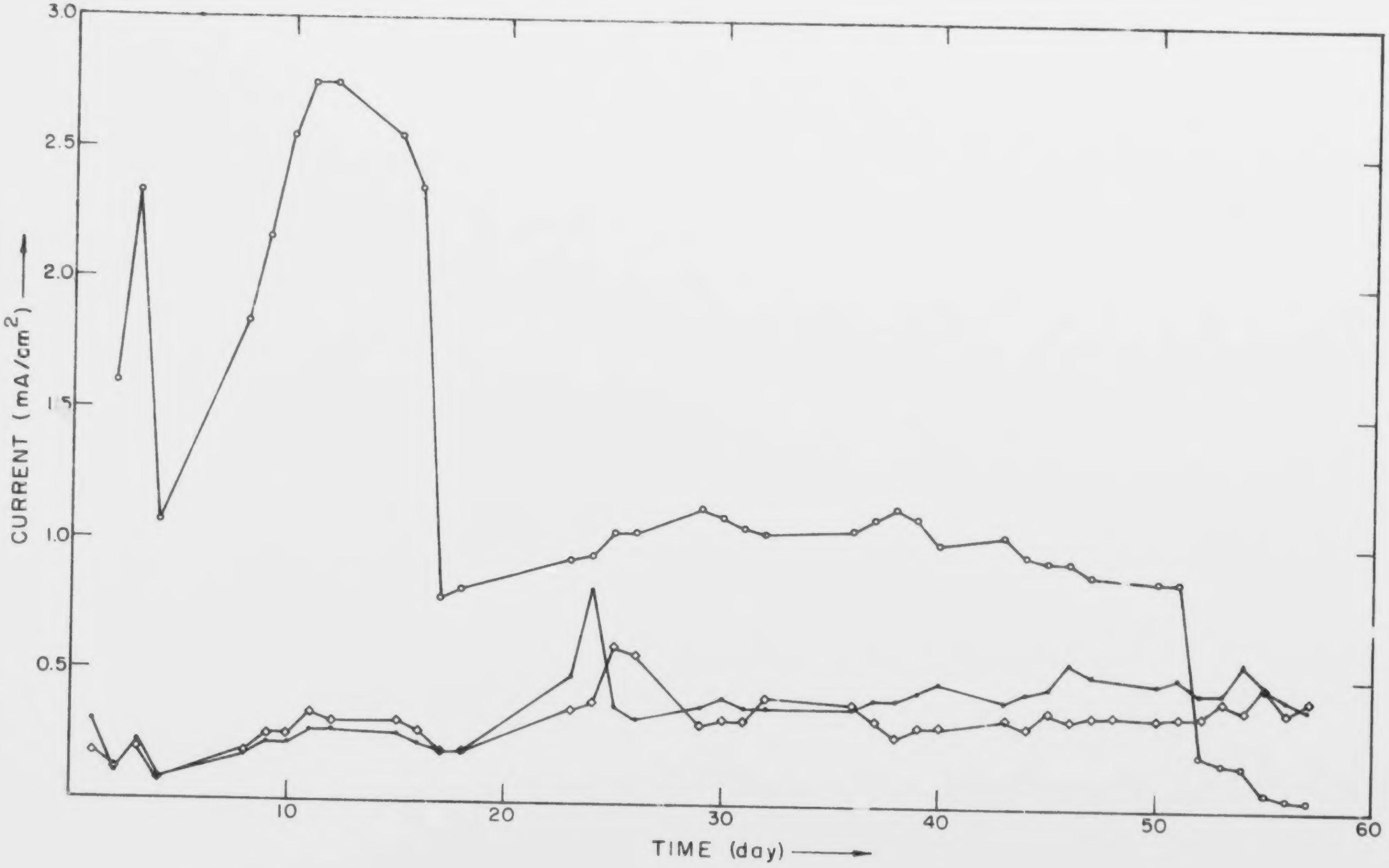

Fig. 32. Corrosion currents of Pb, Pb/Ca and Pb/Sb grid samples held at 1.25 V (Hg/Hg$_2$SO$_4$) in 1.28 sp gr H$_2$SO$_4$ at 90 °C (◇, Pb/Ca; ●, Pb; ○, Pb/Sb)

Reproduced from best available copy.

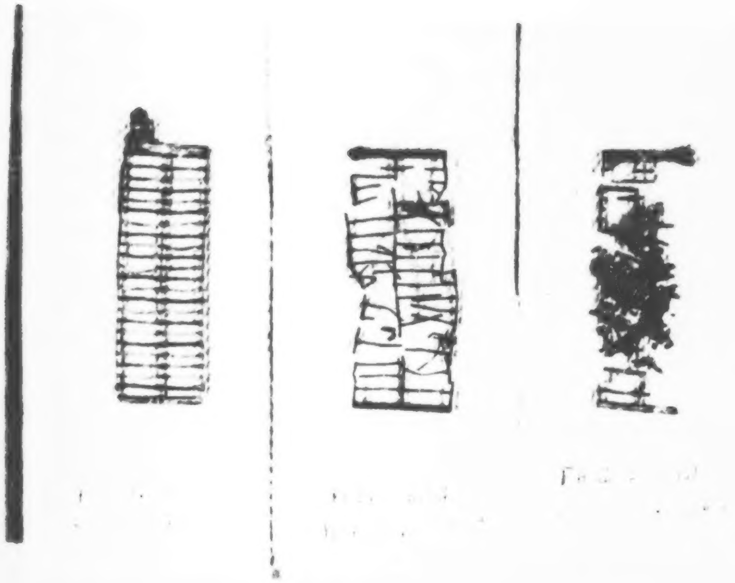

Fig. 33. Photograph of "bare" grids after corrosion in 1.28 sp gr H_2SO_4 at 1.25 V (Hg/Hg_2SO_4) at 90°C after 60 days

Table IV. Comparison of the Weight Losses (g) of Pb and Pb Alloys in 1.28 sp gr H_2SO_4 at Various Temperatures After 60 Days Immersion

	Temperature					
	30°		60°		90°	
Alloy	Original Weight	Weight Change	Original Weight	Weight Change	Original Weight	Weight Change
Pure Pb	14.2865	0.0565	13.7870	0.2270	14.0395	2.4695
Pb/0.08% Ca	13.8223	0.0423	13.7155	0.1455	13.3297	2.0497
Pb/4.5% Sb	18.0567	0.5967	17.9865	2.9965	17.9925	11.2825

Pb/Ca and Pb/Sb grids are almost completely disintegrated, whereas the Pb grid has corroded but still maintained its shape. The latter may be attributed to severe intergranular attack in the Ca and Sb containing alloys.[28] As pointed out by Wesson,[37] corrosion attack in soft lead grids commences along grain boundaries even during the formation process. In lead calcium alloys, grain boundaries are attacked only in service but to such an extent that not only the individual grains, but whole areas, are cut off and consumed giving rise to cavity formation and grid fracture, as we have observed. In Pb/Sb alloys, the eutectic corrodes, but since this is of a finer structure than in the Pb/Ca alloy, the overall corrosion is more uniform and therefore less destructive. The results confirm that pure Pb is the material of choice to maximize corrosion resistance.

The effect of an overpasting of active material (PbO_2) on the corrosion rates of the above three materials was measured also. This was considered to be worth studying since it is the practical situation in a battery and a review of previously recorded corrosion rates on "bare" Pb based alloys had suggested that the life of conventional grids would be much shorter than is actually observed. The inference was that an overpasting of active mass led to decreased corrosion rates but no data were presented to substantiate this fact. Pb, Pb/4.5% Sb and Pb/0.08% Ca grids of the same configuration as those in the above tests were overpasted with active material which was then oxidized to PbO_2 on the grids in 1.08 sp gr H_2SO_4 at 30°C. The samples were then immersed as before in 1.28 sp gr H_2SO_4 at 30°C, 60°C and 90°C for 60 days. After this period, they were cleaned of active mass, the oxide removed in ammonium acetate solution[36] and weight loss then evaluated. This is expressed in Table V on a percentage basis and a correction has been applied for the weight loss incurred during the formation of the positive active mass on the grids before corrosion testing. (The correction factor was obtained simply by forming PbO_2 on exactly similar grids under the same conditions and for the same time as before. The grids were then cleaned of active mass and the oxide removed in acetate solution. Finally, the weight losses incurred during paste formation were measured.) Comparative percentage weight losses are included in Table V for the samples not covered with an overpasting of active mass during corrosion testing.

---

*In all of these tests an attempt was made to keep the geometric area of the test grids of the three different materials as closely similar as possible. This also applied to the tests with overpasted grid samples.

Table V. Comparison of Weight Changes (%) in Pb and Pb Alloy Grids With and Without an Overpasting of Positive Active Mass When Immersed in 1.28 sp gr H_2SO_4 at Constant Potential for 60 Days

	30°C			60°C			90°C		
Alloy	Pb	Pb/Ca	Pb/Sb	Pb	Pb/Ca	Pb/Sb	Pb	Pb/Ca	Pb/Sb
Unpasted Samples	0.4	0.3	3.3	1.6	1.2	17.5	17.5	15.3	62.5
Pasted Samples	3.7	0	3.5	3.7	1.8	11.1	13.7	7.2	15.8

The above method of correcting for corrosion weight losses during formation of the pasted grids was not thought to be very accurate. In the case where comparable weight changes were observed on subsequent corrosion of the samples by immersion at low temperatures in 1.28 sp gr H_2SO_4, an accurate evaluation of the effect of an overpasting of active mass on underlying grid corrosion was not obtained. However, whereas the weight change arising from corrosion of the grid during PbO_2 formation was both constant and low (since formation temperature was low and constant), the magnitude of weight losses arising from subsequent corrosion of the samples immersed in 1.28 sp gr acid, increased with increase in temperature. Especially at 90°C, the correction factor was relatively small when compared with the overall final weight change. At 90°C, it is evident that the samples overpasted with active mass prior to corrosion all exhibit lower corrosion rates than for corresponding unpasted samples. Photographs of the former alloys corroded at 90°C are shown in Fig. 34 after removal of the active mass and ammonium acetate cleaning.

We conclude from the above that reduced corrosion rates may be expected in Pb alloys overpasted with active mass. The extent of the reduction is estimated to be in excess of 20% - which is a substantial improvement in terms of grid lifetime.

Associated with corrosion, there is an expansion of the grid due to the lower density of the formed PbO_2 as compared with lead.[28] This expansion sometimes leads to plate failure due to loosening of the contact between the active mass and the grid. Expansion is somewhat less in Pb [28] than in Pb/Ca due to its slower corrosion rate. With Pb/Sb alloys of high Sb content, expansion is still less of a problem because the Sb dissolution compensates for the volume increase in PbO_2. The choice between Pb and Pb alloys, however, does not rest solely on the above characteristics. For example, Sb also has other effects on Pb acid battery performance which are discussed below.

c. Effect of positive grid material on the negative plate: During corrosion, Sb is released in the electrolyte from the positive grid and migrates to the negative plate where it deposits.[13] Once there, it lowers the overvoltage for hydrogen evolution on the negative plate (see Task III in this report) and this causes the following adverse effects: (1) it facilitates gassing of the negative during charge resulting in higher consumption of electrolyte and increased maintenance requirements;[23-25, 28] (2) it prevents adequate charging of the battery particularly as more Sb plates out on the negative (the current instead goes increasingly into gas evolution); (3) it gives rise to grid corrosion and overcharge (also with gas evolution) on the positive plate; since more current is required on float, and (4) it causes self-discharge of the negative plate by local cell action.

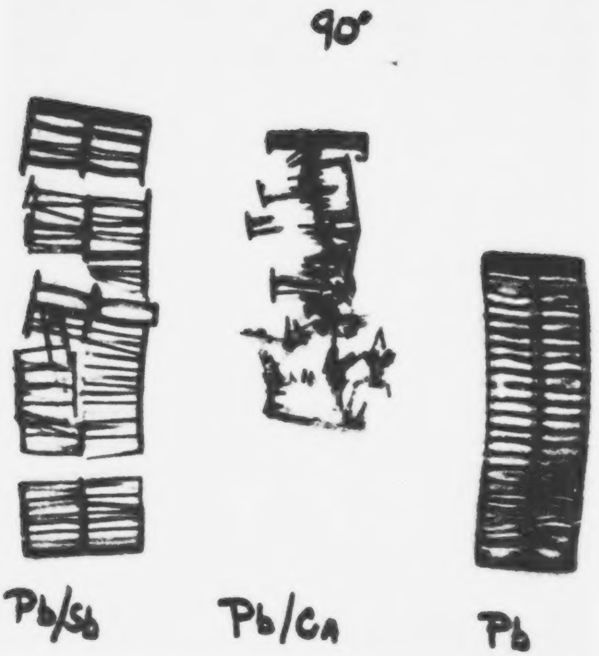

90°
Pb/Sb
Pb/Ca
Pb

Fig. 34. Photograph of grids corroded in 1.28 sp gr H_2SO_4 (with an overcoating of PbO_2) at 90°C for 60 days

d. Effect of grid material on positive paste: A positive aspect regarding the use of Pb/Sb alloys in battery grids is that Sb becomes incorporated in the positive paste improving its performance.[13-17,38] Hence, a larger number of cycles is permitted before failure occurs. We have confirmed this finding (Section III) using high rate/shallow discharge cycles, but have also shown that when no Sb is present in either grid or electrolyte, (i.e., using pure Pb grids) H_3PO_4 additions to the electrolyte have the same positive effect[18-21] on cycle lifetime. This latter observation obviates the need for Sb in the grid in regard to cycle lifetime and thus facilitates the development of a maintenance-free battery.

The preceeding discussion is summarized in Table VI which shows the advantages and disadvantages of pure lead, Pb-Sb alloys and Pb-Ca alloys, as grid materials.

Table VI. A Comparison of the Relative Advantages (+) and Disadvantages (-) of Three Grid Materials in Lead Acid Batteries

	Pb	Pb/Sb	Pb/Ca
1) Strength	-	+	+
2) Expansion of Grid	(+ -)	+	-
3) Corrosion of Grid	+	-	-
4) Self-discharge of -ve	+	-	+
5) Non-charge of -ve	+	-	+
6) Effect on PbO_2 of +ve	-	+	-
7) Gassing of -ve	+	-	+
8) Maintenance of free operation	+	-	+

3. Conclusions

a. Metals such as Ti, TiN, Al and Mg either with or without conductive coatings, Pb overplating, etc. are not suitable for use in Pb acid batteries without additional development work. The materials all corrode severely or form oxides which act as a dielectric.

b. Pb or Pb alloys cannot be used in sheet form as active mass support and current conductor in a practical bipolar high power density battery for hybrid vehicles. To resist corrosion and to be mechanically capable of supporting the active mass, the sheets have to be of impractical thickness with particular regard to battery weigh limitations.

c. The use of Pb or its alloys as current conductors in conjunction with a plastic substrate material support is not precluded from a corrosion or expansion aspect. Pure Pb is the material of choice by virtue of its corrosion resistance in acid compared to Pb/4.5% Sb and Pb/0.08% Ca alloys. It also has less expansion problems than the Pb/0.08% Ca alloy. It is estimated that a covering of active mass will reduce Pb corrosion in H_2SO_4 by at least 20%.

d. For maintenance-free operation, Sb should not be used in the grid material.

B. Plastic Substrates

These are attractive materials for use as plate substrates and as case materials because they are light weight and can have high strength, particularly when reinforced. A difficulty with bipolar plates in sealing each plate within the case is also minimized by the choice of plastic plates. As with metals, these materials also must withstand H_2SO_4 degradation.

The compatibility of plastics with Pb acid batteries has been examined by Butherus, et al.[39] A wide range of materials was also studied here. Basically, the latter can be divided into two classes, namely: thermosetting plastics and thermoplastics. The former materials are generally thought to be less resistant to H_2SO_4 than the latter. On the other hand, thermosets exhibit superior bonding to metals such as Cu, Al, stainless steel, brass, Pb and Pb alloys than do thermoplastics. In view of the desirability of preventing short circuits by electrolyte leakage at those points where the Pb conducting strips extend through the substrate, a more detailed study of the compatibility of the former materials with H_2SO_4 was justified.

Literature surveys of the compatibility of both classes of plastics with sulfuric acid were carried out.[39,40] Additional in house tests were also performed as elaborated below. The engineering thermoplastics, being readily thermoformed, machinable, etc., and having substantial inherent mechanical strength, were judged to be suitable for supporting active material in thin structures (~ 20 mil) without further reinforcement by, e.g., glass cloth, or glass fibers. They were therefore tested in such a form. In contrast, thermosets for structural purposes are most readily employed in reinforced form and are used in laminates for a wide variety of purposes, e.g., printed circuit boards. We have, therefore, considered the H_2SO_4 compatibility of thermosetting resins reinforced with glass cloth and also the compatibility of the base resins themselves. Structural aspects of these materials are discussed subsequently. Below, we give our own data on the compatibility of all these materials in H_2SO_4, followed by literature data on the same subject where they were available. Since the mode of preparation of the laminates is important and affects subsequent corrosion resistance, information on this is also supplied.

The H_2SO_4 compatibility of the plastic was tested by immersion in 1.28 sp gr H_2SO_4 at 30°, 60°, and 90°C for extended periods of time. Data are recorded in Table VII where we show percentage weight losses or gains. In some cases, samples were almost completely destroyed. We have noted this also in the Table. Before weight measurements, samples were washed free of acid and dried at 50°C overnight.

The Table shows the increased severity of attack as the temperature is increased. Of the laminated thermosets, the phenolic and Dapon materials show most stability, while the epoxy and polyester laminates exhibited decreased stability in that order. We have shown the weight change for a phenolic SC 1008 base resin cured in two separate ways. In general, both showed less attack than the corresponding laminates at equivalent temperatures.

Of the thermoplastics, plexiglass exhibited a 0.4% weight gain at 30°C, whereas the other plastics exhibited $\leq 0.1\%$ weight changes. This trend continued at higher temperatures except that hi-impact polystyrene was quite severely attacked at 60° and 90°C. At the latter temperature also, PVC had a 3.5% weight loss. In general appearance, all samples

Table VII. Weight Changes of Various Plastics in 1.28 sp gr H_2SO_4 at 30°C

Resin System	Sample Number	Corrosion Time, Weeks	Weight Change %
Epoxy	1	13	+ 15.0
Micaply	2	13	+ 5.3
No. 102-13			
Laminate	3	13	+ 1.6
Dapon	1	10	- 1.4
(From NELCO)			
Laminate	2	10	+ 4.1
Phenolic	1	10	+ 0.9
SC-1008			
Laminate	2	10	+ 0.4
Polyester	1	9.5	+ 9.6
XP-7289-L			
Laminate	2	9.5	+ 6.6
Noryl	1	6	0.0
Hi-Density Polyethylene	1	6	- 0.1
Hi-Impact Polystyrene	1	6	< 0.1
Lexan	1	14	+ 0.1
Plexiglass	1	14	+ 0.4
Polystyrene	1	14	< 0.1
PVC	1	6	< 0.1
Polypropylene	1	6	< 0.1

Table VII. Weight Changes of Various Plastics in 1.28 sp gr H_2SO_4 at 60°C

Resin System	Sample Number	Corrosion Time, Weeks	Weight Change %
Epoxy Micaply No. 102-13 Laminate	1	13	+ 11.0
	2	13	+ 10.1
	3	13	+ 6.5
Dapon (From NELCO) Laminate	1	10	+ 0.2
	2	10	+ 1.7
Phenolic SC-1008 Laminate	1	10	+ 7.5
	2	10	+ 3.3
Polyester XP-7289-L Laminate	1	9.5	Destroyed
	2	9.5	Destroyed
Noryl	1	6	0.0
Hi-Density Polyethylene	1	6	< 0.1
Hi-Impact Polystyrene	1	6	- 1.0
Lexan	1	14	+ 0.1
Plexiglass	1	14	+ 0.6
Polystyrene	1	14	< 0.1
PVC	1	6	- 0.1
Polypropylene	1	6	- 0.1
Phenolic Resin-SC1008	1	14	+ 0.1
Phenolic Resin-SC-1008	1	14	+ 7.5

Table VII. Weight Changes of Various Plastics in 1.28 sp gr H_2SO_4 at 90°C

Resin System	Sample Number	Corrosion Time, Weeks	Weight Change %
Epoxy Micaply No. 102-13 Laminate	1	13	
	2	13	
	3	13	
Dapon (From NELCO) Laminate	1	10	Samples Destroyed
	2	10	
Phenolic SC-1000 Laminate	1	10	
	2	10	
Polyester XP-7289-L Laminate	1	9.5	
	2	9.5	
Noryl	1	6	+0.1
Hi-Density Polyethylene	1	6	- 0.1
Hi-impact Polystyrene	1	6	+0.4
Lexan	1	14	<0.1
Plexiglass	1	14	+0.5
Polystyrene	1	14	<0.1
PVC	1	6	- 3.5
Polypropylene	1	6	- 0.1
Phenolic Resin-SC1008	1	14	- 1.9
Phenolic Resin-SC1008	1	14	+ 1.2

showed some surface roughening at the higher temperature (90°C) and the polystyrene curled up at this temperature. Below 90°C, only slight surface changes were evident for all samples. The following curing schedules were used in the fabrication of the reinforced thermosets noted in the table:

The epoxy was a Micaply no. 102-13 laminate with three plies of prepreg and was cured at 350°F for 10 min at contact pressure and then 250 psi for 30 min followed by cooling to ~ 70°F at pressure before removal from the press. The Dapon resin (modified polyester) was from New England Laminating Company. This was made from four plies of prepreg (glass cloth style no. 7728) and was cured at 500 psi and 360°F for 30 min followed by reduction in temperature to 70°F under pressure before removal from the press. No precuring cycle was utilized to control resin flow. The polyester laminate no. XP-7289-L from Fabricon Products was prepared using four plies of prepreg. Curing was affected at 250 psi and 300°F for 40 min followed by cooling to 70°F under pressure. Again, no precuring cycle was applied. Phenolic laminates were made from no. 396 prepregs from Spaulding Fiber Company, Inc. Three plies were used and cured at 350°F for 2 min at contact pressure followed by 40 min at 350°F and 300 psi and finally cooled under pressure to ~ 70°F.

The above curing schedules,and indeed, the above resins were not necessarily such as to impart maximum chemical resistance. The materials and techniques were those most readily available commercially. In addition, it was often impossible to obtain exact information on the precise chemical make up of each thermosetting resin system, e.g., resin, curing agent, promoter used. All these, and also the curing temperature, can have a marked effect on the subsequent chemical resistance of the laminate. For example, the relatively rapid rate of attack on our epoxy laminates was particularly surprising from several aspects. Thus, in printed circuit board technology, laminated epoxies with Cu overlays are routinely etched with much stronger acids than 1.28 sp gr H_2SO_4 to selectively remove Cu. No adverse effects are noted under such conditions. Also, Bell Telephone Company routinely encapsulates the terminal posts of their new standby lead acid battery in an epoxy resin.[40] Data shown in Tables VIII-X illustrate the chemical resistance of unfilled Epon 828 resin as a function of curing agent in 25% H_2SO_4 over a 180-day period at up to 225°F. Clearly, there is a change in the rate of attack as the curing agent is varied and attack is also more pronounced as the temperature is increased. The drastic changes we have noted in our test specimens are not however evident here. Further examination of the test specimens indicated that the attack was confined in the major part to the surface of the laminates and particularly to the epoxy/glass reinforcement bond. In some test samples, exposed glass edges were presented to the acid and subsequent greater rates of attack were observed with these samples. Also, in some preparations (for an entirely different reason), resin was deliberately extruded in the form of 20 mil thick ribs on the surfaces of the laminates and, whereas general attack was observed over the surface of the laminate, the ribs appeared untouched (at up to 60°C). We have made similar observations with most of our other laminates and generally find that though there is undoubtedly some attack by the acid at 90°C (an excessively high temperature) the main cause of failure is at the thermoset/glass reinforcement bond. This is not surprising and many surface treatments (following section) are applied to improve the strength of this bond prior to resin impregnation.

Table VIII. Chemical Resistance of Unfilled Epon 828 as a Function of Curing Agent in 25% Sulfuric Acid Over a 189-Day Immersion Period

Curing Agent	Appearance Changes		Change in Flexural Strength, Psi	
	Solution	Specimens	Original	After 180 Days Immersion
	75°F Immersion			
Triethylenetetramine	No Change	No Change		
3 PHR $BF_3 \cdot MEA$	No Change	No Change		
20 PHR Diaminodiphenyl-sulfone (DDS)	No Change	No Change		
20 PHR Curing Agent Z	No Change	Greenish & Some Slight Darkening		
14 PHR Curing Agent CL	No Change	No Change		
75 PHR Phthalic Anhydride	No Change	No Change		
110 PHR Chlorendic (HET) Anhydride	No Change	No Change		
	180°F Immersion			
Triethylenetetramine	Darkened	Some Slight Darkening, Swelling & Sugar Like Odor	17,700	9,200
3 PHR $BF_3 \cdot MEA$	No Change	Some Slight Darkening	16,500	14,500
110 PHR Chlorendic (HET) Anhydride	No Change	Dull & Some Slight Darkening	14,500	13,400
20 PHR Diaminodiphyenyl-sulfone (DDS)	No Change	Some Slight Darkening Particularly Edged	17,900	16,300
20 PHR Curing Agent Z	No Change	Greenish & Some Slight Darkening	20,200	11,300
14 PHR Curing Agent CL	No Change	Slight Surface Dulling	19,800	15,000
75 PHR Phthalic Anhydride	No Change	Darkening	24,000	23,600

(Taken from Shell Epon Resins for Casting 1967)

Table IX. Chemical Resistance of EMI-24 Versus CL Cured Epon 828 Castings

		Formulation:	EMI-24 (2 phr) Epon 828	CL (14 phr) Epon 828
Chemical Compound	Test Temperature, °F	Time of Exposure, Days	Weight Gain, %	
50% Sulfuric Acid	150	30	0.485	1.415
50% Sulfuric Acid	200	30	0.635	1.63
50% Sulfuric Acid	225	30	0.65	3.32

Cure conditions for above samples: Epon 828/EMI-24 4 hr at 70°C, 1 hr at 120°C
3 hr at 204°C

Epon 828/CL: gel at 55°C, 2 hr at 125°C
2 hr at 175°C

Chemical Compound	Test Temperature, °F	Time of Exposure, Days	EMI-24 (2 phr) Epon 828	CL (14 phr) Epon 828
70% Sulfuric Acid	200	14	0.45	Sample Destroyed

Cure conditions for above sample: both - gel at 70°C, 4 hr at 150°C

(Taken from Shell Epon Resins for Casting (1967))

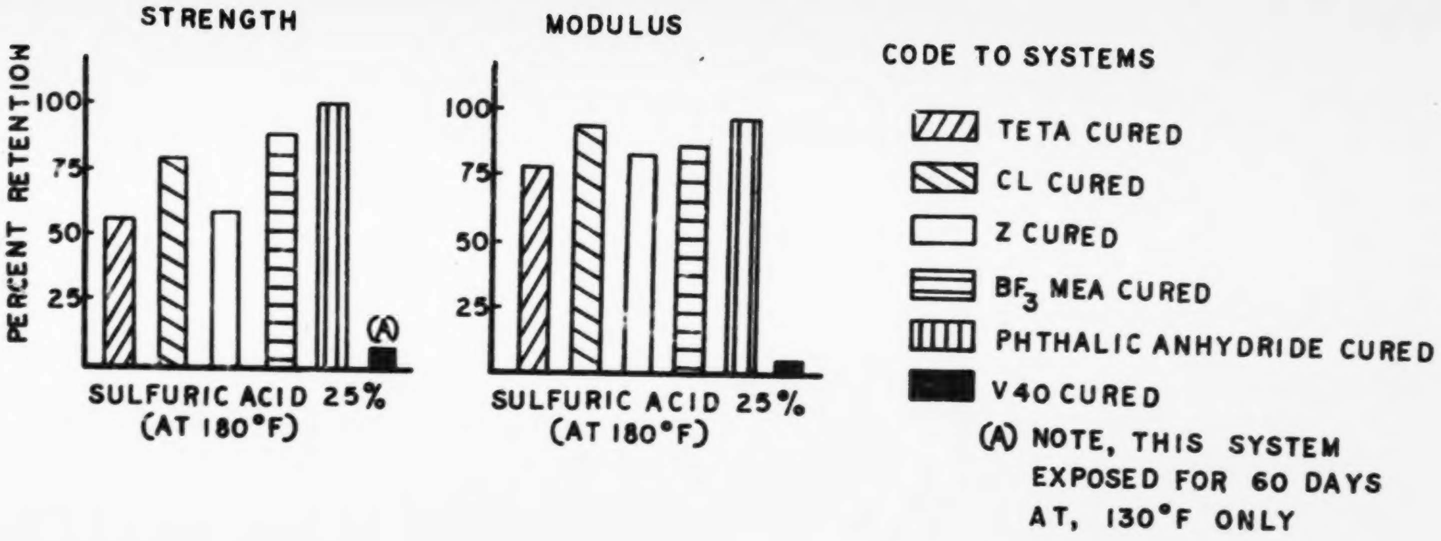

Table X. Flexural Strength and Flexural Modulus Retention (%) of Epon Resin Castings After Six Months Exposure to Various Chemical Media

The above considerations apply to our phenolic laminates also. (Note that W. R. Grace routinely supply a phenolic separator for use in Pb/acid batteries, trade name Darak 2000). Here, during lamination, the resin was extruded along the outside edges of the sample and at these points, little attack by acid was noted even at the higher temperatures. Also, the phenolic laminate is based on Monsanto SC-1008 phenolic resin, and when we tested bulk specimens of this resin at up to 90°C, (Table VII), surface darkening and embrittlement was observed only at the latter temperature with little or no appearance changes below this temperature. We conclude again that the phenolic/glass reinforcement bond is the main point of acid attack.

A final point regarding corrosion susceptibility of laminated resins is that in our early designs we were looking for structures which could be cast in one step and have plastic ribs on the surface to enhance paste adhesion. For this reason, we used high temperature/high pressure curing cycles to maximize resin flow. We have since changed our mode of plate preparation as will be discussed shortly. However, since the corrosion test samples were all prepared at high pressures and consequently had only a minimum of resin content on the actual surface of the laminate protecting the resin/glass bonds, it is obvious that very little local attack is required before acid penetration to the relatively weak resin/glass bonds. When this occurs, accelerated attack throughout the reinforced system can then take place. This, we believe, was a major contributing factor in the observed excessive disintegration of these corrosion samples.

In summary, it is evident that thermosetting resins are attacked by H_2SO_4 but to varying degrees. Of the materials we have examined, polyester and modified polyesters (Dapon) show least stability. Phenolics and epoxies are susceptible to attack but not to the extent indicated by test results. Rather, the resin/glass (or graphite) bond is the weak point in laminated structures. This attack was enhanced in our corrosion test specimens by the relatively high pressure laminating techniques employed. Although different techniques may be used in forming laminates from thermosetting resins (e.g., by using lower pressures and resins having lower flow characteristics), it is felt that the major outlet for use of epoxies or phenolics in lead acid batteries would be as sealants or adhesives rather than as a possible high strength active mass support material. Test data and literature information on epoxies and phenolics reveal that they can have substantial resistance to H_2SO_4 attack, particularly if the resin (e.g., Epon 828 epoxy), curing agent (e.g., acid anhydride), and curing temperature (high temperatures), are carefully chosen.

The thermoplastic materials generally all behaved very well in acid solution, even at 90°C. Lexan (a polycarbonate) and polystyrene exhibited the lowest weight changes at the highest temperature, but in practice all of these materials were deemed to be suitable for use in a practical battery from a corrosion standpoint. Further plastics such as SAN (styrene/acrylonitrile) and polysulfone are also corrosion resistant. In the Appendix further corrosion data on polysulfone and polypropylene are given. The thermoplastic material of choice as active mass support was governed by the factors discussed next.

The following specific conclusions were drawn:

1. The majority of thermoplastics, for example, Lexan, polystyrene, polysulfone, PVC, polypropylene and Noryl are stable in 1.28 sp gr H_2SO_4 at ambient temperature for extended periods. From this aspect they are suitable for use as substrate material.

2. Reinforced laminates with thermosetting resins are subject to attack by H_2SO_4 at the resin to glass reinforcement bond. The base resins, and particularly epoxy and phenolic resins, if suitably selected, and carefully cured, can be quite resistant to acid attack.

3. The major outlet for thermosets in Pb acid batteries is not as a structural paste support material, but as an adhesive or sealant in selected areas of the plate or battery.

4. No data have yet been generated on the corrosion resistance of reinforced thermoplastics in H_2SO_4. Literature information suggest that this is generally as good as that of the unreinforced plastics.

VI. TASK V. DEVELOPMENT AND MECHANICAL TESTING OF STRUCTURES

A. Factors Influencing Choice of Design Materials and Techniques

The additional aspects of plate development not already considered in previous sections were examined here. Due to corrosion problems, structures involving metals other than Pb or Pb alloys were not considered further. Emphasis was placed on those alternative designs outlined in Section III of this report. The selection of materials and techniques for further study was closely controlled by the results of corrosion and other parameters influencing design which are described in earlier sections. Literature surveys of material performance capabilities were carried out and, where necessary, these were backed up by laboratory tests. The following specific factors were considered: -

1. Strength
2. Ease of fabrication
3. Cost and availability
4. Bonding of the plastic to Pb or Pb alloys
5. Adhesion of active mass to the plastic
6. Oxidation of the plastic by PbO_2
7. Temperature and corrosion resistance
8. Ease of handling (e.g., brittleness) and sealing (plastic to plastic) in a battery case.

Only plastic materials were investigated since it was clear by this stage that the maximum chance of success lay in the use of plastic substrate materials as active mass support in the grid.

1. Strength

Both thermoplastics and thermosets were considered for use as a substrate material. Whereas it was thought that thermoplastics might not require any additional reinforcement (particularly the engineering thermoplastics such as Lexan, Noryl, Polysulfone etc.) to achieve the necessary structural stability, in contrast, when using thermosets, some type of reinforcing medium is required. Also, in the event that a substrate thickness of 10 mil was desired in the final design (to minimize the weight of passive battery components) even the engineering thermoplastics must be reinforced. We have therefore considered reinforcement

Preceding page blank

types, techniques and problem areas, together with literature data on the strength of unreinforced plastics.

Plastics are generally reinforced in one or other of two ways, namely: (1) using woven cloth, or (2) using chopped fibers. The reinforcement may be either glass based or carbon or graphite based. Glass cloth reinforcements were available in various types from three main suppliers: (1) Clark-Schwebel Fiber Glass Corp., 245 Park Ave., New York, N.Y., (2) Burlington Glass Fabrics Company, 1345 Ave. of the Americas, New York, N.Y., and (3) J. P. Stevens and Co., Inc., Glass Fabrics Division, 1185 Ave. of the Americas, New York, N.Y. During the weaving of the fabrics, oils and starches are added as binders, Fabrics to which additional finishes are applied go through a heat cleaning process to remove these binders (or sizing). Fabric no. 112 is an example of a heat cleaned material which is not treated further. The various possible additional finishes which are applied to the fabrics serve to improve bonding between the glass and the plastic to be reinforced. The most common of these is the Volan A finish which is suitable for reinforced structures with polyester and epoxy plastics (and also phenolic). Here a treatment with methacrylate chromic chloride enhances bonding to the cleaned glass surface giving a Cr-O-Si bond. Chloride salts formed during the treatment are washed out afterwards. The chromium content of the fabric is 0.03 - 0.06%. Other finishes such as A-1100 are compatible with polyester and epoxy, phenolic, melamine and polyimide resins, respectively. All of these treatments simply improve bonding of the resins to the glass. (We did not anticipate that the finishes would impair battery performance in any way particularly since they would not in any case be exposed directly to the acid.) As is clear from the above, commercial finishes are applied with a view to future applications with thermosetting plastics, for example, in laminated structures for printed circuit boards. Similar finishes can also be applied to chopped glass fibers for use as a reinforcing medium for the above plastics. Glass cloth however is the more usual reinforcing medium for thermosets. The glass cloth syles used vary widely. Typical styles are 108, 128, 7628, and 181 and some properties of these materials are given in Table XI. Style 181 is the strongest of these materials. The prices are also included in the table. Choice of material and finish is governed by many factors such as cost, thickness, resin content desired, lay up technique of the laminante (wet or dry), and strength of final laminate. All of these factors are important in plate design.

It is possible to use carbon or graphite materials as a reinforcement for thermosetting plastics and one further advantage of this is that both of these materials are conductors. The possibility of developing a structurally sound and conducting substrate is thus realized. As will be seen, however, there are other difficulties inherent in such a structure. Two major suppliers of graphite and carbon materials are Union Carbide Corporation (Carbon Products Division, New York) and the Carborundum Company, Graphite Products Division (Brookfield, Ohio). Cloths, yarns, and chopped fibers are available from both companies. The availability of material for structural applications, e.g., laminates, is more limited than for glass reinforcements. However, carbon and graphite materials are available and are treated with sizings

Table XI. Properties of Glass Fabrics

Style	Yarn		Thick-ness	Weight, oz./sq. yd.	Tensile W&F	St. Roll Length, yd	Weave	Width, in.	Un-treated	Typical Finish Prices*	
	Warp	Fill								112	Volan A
108	900-1/2	900-1/2	0.0020	1.45	70×40	625	Plain	19	0.25	0.31	0.38
								38	0.49	0.55	0.62
								40	0.515	0.575	0.645
								50	0.645	0.705	0.795
128	225-1/3	225-1/3	0.0075	6.10	250×200	250	Plain	33	0.62	0.68	0.75
								44	0.72	0.78	0.85
								50	0.82	0.88	0.97
								60	0.98	1.04	1.13
181	225-1/3	225-1/3	0.0090	8.90	350×340	125	8 Sh.	38	0.865	0.925	0.945
						250	Satin	44	1.005	1.065	1.085
						500		50	1.14	1.20	1.22
								60	1.37	1.43	1.47
7628	75-1/0	75-1/0	0.0070	5.80	250×200	750	Plain	38	0.35	0.41	0.43
								39	0.36	0.42	0.44
								44	0.41	0.47	0.49
								50	0.46	0.52	0.54

Tensile Strength - Minimum Average breaking strength, lbs. per inch (ASTM method 579-49).

Property values herein are based on untreated fabric, are approximate guides only, and are not guaranteed values.

Strength, thickness and weight values will change when cloth is finished.

*For quantities of under 5,000 yards, add $0.03 per yard to the listed price

(Burlington Glass Fabrics Co. Sales Data) compatible with epoxy, polyimide, phenolic, and polyester resins. Union Carbide Corporation manufacture a "Thornel" 75S structural graphite yarn in a broadgood form with B-staged epoxy resin. This material contains unidirectional two-ply graphite filaments and is used for high elastic modulus and tensile strength. Its price is $2.65/lb at up to 1000 lb with a nominal yield of 8000 yd/lb. Of more direct interest to us were the carbon and graphite cloth materials which impart high compressive, flexural, and tensile strengths to laminates. Typical data on these materials are given in Tables XII and XIII.

It is clear that a wide range of structural reinforcement materials is available for the present applications. To reinforce structures using woven glass or carbon fabrics (or unidirectional yarn), materials are generally laid up to the desired thickness and then simply hot pressed. This method is generally applied to thermosetting resins, e.g., for printed circuit boards, but we have recently used a similar technique successfully to reinforce thermoplastics - by hot pressing a thin glass cloth (~3 mil) between two 10-mil plastic sheets. With the thermosetting resins, a wide range of structural laminates are commercially available from, e.g., Mica Corporation and New England Laminating Company in prepreg (or stage B) form. In the latter, the cloth or fiber reinforcement is treated with a suitable resin compatible finish, if this is desired, and then impregnated with the resin of choice. Finally the resin impregnated material is partically cured. Sheets of such material are commercially available in various thickness and with various resin contents and types. The reinforcing medium can also be varied and the final materials are classified as high flow, low flow and no flow prepregs.

The latter are used mainly for adhesive purposes. All of these prepregs are shipped in the partially cured state and have the advantage that they can be laid up to the required thickness simply by using a combination of sheets. The prepreg is then polymerized by the application of heat (~340°F for 30 min), pressed to size simultaneously (~25 - 200 psi) and finally cooled to ≤ 140°F under pressure. During the initial stages of preparation, a precure stage can be applied to the prepregs at the curing temperature for 3-4 min at 10 psi. This stage is crucial and controls resin flow. In a further technique to achieve the same result, total pressure is applied immediately and the temperature then raised at a controlled rate. The resin viscosity drops sharply on first application of heat and then increases again as polymerization occurs. By varying the precure time, it is thus possible to vary resin content in the final structure. Properties of typical prepregs are given in Table XIV for epoxy materials.

In the alternative reinforcement procedure which applies mainly (but not soley) to thermoplastics, chopped fibers are employed. A wide range of thermoplastics is available in the pellet form with 20 to 40% fiber reinforcement. Final reinforcement content is achieved by blending the pellets with various amounts of the basic plastic. The drawback here is that injection molding is required to form the final shapes. In the thicknesses we are dealing with, inadequate filling of the mold would be achieved with such reinforced plastics (or even

Table XII. Technical Data for Carbon and Graphite Cloth

Typical Data*

Grade Designation	GSCC-2	GSGC-2	GSCC-8	GSGC-8
Type	Carbon	Graphite	Carbon	Graphite
Weave	Plain	Plain	8-harness	8-harness
Weight (oz/yd^2)	7.5	7.5	7.9	7.5
Thickness (in.)	0.0175	0.0175	0.0175	0.0175
Width (in.)	42	42	30	30
Length, Maximum (yd)	75	75	80	80
Breaking strength, min (lb/in.) warp	64	50	64	50
fill	64	40	64	40
Elongation, ultimate (%)	5	5	5	5
Electrical resistance (ohms/sq)	0.54	0.55	0.51	0.54
Carbon content (%)	99.0	99.9	99.0	99.9
Type of yarn	Continuous	Continuous	Continuous	Continuous
Yarn count warp	27	27	51	51
fill	23	23	51	51
Plys per yarn	2	2	1	1
Filaments per ply	720	720	720	720
Yarn filament diameter (in.)	37×10^{-5}	37×10^{-5}	37×10^{-5}	37×10^{-5}
Yarn denier	1200	1200	600	600

General Cloth Data*

Density (gm/cc)	1.5	
Specific heat (BTU/lb/°F)	0.15	
Heat of combustion (BTU/lb)	14,370	
Heat of sublimation (BTU/lb)	25,740	
Sublimation point	6600°F	
Emissivity	> 0.9	< 1.0

---

* This data does not represent a specification.

(Technical Data, Graphite Products Division, The Carborundum Co.)

Table XIII. Pricing Schedules for Carbon and Graphite Fabrics

CARBON FABRICS

Grade GSCC-2 Carbon Cloth

Type of Weave - Plain
Width of Fabric - Approx. 42 in.
Weight - Approx. 7.5 oz/sq yd
Maximum Roll Length One Piece - 75 yd

1 - 9 lb.	$39.00 /lb
10 lb and over.	31.30 /lb

Grade GSCC-8 Carbon Cloth

Type of Weave - 8 harness satin
Width of Fabric - Approx. 35-1/2 in.
Weight - Approx. 7.4 oz/sq yd
Maximum Roll Length One Piece - 75 yd

1 - 9 lb.	$39.00 /lb
10 lb and over.	31.30 /lb

GRAPHITE FABRICS

Grade GSGC-2 Graphite Cloth

Type of Weave - Plain
Width of Fabric - Approx. 42 in.
Weight - Approx. 7.5 oz/sq yd
Maximum Roll Length One Piece - 75 yd

1 - 9 lb.	$39.00 /lb
10 lb and over.	31.50 /lb

Grade GSGC-8 Graphite Cloth

Type of Weave - 8 harness satin
Width of Fabric - Approx. 35-1/2 in.
Weight - Approx. 7.4 oz/sq yd
Maximum Roll Length One Piece - 75 yd

1 - 9 lb.	$39.00 /lb
10 lb and over.	31.50 /lb

(Technical Data, Graphite Products Division, The Carborundum Co.)

Table XIV. Properties of Prepreg

Micaply Grade	Class Cloth Type	Nema Grade	Mil Spec Type	Nominal Prepreg Thickness, in.	Nominal Cured Thickness, in.	Resin Content. %	Resin Flow, %	Volatile Content, %	Tack Time (grade)	Gel Time, sec	Price, (per sq. ft)
High Flow (Class III) Prepreg											
102-18	**108**	G-10	PC-GE	**0.0035**	**0.0025**	**60±5**	**40±5**	**0.5**	C/D	**225±30**	**0.40**
High Flow Medium Gel Prepreg											
102-13	**128**	G-10	PC-GE	**0.0085**	**0.0065**	**40±5**	**20±5**	**0.5**	B/C	**150±30**	**0.35**
Low Flow (Class II) Prepreg											
102-418	**108**	G-10	PC-GE	**0.0035**	**0.0025**	**60±5**	**25±5**	**0.5**	A	**250±30**	**0.45**

(Micaply Corp. Sales Literature)

unreinforced plastics in ≤ 20 mil thickness). The "sandwich" technique with cloth between sheets of plastic is thus of major interest.

In terms of strength measurements, we have measured tensile strengths of epoxy, polyester, phenolic, and Dapon resins laminated as discussed in the corrosion section and tested on an Instron Tensometer. We used samples 2 in. long by 0.25 in. wide along a 1-in. section and stress was applied parallel to the direction of the minimum number of fibers. Strain rate was 0.05 in./min. Tensile strengths were 35,700 psi, 45,650 psi, 24,000 psi, and 18,950 psi for the epoxy, polyester, Dapon, and phenolic laminates, respectively. Variations arise from glass cloth type and number of plies chosen. The values quoted are more than sufficient for battery plate requirements.

We have a range of values for the thermoplastic materials in the unreinforced state. Tensile strengths for Noryl, Lexan, PVC, polypropylene, and polysulfone are 9,600, 8,750, 7,500, 4,900, and 10,200 psi, respectively. Lexan reinforced with 20 and 40% glass fibers has tensile strengths of 16,000 and 25,000 psi, respectively. Noryl reinforced with 20 and 30% glass fibers has tensile srengths of 14,500 and 17,000 psi, respectively. Polysulfone also has extremely good properties in the reinforced form.

To summarize, it is evident that it is possible to achieve the desired mechanical strength using plastic substrates. With some of the engineering thermoplastics, e.g., Noryl, Lexan and polysulfone, there are indications that this may even be possible in the unreinforced form with ~20 mil substrate thicknesses. Further general engineering data substantiating this conclusion are given for thermoplastics and thermosets in the appendix.

2. Ease of fabrication

These details are discussed more fully later. They are based on many of the facts and techniques outlined in this section.

3. Cost and availability*

Below, a list of the approximate large volume prices of thermoplastic materials is given. Since the cost of battery manufacture is governed not only by the base price of the chosen substrate but also by the constructional problems encountered when using a particular plastic, this must also be considered in the final cost estimations.

Values in Table XV refer to the unreinforced materials unless otherwise stated.

Table XV. Price Schedules for Thermoplastic Materials

Plastic	Cost, ¢/lb
Styrene/acrylonitrile (SAN)	26
Polypropylene	17
PVC	15
Polystyrene	14
Polyethylene	14
Polysulfone	100
Lexan	75
Noryl	72
Noryl (reinforced with chopped glass fibers)	80
Lexan (reinforced with chopped glass fibers)	110

---

* A complete cost analysis of a battery is given in Section VIII of this report.

The cost of thermosetting resins in large volume is more difficult to estimate and varies from resin to resin (in the laminated form). A price of 30-45 ¢/sq ft is reasonable for epoxy prepregs. In these the main cost is incurred in the glass cloth style chosen. With Dapon resins, the price may be closer to 100 ¢/sq ft and is based mainly on resin price. Monsanto phenolic no. SC1008 in the resin form is priced at 33 ¢/liquid lb in large volume. The latter appears to be an approximate price for the more common thermosetting resins but not for specialty products such as resin V341 which has been supplied to us from U.S. Polymeric Company with no available price as yet. Similarly, polyimides, which exhibit good acid stability and also are available in prepreg form, are excessively expensive.

The choice of plastic is governed by cost considerations, not only of the basic material, but also of the fabrication costs and performance characteristics since these ultimately will be the limiting factors. Reinforced plastics, though more expensive as such, nevertheless permit thinner structures to be used with consequent cost and weight savings from materials. These factors are all considered in the final choice of material.

In regard to availability of plastics, there appears to be little problem here with the possible exception of some specialized thermosetting resins suitable for use in H_2SO_4. Materials such as Lexan, PVC, polysulfone, polypropylene, epoxies, phenolics are all available in large quantities. On a small scale for the present experiments, it was sometimes difficult to get sheet or film material of individual plastics at a given thickness. Some thermosetting resins are also difficult to purchase on a small volume. For this reason, we were not always able to gather extensive data on the plastics in question. Noryl, for example, has at first sight good mechanical properties and good acid resistance. It was not available in small volume in $\leq$ 30 mil thickness. In our designs which we discuss later, we required smaller dimensions. For this reason, we have not worked with Noryl. It is evident however, from our discussions with commercial concerns that most of these materials can be custom made if desired. No absolute restrictions in this respect are thus anticipated.

4. Bonding to Pb and Pb alloys

The plastic based plate structures with Pb or Pb alloy conductors on either side and extending through the plastic at localized points have one possible inherent weakness. This is that, if the bonds between metal and plastic are not strong enough, then acid attack there may cause leakage through the plates resulting in short circuits. Furthermore, it is necessary to provide a means of holding the conductors to the substrate on either side. Plausible methods of doing this are to actually bond the conductors to the substrate during plate preparation or, alternatively, to use some type of overlying grid system to mechanically hold the conductors to the substrate at localized points. For the above reasons, it is evident that techniques or materials resulting in good bonding between metal and plastic are desirable.

Table XVI. Lexan Resin Bonding Data

	For Bonds To			Hardener	Proportions (pph)	Cure Temperature (°F)	Time (Hrs)	Adhesion Quality	Tensile Shear Strength (psi)	Service Range (°F)	Color of Adhesive
	Lexan	Metals	Rubber Wood Plastics								
Solvent Cementing											
Methylene Chloride	X					Room	48	Excellent	4500-6500	-40+270	Clear
Ethylene Dichloride	X					Room	48	Excellent	4500-6500	-40+270	Clear
One Part Systems											
A. Room Temp. Curing											
Eastman 910	X	X	X			Room	2-24	Excellent		70 to 212	Clear
Central Coil HB-56		X	X			Room	4-24	Good		70 to 175	Red
Vulcalock R-266-T			X			Room	Air Dry	Good			Amber
G-E RTV-102	X	X	X			Room	2-24	Excellent	350	-75 to 350	White
B. Hot Melt Adhesive											
Terrell Corp. 10 × 104	X	X	X			Melts at 350	Instantaneous	Excellent		32 to 175	Dark
Two Part Systems											
A. Room Temp. Curing											
Epon 828	X	X	X	Diethylene Triamine	100-8	Room	2-48	Excellent	2500	-40+250	Clear
Epon 828				Versamid 115	100-100	Room	24-48	Fair	600	32 to 160	Dark Amber
Epon 828 - Thiokol LP-3		X	X	DMP-30	100-100-10	Room	48	Fair		70 to 160	Dark Amber
Epon Adhesive IV		X	X	Cur. Ag. A	100-6	Room	24-6 Days	Very Good	1800	-60+190	Red-Tan
Epon Adhesive 913		X	X	Part B	100-12	Room	3-4 Days	Very Good	2900	-60+250	Gray - Black
Bondmaster M688		X	X	Ch-8		Room	4-24	Very Good	2000	-40+212	Tan
B. Elevated Temp. Curing											
Uralane 8089	X	X	X	Part B	100-40	70-80 150	2 Days 3	Excellent	1200	–	Tan
Uralane 5716	X	X	X	Part B	100-34	70-80 150	2 Days 3	Excellent	1000	–	Clear
Epon 828		X	X	Methyl Nadic Anhydride DMP-30	100-84-2	175	8 (min)	Very Good	1200	32 to 250	Light Amber
Epon 828			X	Phthalic Anhydride	100-40	250	8 (min)	Very Good	1200	-40+250	Light Amber
Epon Adhesive IV			X	Cur. Ag. A	100-6	200	45 minutes	Very Good	1800	-60+200	Red - Tan
Epon Adhesive 913		X	X	Part B	100-12	180	3	Very Good	2900	-60+250	Gray - Black
Bondmaster M688			X	Ch-8	100-16	200	15 minutes	Very Good	2000	-40+250	Tan
Flexicast 4002	X	X	X	Part B	100-25	212	3	Very Good	600	-90+250	Gray - Black
Pressure and Heat Sensitive											
Lepage 4050			X			Room				Room	Clear
Nafco 101	X	X	X			Room		Excellent	25 psi at point of bond	-40 to 400	Clear
Kleen - Stik 295	X	X	X			120-140	< a minute	Good		-40+200	Amber
Kleen - Stik 298	X	X	X			120-140	< a minute	Good		-40+200	Amber
G-P Transmount	X	X	X			150-250	10-15 minutes	Excellent		-60+250	Amber
G-P Transmount	X	X	X			150-250	10-15 minutes	Excellent		-60+250	Amber

(G.E. Technical Data Revised Report CDC-502) in peel values with such treatments. The results, however, give comparative values for bonding to the four laminates. Note that we would also expect higher peel values to unreinforced resins since in the above case our lead strips were, in part, in direct contact with the underlying glass reinforcing cloths. This was a result of the relatively high pressure used (~ 200 psi) during lamination.

These data and literature information confirm that thermosets exhibit superior bonding to metals than do thermoplastics. Of the thermosets, epoxy and Dapon resins are superior to phenolic and polyester resins. There are, however, several possible alternatives available to enhance bonding to Pb, involving prior surface roughening treatments and using plastic/solvent solutions applied to the Pb before bonding. The use of epoxy type adhesives is also viable, the restriction being that such adhesives should be compatible with H_2SO_4 or, at worst, be only slowly attacked and in the final structures be as much protected from acid attack as possible. Also, if an adhesive is employed, it should either be room temperature cured or have similar shrinkage characteristics to the plastic and metal in question.

5. Adhesion of active mass

The grid in a conventional battery supports the active mass and also carries current to and from the active mass. To do so efficiently there must be good adhesion between the two, otherwise paste shedding results. It is difficult to visualize Pb and Pb oxides adhering adequately on each side of a plastic substrate for any length of time even if there are conducting strips laid down the surfaces of the substrates. Conventional grids are designed to have an interlocking hold on any paste material - which is impossible to achieve when paste is applied separately to each side of a plastic substrate (effectively, one-sided grids). We therefore examined alternative methods of enhancing adhesion to plastic supports.

Apart from using no surface treatment to enhance paste adhesion the alternatives available are to deliberately roughen the plastic by sand blasting, to incorporate a glass mat or dynel fibers on the plastic surface during preparation, or to use a substrate of thin Pb foil (~ 4 mil) on top of the plastic. We anticipate that some surface treatment would be desirable and, most likely, use of glass mats or dynel fiber would be best. It is probable that any Pb foil laid on the plastic surface would increase plate preparation difficulties, increase cost and weight requirements, and also cause excessive corrosion and positive plate buckling problems. The use of glass retainer mats between separators and plates to enhance retention of the paste mechanically to the plastic substrate is also an alternative which is used commercially in some conventional batteries.

6. Oxidation by PbO_2

We do not have complete information on the susceptibility to oxidation of plastic substrates of choice. However, various separators now in use provide useful pointers to this susceptibility. PVC separators have now been used for a long time in the lead acid industry and exhibit no degradation due to oxidation.[43] Similarly, the Darak 2000 supplied by W.R. Grace Company is a phenolic material and is also not oxidized by PbO_2.[27] A Daramic separator supplied by the same company and made of extruded polyethylene material also performs well and a new experimental polypropylene separator,again from W.R. Grace Company,is showing good performance.[26] Polystyrene separators were introduced in the second world war[4] and behaved satisfactorily though only up to 165 ° F. Polystyrene is still being used in Europe as separator and spacer material. Dynel fibers are used throughout the industry to help paste retention in the positive plates. Glass mats are also used as retainers or separators.

We have no information on Lexan, Noryl, and polysulfone plastics but we would not expect oxidation of these materials by PbO_2. SAN, ABS, epoxy, and polyester plastics are used in batteries but as case or sealant material and not in direct contact with active mass. It appears that the problem is not a serious one and can readily be circumvented by suitable choice of plastics.

7. Temperature and corrosion resistance

All of the plastics we have discussed are stable at least up to 150° F – the softening point for PVC. In the reinforced form, the stability to heat increases. Heat deflection temperatures of unreinforced PVC, Lexan, polypropylene, polystyrene, Noryl, and polysulfone are of the order 150, 250, 285, 165, 275, and 300 ° F, respectively. Polysulfone in the unfilled form can be used at temperatures up to 300 ° F even under a stress of 1000 psi. Its heat deflection temperature is 345 ° F at 264 psi and 358 ° F at 66 psi. Long term thermal aging at 300 - 340° F has little effect on the physical properties of polysulfone. Its physical properties are also good down to -150 ° F. The heat deflection temperature of Lexan 500 under stress at 264 psi is 288 ° F. The equivalent value for Noryl at 264 psi is 265 ° F. Polypropylene has values of 220 ° F and 140 ° F under 66 psi and 264 psi load, respectively.

The heat deflection temperature of reinforced Lexan at 264 psi stress is 295 ° F, and at 66 psi it is 300 ° F with 20% glass. For 40% glass, the corresponding temperatures are 295 ° F and 310 ° F. The heat deflection temperature of Noryl reinforced with 20% glass at 264 psi is 270 ° F compared to 275 ° F with 30% glass reinforcement. Polypropylene has heat deflection temperatures of 305° F (66 psi) and 230 ° F (264 psi) when filled with 20% glass fibers (327 ° F at 264 psi with 40% reinforcement). SAN reinforced with 40% glass fiber has a deflection temperature of 250 ° F under 264 psi load. Polysulfone has superior properties to all of the above. More complete details are included in the Appendix.

In the thermosetting series of resins, the materials are not softened by heat once polymerized but are degraded at higher temperatures. Loss in tensile strength and chemical resistance and increase in tensile elongation and flexibility occur above the heat deflection temperature. The temperature stability depends on the choice of starting material. Table XVII gives heat deflection temperatures of Epon resin systems. The lowest value is 320 ° F.

Table XVII. Heat Deflection Temperatures of EPON Resin Systems

Typical Value Range		
Type of System	Cure Cycle	Heat Deflection Temperature, °C
Aliphatic Amine Cured	7 days at 23°C + 1 hr at 100°C	100-125
Anhydride (except dianhydrides)[1]	2 hrs at 90°C + 4 hrs at 150°C	120-150
Aromatic Diamines (except DDS)	2 hrs at 80°C + 2 hrs at 150°C	150-160

[1] When catalyzed with 1 phr BDMA or DMP-30

Values for Systems Designed to Provide High HDT			
Resin System	Material Ratio (parts by wt)	Cure Cycle Required, hrs/°C	Heat Deflection Temperature, °C
EPON 826/EMI-24	100/4	2/80 + 2/150	160
EPON 826/CL	100/14.6	2/80 + 2/150	160
EPON 826/DDS/BF_3·MEA	100/20/1	2/125 + 2/200	175
EPON 826/NMA/EMI-24	100/90/1	4/125 + 2/200 + 2/260	176
EPON 154/CL	100/15	2/80 + 16/150	178
EPON 826/BF_3·MEA	100/3	3/120 + 48/150	184
EPON 826/EPON 1031/NMA/EMI-24	50/50/90/1	2/120 + 2/200 + 2/260	185
EPON 826/EPON 1031/EMI-24	50/50/2	4/70 + 48/150	202
EPON 154/BF_3·MEA	100/3	2/80 + 4/150 + 16/200	245
EPON 1031/NMA/BDMA	100/90/1	4/120 + 18/200 + 7/260	280

The performance of an EPON resin system at a given temperature is governed by the glass transition temperature of the cured resin system and the rate of oxidative or thermal degradation occurring at that temperature.

Amine cured systems generally are not suitable for long-term service at temperatures greater than approximately 375°F, since rapid oxidative degradation of these systems occurs at 400°F (except for DDC-cured systems which do not degrade noticeably below 450°F). With certain specific anhydride curing agents, good long-term performance can be achieved at temperatures as high as 650°F.

(Shell Epon Resins for Casting, 1967)

Our data on phenolic, Dapon, and polyester resins are not so extensive. However, the pH-500 series of phenolic resins from Fabricon Products is based on a Monsanto SC-1008 phenolic resin and has short term capabilities at up to 900° F.

Based on the foregoing, we do not anticipate any problem from retention of physical properties in any of the plastic substrates investigated, as a result of estimated increases in temperature during battery operation. We have given information earlier on the acid stability of various plastics – both thermosetting and thermoplastic. Additional data on stability and changes in physical properties on exposure to H_2SO_4 are given in the Appendix. The results indicate that no severe plastic degradation problems will be observed particularly with thermoplastics. With thermosets we have suggested that the weak point is in reinforced laminates at the resin/glass or carbon bond. Phenolics, epoxies, and polyesters have all been used successfully in lead-acid systems before in bulk form (see earlier corrosion section and the Appendix). At worst we can still employ epoxies as sealants at localized points to prevent short circuit losses through the bipolar plates.

In regard to metal corrosion, pure lead seems to be the best choice due to its more uniform attack compared to Pb/Sb and Pb/Ca alloys. It is also adequate in terms of expansion characteristics.[28] From a practical viewpoint the design of the plate is probably more important in relation to provision for expansion of the Pb conducting strips.

8. Ease of sealing

By this, we refer to sealing of each individual bipolar plate within the battery case. Many techniques are available and various difficulties are encountered. The most interesting techniques are heat sealing, ultrasonic bonding, solvent cementing and adhesive bonding. Most thermoplastic materials can be solvent bonded and adhesive bonded (using epoxies, for example) while the technique of heat sealing and ultrasonic bonding has been applied to Lexan and Noryl plastics. The majority of the thermoplastics we have discussed can be made to soften and flow under the influence of heat and pressure, e.g., PVC, polypropylene, polysulfone, and the above two plastics. We would thus expect to be able to heat seal the latter plastics also. We would not then anticipate problems in sealing these materials within equivalent case materials. Thermosetting resins can best be sealed using the basic resin/curing agent as an adhesive bonding agent. We anticipate that the major problem is not in providing an adequate seal but rather in handling the prepared plates. In this respect, for example, PVC tends to be rather brittle and we are informed by local plastic company personnel that, while Lexan is easy to seal, polyethylene and polypropylene are more difficult. The inherent stiffness of unreinforced Lexan in any event makes it an ideal material to employ rather than polypropylene. Though the latter can be reinforced, it is more difficult to seal such reinforced structures within a case material.

B. Conclusions

The following specific conclusions were drawn as a result of this study:

1. Both thermoplastics and thermosets have adequate mechanical strength to support the active mass in practical design configurations. With thermosets a reinforcement medium is required for this purpose especially for substrates of $\leq$ 20 mil thickness. Engineering thermoplastics may be suitable as support material in the unreinforced form especially when strengthened by the incorporation of a thicker plastic rim surrounding the main substrate area. For substrates of $<$20 mil thickness, the thermoplastics also require reinforcement.

2. A wide range of reinforcement techniques is available using glass, carbon and graphite cloths or chopped fibers as reinforcing media. Suitable surface treatments are applied to these materials to enhance their compatibility with the thermoset of choice.

3. Whereas thermosets are most usually reinforced with cloth material, thermoplastics generally use chopped fibers. Hot press techniques are used to form structural laminates with thermosets. Reinforced thermoplastics are formed to shape by injection molding methods. The latter technique is not suited to the thin plate structures desired here because of inadequate mold filling.

4. A thermoforming technique is suggested when fabricating plates from thermoplastics. The latter may be reinforced if desired by hot pressing a suitable cloth between thin sheets of the plastic in question.

5. Mainly because of H_2SO_4 corrosion stability, thermoplastics are preferred to thermosets as substrate material.

6. Thermosets form superior bonds with Pb than do thermoplastics. The former may then be used to provide seals in plates at localized points if desired. Careful choice of the resin and its curing technique and curing agent are, however, necessary.

7. Because carbon and graphite can be used as reinforcement, a means of obtaining conductive plastic substrates is offered if concurrent problem areas can be solved.

8. Lexan thermoplastic is an ideal starting material for substrate fabrication. It is relatively low cost, is thermoformable, stable in H_2SO_4, light weight/medium strength and is easy to handle.

9. There are techniques available to enhance sealing of thermoplastics to Pb. Also, paste adhesion to such substrates may be enhanced by suitable surface treatments.

C. Preliminary Plate Development

The following describes the practical application of the information presented in previous sections. Only bipolar designs are considered and these are all based on the concepts outlined earlier. Both the information given up to this point, and also information generated as a result of these practical fabrication experiments, are used subsequently in the development of the final design structure and techniques for its fabrication. In the absence of any extensive H_2SO_4 stability data, early plates were fabricated from epoxy laminates since these were readily available, easy to handle and readily fabricated in the desired plate geometry.

The following fabrication techniques were used: Grooves were milled across both faces of an aluminum mold to depths of 15-21 mil and in widths of 1/32 in. up to 1/16 in. A border 20 mil deep and 3/32 in. wide was also drilled around the mold enclosing an area 5 1/2 in. by 4 7/16 in. Down the mold additional grooves 3/32 in. wide and 15-18 mil deep were also drilled. Three to five sheets of epoxy Micaply No. 102-13 were then cured between the faces of the mold by the application of heat and pressure as outlined earlier. During the curing, good resin flow into the grooves cut in the faces of the mold was obtained. The cured plate was approximately 22 mil thick except around the edges where the resin flow into the groove drilled round the mold (and down and across the mold at localized points) resulted in an additional ~ 20 mil border thickness on each side of the structure. This border also served to add flexural rigidity to the structure which was, in fact, sufficiently rigid to begin with. When Pb strips (22-27 mils thick by 3/32 in. wide) were laid in the grooves drilled down the mold prior to lay up of the laminates and the hot press curing cycle then applied, good adhesion of the Pb to the complete laminate was obtained and each Pb strip protruded above the surface of the plastic by 16-18 mil. i.e., corresponding to the depth of the mold groove. We also made electrical connection through the plate between the Pb strips laid in grooves on opposite sides of the plastic prior to layup. For this purpose, holes were drilled in the substrate at the desired connection points before curing. Structural tests, corrosion data and peel strength measurements were carried out on samples from such plates and the results of these have been outlined earlier. The following useful information was obtained from these experiments.

a. It is possible to manufacture a structurally sound thermosetting plastic substrate which has Pb strips as conductors on either side and with electrical connection through the plate at desired points. Fabrication is relatively simple.

b. Plastic ribs can be incorporated across the plate simply by extruding the resin from the prepreg sheets during the fabrication operation. These ribs can help active mass adhesion to the plate (mechanically).

c. The plastic border also extruded round the structure during lamination adds further flexural rigidity to the plate.

Bearing in mind that the experiments were preliminary in nature and that no major attempt was made to optimize the resin content on the surface of the laminate (protecting the underlying glass/plastic bonds from acid attack) the following major problem areas were observed or anticipated with this structure.

a. The plate was extensively attacked in acid solution. Rapid loss in structural stability was observed and Pb strips bonded to the underlying plastic surface, became separated from that surface.

b. As a result of corrosion but also because of excessive stresses induced by expansion of the Pb strips on the positive electrode, it was anticipated that this method of holding the strips rigidly to the underlying plastic would not survive the rigors of extended cycling and lifetime. An alternative design permitting rib expansion without complete separation of the ribs from the underlying substrate or causing substrate buckling, is desirable.

With these views in mind the fabrication techniques outlined below were developed.

D. Second Design Plate

Again, this design was not considered to be final but rather was chosen to rapidly test further fabrication techniques and ideas. The mold for fabrication was made from wrought jig-plate Al, which was machined on both sides. Dimensions are shown in Fig. 35. For plate fabrication we now used PVC or Lexan, both in the unreinforced form. A thermoforming technique, given in detail subsequently, was used to fabricate the plates. A further essential difference from the first design was that a plastic grid was now used to hold the unidirectional Pb conductors to the plastic substrate. This allows conductor expansion down the plate without plate buckling or conductor separation from the substrate. The separation of adjacent Pb strips laid down the plate was held at 0.29 in. in this design. Without going into exact fabrication techniques and advantages inherent in the design (there are all noted below) the following basic problems were observed with bipolar plates made in this mold:

1. The Pb conductor strips were too widely separated (0.29 in.) and contributed to inadequate formation of the active mass.

2. During plate preparation, plastic was extruded along the edges of the Pb ribs laid down the base plate. This reduced the formation rate and capacity of the plates.

3. Plates with no base plate treatment or with sand-blasting only to enhance adhesion were not satisfactory. The paste tended to shed during operation. Those plates with glass backing or dynel fibers showed good paste adhesion properties.

4. There were problems in early test cells using these plates which were caused by gas bubble retention in the glass mats and/or thin separators first used. (10 mil separators and 10 mil glass mats).

Basically however, the fabrication technique worked smoothly and the final plate design and fabrication techniques, with suitable modifications, were based on the above concepts.

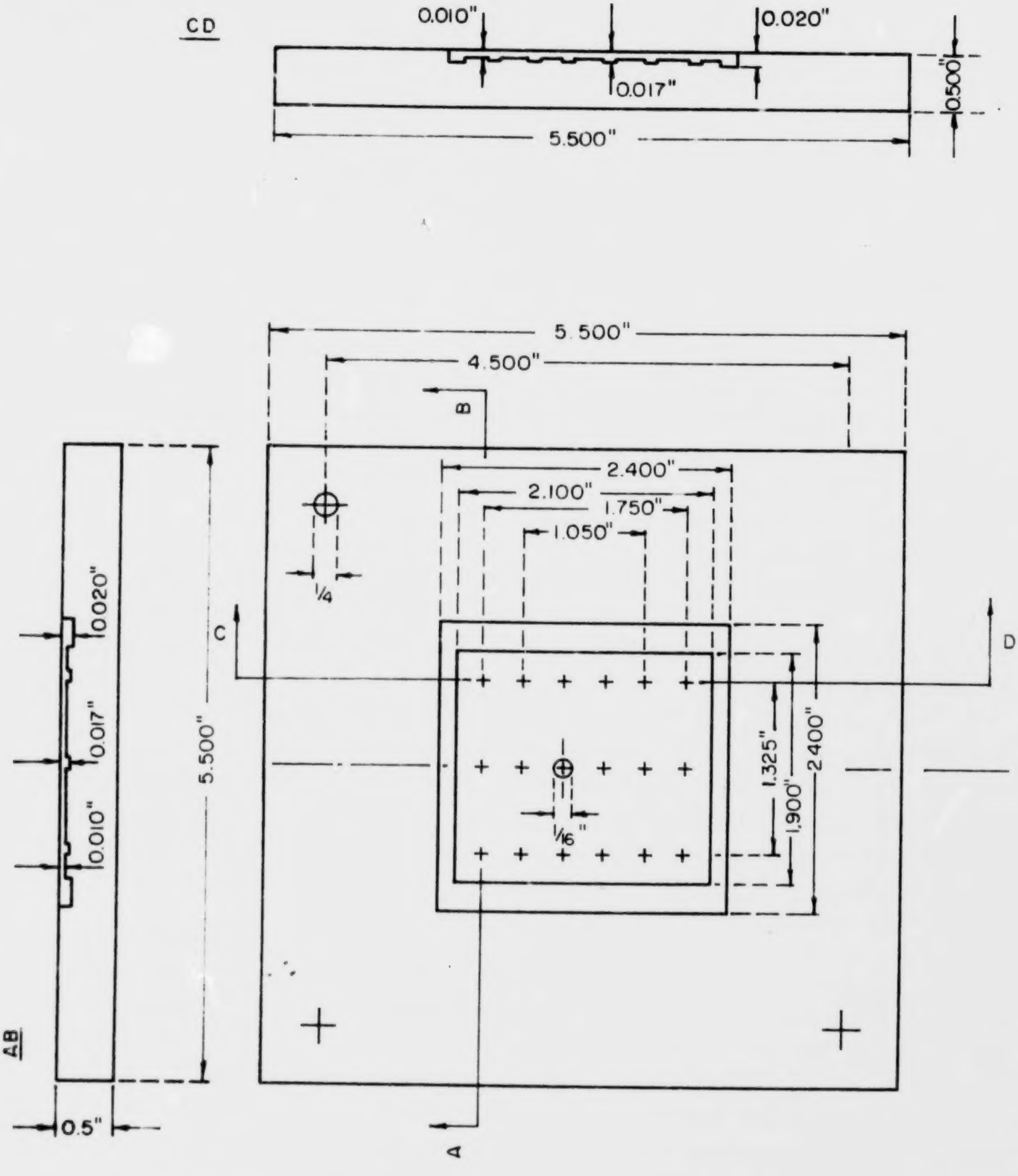
CD
0.010"
0.020"
0.017"
0.500"
5.500"
5.500"
4.500"
B
2.400"
2.100"
1.750"
1.050"
1/4
C
D
1.325"
1.900"
2.400"
1/16"
0.020"
0.017"
0.010"
5.500"
AB
0.5"
A

Fig. 35. First mold design for plastic plate manufacture

E. Final Plate Design

The concept is basically that denoted as number (1) in Task II, section A of this report and is defined here as a "quasi-bipolar" plate. It is based on the use of a flat, insulating plastic substrate. On each of the sides of this substrate there is a parallel array of vertical lead strips which are held to the substrate surface at several points using a plastic grid with horizontal strips. The lead strips are placed in such a way that each strip on the face of the substrate has a corresponding one directly underneath on the other face of the substrate. Electrical contact between one strip and the corresponding one on the other face is made at the top end of the strips via a section cut through the plastic substrate close to its upper edge. This contact is located above the electrolyte level and, in addition, is covered with the frame of the plastic grid to minimize chances of electrolyte leakage. (The two strips in contact can be obviously substituted by a U-shaped strip riding on each side of the plastic substrate over the top of the cut section.) On one side of this structure, the positive mass is pasted, with the negative active mass on the other side. After pasting, the plate is formed by a simple modification of the conventional formation process.

A photograph of such a quasi-bipolar plate prior to pasting is shown in Fig. 36. The most important aspects of this plate are summarized below:

1. It is approximately 1/6 full-size and may be scaled up to full size directly. Final plate dimensions (pasting area) are 8 by 4 in. The 4-in. dimension is in the vertical direction. Relatively long and shallow plates result. The reason for this can be seen from the current conduction paths which in this plate are over the top of the plate only. By making the plate relatively shallow, resistance losses down the plate are minimized.

2. The materials of construction are Lexan as substrate and pure Pb as current conductors. Lexan is a light weight/high strength plastic which permits relatively easy handling of the plate with sufficient flexural strength capabilities. Pure Pb has minimal corrosion problems and also is quite good from an expansion viewpoint.

3. The current conductors of Pb have been held at 20-mil thickness.

4. The conductors are separated by 0.15-in. intervals along the plate. This separation permits easy charge and discharge of active mass without introducing excessive resistive losses. The separation is equivalent to that of horizontal grid members in conventional lead acid batteries, but since each lead strip carries only the current generated around it, the additional leads used in conventional plates to collect the current at the terminal are not necessary here.

Reproduced from best available copy.

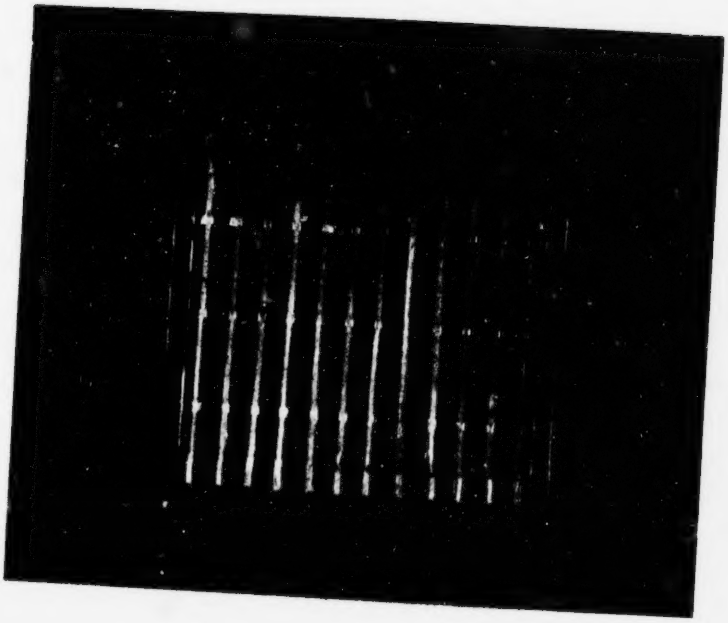

Fig. 36. Typical photograph of an unpasted "quasi-bipolar" plate newly thermoformed (the pasting area is 2.55 in. × 2.04 in.)

5. A plastic rim is provided to facilitate sealing of each plate within a case (lexan). Lexan is an extremely easy material to handle from this aspect.

6. Paste thickness is held at 20 mil per positive and negative electrode with a plastic substrate thickness of 20 mil also. Pasting thickness is governed by the plastic border round the circumference of the plate (as is the case with the outside rim in conventional plates). The rim also adds rigidity to the structure.

7. Paste adhesion to the plastic substrate is enhanced using glass mats or dynel fibers attached to the substrate surface in a prior step. Very good paste adhesion has been observed so far.

8. Current is removed from each electrode over the top of each plate only, using Pb conductors looped over the base plate prior to layup. The points where each conducting strip make contact with its equivalent strip on the opposite face of the substrate are not directly immersed in electrolyte. The problem of intercell leakage is thus minimized significantly.

9. The Pb conductors are held mechanically to the plastic substrate by a plastic overlying grid only at those points where the plastic and the Pb intersect down and across the plate. During cycling, this setup permits expansion of the Pb down the plate without introduction of any stresses resulting in plate buckling and poor paste adhesion.

10. As discussed, production of the entire plate is relatively easy. It appears that it can be carried out on a large scale basis.

11. There is scope in the design for both thinner base plates and also thinner pastes. No substantial changes are required. The plastic base plate can easily be reinforced with glass cloth to provide sufficient flexural rigidity in $<$ 20 mil thicknesses. Paste thicknesses $<$ 20 mil also give superior paste utilization and reduce weight requirements.

The principal advantages of this quasi-bipolar plate are that a serious problem area in bipolar plates, namely intercell leakage, is minimized by not immersing in acid those points where conduction is made through the plastic. The leakage paths are also substantially lengthened. Any corrosion product formed on the Pb conductors would expand under the sealing plastic "cocoon" and tend to close any electrolyte leakage paths. By virtue of the unidirectional Pb conductors, the design also reduces plate expansion and buckling problems which we have shown to seriously limit successful operation of conventional battery positive plates under high rate cycling conditions. The light weight of the substrate material further adds to the plate attractiveness and this, together with the basic advantages of a bipolar plate design which were outlined previously, makes the whole concept very attractive.

F. Construction of the Battery Using Quasi-Bipolar Plates

In construction, the bipolar battery with quasi-bipolar plates is relatively simple and each plate is connected in series in a module to give the required voltage. To increase capacity, individual modules are connected in parallel. Sealing of each individual plate within a module may most readily be affected by preforming a case (~1/8 in. thick) with side and bottom slots. Each plate is then fitted into the slots in the case and sealed by application of heat and pressure around the rim surrounding the plate pasting area. A simple heat sealing technique has been developed by Bell Telephone where plastic components to be heat sealed are treated with an infrared absorbing material.[44] On exposure to infrared light, those areas in contact with each other and treated beforehand in this manner are adequately heat sealed. The method has been used commercially and has the advantage that it is simple and that the heated zone is very localized. It may be more applicable than a conventional heat-sealing process.

The terminal plates in each module are simply thick conventional plates or, to reduce weight requirements, lead coated Al plates. To allow for electrolyte equalization, we have incorporated an "upper rim" in each bipolar plate in which an equilization slot is cut. When the module is turned partially to one side, electrolyte added through a single filling hole can flow into each cell compartment. In the normal horizontal position, the electrolyte level is below the level of these slots. The upper "rim" on the plates also minimizes any possible intercell leakage problems from electrolyte splashing over the top during charge for example. A crude schematic of an individual module is shown in Fig. 37.

Within each cell, we at present incorporate 3-mil glass mats as paste retainers together with commercial Daramic separators with 45-mil ribbing and 30-mil backing. The final requirements as regards separators have not been fully established but these separators do permit trouble free operation with minimal gas bubble retention characteristics.

G. Method of Construction of the Quasi-Bipolar Plate

The design of the bipolar plate has been kept deliberately simple to facilitate large scale fabrications. The various steps in the process are outlined and scale diagrams and photographs are included to ease understanding. Basic test plate dimensions are shown in Fig. 38 where we show one face of the mold in which the final structure is thermoformed. The four basic components of the plates are pure Pb, Lexan plastic, and dynel fibers or glass mats. Plate preparation is as follows:

1. Lead conductor preparation

Strips of Pb were cut from a 20-mil-thick sheet and then bent U-shaped. The length of the strips was tailored to meet the requirements of the final plate. The tops of each strip (the "U") were etched in a H_2O_2 acetic acid solution, washed in H_2O, dried and then painted lightly with a solution of 5% Lexan in methylene chloride. The painted portions are shown in Fig. 39a. The solvent was then permitted to evaporate off at room temperature. The "painted" portions of the Pb conductors were those sections to be encased in plastic during layup. In this way, the bond between Pb and plastic is made as strong as possible. The possibility of cell short circuits by acid leakage at the points where the conductors extend through the plate, is thus minimized.

Exactly similar tasks were performed when the conductors were made from Pb wire of 20 mil diameter.

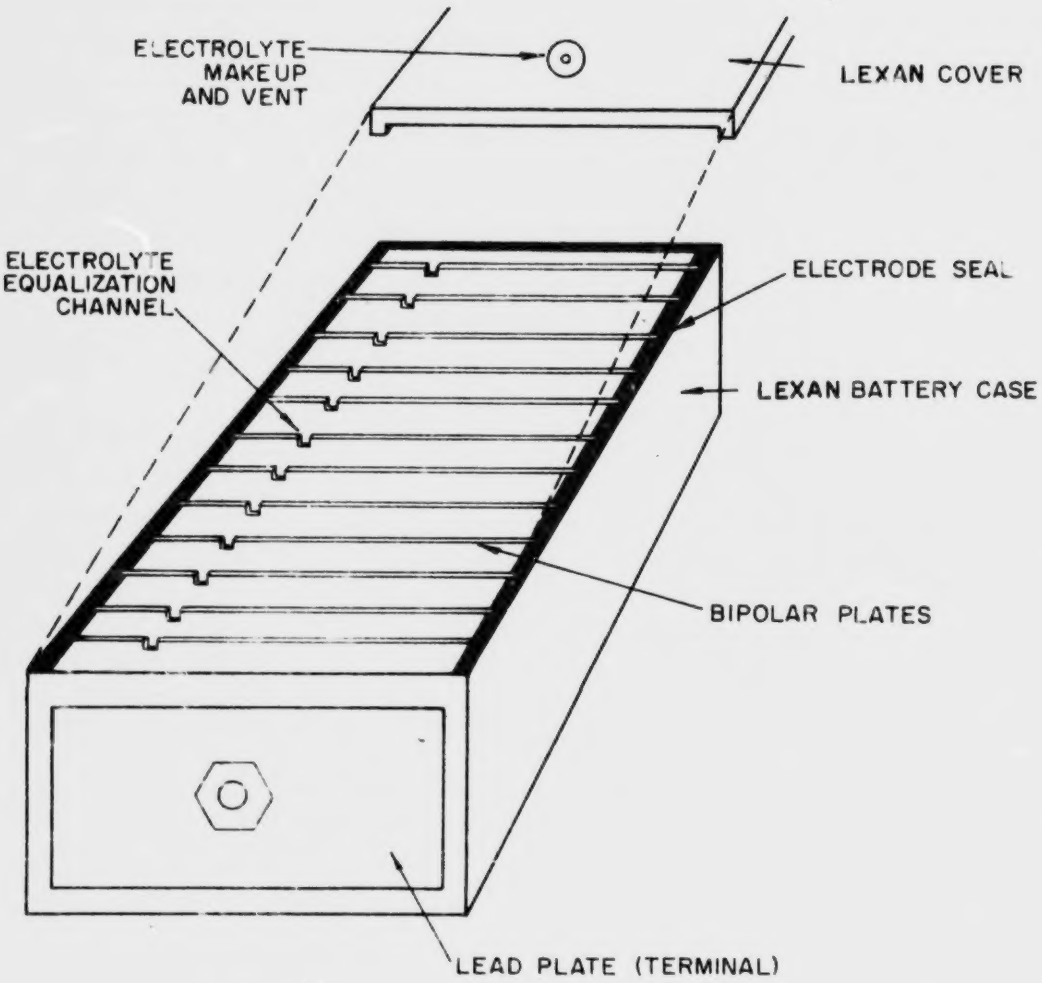

ELECTROLYTE MAKEUP AND VENT
LEXAN COVER
ELECTROLYTE EQUALIZATION CHANNEL
ELECTRODE SEAL
LEXAN BATTERY CASE
BIPOLAR PLATES
LEAD PLATE (TERMINAL)

Fig. 37. Schematic of an individual module

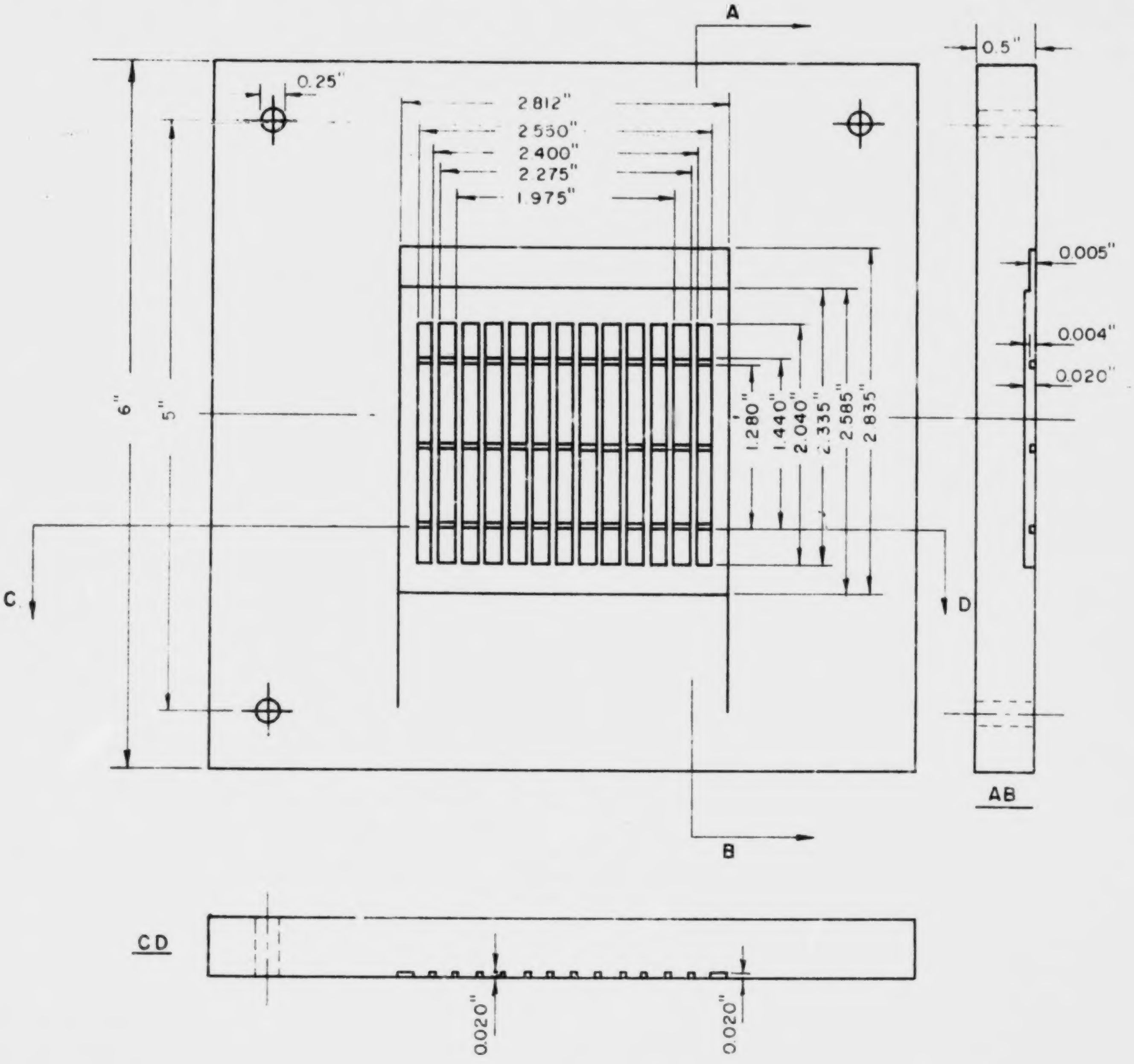
A
0.5"
0.25"
2.812"
2.550"
2.400"
2.275"
1.975"
0.005"
0.004"
0.020"
6"
5"
1.280"
1.440"
2.040"
2.335"
2.585"
2.835"
C
D
B
AB
CD
0.020"
0.020"

Fig. 38a. Dimensions of aluminum mold for quasi-bipolar plate manufacture

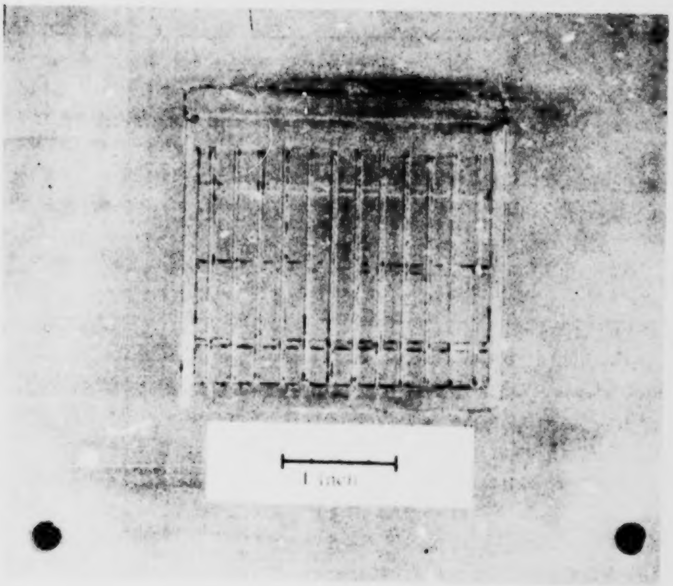

Fig. 38b. Photograph showing one face of the mold used to thermoform the final quasi-bipolar plate

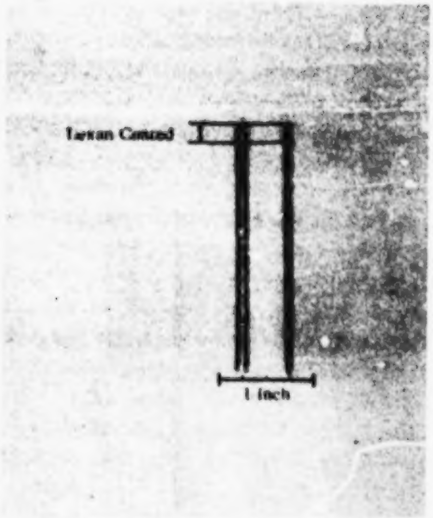
Lexan Coated
1 inch

a. Lead Conductors

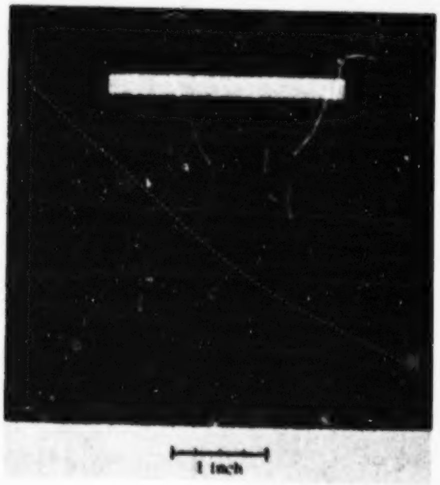

b. Plastic Base Plate

Fig. 39. Preparation sequence for quasi-bipolar plate manufacture

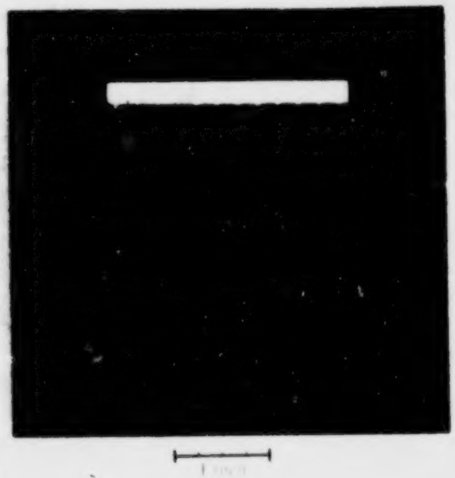

c. Base plate with layup of
some Pb conductors

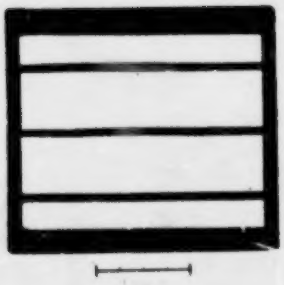

d. Plastic Grid

Fig. 39. Preparation sequence for quasi-bipolar plate manufacture

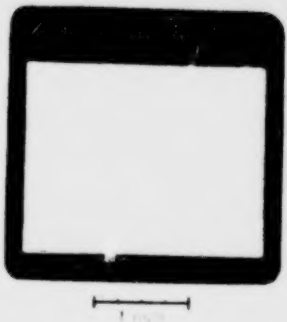

e. Plastic Border

Fig. 39. Preparation sequence for quasi-bipolar plate manufacture

2. Lexan preparation

A sheet of Lexan 20 mil thick* was cut with a metal die to the shape shown in Fig. 39b. This is the "base plate" and the Pb strips are laid over the small cuts at the top of the plate as illustrated in Fig. 39c.

Two further plastic shapes were cut using special dies. Fig. 39d shows the 5-mil Lexan "grid" whose main purpose is to mechanically hold the Pb conductors to the base plate at localized points. Around its circumference, it also combines with a 15-mil "border" to control paste thickness at 20-mil total. The 15-mil Lexan "border" shown in Fig. 39e helps to control paste thickness and also enhances plate rigidity. Note that the border is wider at the top of the plate to minimize acid leakage by splashing over the top of each cell.

3. The plate mold

This is shown in Fig. 38 and is self-explanatory. It was made from wrought jig-plate aluminum which was machined on both sides. Grooves cut in the mold permit incorporation of the plastic and Pb grid structure on the surface of the base plate during the hot pressing. A photograph of one side of the mold is shown in Fig. 38b,

4. Layup technique

The sequence for this is quite simple and after preparation of the various components is as shown in Fig. 40. When layup is complete, suitable stops (generally ≥ 18 mil) are inserted between the faces of the mold to prevent excessive squashing of the desired structure. A hot press is then carried out at a temperature governed by the plastic employed. This is close to 300°F for Lexan. Finally, the mold is watercooled under pressure and the plate removed from the press. A typical plate manufactured in this way is shown in Fig. 36. We see no restriction to performing these operations rapidly and on a large scale.

Following observations of poor paste adhesion on early plates several techniques were developed to overcome this defect. These involved prior treatments of the base plate surface. Thus, we now use glass mats, (112 style with Volan finish, Clarke-Schwebel Corp.), or dynel fiber (an acrylonitrile/vinyl chloride copolymer) backings to enhance paste adhesion. The mats are 3 mil thick. They are cut to a size corresponding to the pasting area of the plates and are then soaked in a 1-2% Lexan solution in methylene chloride. The solvent on the soaked mats is then permitted to evaporate partially on a glass plate before the mats are attached to the plastic base plate of the final structure which is to be made. At this point, Pb strips are etched, treated with Lexan as outlined before, and then laid up over the glass mat on the base plate. The solvent is again allowed to evaporate off this time completely for ≥ 6 hr. The plate is then laid up con-

---

* Photographs of the plastic shown here have been taken on sections sprayed with black paint so that they can be more easily seen.

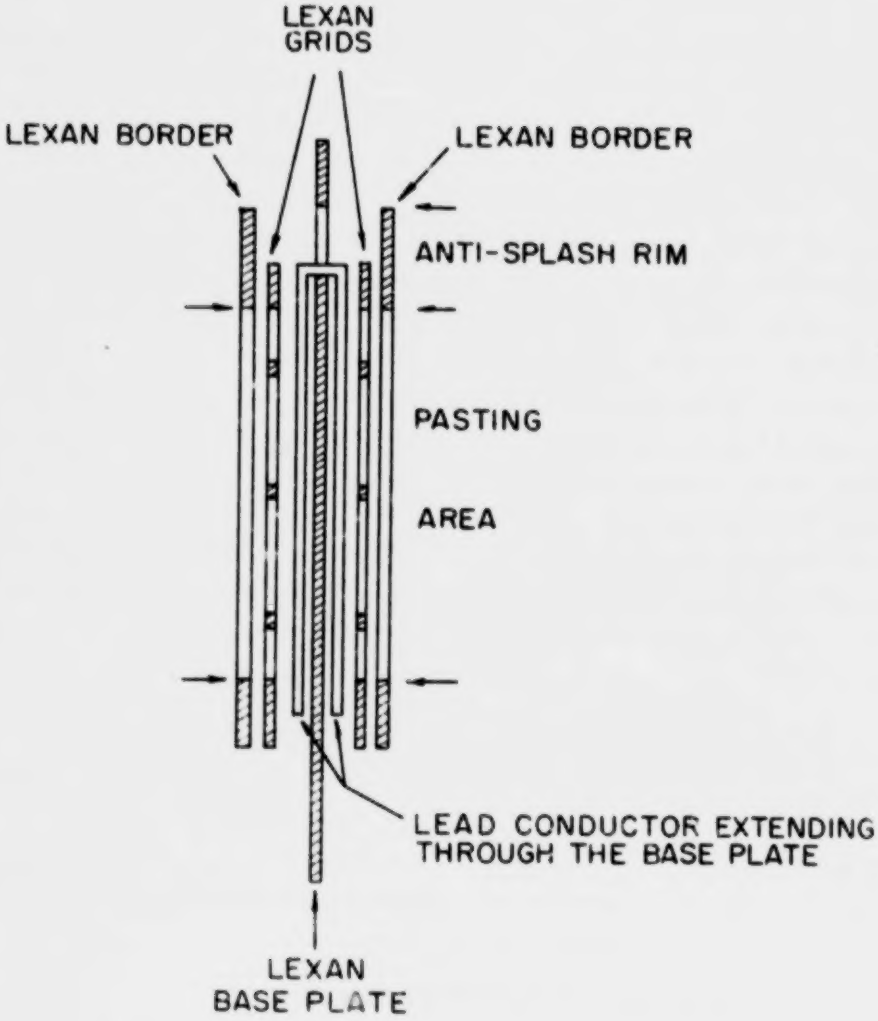
LEXAN GRIDS
LEXAN BORDER
LEXAN BORDER
ANTI-SPLASH RIM
PASTING
AREA
LEAD CONDUCTOR EXTENDING THROUGH THE BASE PLATE
LEXAN BASE PLATE

Fig. 40. Section through the various components of the bipolar plate prior to thermoforming

ventionally in the mold and the entire structure oven dried for > 1 hr at 225° F. If all the solvent is not evaporated off prior to this step, bubbles are formed on the Lexan surfaces. The heated mold is then transferred to the hot press and thermoformed conventionally. One deviation from the norm in this latter step is that 21-mil stops are now used to prevent excessive squashing of the glass mat into the base plate during the forming operation. If this is not done, too much plastic extrusion occurs. The Pb strips tend to become covered with plastic and there is also a tendency towards plate buckling. Additionally, the glass mat becomes completely immersed in the Lexan base plate and loses its effect as a paste-retaining surface. With the 21-mil stops, a 1-2 mil glass surface "sits" on top of the Lexan after layup and is well bonded to the plastic on its underside. In practice, we also deliberately "roughen" this glass surface by scraping it with a metal probe after layup (though this may not stricly be necessary). The Lexan "grids" used to hold the Pb strips to the base plate at localized points also bond well to the Lexan coated (the 1-2% Lexan solution) glass mat surface between the Pb strips.

The preparation of plates with Dynel fiber backing to enhance adhesion of paste is simpler and proceeds in the conventional manner completely through the bipolar plate preparation. When completely manufactured, those portions of the plate between the Pb strips are lightly painted with methylene chloride. Immediately after this, chopped dynel fibers are applied to the surface and the plate is then left until all the solvent has evaporated off. Excess fibers are brushed off the surface. The only care required is to avoid smearing methylene chloride over the Pb conducting strips since the solvent may contain some Lexan dissolved off the base plate. Fig. 41 shows a plate prepared in this manner.

5. Pasting

This was entirely conventional with the exception that ~0.2% Dynel fibers were added to the positive paste and the negative paste to enhance mechanical stability during cycling. Normally such additions are made only to the positive paste. The paste material was Universal Grenox Oxide containing 25% free Pb and a balance of orthorhombic PbO. Curing and formation schedules were conventional and are given in Appendix V.

H. Modifications to the Final Design Structure

The modifications involved the incorporation of further conduction paths through the plates as proposed in numbers (2) and (3) of the preliminary design concepts. For the first modification only two small changes in the entire fabrication procedure are required. Thus, the base plate is cut also at the bottom of the pasting area to the shape shown in Fig. 39b, at the top. The 15 mil Lexan border shown in Fig. 39c is also made equally wide at its top and bottom edges. This serves to give an adequate sealing rim along the bottom edge. In layup, the Pb strips are now completely circled round the base plate via the sections cut out for this purpose (Fig. 39b with the additional bottom cut) and overlapped slightly. The overlap may be located at the top of the plate beneath the plastic border in the final fabricated plate. Both the top and bottom sections of the Pb strips

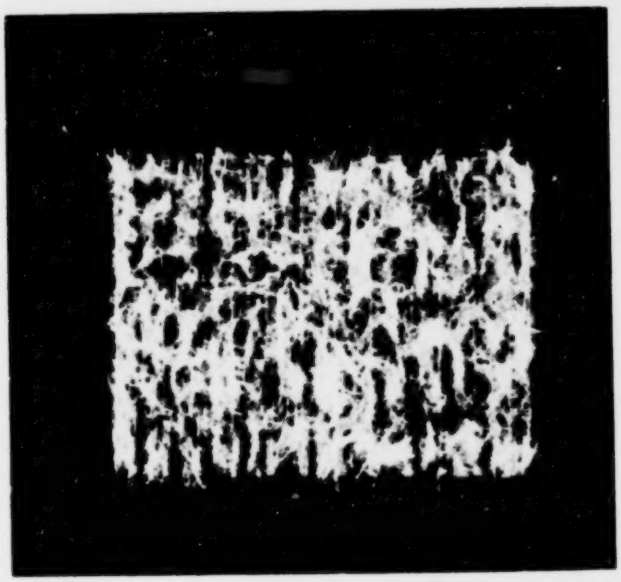

Fig. 41. Photograph of a quasi-bipolar plate prior to pasting with a surface treatment of Dynel fibers to enhance paste adhesion

are treated with plastic solution beforehand to enhance bonding. In the design, the conductor paths are doubled and, therefore, the probability of intercell leakage is increased. The advantage of better paste utilization is also expected by the modification.

In the third modification whose layup is more complex, electrical contact is obtained at the top and bottom of each plate and also at the localized points where the Pb strips and plastic grid intersect in the final layup. The laboratory technique is to drill holes through the plastic at these latter points and to place 15-mil Pb squares on either side of the holes with a smear of methylene chloride between to soften the plastic around the hole. The Pb squares are then mechanically squashed through each hole and at the same time the softened plastic extrudes along the underside of the squashed buttons, coating them. The latter serves to provide good leak-free seals at each point. In addition, after this step, a 5% Lexan solution is pointed around the outside circumferences of each button to further prevent leakage problems. The centers of the buttons are left free, however, to provide electrical contact with Pb strips which are then laid down the plate and over the top of each button. The various steps in this process are shown in Fig. 42. The remainder of the layup process is conventional. As before, corrosion problems may ensue but if corrosion is prevented, there may be significant improvement in plate performance as a result of the changes.

In summary, small scale prototype type plates have been developed which are considered to be suitable for use in a high power density/long life battery. The fabrication techniques are relatively simple and may be readily extended to full size plates on commercial production scale. The complete range of plates which we have fabricated to date (including the preliminary design plates) are tabulated in Table XVIII. Our major operating experience has been with the quasi-bipolar plate described first, which has a plastic substrate with Pb strips as conductors connected only over the top of the plate. Performance data on these are described later (Section VII.B.). Preliminary evaluations of the effects of the changes incorporated in initial quasi-bipolar plates (Fig. 36) on subsequent performance are also discussed. As will be seen, the performance of the first design is such as to negate the necessity for using the latter two if so desired.

I. Design in Which the Plastic Substrate is Conductive

This corresponds to number (4) in the preliminary design concept. In practice we had little hope for its successful application after the conclusion of the evaluations of the acid stability of reinforced thermosetting systems (which were found to lose structural stability as a result of acid attack of the reinforcement/plastic bond). We also found that at the positive plate potential and more particularly at the negative plate potential, O_2 and H_2 gas are rapidly evolved on graphite or carbon in H_2SO_4 electrolyte. Since we anticipated using the latter materials as conducting medium (and as reinforcement) in plastic substrates, this obviously left no choice but to isolate the materials from the acid (with plastic). The acid stability tests did not suggest that the latter was possible without extended experimentation with the structures. However, we attempted to fabricate some structures and the results of this are outlined below:

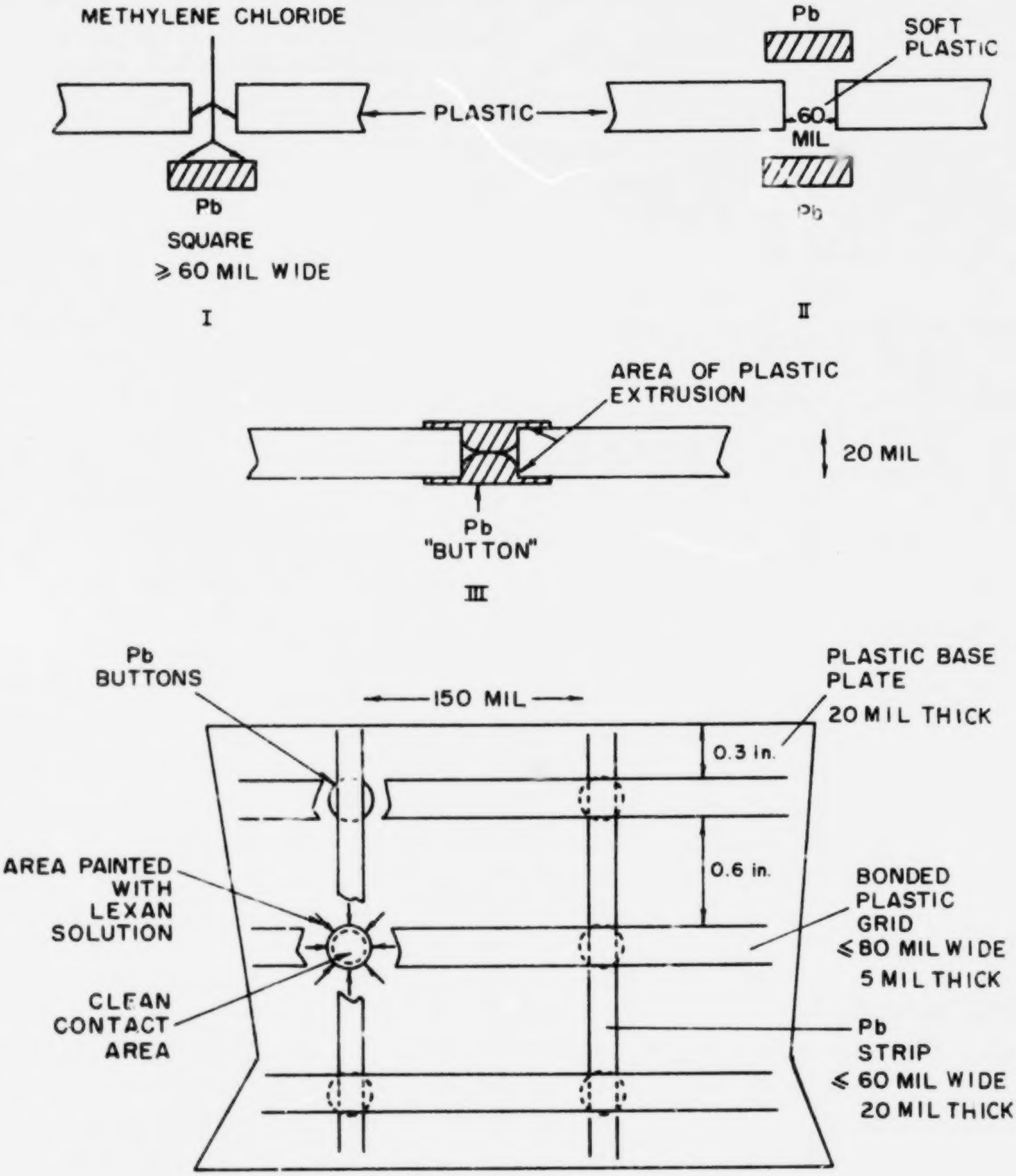
METHYLENE CHLORIDE
PLASTIC
Pb
SQUARE
≥ 60 MIL WIDE
I
Pb
SOFT PLASTIC
60 MIL
Pb
II
AREA OF PLASTIC EXTRUSION
20 MIL
Pb "BUTTON"
III
Pb BUTTONS
150 MIL
PLASTIC BASE PLATE
20 MIL THICK
0.3 in.
0.6 in.
AREA PAINTED WITH LEXAN SOLUTION
CLEAN CONTACT AREA
BONDED PLASTIC GRID
≤ 80 MIL WIDE
5 MIL THICK
Pb STRIP
≤ 60 MIL WIDE
20 MIL THICK

Fig. 42. Construction of a bipolar plastic plate with conduction at the top and bottom of the plate and at those points where the Pb strips and plastic grid intersect on the surface of the plate

Table XVIII. Construction Details on Bipolar Plates with Plastic Substrate and Pb Conductors

	First Plate Design						Second Plate Design									Preanodised Pb Conductors Second Design										
Cell Number	1	2	2 repasted	3	4	5	6	6 repasted	7	8	8 repasted	9	10	11	12	13	14	15	16	17	18	19	20	21	22	23
Plastic	L	L	L	L	L	L	PVC	PVC	PVC	PVC	PVC	L	L	L	L	L	L	L	L	L	L	L	L	L	L	L
Conduction Path	T	T	T	T B	T	T	T	T	T	T	T	T	T	T	T	T B	T B	T B I	T B I	T B	T B	T B	T B	T B	T	T B I
Pb Conductor Width, mil	60	60	60	60	60	60	60	60	20 mil wire	60	60	60	60	60	20 mil wire	60	60	60	60	60	60	60	60	60	60	60
Pb Conductor Thickness, mil	8	8	8	6	8	8	15	15	20 mil wire	15	15	25	20	20	20 mil wire	20	20	20	20	20	20	20	20	20	20	20
Base Plate Treatment	N	N	N	N	G	[illegible]	SB	SBD	[illegible]	N	SBD	D	G	G	G	D	D	D	D	LD	LD	G	G	G	G	D
Paste Weight, gm	13.6	14.7	13.7	13.6	12.4	14.3	16.5	16.5	16.4	17.9	17.8	17.1	16.4	16.5	16.5	14.0	15.4	14.0	15.1	17.1		15.9	15.9	17.4	15.5	18.0
Formation Charge, Ahr	←		poor		→	4.8	10.0	7.0	9.0	5.0	7.35	9.35	9.75	6.3	7.6	6.5	7.2		8.2			7.2			6.6	6.2
Initial C5 Capacity, Ahr	←		poor		→	0.63	0.72	1.18	poor	poor	1.25	1.0	1.06	1.12	1.2	0.98	0.52					0.96			1.09	1.08
Capacity After H_3PO_4 Addition, Ahr								1.05			1.06	0.6	1.0	1.06	1.04	0.84	< 0.1								0.65	0.92
Cycles Before Failure								1000			1000		730	1000	1005	560									200	1158

Key: L → Lexan; PVC → Polyvinyl Chloride; T → Top; T, B → Top and Bottom; T, B, I → Top, Bottom and Pb Plastic Intersection Points; N → No Treatment; G → Glass Mat or Cloth; SB → Sand Blasted; SBD → Sand Blasted and Dynel Fiber; D → Dynel Fiber; LD → Lead Dust.

A prepreg from Union Carbide was used. The material is designated as "Thornel" 75S structural graphite and is B-staged with X-2544 epoxy resin. The material contains unidirectional two-ply graphite filaments. Ply thickness is 7.5 mil. In layup, three plys were used with the middle ply at right angles to the other two. Pb strips were simply laid along the surface of both sides of the laminate at 0.15-in. spacing. It is not necessary to loop the Pb over the top of the structure to provide conduction since this is achieved through the underlying graphite filaments in contact with the Pb strips. Apart from this, layup was as before and Lexan borders and Lexan grids were used to hold the Pb to the base plate (the prepreg) surface at localized points. Where no Pb adhesion to the base plate was desired, the underside of the strips were sprayed with a suitable release agent beforehand. The entire package was placed in the hot press and subjected to the curing shedule below:

Curing schedule	(1)	15 psi at 203°F for 30 min
Bring to	(2)	90 psi at 203°F and hold for 30 min
Heat to	(3)	239°F and hold for 30 min at 90 psi
Bring to	(4)	338°F at 90 psi for 2 hr
Cool to	(5)	122°F at 90 psi in not less than 20 min. (After 1 hr of air cooling, the temperature was down to 150°F: The mold was then water cooled and removed from the press.)

The plate prepared in this manner had the following characteristics:

1. Bonding of the Lexan borders and grid to the laminate base plate was poor.
2. Interply bonding in the base laminate was not good along the outside edges.
3. Resin flow tended to be nonuniform, resulting in some exposed graphite surfaces.
4. There was good conductivity through the plate via the Pb strips.
5. The laminate was bowed and rather brittle.

A phenolic prepreg from Fiber Materials, Inc., (Westford, Mass.) was also used. It had the following properties:

1. It was made from a graphite loaded phenolic resin B-staged on graphite cloth.
2. The cloth thickness was 15 mil and the prepreg thickness 20 mil. The prepreg density was 1.45 g/cc and the cost was 35 dollars per sq yd (for very small volume).

The layup technique was the same as above and the curing schedule was as follows:

1. Bring to 225°F at contact pressure.
2. Increase pressure in 20 psi increments every 5–10 min at 225°F up to 200 psi.
3. Apply total pressure (200–2000 psi) which depends on requirements of final laminate, elg., total thickness desired. [This step was omitted when preparing our laminate which was cured at 200 psi (since the desired laminate thickness was only 20 mil)].

4. Bring to: (1) 250°F for 0.5 hr
then: (2) 275°F for 1 hr
(3) 300°F for 1 hr
(4) 325°F for 2 hr

5. Cool to < 250°F at pressure and then remove the mold from the press.

The plate prepared in this manner had the following characteristics:

1. There was nonuniform resin flow on parts of the surface of the laminate base plate, resulting in some exposure of graphite cloth at the surface.

2. Those areas which were covered by resin showed reduced conductivity.

3. Conductivity through the plate via the Pb strips was good.

4. Bonding of the Lexan border and grid to the phenolic laminate base plate was poor.

5. The plate bowed slightly.

In summary, our preliminary results with these new designs showed both good and bad features. Conductivity was very good through the plate via the Pb strips and underlying graphite. Good conductivity was also achieved through the plate via a Pb strip on one side and on the right hand edge of the plate, and a Pb strip on the reverse side and on the left hand edge of the plate, i.e., along the cloth underneath the resin. Of the two plates, the phenolic with graphite cloth was less bowed and much less brittle and also showed less exposed graphite after preparation. We believe that all these points can be adjusted, however, by adjustment of the various experimental variables, e.g., time of curing and temperature. There is more chance of success with the cloth reinforced prepreg, however. In regard to bonding of the Lexan border (which controls paste thickness) and Lexan grid (which holds the Pb strips to the base plate at localized points), the problem is less easily solved. The best approach would probably be to experiment with other materials, e.g., polysulfone or, if available, thin sheets of the thermosetting resin actually used in the prepreg itself. These problems are not necessarily insurmountable but would require a reasonable time period in which to experiment with the above mentioned materials and techniques.

VII. LIFE TESTING OF NEW DESIGN PLATES

A. Test Cell and Test Procedure

The test configuration and test procedure were held constant for all of the bipolar plates studied. Plexiglass holders were made in which each individual bipolar plate was held between Viton rubber gaskets at the two sides and bottom edge of the plastic rim surrounding the pasting area of the plate. This provided leak-free operation around the plate. Head plates of approximately four times the capacity of each bipolar plate (~5 Ahr total) were inserted in the test holders on either side of the bipolar plate. The head plates were made from antimony free grids. Industrial Daramic separators (extruded polyethylene) from W. R. Grace with 30-mil backing and 45-mil ribbing were used in each cell and a 3-mil glass mat (from W.R. Grace) was used as paste retainer on both positive and negative side of each bipolar electrode. Total electrolyte volume in each cell was ~ 18 ml of 1.28 sp gr H_2SO_4.[4] This is a large excess of acid and cycling tests reported here were carried out using this excess. Recently, we have reduced the acid volume per cell to 6 ml without any apparent degradation in cell performance. The theoretical volume of electrolyte required for high rate/shallow discharge cycles is less than the latter value.* In our battery weight calculations (based on full size plates of the quasi-bipolar design), we have incorporated an allowance for 100% excess of acid. Even with this excess, electrolyte weight is only 10% of total battery weight. Clearly there is adequate scope for varying practical electrolyte requirements without overstepping final battery weight specifications. Additions of 1.8 vol% of 85% H_3PO_4 were made to the electrolyte after formation of each plate and after initial C/5 capacity evaluations.[21] The capacity evaluations before H_3PO_4 additions were minimized to reduce any plate degradation prior to cycling performance tests.

Table XVIII shows the plates we have prepared to the above specifications. The exact details of individual plate construction are given therein. Plate area was held constant at ~ 34 cm^2 per positive or negative electrode. Initial capacity data are given also. Photographs of typical pasted and formed bipolar plates are shown in Fig. 43a and 43b, respectively.

The steps leading up to cycling evaluations after the initial capacity measurement in 1.28 sp gr H_2SO_4 were as follows:

1. Add 1.8% H_3PO_4 to the electrolyte and recharge the plate.
2. Reevaluate the capacity at the C/5 rate.

---

* See page 137 in the text with respect to this point.

Reproduced from best available copy.

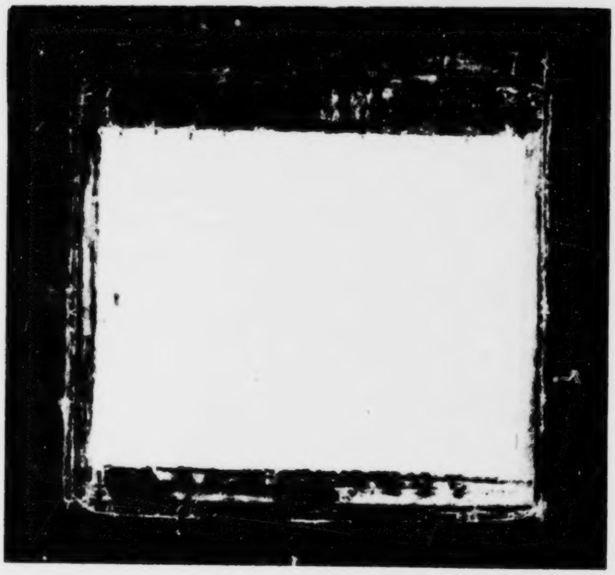

a. Pasted Plate

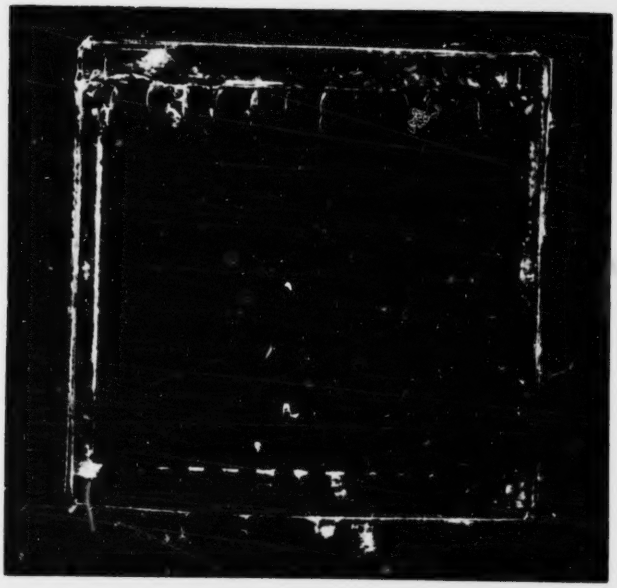

b. Formed Plate

Fig. 43. Photographs of a pasted and cured quasi-bipolar plate and of a formed quasi-bipolar plate

3. Charge at the C/5 rate to full capacity (based on the initial capacity).

4. Partially discharge the plate to 80% total capacity [based on the value in (2) above].

At the end of this sequence, testing is started with exactly the same procedures as outlined previously for commercial plates (page 8, point 4). Temperature was also held at 30°C ± 1°C. Charge and discharge currents were those required to obtain the power ratings of 55 KW and 30 KW within the weight (550 lb maximum) and voltage (150 V minimum) limitations using a battery system based on these quasi-bipolar plates. Based on this, an operating point of 150 mA/cm^2 was chosen. Note that this is lower than the current density required from commercial plates to achieve the same power ratings. Superior life-time on cycling would thus be expected. As before, discharge time was 25 sec. Charge time was held at 67 sec giving a ~ 10% overcharge on each cycle. It is difficult to measure individual positive or negative electrode potentials in a bipolar battery since there are no current take-off terminals. Therefore, complete cell voltages are given for each bipolar plate plus head plates. However, the head plates were shown to vary in voltage during charge and discharge in a characteristic manner which did not change throughout the cycling. Changes in voltage characteristics during cycling are thus a function of bipolar plate performance only. The capacity retained as shown in the data is also that retained by the bipolar test plates only. Because of the difficulty in determining individual positive or negative electrode potentials it has not yet been possible to evaluate which electrode is actually failing as a result of the cycling.

B. Test Results

Test results are recorded in Table XVIII (page 107) and in Figs. 44-52. A synopsis of the relatively poor performance of plates based on the first design has been given already. A major problem was that the Pb strips were too widely separated (0.29 in.) in the design to permit adequate plate charging. Plates numbered 6, 7, 8 and 9 in the final design also did not perform well at first. Thus, paste adhesion was poor in 6, where only sand blasting was used to improve adhesion. Though it formed well initially, the paste rapidly shed from the plastic base plate on subsequent cycling. The same was true for plate number 8 which had no prior surface treatment. Plate number 7, which had Pb wires as conductors, had plastic extruded over many of the wires during fabrication and thus did not form well. Plate number 9 had relatively thick (25 mil) Pb strips as conductors and on plate fabrication, some of these cut completely through the substrate causing short circuit paths when immersed in acid. We overcame these defects by adjusting the fabrication techniques as outlined earlier and were able to salvage plates number 6 and 8 for repasting. These are thus denoted as 6"repasted" and 8 "repasted" in the table. These two plates subsequently showed superior formation characteristics compared to further plates made in exactly the same way and avoiding the defects noted above. We attributed this to better contact between paste and conductors caused, in turn, by the prior surface roughening which the conductors had undergone in the plates during their initial pasting and testing. Subsequently, we now deliberately pre-anodize all the strips on the fabricated plates at 0.5 A for 10 min before pasting. This is noted also in the table.

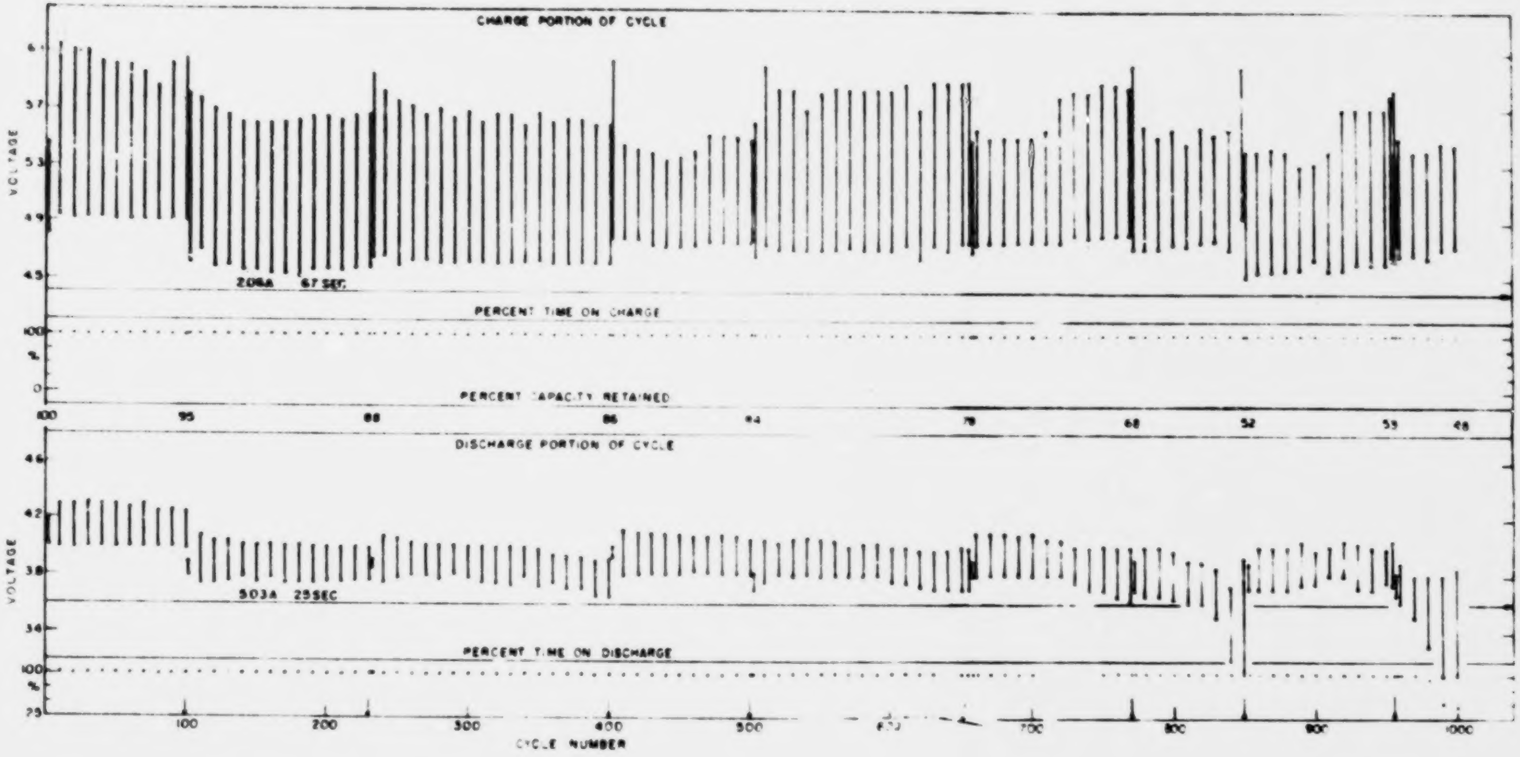

Fig. 44. Performance of quasi-bipolar plate no. 6 "repasted" under severe cycling conditions (two cell voltage)

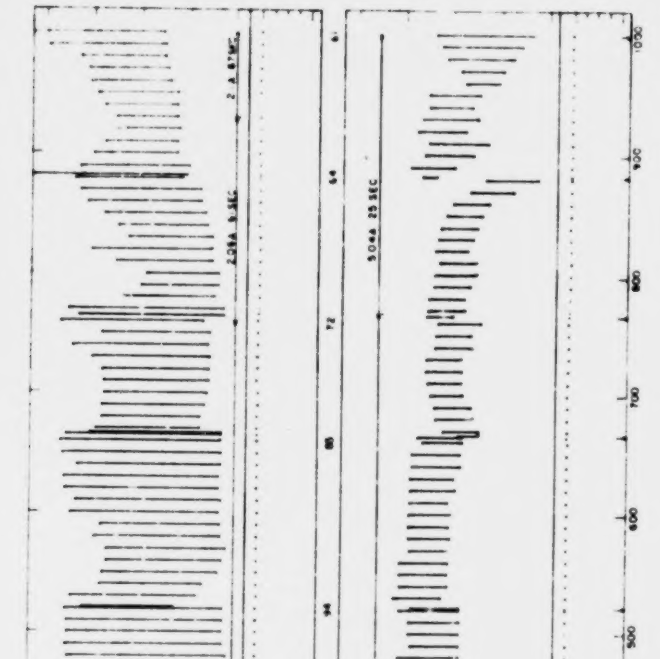

Fig. 45. Performance of quasi-bipolar plate no. 8 "repasted" under severe cycling conditions (two cell voltage)

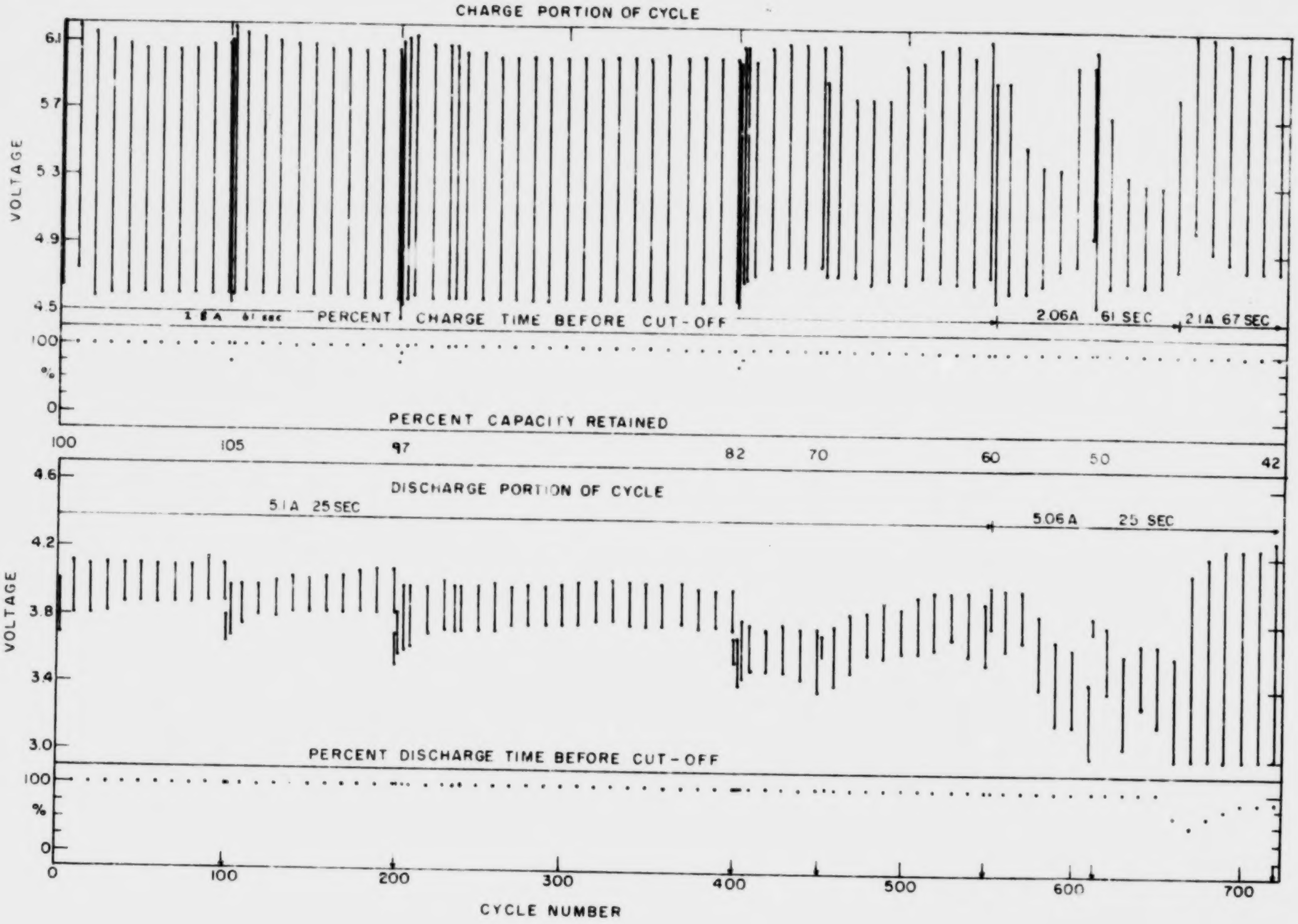

Fig. 46. Performance of quasi-bipolar plate no. 10 under severe cycling conditions (two cell voltage)

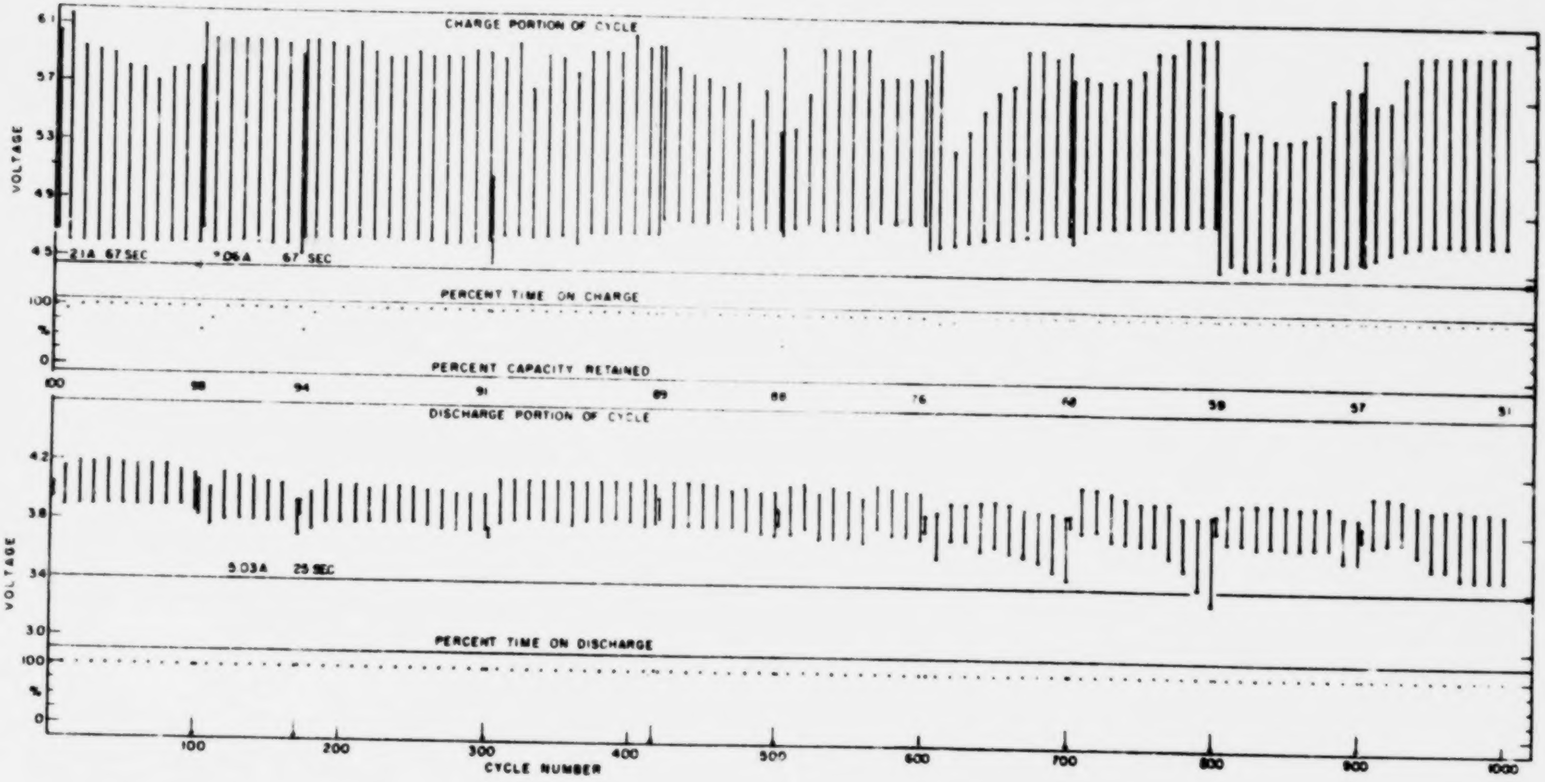

Fig. 47. Performance of quasi-bipolar plate no. 11 under severe cycling conditions (two cell voltage)

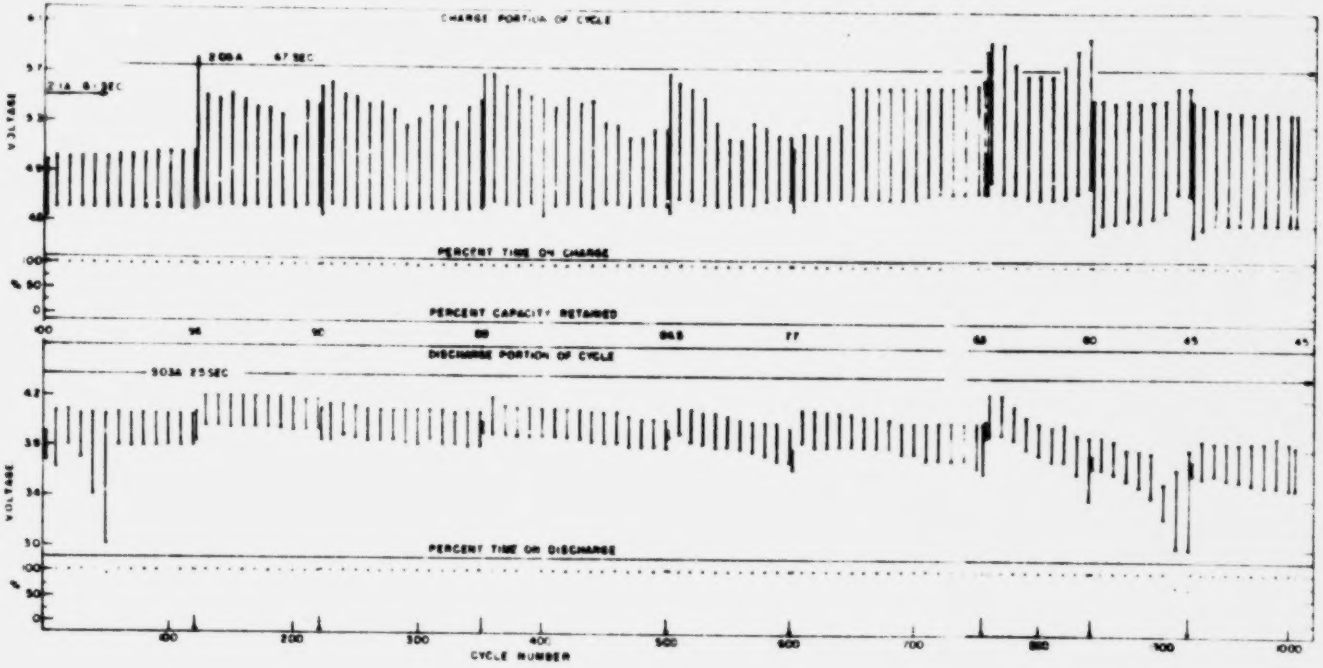

Fig. 48. Performance of quasi-bipolar plate no. 12 under severe cycling conditions (two cell voltage)

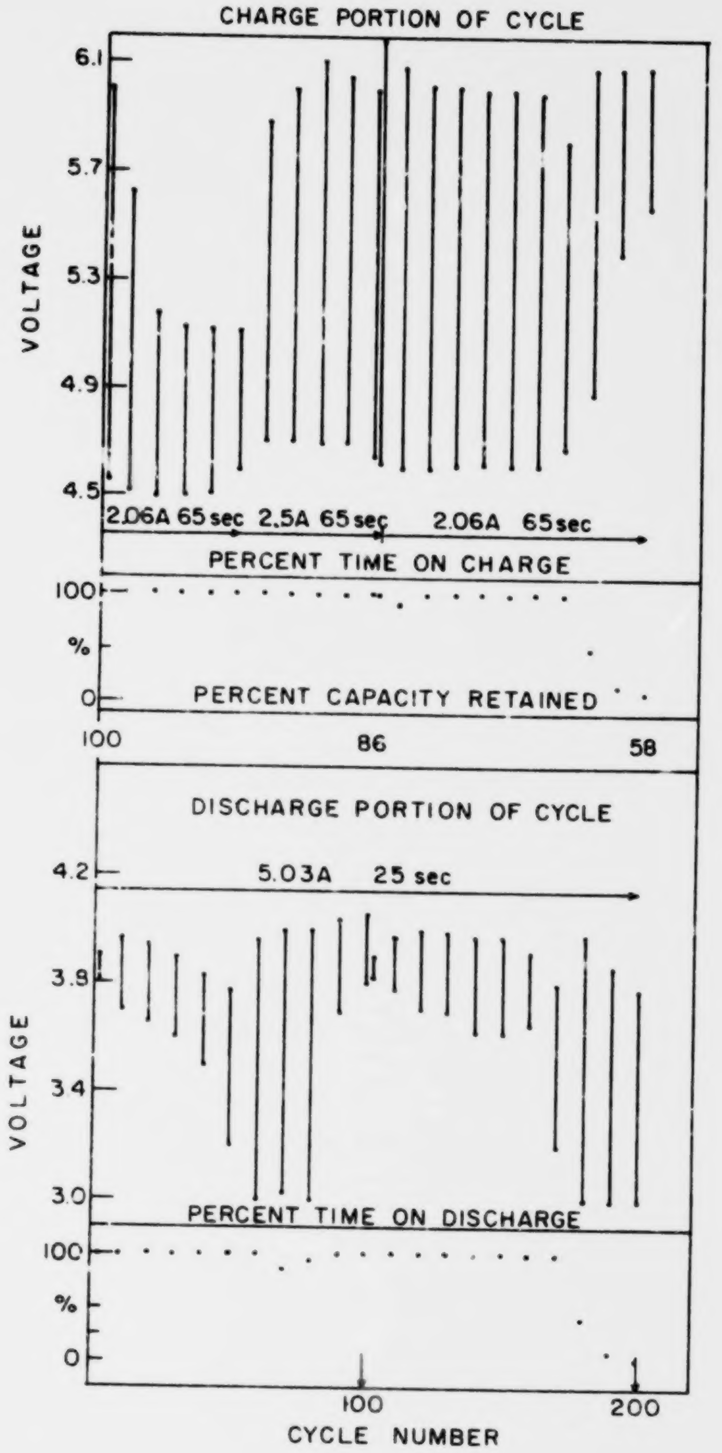

Fig. 49. Performance of quasi-bipolar plate no. 22 under severe cycling conditions (two cell voltage)

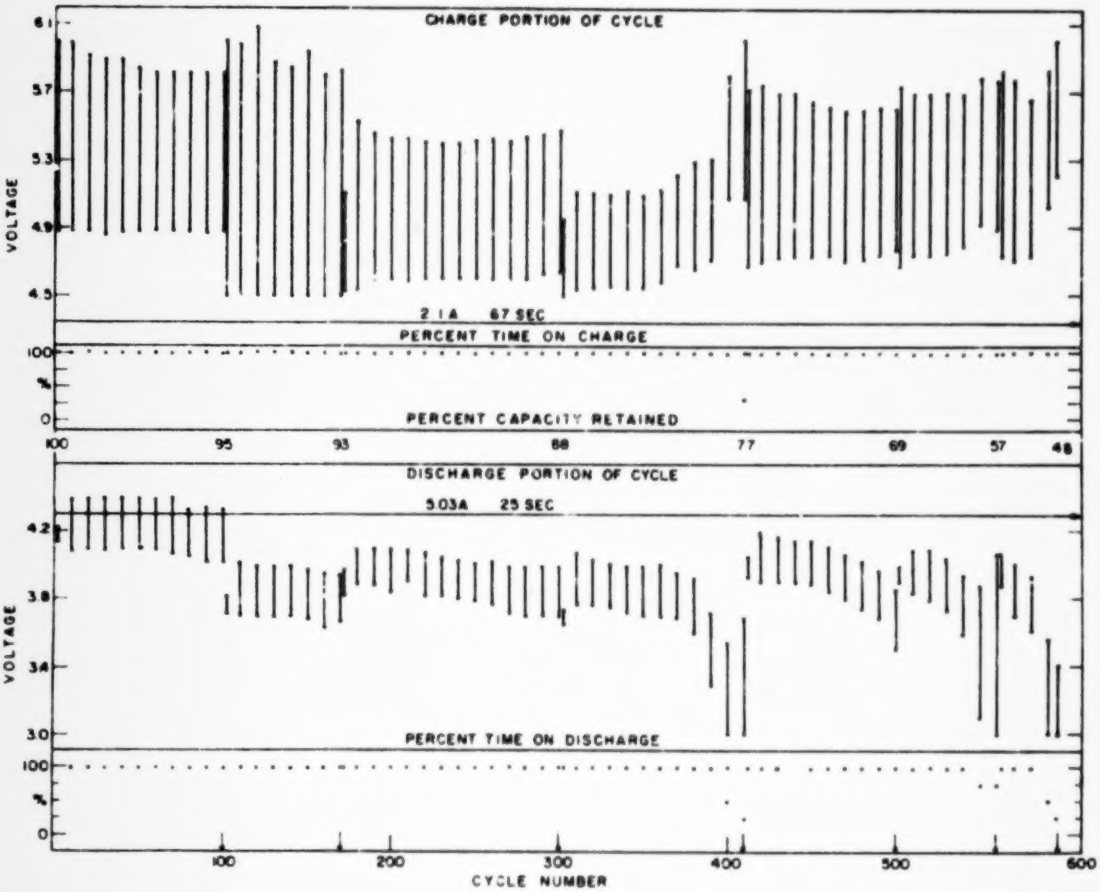

Fig. 50. Performance of quasi-bipolar plate no. 13 under severe cycling conditions (two cell voltage)

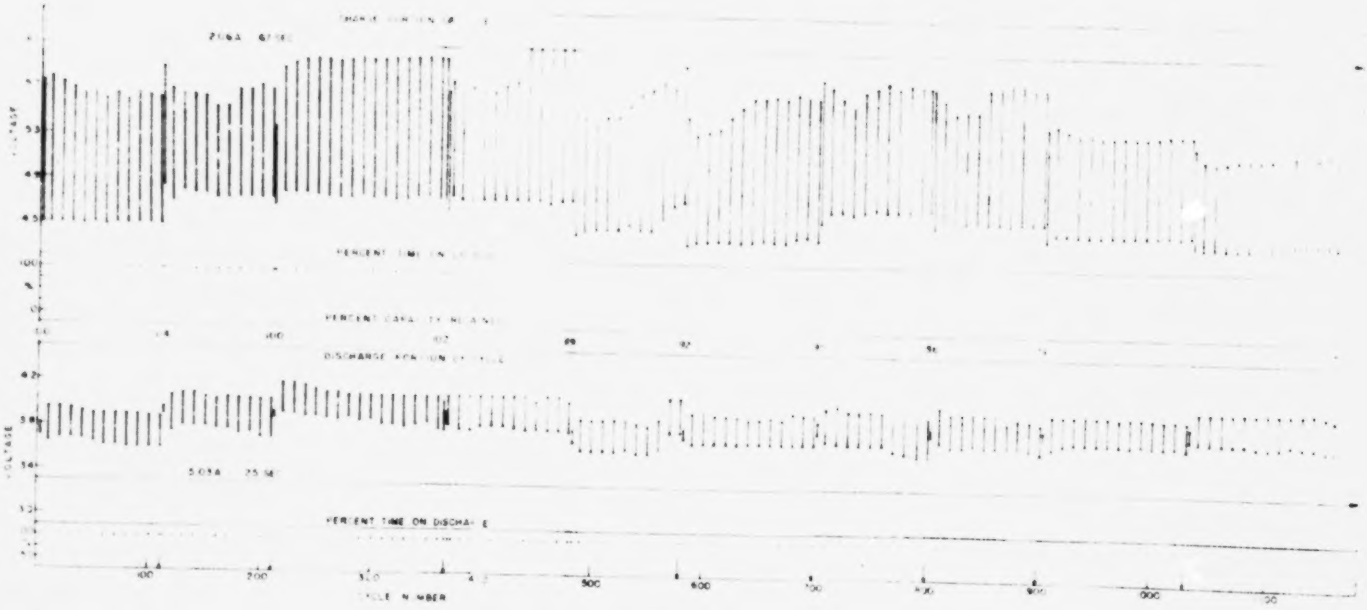

Fig. 51. Performance of quasi-bipolar plate no. 23 under severe cycling conditions (two cell voltage)

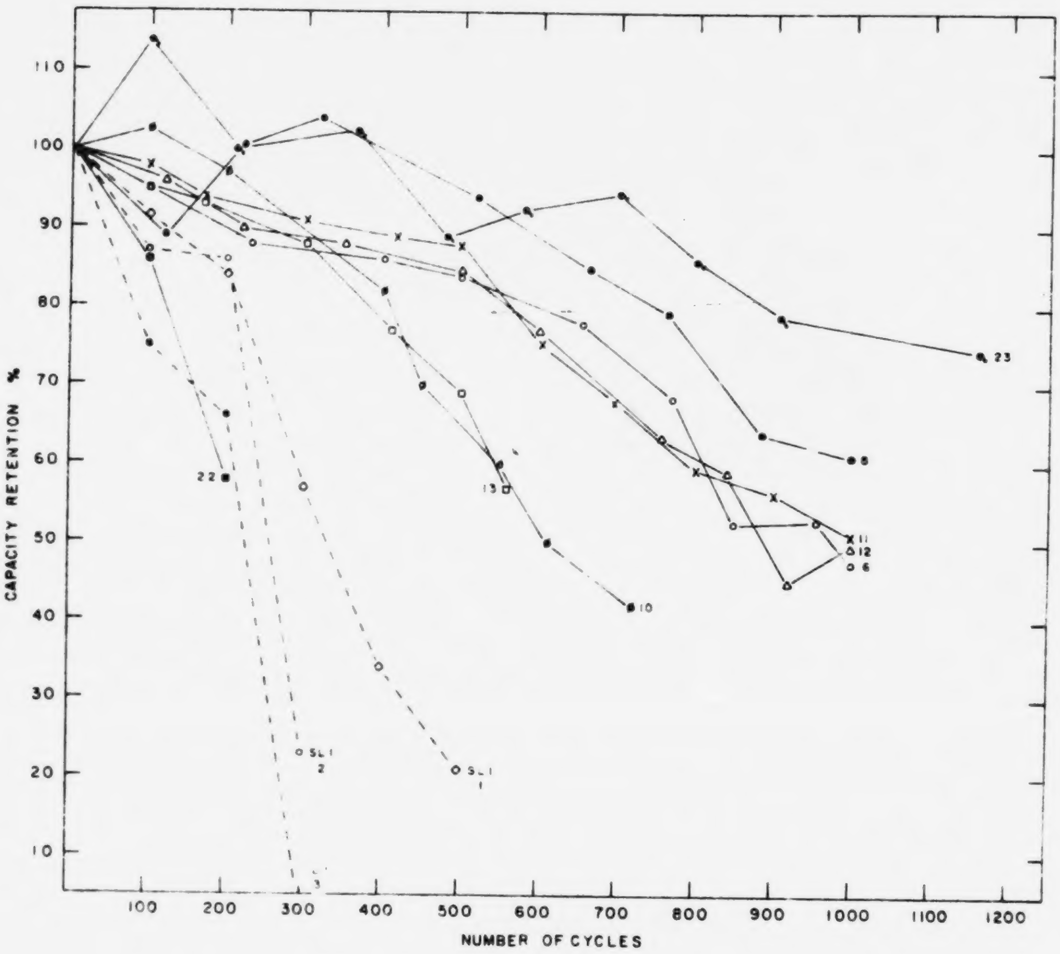

Fig. 52. Capacity retention (C/5) for the limiting electrode of quasi-bipolar test plates as a function of the number of prior high rate cycles undergone. The dotted curves show the equivalent data for three conventional positive plates tested under slightly less severe conditions (cf pages 10 and 113).

The maximum data have been recorded on plates 6 repasted, 8 repasted, 10-12, 22 which all have conduction only over the top of the plate. Other details of the plates are indicated in Table XVIII. They all exhibited good characteristics requiring an average 7.37 Ahr for formation. Visually, they could be seen to form well and evenly over the entire surface. The initial C/5 capacity values were also high, averaging at 1.09 Ahr prior to H_3PO_4 addition. The average paste weight was 16.1 g total and assuming that the positive and negative sides of each bipolar plate have equal weights, this gives a value of 8.05 g/positive or negative paste. The expected capacity for the plates based on Berndt's value[6] of 0.125 Ahr/g (at 2.5 mA/cm^2 discharge current) is 1.01 Ahr. The observed value of 1.09 Ahr is 8% greater than this and was in addition measured at a current density approximately two-and-a-half times greater than the value on which Berndt's figure was based. The plates thus perform well based on this simple evaluation. An interesting observation, and one which we have no real explanation for as yet, was that the addition of H_3PO_4 to the electrolyte caused on average only a 10% drop in capacity of these plates. This is less than the average 25% capacity drop following H_3PO_4 additions to the iR-free plates containing no Sb. (Tudor, et al.[21] also observed a fall in capacity of up to 50% following H_3PO_4 additions to Sb-free cells.) It has been suggested elsewhere[45] that if battery plates are left to sit for an extended period of time after H_3PO_4 addition, the decrease in capacity is not so large. In practice, we did leave all the bipolar plates for more than 6 hr in the discharged state after H_3PO_4 additions. The iR-free plates, in contrast, were immediately recharged after H_3PO_4 additions to the cell. This may or may not be the important difference. For whatever the cause, the observation is important since minimum reductions in plate capacity following H_3PO_4 additions are desirable. Here, it was not deemed necessary to "work" the phosphate into the paste by cycling as recommended by Tudor, et al.[21] to minimize capacity losses in the paste. (That is, the latter authors found that the initial capacity loss could be minimized by subjecting the paste to a number of deep cycles after H_3PO_4 additions).

Results of the cycling on these plates are shown in Figs. 44-52. Apart from plate 22 (Fig. 49) in which some conductors had cut through the substrate during fabrication, all the plates tested stood up extremely well to the cycling regime. The plates are much superior to commercial plates tested under similar circumstances, and four plates which have conduction only over the top of the plate have successfully completed 1000 cycles before onset of failure. Conventionally, due to time limitations, results were terminated after the completion of 1000 successful cycles. It is apparent that each plate underwent capacity degradation as a result of cycling (Fig. 52) and that towards the end of the ninth and tenth groups of 100 cycles, that is, after close to 900 complete cycles and 1000 complete cycles, the voltage of the test cells generally started to decrease sharply towards the 3.0 V cutoff point. However, in each case where such a decrease was observed, the good performance characteristics of each plate were re-attained on re-charging the plates (after the usual capacity evaluations). It is thus anticipated that on these plates, particularly plates numbered 8, 11, and 12, in excess of 1000 cycles could be successfully completed if time permitted. With plate number 10, which also had conduction only over the top of the plate, 730 complete cycles were obtained prior to failure. Time again did not permit an investigation of the failure mode here, but no severe paste shedding was observed on this plate. The negative electrode paste, however, was softened and severely blistered.

The completion of 1000 successful high rate cycles with these plates compares very favorably with the 350 cycle maximum of commercial positive plates. The capacity retained by these bipolar plates is also well in excess of that retained by the commercial plates after equivalent numbers of cycles (see Fig. 52). Thus, for example, after 300 complete cycles, the capacity retained by bipolar plates 6, 8, 10-12 was 87%, 102%, 90%, 91% and 89%, respectively (the maximum capcity retained by the commercial positive plates after 300 cycles was 57%). The voltage on discharge of the bipolar plates is also high when compared to that of the commercial plates (for example, compare Fig. 2). During charge, the voltage of the bipolar plates is quite high, reaching ~ 3 V/cell, but this does not appear to accelerate plate degradation. The difference is due to the absence of Sb in the bipolar plates, and also due to the fact that the plates also receive overcharge at rates up to 40 KW, e.g., in some cycles on plates 8 repasted and 10. Sb lowers the polarization of the positive plate and also lowers H_2-evolution on the negative plate.[46] Because we are able to eliminate Sb from the plates and yet still maintain cycling life, the advantage of maintenance-free performance is thus realized with these bipolar plates.

The results were extremely encouraging. The capacity retained by plates 6 repasted, 8 repasted, 10, 11, and 12 was 47%, 61%, 42%, 51% and 48%, respectively, on completion of 1000, 1000, 730, 1000 and 1005 cycles (Fig. 52). Even at this stage the appearance of the plates was quite good, as can be seen in Figs. 53 and 54, which are of plates 8 "repasted" and 12 after the above number of cycles. Little shedding was observed and the positive electrode paste appeared to undergo less physical changes than the negative. The negative electrode paste was somewhat softened in a manner similar to that observed in commercial negative paste material after cycling (cf. Fig. 10). Note also the whitish tinges (probably due to phosphate) on the positive electrode paste of plate 8 "repasted." Insignificant buckling of the plates was observed and no degradation of the plastic substrate was found. Though some corrosion product was observed on the Pb conducting strips under the plastic border at the top of the plate on the positive electrode, no leakage paths were apparent. After removing the paste from all these plates, the Pb conductors were examined for corrosion attack. Even with 20 mil wires (in plate number 12), no excessive corrosion was observed.* Taken together, the results indicate that the above plates, without further modification, are extremely promising for use in a high rate/long life battery. Though only quasi-bipolar in nature, they apparently are sufficiently well designed to stand up to the rigors of high rate cycling and still exhibit good performance after extended periods.

Nevertheless, we also tested two plates, numbered 13 and 14, in which the Pb conductors were connected through the substrate at the top and bottom of the plate, and one plate

---

* An examination of the minimum conductor cross-section which is compatible with desired lifetime is one of the factors proposed to further characterize these plates on a more realistic time basis.

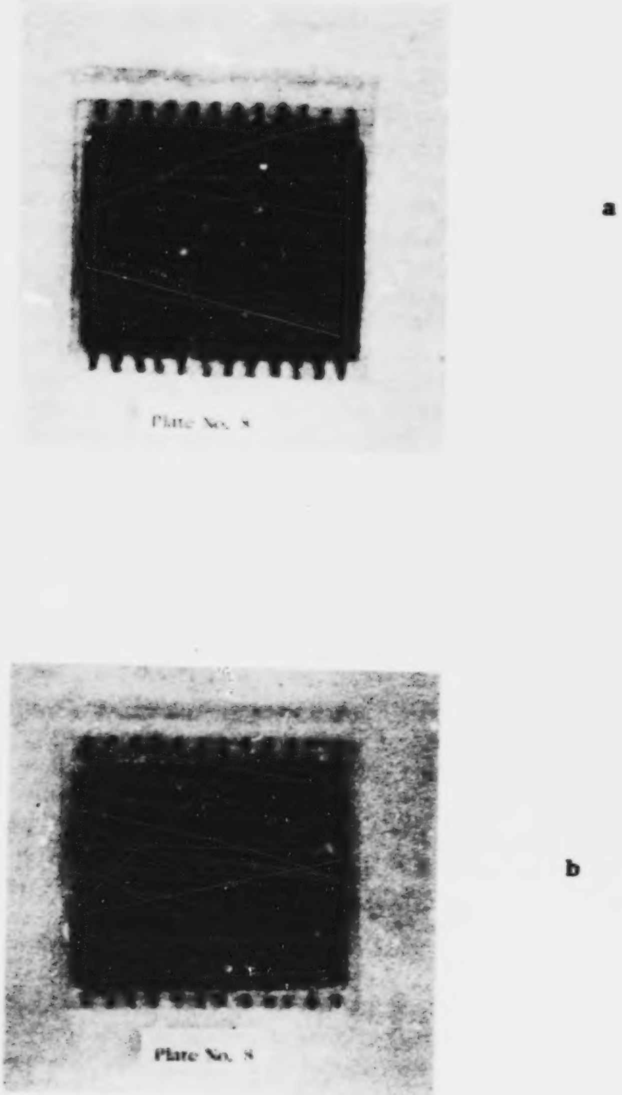
Plate No. 8
a
Plate No. 8
b

Fig. 53. Photographs of the positive (a) and negative (b) electrodes of plate no. 8 after extended (1000) high rate/shallow discharge cycles

Plate No. 12
a
Plate No. 12
b

Fig. 54. Photographs of the positive (a) and negative (b) electrodes of plate no. 12 after extended (1000) high rate/shallow discharge cycles

number 23, in which connection was made also at multiple points down and across the plate. Plate number 14 did not perform well and some conductors were found to have sliced through the substrate during plate fabrication. Plate number 13 lasted for 595 complete cycles, and the capacity retention was 47%. As can be seen from Fig. 50, its voltage characteristics are not excessively different from that of the unmodified quasi-bipolar plates. Plate number 23 (Fig. 51) was tested for 1158 complete cycles and after these, its capacity retention was 74%. On the last 123 of these cycles the plate was operated successfully in the starved electrolyte condition, that is, with electrolyte in the paste and a slight excess outside the paste (approximately 6 mil compared to 18 mil per cell in all the other tests). The data plotted for this plate are shown in Fig. 51. Though the voltage characteristics on cycling are again not markedly changed from those of the above plates, the plate does appear to stand up somewhat better to the high rate cycling as evidenced by the higher final capacity retention figures (after a greater number of cycles). Note also that testing was terminated with this plate after 1158 cycles, not because of failure, but due to time limitations. More so than with the previous plates discussed, an extended cycling lifetime beyond 1158 cycles is anticipated.

Obviously, no exact conclusions may be drawn from the last results since not enough test data are available. However, it is apparent that if sufficient care is taken in fabrication, plates with plastic substrates and multiple connections through the plate between Pb conducting strips placed on either side, can be made and operated successfully. The performance of such a plate suggests that superior life time on cycling may ensue due to better paste utilization, compared to plates where connection is made only over the top of the plate.

VIII. BATTERY DESIGN AND PRELIMINARY COST ANALYSIS

In this section, details of the design, operation, and characteristics of full-scale battery systems made from the quasi-bipolar plates are given. Since the actual experimental test program and design concepts were based on the Preliminary Power Profile specified by EPA (pages 1 and 2), the specifications of a full-scale battery operating at the minimum permissible limits given in this profile, i.e., at 100 W/lb, are discussed first. The maximum power density demonstrated in the program period for a full-sized battery system based on the plates is then calculated. Also, the energy density of the battery operating at 100 W/lb and at a moderate rate (C/5) is included and contrasted with that of an equivalent battery constructed from thin conventional SLI plates operating at the same power densities. Finally, the modifications to the above battery system which are necessary to make it conform to the Final Power Profile specified by EPA (Fig. 1 and pages 2 and 4) are then discussed. In this respect, the specifications are given first for such a modified battery operating at the minimum permissible limits given in the profile, i.e., 128 W/lb. Then, the specifications are given for operation at the final preferred goal of 156.6 W/lb (the latter is the average power density over a 25 sec period - at the 70.5 KW rate). Finally, the specifica- the average power density over a 25 sec period - at the 70.5 KW rate). Finally, the specifica- tions of the battery operating at the maximum desired power output (92.5 KW for 10 sec) of 205.5 W/lb are given; and here the preferred changes to the basic (Fig. 36) quasi-bipolar plate design, which are considered desirable to enable a system constructed from the plates to conform to the latter limits, are also detailed.

Of necessity, several assumptions were made in all these calculations and they are rationalized below. Where possible, however, projected full-scale battery performance is based on actual test results and calculations have been based on the use of those materials which have been shown here to be suitable for use in lead acid batteries.

A. Design, Operation, and Characteristics of a Quasi-Bipolar Battery System Based on the Preliminary Power Profile Specified by EPA

The design of the system is based on the same modular approach discussed in Section III Concept I and in Appendices I and II for Preliminary Bipolar Concepts A and B. The basic plate design is exactly as discussed in Sections VI (E, F, and G) for the small scale quasi-bipolar plates, with conduction only over the top of the plate. The pasting area is approximately six

Preceding page blank

times that of the small scale quasi-bipolar plates and is made relatively long (8-in.) and shallow (4-in.) to minimize resistance losses. As before, each module consists of a series arrangement of 100 such plates, with two conventional head plates (~ 80 mil thick) pasted in Pb or Pb/Ca grids and placed at each end of the module to remove the current. The modules are placed in parallel to provide the necessary capacity. In this design, the total plate dimension is held at 9-in. long × 5.3-in. deep. Thus, approximately 0.37-in. is available on each side of the plate for sealing within the case and approximately 0.5-in. is available at the bottom for sealing in the case. The additional space at the bottom of each module also tends to prevent short circuits in each cell due to accumulation of paste which may shed from the plates during operation. Sealing is accomplished within the case (such as that shown in Fig. 37), preferably in the manner used by Bell Telephone, which is outlined on page 97 of this report. At the top of the plate, the 0.55-in. rim prevents acid splashing over the plate. In each module an acid equalization slot is also cut in each plate, as shown in Fig. 37. The following specific points rationalize the choice of design parameters for the full-scale battery:

1. Choice of Pb conductor dimensions

For calculation purposes, these were taken as 20 mil Pb wires. Pb has a minimal corrosion rate in H_2SO_4. In effect, the minimum cross-section through the conductor governs its life due to corrosion. In some test plates, the minimum dimension was actually 15 mil per conductor, and plates with such conductors performed very well on cycling. Within the short time scale (~ 1 mo.) of the tests, there was no recorded instance in which severe corrosion of these strips (e.g., complete corrosion through of any strip) was observed. On the contrary, the conductors in all of the plates after 1000 cycles, though corroded somewhat on the positive side, still looked very good. Plate number 12, which was made using 20 mil Pb wires as conductors, also performed very well. In addition, the minor change in conductor separation across the plate, affected by using conductors of thinner cross-section, also did not limit plate performance. Nevertheless, in any subsequent development of the battery system, a more extensive evaluation of the minimum conductor dimension necessary to maintain a 5 yr lifetime under the specified operating conditions is required.

2. Electrolyte weight

The electrolyte weight was a calculated value for the final design battery, and the calculations are exactly as shown for the preliminary bipolar concepts (A) and (B). As before, this electrolyte weight was based on the two consecutive 55 KW, 25 sec power pulses. An acid utilization factor of 0.5 was selected, and this has been shown to have only a minor effect on overall battery weight (Fig. 16). In practice, we doubled the calculated amount of H_2SO_4 to allow for the volume of electrolyte required physically to soak the retainer and separator in the intervening space between adjacent electrodes. In fact, the volume of electrolyte required for the most severe high rate discharge cycles can be incorporated totally in the volume of the paste.

Even with the above allowances, electrolyte contributes only 10% to total battery weight, leaving scope for further incorporation of more electrolyte if desired. In practice, thougn the majority of the tests reported here were carried out with excess of electrolyte, in one instance with cell 23, we used a starved electrolyte condition (6 mil cell compared to 18 mil normally) and observed no degradation in plate performance during the high rate cycling. It is, nevertheless, true that even in this starved condition the electrolyte volume (converted to a volume per full size cell) is still twice that used for calculation purposes. Therefore, further development work in this field is required. We re-emphasize, however, that in actual fact there is scope for more than doubling the acid volume without exceeding battery weight requirements.

3. Separators and retainers

A major problem area anticipated was that of gas bubble retention, particularly during charging. In the latter experiment, outlined above, we used a 3 mil glass mat and a Daramic separator with 10 mil backing and 10 mil ribbing. No severe gas retention problems were observed. Note that with the latter separators and retainers, the total weight contribution per battery is only 1.5% and 1.0%, respectively. Therefore, no weight restrictions are found with these two components, nor apparently is gas bubble retention a problem with such materials. However, at the electrolyte volume chosen per cell for calculation purposes, the calculated spacing between adjacent electrodes is only 0.011-in. Therefore, a compromise is required between the retaining mat thickness, separator thickness, and configuration and the desirability of reducing the acid volume (weight component) per cell. In such a tightly packed cell configuration as that proposed in a module, it is questionable if retaining mats are necessary, or even desirable, but we have included their weight in the final calculations. We have considered the use of 10 mil flat sheet separators for calculation purposes, but this is another area requiring further development work. An ideal compromise may be to use a ribbed separator with 10 mil backing and 5 mil ribbing (which can be made available from W. R. Grace Co.) and with a retainer only on the positive electrode side. Alternatively, the desired approach may involve modifications to the electrode structure incorporating channels for gas bubble release in conjunction with the use of a flat sheet separator.

4. Choice of paste thickenss

The paste thickness necessary to supply the required capacity during the most severe energy transfer cycle of 760 Whr was initially calculated as 7-mil (for a 8-in. × 4-in. plate or 5-in. × 3-in. plate - see Appendices I and II). These calculations were based on paste utilization factors taken from Berndt's[6] data and assuming a decay allowance (F in Section III and in Appendices I and II) of 0.5. The values assumed were recognized as being conservative since they referred to conventional thick plate designs (see for example, Fig. 21, and the related discussion). Nevertheless, the paste thickness was held at 20-mil per electrode during plate development and also for the present calculation purposes. The reason for the choice of this large excess of active material was simply to ease any plate fabrication and handling problems. In fact, as discussed, there were no problems, and the quasi-bipolar plates with 20-mil paste thickenss all behaved very well (see Section VII). Moreover, the capacity of these full-size quasi-bipolar plates is 6.4 Ahr at the C/5 rate and is ~ 3 Ahr/plate at a power density of 135 W/lb (150 mA/cm^2 discharge current). On discharging at 55 KW for two consecutive 25 sec pulses, 4.25 Ahr battery (or 0.425 Ahr/plate with 10 parallel modules) are consumed. Clearly, with the present design, there is a very large excess (sevenfold) of capacity available even at the highest discharge rates. This excess of active mass is also very desirable in view of the more extreme power ratings recently specified by EPA (Fig. 1).

The calculations for the preliminary bipolar concept A (see Fig. 16) also revealed the significant impact on battery weight of the reserve capacity in the plates, suggesting that a marked reduction in overall battery weight can be achieved simply by reducing the paste thickness to 15 mil per electrode. Finally, it is normal practice to make a conventional positive electrode slightly thicker than the negative since the former is usually limiting at high rates. Possibly then, the negative electrode in the present quasi-bipolar plates may be made even thinner than 15-mil with further optimization in power density. For the present purposes, however, it is sufficient to reiterate that the battery weight was calculated on the basis of a 20-mil paste thickness per electrode and that the plates in the battery have consequently more than adequate reserve capacity after extended cycling at high rates.

5. Paste adhesion

For the calculations, no Pb plate was incorporated to prevent corrosion through the substrate and enhance paste adhesion. In fact, this is a desirable omission. Final battery cost and weight are reduced and expansion on the positive electrode (with plate buckling) is minimized (see Preliminary Concept A in Section II and particularly Fig. 15). We observed very good adhesion to the substrate using dynel fibers or glass mat, and, because of the design of the plate, no corrosion probelms are evident.

The design values used for power density calculations of a battery system based on the above discussion are summarized below in Table XIX. The values (not the current density) are also the same in a battery conforming to the final power profile.

Table XX gives a summary of the weight requirements for each module designed to operate under the preliminary power profile specified by EPA, and Table XXI is a comparison of the component weight distribution in a conventional battery (ex. Vinal[4]) and the module above.

Table XIX. Basic Assumptions and Design Parameters of a Full-Size Battery Based on the Quasi-Bipolar Plate with Conduction Over the Top (Concept I)

Average Discharge Voltage	:	1.8 V/cell
Pasted Area	:	32 sq in./positive or negative electrode
Total Plate Area	:	48 sq in.
Operating Current Density	:	150 mA/cm^2
Lexan Density	:	1.2 g/cc
Plastic Base Plate	:	20 mil thick
Plastic Grid	:	5 mil thick
Plastic Border	:	15 mil thick
Plastic Border Surrounding the Active Mass	:	Same dimensions as in small scale test plate
Lead Conductors	:	20 mil Pb wire
Paste Thickness	:	20 mil per electrode
Case Material	:	0.2 in. thick
Separator Thickness	:	10 mil (0.9 g/cc)
Retainers	:	3 mil (1.9 gm/cell)
Inter-Module Wiring	:	≈ 1 ft/module of heavy gauge aluminum at 59 gms/ft
Electrolyte	:	1.28 sp gr

Table XX. Summary of Weight Requirements for Each Module Based on the Quasi-Bipolar Plates (Concept I) and Operating Under the Preliminary Power Profile

		lb	% of Total Wt
1. Paste/module	=	22.50	55
2. Head plates/module	=	0.79	2
3. Plastic components (grid) in the Plate/module	=	5.22	13
4. Lead conductors (grid)/module	=	4.50	11
5. Glass retainers/module	=	0.43	1
6. Separators/module	=	0.60	1.5
7. Case material/module	=	2.88	7
8. Inter-module wiring	=	0.11	0.3
9. Electrolyte/module (double the calculated requirement)	=	3.92	9.5
Total wt/module	=	40.95	
Number of modules/battery	=	10	
Total wt/battery	=	409 lb	

Table XXI. Percentage Weight Distribution Comparison in Conventional and Quasi-Bipolar Batteries

	Conventional	Bipolar	
Active materials ($Pb + PbO_2$)	37	55	
Electrolyte	23	9.5	
Pb grid	25	11	Equivalent to a Conventional grid
Case	6	7.	
Connectors	6	0.3	
Separators	1	1.5	
Plastic grid	-	13	
Retainers	-	1	

The above module weighs only 40.95 lb, and the quasi-bipolar plates in it have been demonstrated to operate successfully at 150 mA/cm^2 on discharge and up to 83 mA/cm^2 on charge for 1000 cycles. Concurrently, conventional lead plates in each test cell which incorporated Universal Grenox oxide pasted in 50 mil Pb or Pb/Ca grids did tend to shed somewhat but still readily withstood the same cycling regime. This is not surprising since the effective current density for these conventional plates is only 75 mA/cm^2 and 41.5 mA/cm^2 on discharge and charge, respectively. Under a small drain, the voltage of such a module is close to 200 V and is, on average, close to 180 V at a discharge current of 150 mA/cm^2. To obtain the minimum power density of 100 W/lb originally specified by EPA, 14 such modules can be used in parallel and the operating current density is only 110 mA/cm^2. Since 1000 cycles were performed successfully at 150 mA/cm^2, it is inferred that even more could be performed at 110 mA/cm^2.

Alternatively, an exact calculation of the maximum power density of a full-size system which has been experimentally demonstrated using these quasi-bipolar plates is instructive. Thus, based on the maximum discharge current examined of 150 mA/cm^2, a power density of 136 W/lb is calculated. To achieve the maximum 55 KW discharge rating initially specified, only 10 modules are required and the total battery weight is 409.5 lb.

The modifications to the above design which are necessary to achieve the more recent power profile (Fig. 1) specified by EPA are discussed below.

B. Design, Operation and Characteristics of a Quasi-Bipolar Battery System Based on the Final Power Profile Specified by EPA

There are basically no design changes, as such, required to conform to the more severe power profile. Thus, the same modular approach is followed and the plate design and sealing techniques are exactly as before. The plates are still mounted in series in a module and the modules are placed in parallel also. However, the number of plates required per module is changed and so also is the operating current density.

The most pertinent changes in the power profile are as follows:

1. The minimum working voltage is increased from 150 V to 200 V.

2. The average maximum power over a 25 sec pulse is 70.5 KW (compared to 55 KW previously).

3. The most severe power pulse called for is 92.5 KW for 10 sec (compared to 55 KW previously).

4. The maximum total energy output during two consecutive 25 sec pulses at an average power of 70.5 KW is 980 Whr. This is ~ 30% more than the previous 760 Whr during two consecutive 55 KW pulses for 25 sec each, as specified in the preliminary power profile.

Because of (1) and the specified minimum voltage per cell of 1.5 V, an additional 33 plates per module are now required. Thus, the module weight is increased from 40.95 lb to 54.5 lb. Fortunately, however, no further changes in the module are necessary, for example, in the amount of paste or electrolyte required, due to the higher power ratings specified in (2) and (4). The latter points are illustrated in the comparative calculations given below.

a. Operation at 55 KW with a maximum energy output of 760 Whr for a system using 100 cells per module (and assuming 1.8 V/cell discharge).

The active plate size is 8-in. × 4-in.^{2} = 206 cm^2.

For the entire battery, the highest discharge current at 55 KW and 180 V is 305 A.

The current per module is 0.206 X (amperes), where X = operating current density (mA/cm^2).

The number of modules required in parallel is:

$$\frac{305}{0.206\ X} = \frac{1480}{X}$$

Deepest depth of discharge over two 25 sec consecutive pulses is:

$$\frac{760\ \text{Whr}}{180\ \text{V}} = 4.25\ \text{Ahr, or}$$

$$\frac{4.25\ X}{1480} = \underline{\underline{0.00287\ X\ \text{Ahr/plate}}}$$

The amount of acid required is calculated from the value 0.103 Ahr/gm of 1.28 sp gr acid.[4]

Therefore, the weight of acid per cell is $\frac{0.00287\ X}{0.103\ A}$,

where A = fraction of acid to be used (0 – 1) = 0.0278 $\frac{X}{A}$ gr H_2SO_4/cell.

b. Operation at 70.5 KW with a maximum energy output of 760 Whr for a system using 133 cells per module (and assuming 1.8 V/cell on discharge)

The active plate size is 8 in. × 4 in.^{2} = 206 cm^2.

For the entire battery, the highest discharge current at 70.5 KW and 239 V is 295 A.

The current per module is 0.206 X(amperes), where X = operating current density (mA.cm^2).

The number of modules required in parallel is:

$$\frac{295}{0.206\ X} = \frac{1432}{X}\ .$$

Deepest depth of discharge over two 25 sec consecutive pulses is:

$$\frac{980\ \text{Whr}}{239\ \text{V}} = 4.10\ \text{Ahr, or}$$

$$\frac{4.10\ X}{1432} = \underline{\underline{0.00286\ X\ \text{Ahr/plate}}}$$

assuming 0.103 Ahr/gm of 1.28 sp gr acid.[4]

The weight of acid per cell is again $\frac{0.00286\ X}{0.103\ A} = 0.0278\ \frac{X}{A}$ gm H_2SO_4/cell.

Thus, no more paste or excess electrolyte are required for the modified system. Exact operating characteristics for the full-scale battery are given below for a series of possible power densities. A summary of the weight requirements of a modified module conforming to the final power profile is given in Table XXII.

Table XXII. Summary of the Weight Requirements for Each Module Based on the Quasi-Bipolar Plates (Concept I) and Operating Under the Final Power Profile

	lb	% of Total Wt
1. Paste/module	30.0	55
2. Head plates/module	0.79	1.5
3. Plastic components (grid) in the plate/module	6.96	13
4. Lead conductors (grid)/module	6.00	11
5. Glass retainers/module	0.57	1
6. Separators/module	0.80	1.5
7. Case material/module	3.84	7
8. Inter-module wiring	0.11	0.2
9. 1.28 sp gr electrolyte/module	5.23	9.8
Total wt/module	54.3	

1. 70.5 KW rate, 128 W/lb power density

The above is the maximum average rate desired over 25 sec pulses, and the power density is a minimum desired value from a 550 lb system. The battery is constructed from the same quasi-bipolar plates and the modules are modified as above to include 33 more plates in series (133 total). To obtain the 70.5 KW discharge rate, 10 parallel modules are employed and the operating current density per plate is 143 mA/cm^2. This is within the limit at which the plates were already successfully tested in the present program (150 mA/cm^2, and so no extrapolations are required to predict successful performance on cycling.

2. 70.5 KW rate, 156.6 W/lb

The system is exactly the same as above, but the preferred final battery weight is 450 lb maximum. Since the module weight is 54.3 lb, only 8 parallel modules could be used giving a system weight of 436 lb. The operating current density per plate is increased to 178.6 mA/cm^2 and the exact power density is 161.6 W/lb. Though this current density is somewhat higher than the 150 mA/cm^2 value actually used to test the plates, it is still anticipated that no severe degradation on cycling would occur.

3. 92.5 KW rate, 205.5 W/lb

This corresponds to the maximum power required only over a 10 sec period. With 8 parallel modules (212 W/lb), the current density per plate to achieve this power density from a full size battery, (450 lb desired weight) is increased to 234 mA/cm^2 for those 10 sec.

It is clear that to project battery performance at the power densities specified in (2) and (3) above, some further test data are desirable. The depth of discharge per plate is increased at these higher operating current densities. Fortunately, however, there is already a sevenfold excess of active mass in each plate to compensate for this, so we anticipated no problems in this respect. The question arises as to whether or not repeated cycling at these higher rates would adversely affect performance. Though it is believed that the plates would perform well under such circumstances, further tests are required to demonstrate this.

Rather than raise the operating current density to achieve the power densities specified in (2) and (3), a more feasible approach would be to reduce, by 25% say, the active mass thickness for electrode (to 15 mil) since this is present in such excess anyway. Such a reduction would still leave a large excess (about five times) of active material in the plates over the required amount. The utilization of active mass would also be increased in the thinner plate and the operating current density of the full-size system would be < 190 mA/cm^2 even at the 92.5 KW rate. From our test results, there are no design restrictions involved in such a procedure. It is possible that the Pb conductors may have to be kept at 20 mil (even though the paste thickness is reduced to 15 mil) from a corrosion aspect, but our plates with 15 mil Pb conductors have, in fact, shown very good performance capabilities to date.

In summary, a modular high power density battery system incorporating quasi-bipolar plates with conduction only over the top of each plate (Concept I) is promising. Each module contains 133 plates in series, and there are 8 modules in parallel (436 lb total) in the final battery. The plates must operate at close to 180 mA/cm^2 to achieve a power density of 161.6 W/lb (the 70.5 KW rate). To operate at 92.5 KW for 10 sec periods (212 W/lb), the required operating point is 234 mA/cm^2. There is more than adequate paste and electrolyte in the present design to achieve these rates, but the plates have not been tested on extended cycling above 150 mA/cm^2. A preferred approach is to reduce the amount of active mass per plate by 25%, and thus the operating current density per plate may be reduced to < 190 mA/cm^2 even at a power density of 212 W/lb.

C. Energy Density of a Full-Size Battery System Based on the Quasi-Bipolar Plates (Concept I)

A calculation of the energy density of the battery built with the quasi-bipolar plates and operating at 100 W/lb is instructive. Additional allowance is required for the excess electrolyte used to discharge the plates to 100% of available capacity at this high rate. Initially, there were no data available on paste utilization at high rates for the quasi-bipolar plates. Therefore, we abstracted the data from Fig. 21 using the performance of the iR free one sided 20 mil pasted positive electrode. The operating current density at 100 W/lb and with excess acid is > 110 mA/cm^2 and is estimated as 130 mA/cm^2 for these calculations. Paste utilization in Fig. 21 is ~ 42% at this point (for the positive paste). No data were available for utilization of the negative electrode at high rates. However, because the negative uses less electrolyte,[4] it would be expected to perform as well as, if not better, than the positive, at high rates. Also, when we recently discharged quasi-bipolar plate number 23 to test paste utilization, we recorded a 63% utilization factor at the 150 mA/cm^2 operating point. This was even better than expected and, in addition, is a measure of the utilization of the limiting electrode at high rates – whether this is the positive or negative electrode is not known, nor does it matter for these calculation purposes. The measured capacity of the small scale quasi-bipolar plates is 1.04 Ahr and is, therefore, 6.4 Ahr for the full size plate. Effective capacity for the plate at 100 W/lb is, conservatively, 42% of this, i.e., 2.7 Ahr. Taking an acid utilization factor of 50% and assuming, as before, a value of 0.103 Ahr/gm H_2SO_4, the total module weight is recalculated as 49.3 lb. Thus, 11 parallel modules can be taken to conform to the specified 550 lb weight maximum. Total battery capacity is 29.7 Ahr and the calculated energy density is 9.7 Whr/lb. This compares favorably with the calculated value of 5.9 Whr/lb for a conventional battery discharged at 100 W/lb. Also, positive plates from the conventional battery did not meet the cycle life requirements at this rate. For the conventional battery calculation, allowance was also made for the reduced volume of acid needed at high discharge rates.

At medium discharge rates (C~5), even more acid is required for both conventional and bipolar batteries (29 lb/module in the latter case). Total bipolar module weight is recalculated as 66 lb. At medium discharge rates, the effective capacity of the quasi-bipolar plate is 6.4 Ahr, and using 8 parallel modules in the full-size battery, the energy density is close to 20 Whr/lb. The conventional battery with the excess acid required can be rearranged in 100 parallel cells[4] with 4 positives (and 5 negatives) in parallel per cell. Total weight is 550 lb in this configuration. At the C/5 rate, the capacity of each conventional plate is 11.9 Ahr and the energy density of the complete 200 V battery is 17.3 Whr/lb, i.e., 13.5% less than the complete bipolar battery. Interestingly, whereas the bipolar battery exhibits 48.5% of its medium rate energy density at

100 W/lb, the conventional battery exhibits only 34.1% at 100 W/lb. That is, the bipolar battery, which has an improved energy rating at medium rates, is even more superior to the conventional system at high discharge rates.

D. Preliminary Cost Estimate for the Quasi-Bipolar Battery (Concept I)

No detailed analysis has been carried out here, but the respective large volume cost estimates for the component parts of the system are given below in Table XXIII, and the cost of an individual module is estimated from these figures.

Table XXIII. Preliminary Large Volume Material Costs and Individual Component Cost Estimates for a Module Conforming to the Final Power Profile and Incorporating the Quasi-Bipolar Plates Outlined in Concept I

		Large Volume	Module Cost
1. Paste/module		15. 1 ¢/lb	4.53 $
(Universal Grenox)			
2. Head plates/module		16 ¢/lb	0.13 $
(plus Dynel fiber)		2.50 $/lb	0.15 $
[(Lead grid + paste)/module]			
3. Plastic components (grid) in		75 ¢/lb (Lexan)	5.22 $
the plate/module	or	15 ¢/lb (PVC)	1.04 $
Plus Dynel fiber		2.50 $/lb	0.17 $
4. Lead conductors (grid)/module		17 ¢/lb	1.02 $
5. Glass retainers/module*		4 $/1000	0.80 $
6. Separators/module**		20 $/1000	2.00 $
(Daramic)			
7. Case materials/module	or	75 ¢/lb (Lexan)	2.88 $
		15 ¢/lb (PVC)	0.58 $
8. Inter-module wiring		84 ¢/lb	insignificant
9. 1.28 sp gr electrolyte module		3.3 ¢/lb	0.17 $
		Total Cost/Module	18.69 $

Thus, the total module cost is very small based on this simple analysis and, for example, a full-scale battery based on 8 parallel modules would cost 149.5 $ or 0.344 $ per lb. The manufacture and assembly of materials are the major items in terms of total cost, and these have not been estimated here. However, they are not expected to be excessive since the system was designed with ease of manufacture and assembly in mind. In addition, no extraordinary capital equipment costs are anticipated for any part of the process. On this basis, it is not expected that there will be any cost restriction to further development of the system.

---

* Cut to size 8 in. × 4 in.
** Cut to size 9 in. × 5 in.
{ Both prices are rated on the high side pending delivery of more exact production volume information to W.R. Grace Co.

IX. SUMMARY OF ACHIEVEMENTS, EVALUATION OF THE MAIN AREAS REQUIRING FURTHER DEVELOPMENT, AND PRELIMINARY PROPOSED WORK PLAN

A. Summary of Achievements

1. A new quasi-bipolar plate has been developed in which the active material support is plastic, and conduction through the plate is achieved by parallel Pb strips laid vertically over the top of each plate and along it. The conduction paths through the support are so arranged as to be not immersed in electrolyte during normal cell operation. The possibility of short circuits via intercell electrolyte leakage is thus minimized.

2. The Pb conductors are held at fixed points to the plastic substrate via a plastic grid with horizontal cross-members. Expansion is thus permitted in a vertical direction without introduction of excessive strains resulting in plate buckling.

3. The plate uses dynel fiber or glass mat backing to enhance paste adhesion. Pure Pb strips act as conductors and no Sb is used in the plate components. Cycling life is maintained using H_3PO_4 additions to the electrolyte.

4. On operation at high rates of charge and discharge (150 mA/cm^2), the bipolar plates show very good performance characteristics. They last typically for 1000 high rate shallow discharge cycles, and capacity retention at the C/5 rating is also extremely good. Comparatively, fresh commercial battery positive plates degrade excessively after ≤ 350 cycles and capacity retention is relatively poor.

5. In the preliminary power profile, the maximum discharge rate specified is 55 KW and the minimum desired power density is 100 W/lb. In a full-size system using the above quasi-bipolar plates, 14 parallel modules may be used, each with 100 bipolar plates in series and weighing 40.9 lb/module. The required operating current density per plate is only 110 mA/cm^2. A modular system constructed from the above plates operating to the limits of their tested cycling capabilities, i.e., at 150 mA/cm^2, incorporates 10 parallel modules and exhibits a power density of 136 W/lb.

6. To conform to the specifications given by EPA in their final power profile (Fig. 1), the only change required in the above modular system is to incorporate 133 quasi-bipolar plates in series per module instead of 100 plates/module. Module weight is recalculated at 54.3 lb. At the 70.5 KW average maximum discharge rate and the minimum required power density of 128 W/lb, the operating current density per plate is 143 mA/cm^2 (10 parallel modules).

Preceding page blank

At the preferred operating point of 156.6 W/lb, the operating current density is close to 180 mA/cm^2, while to achieve the maximum discharge rate of 92.5 KW for 10 sec (205.5 W/lb) the rate must be increased to 234 mA/cm^2. In the latter two cases, only 8 parallel modules are used. Also, though cycling behavior is not demonstrated in the latter cases, the plates with 20 mil thickness of paste per electrode do contain an adequate excess of active mass (sevenfold).

7. In the preferred mode, it is anticipated that the best module design for operation under the final power profile would be one incorporating 133 quasi-bipolar plates in series, but on each plate the paste thickness would be reduced by at least 25% to 15 mil per electrode. More than sufficient capacity is still available in the plates to meet the most extreme capacity demands (980 Whr on two consecutive cycles for 25 sec at an average 70.5 KW rate). In this manner, the operating current density can be reduced to $<$ 190 mA/cm^2 even at a power density of 205.5 W/lb.

8. A battery built from 11 parallel modules, each with 100 quasi-bipolar plates in series and with incorporation of sufficient acid, can operate at $\sim$ 130 mA/cm^2, and its energy density is 9.7 Whr/lb at this rate. Under the same circumstances, a battery constructed from conventional plates must operate at $\geq$ 200 mA/cm^2, and its energy density is 5.9 Whr/lb.*

9. At medium discharge rates (C/5-rate), the respective energy densities for the bipolar and conventional systems are 20 Whr/lb and 17.3 Whr/lb, respectively. The bipolar battery clearly retains more of its energy density (48.5%) at high rates compared to the conventional battery (34%).

10. A modification of the quasi-bipolar plate in which multiple Pb conduction paths are made across and down the plate has also been constructed, and an initial plate exhibits superior performance on extended cycling (compared to the initial quasi-bipolar plate above).

B. Areas Requiring Further Development

The most important areas requiring further study to develop the quasi-bipolar plate and battery discussed above are as follows:

1. Extend cycling data on a large number of quasi-bipolar plates under a range of conditions and at higher rates as specified in the more recent EPA requirements. This will establish plate reliability on a more realistic basis.

2. Construct full scale plates to demonstrate structural stability and feasibility of large scale fabrication techniques.

3. Extend evaluations of long term plate corrosion resistance, particularly of the thin cross section Pb conductors but also of the plastic substrate. This will establish a realistic value for the minimum cross-section per conductor, which is compatible with cell performance, weight, and reliability.

4. Establish the exact volume of electrolyte and electrode gap separation necessary to permit successful operation of the plates under high rate/shallow discharge cycling. Here the dimensions of separator and retainer are crucial regariding their effect on interelectrode volume and also gas bubble retention between electrodes.

---

* In such an operating mode, the conventional battery does not perform satisfactorily on extended cycling.

5. Construct prototype modules to develop technology in this area and isolate any plate scaling problems.

6. Complete a more thorough cost analysis, particularly with relation to manufacturing and assembly costs.

7. Identify alternate applications for such a system.

8. Investigate the behavior of the bipolar plates under two consecutive high rate power pulses for 25 sec within a 60 sec interval and followed by high rate recharge.*

C. Work Plan

A suggested plan of approach to further develop the quasi-bipolar plate and battery is outlined as follows: (1) scaleup the plate to a practical size, (2) build a battery using the scaled-up version of the plate developed up-to-date, (3) test this battery to determine its characteristics, including its more probable failure mechanisms, (4) study the further optimization of the plate, and (5) build and preliminary test a battery based on optimized configuration.

Task I: The primary purpose of this task would be to develop a technology for the construction of a complete quasi-bipolar battery based on the final design discussed in this report. Two 25 V prototypes would be made, one using plates described here (1/6 full size) and the other with full-size plates (8-in. × 4-in.) of exactly the same design. Since time is always a limiting factor in evaluating the performance (expecially cycle life) of novel batteries, a significant advantage could be gained by starting this at the beginning of the contract period. Possible constructional and operational problems could then be isolated and overcome at an early stage leaving maximum time for optimization work.

For the above task, we would employ the technology so far gained during the present program. That is, plate design, retainers, separators, etc., would be "frozen" and incorporated in the prototypes. The small scale prototype would be constructed within the first 1.5 months followed by the large scale prototype development. Testing of prototypes would proceed throughout the contract period.

Task II: Taking into consideration problems uncovered in Task I and theoretical analysis of the system, experimental work aimed at the optimization of the plate design and the battery would be performed. This optimization would include the following factors.

---

* In a one time test with plate number 6, which had already been cycled successfully under the stated mode for 770 cycles, we did carry out two consecutive pulses for 25 sec each, with a 1 sec interval, at a current (150 mA/cm^2) corresponding to the 55 KW rate for a full scale system constructed from the plates. After this the plate was re-charged at a current corresponding to the 36.8 KW rate for 120 sec. The latter corresponds to a 20% overcharge. The plate performed well for the 6 cycles examined in this mode. The test cell exhibited a final discharge voltage of 3.2 V (i.e., bipolar plate plus head plates) and a final charge voltage of 6.2 V. No failure was observed which is encouraging for future battery development, particularly since the plate had already undergone severe testing prior to the above.

1. Conductor rib thickness: A realistic examination of the cross-sectional area per conductor required to maintain a balance between cell performance, weight, and reliability will be undertaken.

2. Conductor rib separation: As it affects paste formation, cycling capabilities, etc.

3. Electrolyte gap separation: We have calculated, but not yet established experimentally, the volume of 1.28 sp gr electrolyte necessary to supply the energy required at high power ratings. Since the concentration and volume of electrolyte affect both battery life (by corrosion) and weight requirements, this aspect would be of major interest.

4. Glass retainer type: That is, as it affects paste retention and gas bubble retention during charging of the plates.

5. Separator type: That is, the minimum thickness and type of separator (weight and ribbing geometry) which are consistent with electrolyte volume, gas bubble retention, and how they effect the voltage characteristics of the cells.

6. Paste microstructure: The effect of microstructure of the positive electrode paste will be studied in the "quasi-bipolar plates" with three additional paste formulations on the positive face: (a) N.L. Industries Barton VLY oxide, (b) Barton VLY oxide plus 15% Pb_3O_4, and (c) Bell Telephone Laboratories tetrabasic lead sulfate. The performance of these plates would be analyzed to decide whether or not a significant advantage is to be gained by using one or the other of these rather different formulations.

7. Optimum end plate construction would be briefly investigated.

8. Paste thickness: The performance of plates with paste thickness per electrode of the order of 15 mil would be investigated.

A time scale of approximately 8.5 months is estimated for the above.

Task III:

1. Construction of further 25 V prototypes: Based on the above tasks, further prototypes would be constructed, and their performance evaluated. Initial prototypes would again be on the small scale version, with expansion to full plate size as performance demanded.

2. Prototype specifications: Complete performance specifications would be detailed for prototypes of choice with detailed analysis of weight requirements, constructional procedures, estimated lifetime capabilities, and cost.

This phase of the program would commence after approximately 6 months of the contract and continue for the remaining period.

X. REFERENCES

1. Hybrid Heat Engine/Electric Systems Study, Aerospace Report No. TOR-0059(6769-01)-2, Aerospace Corporation, June 1971.

2. Analysis and Advanced Design Study of an Electromechanical Transmission, TRW Systems, April 1971, Contract EHSH71-002.

3. R.F.P. No. EHSD 71-Neg-100 from the "Division of Advanced Automotive Power Systems Development of the Environmental Protection Agency," October (1970).

4. G.W. Vinal, "Storage Batteries," 4th Ed., John Wiley and Sons, Inc., New York (1965).

5. Proposal No. P119 prepared by Tyco Laboratories, Inc., in response to RFP No. EHSD 71-Neg-100 for the Division of Advanced Automotive Power Systems Development of the Environmental Protection Agency," November (1970).

6. D. Berndt, Power Sources, 2, D.H. Collins, Ed., Pergamon Press, (1968).

7. W. Peukert, Elektrotech, 2, 18, 287 (1897).

8. K. Ebert, Power Sources, 2, D.H. Collins, Ed., Pergamon Press (1968).

9. J.R. Symth, J.P. Malloy, and D.T. Ferrell, Jr., Lead 65, Proceedings 2nd International Conference on Lead, Anaheim, Pergamon Press (1967).

10. K. Peters, A.I. Harrison and W.H. Durant, Power Sources, 2, Ed., D.H. Collins, Pergamon Press (1968).

11. J.E. Puzey and W.M. Orriel, ibid. p121.

12. Voss and Huster in Performance Forecast of Selected Static Energy Conversion Devices, 29th Meeting of Agard Propulsion and Energetics Panel, Eds., G.N. Sherman and L. Devol (1967).

13. J.L. Dawson, M.I. Gillibrand and J. Wilkinson, Power Sources 3, Ed., D.H. Collins, Oriel Press (1970).

14. J. Burbank, J. Electrochem. Soc., 111, 112 (1964).

15. J. Burbank, Abstract 50 ECS Meeting, October 1970.

16. J. Burbank, Power Sources 3, Ed. D.H. Collins, Oriel Press (1970).

17. A.C. Simon, S.M. Caulder and E.J. Ritchie, J. Electrochem. Soc., 117, 1264 (1970).

18. U.S. Pat. 3, 011, 007, November 28, 1961.

19. U.S. Pat. 1,748, 485, February 25, 1930.

20. German Pat. 516, 173 and 516, 556, May 22, 1931.

21. S. Fodor, A. Weisstuch and S. H. Davang, Electrochemical Technology, 3, 90 (1965); ibid., 4, 406 (1966).

22. E.A. Willihnganz, Abstract 25, ECS Meeting, October 1968.

23. J. Dunne, Popular Science, November 1970.

24. T.A. Orsino, H.E. Jensen, J.B. Thomas, D.R. Walter and J.P. Malloy, 21st Annual Power Sources Conf., 60, (1967).

25. H.E. Jensen, C and D Storage Battery Report, Private Communication.

26. J. Rooney, W.R. Grace Co., Private Communication.

27. Technical Bulletin No. 326, W.R. Grace Co., Polyfibron, Division, Cambridge, Mass., 1970.

28. A.G. Cannone, D.O. Feder and R.V. Biagetti, Bell System Technical Journal, 49, 1279 (1970).

29. A.M. Howard and E.A. Willihnganz, Abstract 26, ECS Meeting, October (1967).

30. A.C. Simon, Abstract 364, ECS Meeting, October (1968).

31. J.B. Cotton and I. Dugdale, "Batteries," D.H. Collins, Ed., Pergamon Press, 297 (1963).

32. U.S. Pat. 3, 486, 940, S. Ruben, December 30, 1969.

33. U.S. Pat, 3, 499, 795, S. Ruben, March 10, 1970.

34. U.S. Pat. 3, 343, 995, R.W. Reid, Sanford and Percy F. George, Midland, Mich., The Dow Chemical Co., September 20 (1967).

35. G.W. Mao, T.L. Wilson and J.G. Larson, J. Electrochem. Soc. 117, 1323 (1970).

36. J.J. Lander, J. Electrochem. Soc., 6, 213 (1951).

37. H.C. Wesson, A Survey of Grid Corrosion in Lead-Acid Batteries, Lead Association, England.

38. E.J. Ritchie and J. Burbank, J. Electrochem. Soc., 117, 229 (1970).

39. A.D. Butherus, W.S. Lindenberger and F.J. Vaccaro, Bell System Technical Journal, 49, 7, 1377 (1970).

40. L.H. Sharpe, J.R. Shroff and F.J. Vaccaro, Bell System Technical Journal, 49, 7, 1405 (1970).

41. B.H. Krevsky, Union Carbide Corp., New Polymers Dept., private communication.

42. W. Goldie, "Metallic Coating of Plastics," Vol. 2., Electrochemical Publications Ltd., England, 444 (1969).

43. F. Booth, "Comparative Study on Battery Separators for Lead-Acid Starter Batteries," Reprint from W.R. Grace Co., Cambridge, Mass.

44. D.W. Dahringer and J.R. Shroff, Bell System Technical Journal, 49, 1393 (1970).

45. K. Eberts, Power Sources 2, D.H. Collins, Ed., Pergamon Press, 89, (1968).

46. "The Encyclopedia of Electrochemistry," C.A. Hampel, Ed., Reinhold Publishing Corp., N.Y., 870 (1964).

Appendix I: CALCULATION DETAILS FOR A FULL SIZE BATTERY BASED ON THE PRELIMINARY BIPOLAR CONCEPT A, WITH PLASTIC SUBSTRATE AND Pb CONDUCTORS, USING THE PRELIMINARY POWER PROFILE

The active plate size is 5 in. × 3 in. = 96.75 cm^2.

For the entire battery, the highest discharge current at 55 KW and 180 V is 305 amperes.

The current per module is 0.097 X (amperes), where X = operating current density (mA/cm^2).

The number of modules required in parallel is:

$$\frac{305}{0.097\,X} = \frac{3150}{X}\ .$$

Deepest depth of discharge is:

$$\frac{764\ \text{Whr}}{180\ \text{V}} = 4.25\ \text{Ahr, or}$$

$$\frac{4.25\ X}{3150} = 0.00135X\ \text{Ahr/plate.}$$

Or expressed as paste volume (assuming density of 4.2 g/cm^3):

$$\frac{0.00135X}{FY \times 4.2\ \text{g/cm}^3} = 0.00032\ \frac{X}{FY}\ \text{cm}^3\ \text{of paste/electrode,}$$

where Y = initial amperes/hour/gram of paste and F = decay factor (0 → 1).

This corresponds to a thickness of active material on each side of

$$\frac{32 \times 10^{-5}}{96.75\ \text{cm}^2}\ \frac{X}{FY} = 33 \times 10^{-7}\ \frac{X}{FY}\ \ (\text{cm}).$$

For 100 cells, the active paste weighs:

$$\frac{200 \times 0.00135X}{FY} = 0.269\ \frac{X}{FY}\ \ \text{grams.}$$

Preceding page blank

Weight of plastic sheet:

$$4 \text{ in.} \times 6 \text{ in.} \times T_p \times 16.38 \times 1.4 \text{ g/cm}^3 = 550\, T_p \text{ grams (where } T_p = \text{thickness of PVC}$$

in inches).

Weight of lead ribs:

$$T_L \times 6.45 \times 5 \text{ in. } (0.7\, T_p \times 2.54 + 100 \times 10^{-7} \frac{X}{FY}) \times 11.3 \text{ grams}$$

(where T_L is thickness of lead ribs inside of the plastic plate in inches, the first term of the parenthesis represents the part of the rib inside of the plastic, assumed 30% void, and the second term represents the sum of the two outer sections of the rib with an allowance for their larger average thickness.)

$$647\, T_L\, T_p + 3.64 \times 10^{-3} \frac{XT_L}{FY} \quad \text{grams}$$

There are 3/S lead ribs on each plate (where S = rib spacing in inches).

Weight of lead plate:

$$P \times 15 \text{ in.}^2 \times 2 \text{ sides} \times 16.38 \times 11.3 \text{ g/cm}^3 = 5.5 \times 10^3\, P \text{ grams, (where P = lead plate}$$

thickness, inches).

Total weight of substrate:

$$100 \text{ plates} \left[550\, T_p \div \frac{3}{S} \left(647\, T_L\, T_p + 3.64 \times 10^{-3} \times \frac{T_L}{FY}\right) + 5.5 \times 10^3\, P\right] =$$

$$5.5 \times 10^4\, T_p + \frac{1.94 \times 10^5\, T_L\, T_p}{S} + 1.09 \frac{XT_L}{SFY} + 5.5 \times 10^5\, P \text{ grams}$$

Electrolyte weight:

Theoretical value is 0.095 Ahr/g of 1.26 sp gr acid, or

$$0.12 \text{ Ahr/cm}^3.$$

Weight of acid per cell is

$$\frac{0.00135X}{0.095\, A} = 0.0142 \frac{X}{A}, \quad \text{gr } H_2SO_4\text{/cell, where A = fraction of acid to be used (0–1).}$$

and

$$0.0113 \frac{X}{A} \text{ cm}^3 \text{ of } H_2SO_4\text{/cell.}$$

Distance between plates:

$$\frac{0.0113\ \frac{X}{A}}{96.75\ \text{cm}^2} = 1.17 \times 10^{-4}\ \frac{X}{A}\quad \text{cm}$$

The length of the module (100 cells):

$$1.17 \times 10^{-2}\ \frac{X}{A} + 254\ T_p + 66 \times 10^{-5}\ \frac{X}{FY} + 508\ P\quad \text{cm}$$

Case weight (assuming 0.635 cm thick wall, with 1.4 g/cm^3 density):

Bottom and top $2[\,0.635 \times 6 \times 2.54\ (1.17 \times 10^{-2}\ \frac{X}{A} + 254\ T_p + 66 \times 10^{-5}\ \frac{X}{FY} + 508\ P)\,]$

2 ends $2 \times 24 \times 6.45 \times 0.635 = 197\ \text{cm}^3$

2 sides 4/6 (bottom and top)

Total $0.53\ \frac{X}{A} + 11500\ T_p + 2.98 \times 10^{-2}\ \frac{X}{FY} + 276 + 23000\ P$ grams

Lead end plates:

Assume these are mostly aluminum wires at density of ~ 5.5 g/cm^3 and they are 0.25 in. thick

$$96.75\ \text{cm}^2 \times 0.635\ \text{cm} \times 5.5 \times 2\ \ \text{grams/module}$$

Inter-module wiring:

≈ 1 foot/module is needed: $\frac{3150}{X}$ ft. are required for entire battery

Aluminum heavy gauge wire at 50 g/ft

Total weight: $\frac{50 \times 3150}{X} = \frac{157.5}{X}$ (Kg)

Refer also to Section III for summary details on the above.

Appendix II. NEW DESIGN EQUATIONS FOR THE PRELIMINARY BIPOLAR CONCEPT B WITH A PLATE DIMENSION OF 8 in. × 4 in. USING THE PRELIMINARY POWER PROFILE

Component	Weight/Module/g
Active Paste	$\frac{0.575\,X}{FY}$
Plates	$1.03 \times 10^{5}\,T_P + \frac{4.12 \times 10^{5} T_L\,T_P}{S} + \frac{2.3\,X\,T_L}{SFY} + 1.18 \times 10^{6}\,P$
Acid	$\frac{3.02\,X}{A}$
PVC Case	$\frac{0.73\,X}{A} + 16058\,T_P + \frac{4.17 \times 10^{-2}\,X}{FY} + 32116\,P + 516$
Terminal Plates	1442
Interelectrode Wiring	50
No. of Modules	$\frac{1480}{X}$
Battery Weight	$\frac{2.01}{FY} + \frac{3.9 \times 10^{5}\,T_P}{X} + \frac{1.34 \times 10^{6}\,T_L\,T_P}{SX} + \frac{7.5\,T_L}{SFY} + \frac{3.9 \times 10^{6}\,P}{X} + \frac{12.24}{A} + \frac{6559}{X}$ lb.

The following parameters were not varied:

Module height and width	5 × 9 in.
Plastic case thickness	0.25 in.
Electrode size	4 × 8 in.
Paste density	4.2 g/cc
Acid density	1.26 g/cc
Interelectrode wiring	50 g/ft wire
Module terminals	0.25 cm lead plated Al

Preceding page blank

Appendix III. COMPARISON OF BATTERY SYSTEMS BASED ON THE PRELIMINARY POWER PROFILE AND ON THE TWO DIFFERENT BIPOLAR PLATES OUTLINED IN PRELIMINARY CONCEPTS A AND B

System Design Values	8 in. × 4 in. Plate	5 in. × 3 in. * Plate
Current Density mA/cm^2 (X)	150	150
Coulombic Yield Ahr/g (Y)	0.054	0.054
Decay Allowance (F)	0.5	0.5
Plastic Plates in. (T_P)	0.03	0.03
Lead Ribs in. (T_L)	0.03	0.03
Lead Plates in. (P)	0.004	0.004
Rib Spacing in. (S)	0.5	0.5
Acid Use	0.5	0.5
Module Length, ft	0.55	0.47
No. of Modules	10	21
System Weight, lb	364	380
System Volume, ft^3	1.8	1.8

* See Section III, p 27, 28 for more details

Design Values for the 150 mA/cm^2 Operating Point Using the 8-in. × 4-in. Plate

Active Paste, lb	7.00	Distance Between Plates, in.	0.014
Plates (Pb + PVC), lb	20.60	Active Paste Thickness, in.	0.007
Acid, lb	2.00	Substrate Thickness, in.	0.038
PVC Case, lb	3.47	Case Thickness, in.	0.25
Terminal Plates, lb	3.20		
Intermodule Wiring, lb	0.10	Module Length = 0.59 for 100 cells, ft	

Total Module Weight, lb 36.4

Preceding page blank

Appendix IV: ENERGY DENSITY COMPARISON OF THIN PLATE CONVENTIONAL SLI AND QUASI-BIPOLAR BATTERIES (Final Design Plates) AT HIGH AND LOW DISCHARGE RATES

	Conventional	Bipolar
Operating Current Density	250 mA/cm^2 (100 W/lb)	~ 130 mA/cm^2 (100 W/lb)
Efficiency of Paste Utilization	~ 27%	~ 27%
Effective Plate Capacity at 100 W/lb	3.7 Ahr	2.7 Ahr
Average Discharge Voltage (200 V system)	180 V	180 V
Cell Configuration	100 cells in series 5 positives in parallel per cell	11 parallel modules 100 series cells/module
Total Capacity	18.5 Ahr	29.7 Ahr
Total Weight	550 lb	550 lb
Energy Density	5.9 Whr/lb	9.7 Whr/lb
At Low Discharge Rates:		
Average Discharge Voltage	200 V	200 V
Total Capacity	47.6 Ahr	51.2 Ahr
Energy Density	17.3 Whr/lb	20 Whr/lb

For the conventional battery, the energy density at high rates is 34.1% of the low rate energy density.

For the quasi- bipolar battery, the energy density at high rates is 48.5% of the low rate energy density.

The improved performance of the quasi-bipolar plate at increased discharge rates is, thus, self-evident.

Preceding page blank

Appendix V: CURING AND FORMATION TECHNIQUES

A. Universal Grenox Oxide (25% free Pb, balance orthorhombic PbO)

For the positive paste, 8 lb of oxide were first dry mixed with 2.8 g (0.2%) of Dynel fibers (to impart stability to the paste). 440 ml of distilled water were then added with continuous mixing for a further 10 min when a uniform wet paste was obtained. Then, 340 ml of 1.4 sp g H_2SO_4 were added over at least a 1 min period while still mixing. Paste temperature was not allowed to exceed 140°F during this latter process. The paste was well mixed for ~ 10 min, resulting in a homogeneous paste structure. For the mixing, a heavy duty mixer from Charles Ross and Sons was used incorporating a variable speed motor, planetary mixing action, and stainless steel mixing components. The procedure was exactly the same when preparing the negative paste. Here, 8 lb of oxide plus 2.8 g of Dynel fiber were again used, but 72 g of an industrial KX expander (N.L. Industries) were also added. In addition, 412 ml H_2O and 304 ml of 1.4 sp gr H_2SO_4 were now used in the mixing process.

The paste was applied to the grids placed on a glass plate using a wide plastic spatula. The pasted plates were then cured by covering them with damp cloth and leaving them for ~ 80 hr in this condition. Finally, they were air dried at ~ 150°F for at least 60 hr.

Prior to formation, each plate was soaked in 1.08 sp gr acid, generally for an overnight period. For formation in 1.08 gravity acid, approximately 1 Ahr/g of paste was used. For the bipolar plates, for example, formation was generally at 5.9 mA/cm^2 while for the iR-free laboratory test plates, formation was at 5 mA/cm^2 and then 3 mA/cm^2.

The above procedures are exactly the same as emplyed by Tyco's Mule Battery Division in commercial plate preparation, and the pasted plates so obtained performed very well.

B. Barton VLY Oxide (40% tetragonal PbO, 60% orthorhombic PbO < 2% free Pb)

The performance of this paste was generally not satisfactory, particularly after a high temperature cure.

Our initial techniques are summarized below:

1. 45 cc H_2O/lb oxide
2. 45 cc H_2SO_4/lb oxide: - 1.25 sp gr acid added over a 10 min period

Preceding page blank

3. Immersion in a 100% rh chamber at 100° F followed by a temperature increase over a 7 min period to 170-180° F. The paste was then left for ~ 2-1/2 hr and finally was air dried.

We modified the techniques as follows:

4. 30 cc and 37 cc H_2O/lb oxide
5. 45 cc H_2SO_4/lb oxide: 1.25 sp gr acid added in 1 min
6. Immersion in the 100% rh chamber at 100° F followed by a temperature increase at 25° F/hr to 170-180° F. The paste was again left for 2-1/2 hr and finally dried in air at 150-160° F for 6 hr.

The major deviations above were in the amount of H_2O additions to control paste consistency and in the rate of H_2SO_4 addition to control the heat evolution during the mixing process. As the H_2O content is reduced, the paste becomes firmer, and as the H_2SO_4 addition rate is increased, more heat is evolved. Thus the temperature rose to 140° F (and remained there for 5 min) after a 1 min acid addition. On addition of the acid over a 10 min period, a maximum temperature of 134° F only was attained briefly after the first two additions. We chose also a slower heating rate during curing to allow for the large heat capacity of our plate structures. During the curing, we strictly controlled rh in our rh chamber since we had observed severe shrinkage of our pastes in some instances under apparent 100% rh conditions. For this reason also, we cured some plates separately in a simple forced convection oven containing a bowl of water. Finally, after curing, we air dried our plates at 150° F-160° F for 6 hr, compared to a previous room temperature drying. This was to ensure complete removal of water from the cured plates. If water is present in the paste when it is immersed in acid, excessive heat may be generated and the gas evolved then "pops" the paste out of the grid structure.

Formation techniques were the same as for the Grenox paste. The above paste, cured in the relative humidity chamber, using the modified techniques, was used for some investigations of paste performance versus paste thickness in the iR-free laboratory test structures.

Appendix VI: ENGINEERING DATA FOR BATTERY MATERIALS OF POSSIBLE INTEREST

THERMAL PROPERTIES OF POLYPROPYLENES

Property	General Purpose	Long-Term Head Aging	Copolymers		Polyblends		Asbestos Filled	Glass Fiber (20%) Reinforced
			Impact	High Impact	Impact	High Impact		
Heat Deflection Temp, F								
At 264 psi	140	140	135	130	125	115	200	230
At 66 psi	210	210	215	205	175	145	295	305
Coef of Ther Cond, Btu/hr/sq ft/°F/in.	1.48	1.48	–	–	1.62	1.72	1.55	–
Coef of Linear Ther Exp[a], in./in./°F × 10^{-5}	6.46	6.46	8.3	10	7.00	7.23	2.9	2.9
Melt Point (crystalline), F	333	333	333	340	–	–	333	–
Ther Aging at 300 F, days[b]	40-80	40-80	–	–	–	–	>100	–

[a] Above 86 F. [b] End point defined by crazing and/or discoloration.

CHEMICAL RESISTANCE OF POLYPROPYLENES[a]

	30 Days at 72 F		30 Days at 140 F	
	Weight Change, %	Tensile Elong Change	Weight Change, %	Tensile Elong Change
INORGANIC CHEMICALS				
Distilled Water	+0.7	O	+0.2	O
Sulfuric Acid (98%)	-0.2	O	-0.2	X
Sulfuric Acid (2N)	-0.3	O	+0.3	O
Nitric Acid (fuming)	-0.1	O	ND	X
Nitric Acid (2N)	+0.1	O	+0.8	O
Hydrochloric Acid (30%)	-0.2	O	+1.2	O
Phosphoric Acid (85%)	ND	O	-0.5	O
Potassium Hydroxide (54%)	-0.3	O	+1.3	O
Sodium Hydroxide (52%)	-0.2	O	+0.7	O
Ammonia (30%)	+0.3	O	ND	ND
Sodium Hypochlorite (20%)	+0.1	O	-2.1	X

[a] O = reduction in tensile strength of less than 10% and change in elongation of less than 25%; X = reduction in tensile strength of more than 10% and/or more than 25% change in elongation; P = a plasticizing effect; ND = not determined.

(Materials and Processes Manual, No. 238, p89 (1966)).

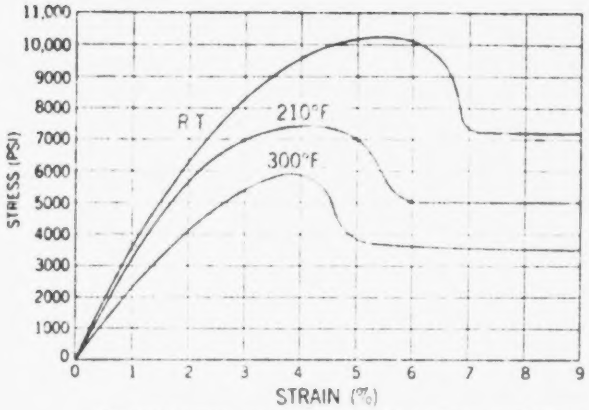

POLYSULFONE TENSILE STRESS-STRAIN CURVES

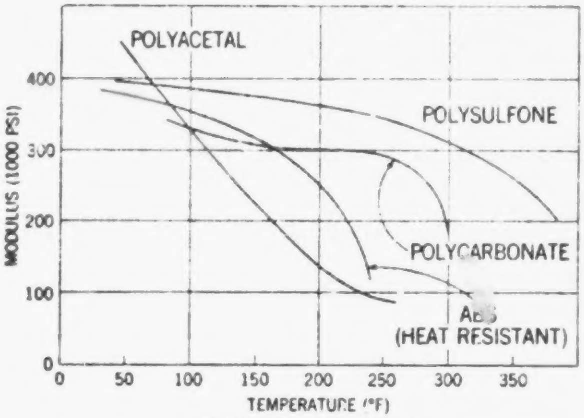

FLEXURAL MODULUS VS. TEMPERATURE

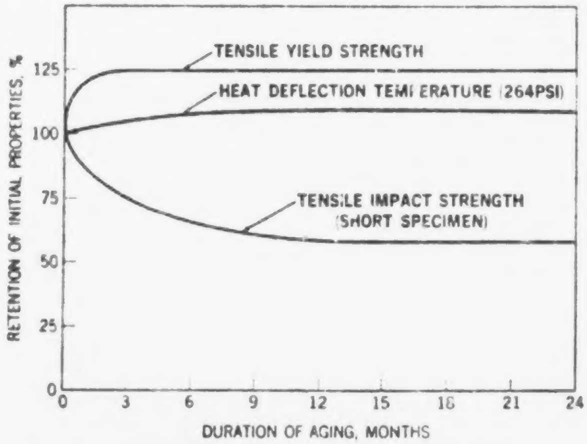

EFFECT OF HEAT AGING AT 300°F ON THE PROPERTIES OF POLYSULFONE

ALL PROPERTY TESTS MADE AT ROOM TEMPERATURE ON 1/8-IN.-THICK SPECIMENS.

(Union Carbide Corporation
Product Data Article)

TYPICAL PROPERTIES OF "BAKELITE" POLYSULFONE

Property	ASTM Method	Value
General		
Melt Flow, @ 650°F. (343°C.) 44 psi. dg/min..	D1238	6.5—P-1700, P-1710 3.5—P-3500, P-3510
Specific Gravity	D792	1.24—P-1700, P-3500 1.25—P-1710, P-3510
Mold Shrinkage, in./in.		.007
Water Absorption, % in 24 hrs.	D570	0.22
Mechanical		
Tensile Strength at Yield, psi	D638	10,200
Tensile Modulus, psi	D638	360,000
Tensile Elongation at Break, %	D638	50-100
Flexural Strength, psi	D790	15,400
Flexural Modulus, psi	D790	390,000
Izod Impact, @ 72°F., 1/8" spec., ft.-lb./in. notch ...	D256	1.3
Izod Impact, @ −40°F., 1/8" spec., ft.-lb./in. notch ...	D256	1.2
Tensile Impact, ft.-lb./in.^{2} ..	D1822	200
Rockwell Hardness	D785	M69 (R120)
Thermal		
Heat Deflection Temp., @ 264 psi, °F.	D648	345
Coefficient of Linear Thermal Expansion, in./in./°F. ...	D696	3.1×10^{-5}
Flammability	D635	Self-Extinguishing
....	UL	Self-Extinguishing Group II
Thermal Conductivity, BTU/hr./sq. ft./°F./in. ..		1.8
Electrical Properties		
Dielectric Strength, 1/8" spec., ST, v/mil	D149	425
Arc Resistance, sec. (Tungsten Electrodes) ..	D495	122
Volume Resistivity, @ 72° F., ohm-cm	D257	5×10^{16}
Volume Resistivity, @ 347°F., ohm-cm	D257	1×10^{13}
Dielectric Constant, @ 72°F., 60 cps-1 Mc	D150	3.07-3.03
Dielectric Constant, @ 347°F., 60 cps-1 Mc ..	D150	2.82-2.73
Dissipation Factor, @ 72°F., 60 cps-1 Mc	D150	0.0008-0.0034
Dissipation Factor, @ 347°F., 60 cps-1 Mc ..	D150	0.006-0.003
Chemical Resistance		
Inorganic Acids		No effect
Alkalies		No effect
Alcohols		No effect
Esters		Partly soluble, swells
Ketones		Partly soluble, swells
Aliphatic Hydrocarbons		No effect
Aromatic Hydrocarbons		Partly soluble, swells
Chlorinated Hydrocarbons .		Dissolves

LEXAN® SHEET

A Comparison with Other Metals and Plastics

The strength of LEXAN sheet compares favorably with other plastics and the more commonly used metals. Having one of the lowest specific gravities, LEXAN sheet offers a particular advantage in having a high strength-to-weight ratio and a low cost per finished part.

	LEXAN	NORYL 1000	Acrylic	Polysulfone	SE ABS	Butyrate	PVC KYDEX	Test Procedure*
Specific Gravity	1.20	1.09	1.19	1.27	1.24	1.18	1.35	D 792
Impact Strength—notched Izod—¼" specimen	16.2	6.0	4	1.3	1.6–3.5	0.8–6.3	12.0–15.0	D 256
Heat Deflection Temp 66 psi 264 psi	285 275	220	225 205	358 345	180	130–227 113–202	177 160	D-648
Flammability ASTM D 635	SE	SE	Slow Burning	SE	SE	Slow Burning	SE	ASTM D 635
Tensile Yield Strength	9000–9500	7800–9500	8000–11 000	10 200	3000–5500	2600–6900	6500	D 638
Tensile modulus 10^5 psi	3.5	3.55–3.8	3.5–4.0	3.6	2.2–3.1	2.0–2.5	3.35	D 638
Flexural Yield Strength	13 500	12 800–13 500	12 000–17 000	15 400	6000–7500	4000–9000	10 700	D-790
Flexural Modulus	3.4	3.5–4.0	3.9–4.75	3.7–3.9	2.2–3.0	—	4.0	D 790
H_2O Absorption %	0.15	0.06	0.30	0.22	0.30	1.50	0.06	D 570
Thermoforming Shrinkage in/in	005–007	005–007	—	0076	003–008	—	006–001	D 955
Rockwell Hardness	M70–R118	R119	M80 M100	M69 R120	R75–R90	R30–R115	[illegible]	D 785
Elongation	100%	35%	5%	50%	20%	50–100%	100%	D 638
Clarity	Transparent to Opaque	Opaque	Transparent to Opaque	Transparent to Opaque	Opaque	Transparent to Opaque	Opaque	—

*Table represents average values. Tested under standard ASTM conditions.

	LEXAN	Polyester preform/mat	Polyester spray-up/mat	Polyester premix	Aluminum die cast	Zinc die cast
Specific Gravity	1.20	1.5–1.7	1.4–1.6	1.8–2.0	2.57–2.96	6.6
lbs/in	0.043	0.061	0.058	0.072	0.100	0.240
Izod Impact Strength lb/in notch (⅛" TK Specimen)	14–16	4–12	10–20	1.0–10	N.A.*	4.3
Elongation Percent	110	1.0–1.5	1.0–1.2	0.3–0.5	6–8	10
Bending Strength psi x 10^3	13.5	45	28	26	18	—
Flexural Modulus psi x 10^6	0.34	0.8–1.8	0.8–1.8	1.6–2.0	10	—
Stiffness psi x 10^6	0.38	1.8	1.2	2.5	10	—
Tensile Strength psi x 10^3	9.5	24	[illegible]	10	8	14

G.E. Product Data Sheet CDX-80A

Typical Properties

Property	ASTM METHOD	NORYL 731	NORYL SE-1	NORYL SE-100	NORYL GFN2	NORYL GFN3	NORYL SE1-GFN2	NORYL SE1-GFN3
Specific Gravity, 73°F	D792	1.06	1.06	1.10	1.21	1.27	1.30	1.36
Specific Volume, cu. in./lb.	–	26.1	26.1	25.2	22.9	21.8	21.3	20.2
Water Absorption, 24 hrs., 73°F, %	D570	0.066	0.066	0.07	0.06	0.06	0.06	0.06
Heat Deflection Temperature (264 psi), °F	D648	265	265	212	290	300	270	275
Thermal Conductivity, Btu/hr./ft.^{2}/°F/in.	C177	1.5	1.5	1.1	1.15	1.1	1.15	1.1
Coefficient of Thermal Expansion, in./in./°F (–20° to 150°F)	D696	3.3×10^{-5}	3.3×10^{-5}	3.8×10^{-5}	2.0×10^{-5}	1.4×10^{-5}	2.0×10^{-5}	1.4×10^{-5}
Mold Shrinkage, in./in. x 10^{-3}	D1299	5-7	5-7	5-7	2-4	1-3	2-4	1-3
Flammability	(see note)	SE	SE-1	SE-1	SE	SE	SE-1	SE-1
Dielectric Constant (50% RH, 73°F at 60 cps)	D150	2.64	2.69	2.65	2.86	2.93	2.98	3.15
Dissipation Factor (50% RH, 73°F at 60 cps)	D150	0.0004	0.0007	0.0007	0.0008	0.0009	0.0016	0.0020
Volume Resistivity, dry, ohm cm., 73°F	D257	10^{17}	10^{17}	10^{16}	10^{17}	10^{17}	10^{17}	10^{16}
Surface Resistivity, ohm/sq.	D257	10^{17}	10^{17}	10^{16}	10^{17}	10^{17}	10^{17}	10^{17}
Dielectric Strength (1/8" sample), volts/mil.	D149	550	500	400	420	550	600	530
Arc Resistance (Tungsten), sec	D495	75	75	70	70	120	70	120
Tensile Strength, psi at 73°F	D638	9,600	9,600	7,800	14,500	17,000	14,500	17,000
Elongation at Break, %	D638	60	60	50	4-6	4-6	4-6	4-6
Tensile Modulus, psi at 73°F	D638	355,000	355,000	380,000	925,000	1,200,000	925,000	1,200,000
Flexural Strength, psi at 73°F	D790	13,500	13,500	12,800	18,500	20,000	18,500	20,000
Flexural Modulus, psi at 73°F	D790	360,000	360,000	360,000	750,000	1,100,000	750,000	1,100,000
Compressive Strength (10% Deformation), psi	D695	16,400	16,400	16,000	17,600	17,900	17,600	17,900
Shear Strength, psi	D732	10,500	10,500	6,900	10,400	10,600	10,400	10,600
Deformation Under Load, % at 2,000 psi, 122°F	D621	0.30	0.30	0.50	0.20	0.12	0.30	0.25
Creep (300 hrs. 73°F at 2,000 psi), %	D674	0.75	0.75	0.50*	0.33	0.2	0.33	0.20
Izod Impact Strength, ft. lbs./in. notch	D256	5.0	5.0	5.0	2.3	2.3	2.3	2.3
Rockwell Hardness	D785	R119	R119	R115	L106	L108	L106	L108
Taber Abrasion, mg.	D1044	20	20	100	35	35	–	–
Fatigue Endurance Limit, psi, 2 x 10^6 cycles	D671	2,500	2,500	1,850	4,000	5,000	–	–
Colors	–	Unlimited	Unlimited	Unlimited	Unlimited	Unlimited	Unlimited	Unlimited
Clarity	–	Opaque	Opaque	Opaque	Opaque	Opaque	Opaque	Opaque

SE – Self-Extinguishing Non-Dripping (ASTM D635)
SE-1 – Self-Extinguishing Non-Dripping Group 1 (U.L. Bulletin 94)
* 1500 psi

TYPICAL PROPERTIES

G.E. Product Data Article CDX-81 (20M) 2/70

PROPERTY	ASTM METHOD	NORYL 731	NORYL SE1	NORYL SE100	NORYL GFN2	NORYL GFN3	NORYL SE1 GFN2	NORYL SE1 GFN3
PHYSICAL								
Specific Gravity 73 F	D792	1.06	1.06	1.10	1.21	1.27	1.30	1.30
Specific Volume, cu in /lb		26.1	26.1	25.2	22.9	21.8	21.3	20.2
Water Absorption (24 hrs), %	D570	0.066	0.066	0.07	0.06	0.06	0.06	0.06
THERMAL								
Heat Deflection Temperature (264 psi), F	D648	265	265	190	290	300	270	275
Thermal Conductivity Btu/hr/ft²/°F/in	C177	1.5	1.5	1.1	1.15	1.1	1.15	1.1
Coefficient of Thermal Expansion in /in /°F (−20 to 150 F)	D696	3.3×10^{-5}	3.3×10^{-5}	3.8×10^{-5}	2.0×10^{-5}	1.4×10^{-5}	2.0×10^{-5}	1.4×10^{-5}
Mold Shrinkage, in /in $\times 10^{-3}$	D1299	5–7	5–7	5–7	2–4	1–3	2–4	1–3
Flammability	(See Note)	SE	SE-1	SE-1	SE	SE	SE-1	SE-1
ELECTRICAL								
Dielectric Constant (50% RH 73 F @ 60 cps)	D150	2.64	2.69	2.65	2.86	2.93	2.98	3.15
Dissipation Factor (50% RH 73 F @ 60 cps)	D150	0.0004	0.0007	0.0007	0.0008	0.0009	0.0016	0.0020
Volume Resistivity dry, ohm cm , 73 F	D257	10^{17}	10^{17}	10^{16}	10^{17}	10^{17}	10^{17}	10^{17}
Surface Resistivity ohm/sq	D257	10^{17}	10^{17}	10^{16}	10^{17}	10^{17}	10^{17}	10^{17}
Dielectric Strength (⅛ sample), volts/mil	D149	550	500	400	420	550	600	530
Arc Resistance (Tungsten), sec	D495	75	75	—	70	120	70	120
MECHANICAL								
Tensile Strength psi	D638	9,600	9,600	7,800	14,500	17,000	14,500	17,000
Elongation at Break %	D638	20–30	20–30	35	4–6	4–6	4–6	4–6
Tensile Modulus psi	D638	355,000	355,000	380,000	925,000	1,200,000	925,000	1,200,000
Flexural Strength psi	D790	13,500	13,500	12,800	18,500	20,000	18,500	20,000
Flexural Modulus psi	D790	360,000	360,000	360,000	750,000	1,100,000	750,000	1,100,000
Compressive Strength (10% deformation), psi	D695	16,400	16,400	16,000	17,600	17,900	17,600	17,900
Deformation Under Load 90 at 2,000 psi at 122°F	D621	0.30	0.30	0.50	0.20	0.12	0.30	0.25
Creep (300 hrs , 73 F at 2,000 psi), %	D674	0.75	0.75	0.50*	0.33	0.20	0.33	0.20
Izod Impact, notched ⅛ x ½ x 5 bar, at 73 F, ft lb /in notch	D256	2.5	2.5	2.5	2.3	2.3	2.3	2.3
Rockwell Hardness	D785	R119	R119	R115	L106	L108	L106	L108
Taber Abrasion mg	D1044	20	20	100	35	35	—	—
Fatigue Endurance Limit, psi at 2 x 10⁶	D671	2,500	2,500	1,850	4,000	5,000	—	—

SE Self-extinguishing, non-dripping (ASTM D635)
SE-1 Self-extinguishing, non-dripping (Group 1 (U.L. Bulletin 94)
*[illegible] psi

G.E. Thermoplastic Resins Data Article CDX 81 (20M) 2/70

PRICE, PROPERTIES COMPARISON

NORYL
THERMOPLASTIC RESINS

COST COMPARISON

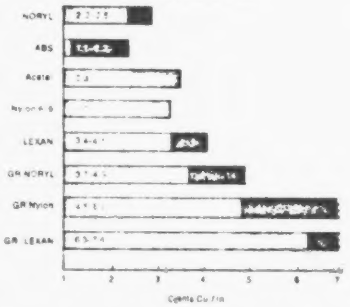

MOLD SHRINKAGE

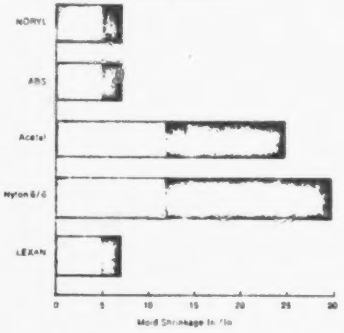

FATIGUE ENDURANCE

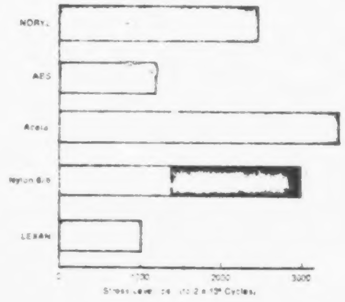

TENSILE STRENGTH

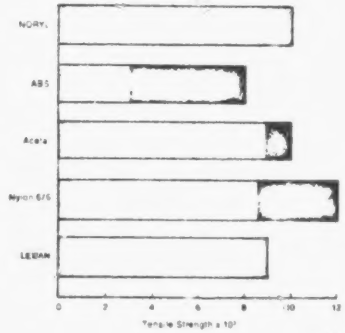

KEY: RANGE ▨

WATER ABSORPTION

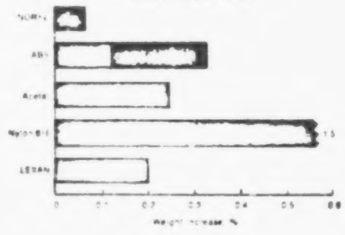

IZOD IMPACT STRENGTH

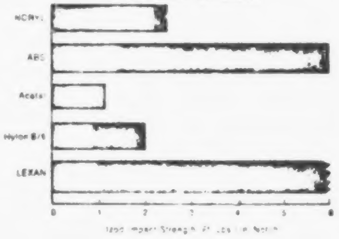

TENSILE CREEP – NORYL GFN3

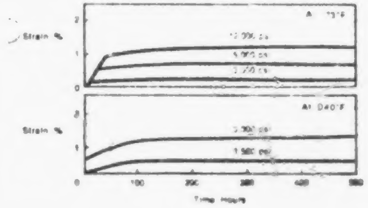

HEAT DEFLECTION TEMPERATURES

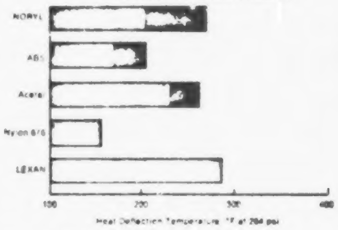

FLAMMABILITY COMPARISONS

U.L. BULLETIN 94 – ⅛" THICK SECTIONS					
	ABS	NORYL	ACETAL	LEXAN	NYLON 6/6
SE-1	●	Grades SE 100 SE 1 SE1-GFN2 SE1-GFN3		Grades 2014 NB-155	
SE-2				Grades 130 141	●
BURNS	●	Grades 731 GFN2 GFN3	●		

MELT FLOW VS. TEMPERATURE

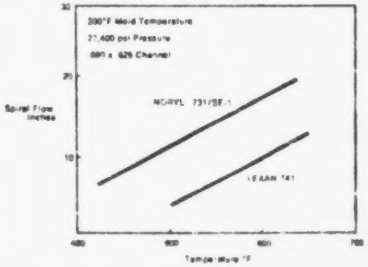

Reproduced from best available copy.

[illegible] properties

The largest selection of engineering plastics comes from GENERAL ELECTRIC!

Property	RESIN ASTM TEST METHOD	NORYL RESIN 731	NORYL RESIN SE 1	NORYL RESIN SE 100	NORYL RESIN GFN2	NORYL RESIN GFN3	NORYL RESIN SE1 GFN2	NORYL RESIN SE1 GFN3	LEXAN RESIN Standard	LEXAN RESIN 40% Glass Reinforced	LEXAN RESIN 500	LEXAN RESIN ML 135	LEXAN RESIN 2014	GENAL 4000	GENAL 4050	GENAL 4700	GENAL 4300	GENAL 4301	PHENOLIC G P GRADES	PHENOLIC IMPACT GRADES	PHENOLIC HEAT RESISTANT GRADES	SHEET NORYL SHEET 1000	LEXAN SHEET 9030 & 9400 SERIES	LEXAN SHEET 9600	SHEET ASTM TEST METHOD
PHYSICAL																									
[illegible]	D792	1.06	1.06	[illegible]	[illegible]	[illegible]	[illegible]	[illegible]	[illegible]	1.52	[illegible]	[illegible]	[illegible]	[illegible]	[illegible]	[illegible]	[illegible]	[illegible]	[illegible]	[illegible]	[illegible]	[illegible]	1.2	1.2	D792
[illegible]	[illegible]	[illegible]	[illegible]	[illegible]	[illegible]	[illegible]	[illegible]	[illegible]	[illegible]	[illegible]	[illegible]	[illegible]	[illegible]	[illegible]	[illegible]	[illegible]	[illegible]	[illegible]	[illegible]	[illegible]	[illegible]	[illegible]	0.15	0.15	D570
Heat deflection temperature 264 psi [illegible]	D648	265	265	[illegible]	290	[illegible]	[illegible]	[illegible]	[illegible]	295	288	[illegible]	[illegible]	[illegible]	[illegible]	[illegible]	[illegible]	[illegible]	[illegible]	[illegible]	[illegible]	[illegible]	275	285	D648
[illegible]	[illegible]	[illegible]	[illegible]	[illegible]	[illegible]	[illegible]	[illegible]	[illegible]	[illegible]	[illegible]	[illegible]	[illegible]	[illegible]	[illegible]	[illegible]	[illegible]	[illegible]	[illegible]	[illegible]	[illegible]	[illegible]	[illegible]	1.35	1.35	[illegible]
[illegible] thermal expansion [illegible]	D696	[illegible]	[illegible]	[illegible]	[illegible]	[illegible]	[illegible]	[illegible]	[illegible]	[illegible]	[illegible]	3.3 x 10	[illegible]	[illegible]	[illegible]	[illegible]	1.2 x 10	[illegible]	[illegible]	[illegible]	[illegible]	[illegible]	1.8	1.8	[illegible]
[illegible]		[illegible]	[illegible]	[illegible]	[illegible]	[illegible]	[illegible]	[illegible]	[illegible]	SE	SE-0	SE	[illegible]	NB	NB	NB	NB	NB	NB	NB	NB	[illegible]	[illegible]	[illegible]	[illegible]
[illegible]		Unlimited	Unlimited	Unlimited	Unlimited	[illegible]	[illegible]	[illegible]	[illegible]	Black	Black	Black	Unlimited	Black	Black	Black	Black	Black	Black Brown	Black Brown	Black Brown	[illegible]	Unlimited	Unlimited	
		Opaque	Opaque	Opaque	Opaque	Opaque	Opaque	Opaque	[illegible]	Opaque	Opaque	Translucent	Translucent	Opaque	Opaque	Opaque	Opaque	Opaque	Opaque	Opaque	Opaque	Opaque	Clear	Clear	
[illegible]		NA	NA	NA	NA	NA	NA	NA	85				85										85	87	
MECHANICAL																									
[illegible]	[illegible]	[illegible]	[illegible]	[illegible]	[illegible]	[illegible]	[illegible]	[illegible]	[illegible]	[illegible]	[illegible]	[illegible]	[illegible]	[illegible]	[illegible]	[illegible]	[illegible]	[illegible]	[illegible]	[illegible]	[illegible]	[illegible]	[illegible]	[illegible]	[illegible]
[illegible]	[illegible]	[illegible]	[illegible]	[illegible]	[illegible]	[illegible]	[illegible]	[illegible]	[illegible]	25,000	[illegible]	[illegible]	[illegible]	[illegible]	[illegible]	[illegible]	[illegible]	[illegible]	[illegible]	[illegible]	[illegible]	[illegible]	[illegible]	[illegible]	[illegible]
[illegible]	[illegible]	[illegible]	[illegible]	[illegible]	[illegible]	[illegible]	[illegible]	[illegible]	[illegible]	4	[illegible]	[illegible]	[illegible]	[illegible]	[illegible]	[illegible]						[illegible]	[illegible]		[illegible]
[illegible]	[illegible]	[illegible]	[illegible]	[illegible]	[illegible]	[illegible]	[illegible]	[illegible]	[illegible]	[illegible]	[illegible]	[illegible]	[illegible]									[illegible]	340,000	[illegible]	[illegible]
[illegible]	[illegible]	[illegible]	[illegible]	[illegible]	[illegible]	[illegible]	[illegible]	[illegible]	[illegible]	32,000	15,000	14,000	[illegible]	9,000	9,000	9,000	11,000	[illegible]	[illegible]	[illegible]	[illegible]	[illegible]	[illegible]	[illegible]	[illegible]
[illegible]	[illegible]	[illegible]	[illegible]	[illegible]	[illegible]	[illegible]	[illegible]	[illegible]	[illegible]	[illegible]	[illegible]	345,000	[illegible]	[illegible]	1,000,000	[illegible]	1,000,000	[illegible]	[illegible]	[illegible]	[illegible]		340,000	[illegible]	[illegible]
[illegible]	[illegible]	[illegible]	[illegible]	[illegible]	[illegible]	[illegible]	[illegible]	[illegible]	[illegible]	[illegible]	[illegible]	[illegible]	[illegible]	[illegible]	[illegible]	[illegible]	[illegible]	[illegible]	[illegible]	25.00 x 10	[illegible]		12,500	[illegible]	D695
[illegible]	D732	10,500	10,500	[illegible]	[illegible]	10,500	[illegible]	[illegible]	[illegible]	[illegible]	[illegible]	11,500	[illegible]										6,000	[illegible]	[illegible]
[illegible]	D621	[illegible]	[illegible]	[illegible]	0.32	[illegible]	0.32	[illegible]						[illegible]	[illegible]	[illegible]	[illegible]								
[illegible]	[illegible]	[illegible]	[illegible]	[illegible]	[illegible]	[illegible]	[illegible]	[illegible]	[illegible]	[illegible]	[illegible]	[illegible]	[illegible]	[illegible]	[illegible]	[illegible]	[illegible]	[illegible]	[illegible]	[illegible]	[illegible]	[illegible]	[illegible]	[illegible]	[illegible]
[illegible]	D785	[illegible]	[illegible]	[illegible]	[illegible]	[illegible]	[illegible]	[illegible]	[illegible]	[illegible]	[illegible]	[illegible]	[illegible]	[illegible]	[illegible]	[illegible]	[illegible]	[illegible]	[illegible]	[illegible]	[illegible]	[illegible]	[illegible]	[illegible]	[illegible]
[illegible]	[illegible]	[illegible]	21	[illegible]	[illegible]								[illegible]										13	9	[illegible]
[illegible]	D621	[illegible]	2,500	2,850	4,000	[illegible]			300	[illegible]	[illegible]		[illegible]										2,000	[illegible]	[illegible]
ELECTRICAL																									
[illegible]	[illegible]	[illegible]	[illegible]	[illegible]	[illegible]		[illegible]	[illegible]	[illegible]	[illegible]	[illegible]	[illegible]	[illegible]	[illegible]	[illegible]	[illegible]	[illegible]	[illegible]	[illegible]	[illegible]	[illegible]	[illegible]	[illegible]	[illegible]	[illegible]
[illegible]	[illegible]	[illegible]	[illegible]	[illegible]	[illegible]	[illegible]	[illegible]	[illegible]	[illegible]	[illegible]			[illegible]	[illegible]	[illegible]	[illegible]	[illegible]		[illegible]	[illegible]	[illegible]	[illegible]	[illegible]	[illegible]	[illegible]
[illegible]	[illegible]	[illegible]	[illegible]	[illegible]	[illegible]		[illegible]	[illegible]	[illegible]	[illegible]	[illegible]	[illegible]	[illegible]	[illegible]	[illegible]	[illegible]	1.4 x 10	[illegible]	[illegible]	[illegible]	[illegible]	[illegible]	[illegible]		[illegible]
[illegible]	[illegible]	[illegible]	500	500	[illegible]	[illegible]	500	[illegible]	[illegible]	430	[illegible]	[illegible]	[illegible]	300	[illegible]	[illegible]	[illegible]	[illegible]	[illegible]	[illegible]	[illegible]	[illegible]	[illegible]	[illegible]	[illegible]
	[illegible]	[illegible]	[illegible]		[illegible]	[illegible]	70	[illegible]	[illegible]	120	[illegible]	[illegible]	120				180		[illegible]	[illegible]	[illegible]	5	[illegible]	[illegible]	[illegible]

SE: Self Extinguishing Non Dripping ASTM D635
SE-1: Self Extinguishing Non Dripping Group 1 U.L. Bulletin 94
SE-0: Self Extinguishing Non Dripping Group 0 U.L. Bulletin 94
NB: Non Burning ASTM D635
NA: Not Applicable

G.E. Product-Data Article CDP-1B

Reproduced from best available copy.

LEXAN®

POLYCARBONATE RESINS

PRODUCT DATA

LEXAN 500

Issued February 1, 1970

DESCRIPTION

LEXAN® 500 is a new member of the LEXAN family of polycarbonate resins particularly suited to applications requiring high rigidity combined with the toughness and impact strength of LEXAN.

LEXAN 500 has the highest combination of rigidity and impact strength available in any thermoplastic, plus self-extinguishing characteristics, excellent dimensional stability, low mold shrinkage, and colorability.

LEXAN 500 has these advantages:

Mechanical:

Flexural modulus increased nearly 60% over standard LEXAN, while high impact strength is retained.

Thermal:

Self-extinguishing SE-1 per UL bulletin 94. UL approved for sole support of current carrying parts.

Molding:

Mold shrinkage is reduced to about ½ that of standard LEXAN, making production of more precise parts possible.

PROPERTIES

The following data are typical for LEXAN 500:

	Property	Value	ASTM Test
Physical Properties	Specific Gravity	1.25	D 792
	Izod Impact strength		D 256
	Notched Bar, ⅛" x ½" (ft lbs/in.)	4-6	
	Unnotched Bar, ⅛" x ½" (ft lbs/in.)	20-40	
	Falling Dart Impact, 1" dart (ft lbs/in.)	>125	
	Tensile Strength, psi	9,600	D 638
	Tensile Modulus, psi	450,000	D 638
	Elongation, (%)	10	D 638
	Shear Strength	8,500	D 732
	Compressive Strength, psi	14,000	D 695
	Compressive Modulus, psi	320,000	D 695
	Flexural Strength, psi	15,000	D 790
	Flexural Modulus, psi	500,000	D 790
	Deformation under load (%)		D 621
	4,000 psi 77°F	.10	
	Fatigue Endurance, psi	3,500	
	Rockwell Hardness	M-85 R-124	D 85
	Water Absorbtion (%)		D 570
	24 hours	.12	
	Equilibrium @ 73°F	.31	
THERMAL PROPERTIES	Heat Deflection °F @ 264 psi	288	D 648
	°F @ 66 psi	295	
	Coefficient of Linear Thermal Expansion		D 696
	in./in./°C	3.42×10^{-5}	
	in./in./°F	1.79×10^{-5}	
	Thermal Conductivity (cal/sec/cm²/°C/cm	4.8×10^{-4}	D 696
	Flammability (UL Bulletin 94)	SE-1	
	Flammability	Self-ext.	D 635
	Mold Shrinkage, in./in.	0.002-0.003	D 955
ELECTRICAL PROPERTIES	Dielectric Constant (73°F)		D 150
	50 cycles	3.10	
	10^6 cycles	3.05	
	Power Factor (73°F)		D 150
	50 cycles	0.0008	
	10^6 cycles	0.0075	
	Dielectric Strength (73°),		D 149
	s/t, volts/mil, ⅛ thick	450	
	s/s, volts/mil, ⅛ thick	450	
	Volume Resistivity (ohm-cm), 73°F	3×10^{6}	
	Arc Resistance (secs.)		
	Tungsten Electrodes	120	
	Stainless Steel	5-10	

---

*Properties for some colors may vary slightly from the average values listed. For additional information see your General Electric representative.

LEXAN®

POLYCARBONATE RESIN

PRODUCT DATA

Glass-Reinforced Grades

Issued February 15, 1969

DESCRIPTION

LEXAN resin reinforced by glass fiber is available in two standard grades. The 3412 products contain 20% glass, the 3414 products 40% glass. Unreinforced LEXAN resin is outstanding among engineering thermoplastics in the areas of impact strength, heat resistance, dimensional stability, and creep resistance. Reinforcement with glass fiber raises performance to levels approaching those of metals while retaining the basic plastic attributes of low cost processing, dielectric character, resistance to corrosion, and inherent color.

The outstanding differences between reinforced (40% glass) and natural LEXAN are these:

Mechanical:

tensile modulus is as much as five times greater—

flexural, compressive and tensile strengths are nearly doubled or more than double

fatigue endurance is dramatically changed, increasing more than 7 times to permit tolerance of a 7500 psi load at 1800 cycles per minute—

deformation under load, a more than satisfactory 0.20% for unreinforced resin, drops to a mere 0.12%, even under 4000 psi.

Thermal:

coefficient of thermal expansion, reduced nearly 75%, equals that of many metals.

Molding:

mold shrinkage is reduced to about 1/3rd that of LEXAN resin, making possible production of very precise parts.

PROPERTIES

The following data are typical for LEXAN 3412 and 3414:

	Property	LEXAN GR 3412 (20% glass)	LEXAN GR 3414 (40% glass)	ASTM Test
Physical Properties	Specific Gravity	1.35	1.52	D 792
	Izod Impact Strength			
	Notched Bar, 1/8" x 1/2" (ft lbs in.)	2.0	2.5	D 256
	Unnotched Bar, 1/8" x 1/2" (ft lbs in.)	19.0	24.0	
	Tensile Strength, psi	16,000	25,000	D 638
	Tensile Modulus, psi	860,000	1,680,000	D 638
	Elongation, (%)	4	4	D 638
	Shear Strength	10,000	11,000	D 732
	Compressive Strength, psi	16,000	21,000	D 695
	Compressive Modulus, psi	760,000	1,500,000	D 695
	Flexural Strength, psi	21,000	32,000	D 790
	Flexural Modulus, psi	800,000	1,400,000	D 790
	Deformation under load (%)			D 621
	4,000 psi 77°F	0.04	0.02	
	122°F	0.04	0.02	
	158°F	0.10	0.06	
	2,000 psi 122°F	0.03	0.01	
	Fatigue Endurance, psi	5,000	7,000	
	Rockwell Hardness	M-91 R-113	M-93 R-114	D 785
	Water Absorption (%)			
	24 hours	0.16	0.12	D 570
	Equilibrium @ 73°F	0.20	0.23	
Thermal Properties	Heat Deflection °F @ 264 psi	295	295	D 648
	°F @ 66 psi	300	310	
	Coefficient of Linear Thermal Expansion			D 696
	in./in./°C	2.68×10^{-5}	1.68×10^{-5}	
	in./in./°F	1.49×10^{-5}	0.93×10^{-5}	
	Thermal Conductivity (cal/sec/cm²/°C/cm	5.0×10^{-4}	5.2×10^{-4}	D 696
	Flammability	Self-ext. I	Self-ext. I	D 635
	Mold Shrinkage, in./in.	0.002-3	0.001-2	D 955
Electrical Properties	Dielectric Constant (73°F)			D 150
	50 cycles	3.17	3.53	
	10^6 cycles	3.13	3.48	
	Power Factor (73°F)			D 150
	50 cycles	0.0009	0.0013	
	10^6 cycles	0.0073	0.0067	
	Dielectric Strength (73°F),			D 149
	s/t, volts/mil, 1/8 thick	490	450	
	s/s, volts/mil, 1/8 thick	490	400	
	Volume Resistivity (ohm-cm), (73°F)	5×10^{-6}	4×10^{-6}	
	Arc Resistance (secs.)			
	Tungsten Electrodes	120	120	
	Stainless Steel	5	5	

GLASS-REINFORCED NORYL®
THERMOPLASTIC RESIN

PRODUCT DATA

GRADES
SE 1-GFN2
SE 1-GFN3

PRODUCT DESCRIPTION

Self-extinguishing glass-reinforced NORYL® thermoplastic resin is offered in addition to General Electric's standard glass-reinforced NORYL-2 and NORYL-3. This resin contains well dispersed, randomly oriented short glass fibers and is rated self-extinguishing, non-dripping, Group 1 according to UL Bulletin 94. Compared with the base NORYL thermoplastics, this SE-1 filled resin offers even better mechanical, thermal, dimensional and molding-to-tolerance characteristics while at the same time maintaining excellent electrical properties and hydrolytic stability.

PRODUCTS AVAILABLE

SE-1 glass-reinforced NORYL is available at the 20 and 30% level of glass loading, designated SE 1-GFN2 and SE 1-GFN3 respectively.

These resins are supplied in 1/8" diameter pellet form in a standard gray color (designation 780) for molding and extrusion. A range of opaque colors is available on special order. SE 1-GFN2 and SE 1-GFN-3 NORYL products are generally recommended for applications requiring high mechanical strength, dimensional stability and UL rated self-extinguishing characteristics.

TYPICAL PROPERTIES OF NORYL GRADES SE 1-GFN2 and SE 1-GFN3

Property	ASTM Method	SE 1-GFN2	SE 1-GFN3
Specific Gravity	D792	1.30	1.36
Specific Volume	—	21.3	20.2
Water Absorption, 73°F, 24 hr	D570	0.06	0.06
Heat Deflection Temp., 264 psi, °F	D648	270	275
Mold Shrinkage, in./in.	D955	0.002	0.001
Flammability	D635 U.L. Bulletin 94	Self-Exting. Non-Dripping Group 1	Self-Exting. Non-Dripping Group 1
Tensile Strength, Yield, psi at 73°F	D638	14,500	17,000
Elongation at Break, %	D638	4-6	4-6
Tensile Modulus, psi at 73°F	D638	925,000	1,200,000
Flexural Strength, psi at 73°F	D790	18,500	20,000
at 200°F		13,500	15,000
Flexural Modulus, psi at 73°F	D790	750,000	1,100,000
at 200°F		625,000	1,000,000
Izod Impact, Notched 1/8" × 1/2" Bar	D256		
Ft. Lb./in. notch, at −40°F		1.4	1.3
at 73°F		1.5	1.4
Tensile Creep, 300 hrs. 2000 psi, 73°F, %	D674	0.33	0.2
Hardness, Rockwell	D785	M90 L106	M93 L108
Dielectric Constant, 73°F, 50% RH	D150		
at 60 cps		2.98	3.15
at 10^6 cps		2.95	3.11
Dielectric Constant, 150°F, at 60 cps	D150	2.96	3.14
at 10^6 cps		2.93	3.10
Dissipation Factor, 73°F, 50% RH at 60 cps	D150	.0016	.0020
at 10^6 cps		.0017	.0021
Dissipation Factor, 150°F, at 60 cps	D150	.0021	.0023
at 10^6 cps		.0018	.0022
Volume Resistivity, dry, 73°F, ohm cm	D257	10[illegible]	10[illegible]
Surface Resistivity, ohm sq	D257	10[illegible]	10[illegible]
Dielectric Strength, volts/mil, ST, 1/8" sample	D149	600	530

CURING AGENTS FOR EPON RESINS – CASTING APPLICATIONS (1967)

Curing Agent	Chemical Type	Physical¹ State	Equivalent² Weight	Recommended³ Concentration Range, phr	Curing Conditions⁴ Curing Temperature Range °F (°C)	Cure Characteristics⁵ Gel Time (1 gl mass) °F (°C)	Cure Characteristics⁵ Complete Cure (typical schedule) °F (°C)	Heat Deflection Temperature⁶ °F (°C)	Suppliers⁷	Remarks
1. Diethylenetriamine (DTA)	Polyamine	Liquid	20.6	10-12	60-300 (15-150)	[illegible] min, 77 (25)	7 days, 77 (25)	250 (120)	A, B, C¹¹	Fast cure, short pot life, good R.T. strength, low initial viscosity
2. Triethylenetetramine (TETA)	Polyamine	Liquid	24.1	11-13	60-300 (15-150)	30 min, 77 (25)	7 days, 77 (25)	250 (120)	A, B, C	Fast cure, short pot life, good R.T. strength, low initial viscosity
3. Diethylaminopropylamine (A)	Polyamine	Liquid	65	4-8	77-300 (25-150)	3-4 hr, 77 (25)	30 min, 240 (115)	212 (100)	C	Requires moderate heat cure, gives good moderate temperature strength. Longer pot life than DTA and TETA
4. EPON® Curing Agent T	Modified Polyamine	Liquid	ca 38	15-25	77-300 (25-150)	30-40 min, 77 (25)	7 days, 77 (25)	180 (82)	R	Mostly used with low viscosity resins in tooling. Low toxicity
5. EPON® Curing Agent T-1	Modified Polyamine	Liquid	ca 47	20-30	77-300 (25-150)	20-30 min, 77 (25)	7 days, 77 (25)	195 (90)	R	Similar to T but cures at slightly lower temperature
6. EPON® Curing Agent U	Modified Polyamine	Liquid	ca 48	20-30	60-300 (15-150)	20-30 min, 77 (25)	7 days, 77 (25)	250 (120)	R	Fast cure, short pot life, low toxicity, gives strong laminated tools
7. EPON® Curing Agent V-25	Polyamide	Liquid	ca 162	33-133	60-300 (15-150)	45-60 min, 77 (25)	7 days, 77 (25)	195 (90)	R	Concentration range with EPON resins can be varied widely without affecting properties of the cured system. Used to provide flexible systems
8. EPON® Curing Agent V-40	Polyamide	Liquid	ca 140	33-133	60-300 (15-150)	45-60 min, 77 (25)	7 days, 77 (25)	240 (115)	R	Similar to V-25 but with lower viscosity and slightly longer pot life
9. EPON® Curing Agent D	Polyamine Salt	Liquid	—¹²	10.5-13.5	150-300 (65-150)	2-4 hr, 77 (25)	1 hr, 145 (60) & 2 hr, 300 (150)	175 (80)	R	Requires moderate heat cure. Excellent in castings up to 200° F service
10. N-Aminoethylpiperazine (AEP)	Polyamine	Liquid	43	20-23	80-300 (25-150)	20-30 min, 77 (25)	24 hr, 77 (25) & 1 hr, 300 (150)	250 (120)	B	Requires moderate heat cure, fast curing, low mix viscosity, gives castings with high impact strength
11. DP17	Modified Polyamine	Liquid	ca 35	16-20	140-400 (60-200)	8 hr, 77 (25)	2 hr, 175 (80) & 2 hr, 300 (150)	300 (150)	G	Requires heat cure, gives excellent high temperature properties, electrical properties & chemical resistance
12. EPON® Curing Agent Z	Modified Polyamine	Liquid	38	19-21	140-400 (60-200)	8 hr, 77 (25)	2 hr, 175 (80) & 2 hr, 300 (150)	300 (150)	R	Requires heat cure, gives excellent high temperature properties, electrical properties & chemical resistance
13. meta-Phenylenediamine (CL)	Polyamine	Solid	27	13-14	140-400 (60-200)	8 hr, 77 (25)	2 hr, 175 (80) & 2 hr, 300 (150)	300 (150)	R, F, G	Requires heat cure, imparts excellent high temperature properties, electrical properties & chemical resistance
14. Methylene Dianiline (MDA) or Tonox	Polyamine	Solid	50	28-30	140-400 (60-200)	8 hr, 77 (25)	2 hr, 175 (80) & 2 hr, 300 (150)	300 (150)	A, J	Requires heat cure, imparts excellent high temperature properties, electrical properties & chemical resistance
15. Diaminodiphenyl Sulfone (DDS)	Polyamine	Solid	61	20-30	240-400 (115-200)	45-60 min, 250 (120)	2 hr, 250 (120) & 2 hr, 300 (150)	250 (120)	D, E	Excellent high temperature properties, high mix viscosity, excellent resistance to high humidity environment
16. BF_3 Monoethylamine (BF_3·MEA)	Lewis Acid Amine Complex	Solid	—¹²	2-4	240-400 (115-200)	6-9 mo, 77 (25)	1 hr, 250 (120) & 2 hr, 300 (150)	340 (170)	F, H	Long pot life at R.T., cure rate highly dependent on temperature, gives good strength and heat resistance, good electrical properties, brittle at room temperature
17. Dodecenylsuccinic Anhydride (DDSA)	Anhydride	Liquid	266	130-140	140-300 (60-150)	5-6 days, 77 (25)	1 hr, 212 (100) & 2 hr, 300 (150)	160 (70)	R, F, K, M	Long pot life at R.T., gives excellent electrical properties in castings and retains them above heat deflection temperature, imparts a degree of flexibility to castings. Should be used with an accelerator.⁹, ¹⁰
18. NADIC Methyl Anhydride (NMA)	Anhydride	Liquid	178	85-95	175-500 (80-260)	5-6 days, 77 (25)	1 hr, 250 (120) & 4 hr, 400 (200) & 24 hr, 500 (260)	356 (180)	R, F	Low viscosity liquid at room temperature, long pot life, excellent for high temperature applications, requires extensive post cure for maximum heat resistance
19. Phthalic Anhydride (PA)⁸	Anhydride	Solid	148	70-80	200-300 (94-150)	5 hr, 250 (120)	12 hr, 250 (120) or 4 hr, 300 (150)	300 (150)	C, F,	Insoluble below curing temp., difficult to handle, used in electrical potting, inexpensive
20. Hexahydrophthalic Anhydride (HHPA)	Anhydride	Solid	154	75-85	200-400 (94-200)	30-60 min, 175 (80)	1 hr, 175 (80) & 2 hr, 300 (150)	265 (130)	R, F	Low melting point, gives low mix viscosity, long pot life, good electrical properties. Gives light colored castings and laminates with good color stability to ultraviolet. Should be used with an accelerator.⁹
21. Chlorendic Anhydride (HET)	Anhydride	Solid	371	100-120	200-400 (94-200)	10-15 min, 250 (120)	1 hr, 250 (120) & 2 hr, 300 (150)	356 (180)	L, N	Short pot life, gives castings of low flammability and high heat deflection temperature
22. Trimellitic Anhydride (TMA)	Anhydride	Solid	192	30-40	210-400 (100-200)	30-60 min, 250 (120)	1 hr, 250 (120) & 2 hr, 300 (150)	460 (250)	P	Good electrical properties, reacts very rapidly at high temperatures, good for high temperature applications
23. Tetrahydrophthalic Anhydride (THPA)	Anhydride	Solid	152	75-80	200-300 (94-150)	1-2 hr, 212 (100)	1 hr, 200 (94) & 2 hr, 300 (150)	250 (120)	R, F	Low mix viscosity, good electrical properties, relatively inexpensive, insoluble below melting point
24. EMI-24	Substituted Imidazole	Supercooled Liquid	—¹²	2-10	140-300 (60-150)	8-24 hr, depending on concentration	4 hrs, 140 (60) & 2 hr, 300 (150)	230-320 (110-160)	Q	Good high temperature strength with moderate temperature cure.

1. At room temperature
2. Amount required to react with one mole of epoxide
3. With EPON Resins 815, 820, 826, 828, and 830 except phthalic anhydride (See Note 8)
4. Cures can be effected with these curing agents at any temperature within the applicable ranges given in the table. Higher temperatures always yield shorter cure times for a given resin. The typical schedules given are intended only to illustrate curing conditions commonly used. In practice, wide variations in cure time can be achieved by varying curing temperature.
5. With EPON Resin 828 except phthalic anhydride. See Note 8. Note: The symbol "&" in this column means "followed by"
6. Obtained with EPON 828 using optimum concentration and curing conditions (not necessarily those specified herein). ASTM D648, 264 psi.
7. Supplier Code

A	Dow Chemical Company
B	Jefferson Chemical Company
C	Union Carbide Chemicals Company
D	RSA Corporation
E	Polychemical Laboratories
F	Allied Chemical Co. Industrial Chemicals Division
G	E. I. DuPont de Nemours Co. Dyes and Chemicals Div.
H	Harshaw Chemical Company
J	Naugatuck Chemical Company
K	Monsanto Chemical Company
L	Hooker Chemical Company
M	Heyden Newport Chemical Co.
N	Velsicol Chemical Company
P	Amoco Chemical Company
Q	Houdry Proc. & Chem. Co. Division of Air Products & Chemicals, Inc.
R	Shell Chemical Co. Plastics and Resins Div.

8. Used with solid rather than liquid resins. Data herein refers to use with EPON Resin 1001
9. Certain epoxy compositions described in this bulletin are the subject of U.S. Patent 3,052,650. We have been informed that Minnesota Mining and Manufacturing Co. is prepared to license those making, using or selling compositions covered by that patent.
10. Gel times of systems making use of accelerators, e.g., anhydride cured systems, will be dependent on concentration of accelerator used.
11. Also consult manufacturers' bulletins for curing agents not manufactured by Shell.
12. Cure catalytically

This information is based on data obtained by our own research and is considered accurate. However, no warranty is expressed or implied regarding the accuracy of these data, the results to be obtained from the use thereof or that any such use will not infringe any patent. This information is furnished upon the condition that the person receiving it shall make his own tests to determine the suitability thereof for his particular purpose.

Sales specifications, although current at time of publication, are subject to change due to process improvements. For latest product specifications, contact our nearest sales office.

Reproduced from best available copy.

VOLUMETRIC SHRINKAGE OF EPOXY RESIN SYSTEMS

(Shell 1967)

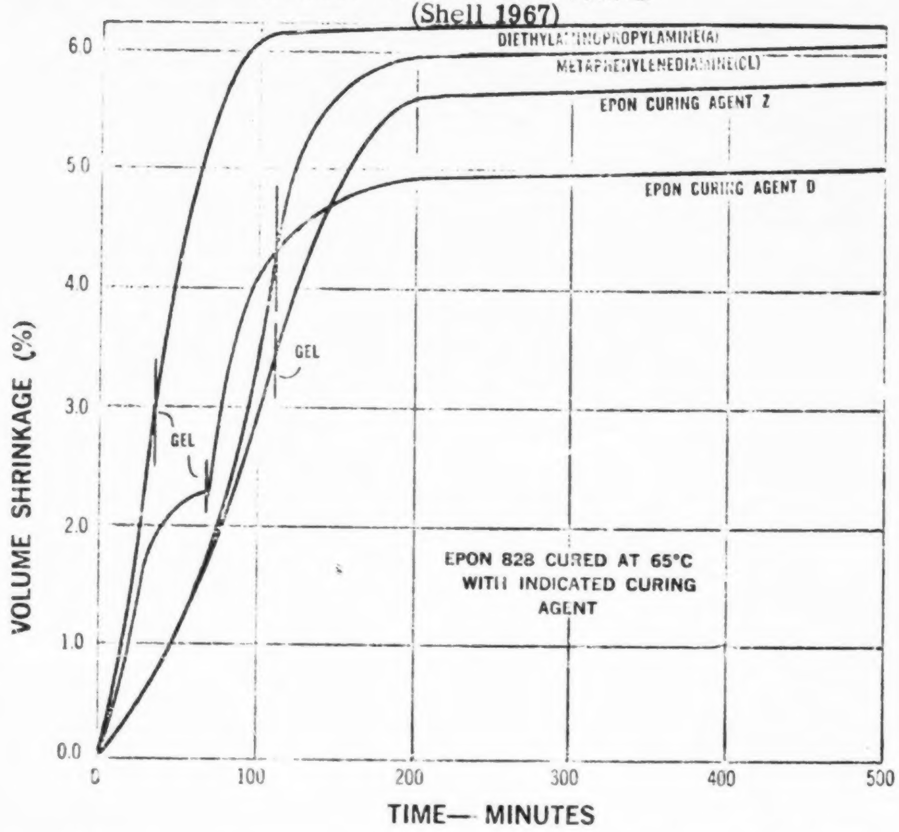

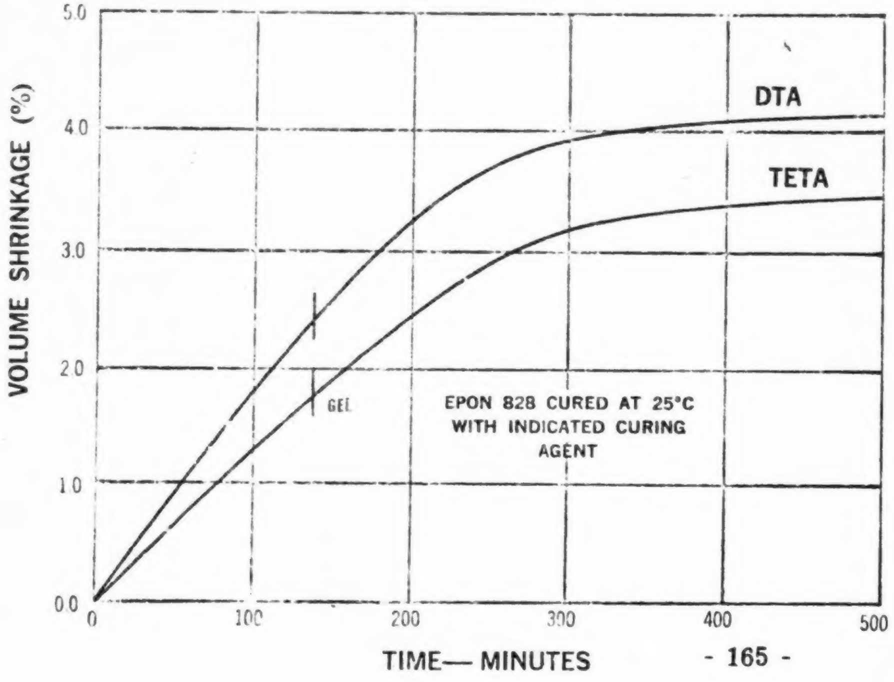

TENSILE PROPERTIES OF "HIGH STRENGTH" EPON® RESIN SYSTEMS

(Systems Providing Tensile Strength Values of Approximately 10,000 psi)

(Shell Epon Resins for Casting 1967)

Resin System	Material Ratio	Cure Cycle¹ (hrs/°C)	Tensile Strength at 23°C, Max. Value, psi	Tensile Modulus at 23°C, psi	Elongation at 23°C, %	HDT °C
Aliphatic Amine Cured						
828/DTA	100/12	RT Gel + 2/150	10,900	410,000	6.3	115
828/AEP	100/20	RT Gel + 1/200	9,600	400,000	8.8	104
Aromatic Diamine Cured						
826/CL	100/15	2/80 + 2/150	13,300	440,000	6.1	156
826/[illegible]	100/18	2/90 + 4/150	12,400	430,000	7.0	[illegible]
8[illegible]/Z	100/20	2/80 + 2/150	13,000	360,000	4.8	147
828/CL	100/14	2/80 + 2/150	12,400	480,000	5.1	[illegible]
828/TONOX	100/22	2/80 + 4/150	12,800	403,000	5.8	[illegible]
815/Z	100/22	2/80 + 2/150	15,000	560,000	5.8	[illegible]
Anhydride Cured						
828/NMA/DMP 30	100/87/1	2/125 + 2/200 + 2/245	8,400	420,000	2.3	140
826/NMA/EMI-24	100/90/1	2/90 + 4/135	7,600	460,000	1.9	[illegible]
[illegible]/HHPA/BDMA	100/84/1	2/90 + 4/150	12,300	440,000	6.0	125
[illegible]/THPA/BDMA	100/76/1	2/120 + 4/150	10,700	400,000	4.5	125
[illegible]/PA/BDMA	100/75/0.1	2/120 + 4/150	11,500	400,000	4.1	135
Catalyzed Systems						
828/BF$_3$/MEA	100/3	3/120 + 1/200	8,700	390,000	3.0	174
828/D	100/10.5	3/75	11,100	500,000	4.7	60

---

¹The values listed are those provided by cure cycles designed to present the highest values in the tensile test. See formulary for effect of cure cycle on properties of given resin system

TENSILE PROPERTIES OF "FLEXIBLE" EPON RESIN SYSTEMS

(Systems Providing an Elongation of 5% or Greater)

Resin System	Material Ratio	Cure Cycle hrs/°C	Tensile Strength Max. Value, psi, at 23°C	Tensile Elongation %, at 23°C
Aliphatic Amine Systems				
872/828/V-40	50/50/50	RT Gel + 1/100	7,000	5.3
828/872/AEP	50/50/14	RT Gel + 1/100	9,000	5.6
830/HMDA/DDA¹	100/12.7/6.7	RT Gel + 2/150	8,900	8.7
872/AEP	100/6	RT Gel + 1/100	2,900	95
872/871/AEP	50/50/8	7 Days at RT	400	100
872/871/AEP/Octyl Amine	50/50/4.0/6.8	7 Days at RT	150	140
Aromatic Diamines				
834/CL	100/10.9	2/80 + 2/150	12,400	7.1
828/872/Z	50/50/13	2/80 + 4/150	9,000	7.4
828/872/Z	25/75/9	2/80 + 4/150	6,500	8.3
826/CL/Aniline	100/12/4	2/80 + 4/150	13,000	8.0
Anhydrides				
828/871/DDSA/EMI 24	50/50/100/1	2/90 + 4/150	4,600	8.4
825/Harcure A/DDSA/EMI 24	100/65/23/1	2/90 + 4/170	4,200	64
830/Harcure A/EMI-24	100/102/1	2/90 + 4/150	3,300	96
826/Harcure A/DDSA/EMI-24	100/108/38/1	2/90 + 4/170	2,000	134
828/EMPOL-1040/DMP-10	100/110/0.75	1½/120 + 5/120	2,500	127
828/EMPOL-1040/DMP-10	100/140/0.75	1½/120 + 5/120	900	260

¹HMDA = Hexamethylenediamine, DDA = Dodecylamine